

Application of field theoretical methods to problems in mesoscopic physics

Inaugural-Dissertation

zur

Erlangung des Doktorgrades

der Mathematisch-Naturwissenschaftlichen Fakultät

der Universität zu Köln

vorgelegt von

Tobias Micklitz

aus München

2006

Berichterstatter: Prof. Dr. A. Altland

Prof. Dr. A. Rosch

Tag der letzten mündlichen Prüfung: 09.02 - 28.02.07

Abstract

The subject of this thesis are three different topics related to quantum interference and dephasing in weakly disordered mesoscopic systems.

The first topic covers the so-called “current echo”, which is a quantum-interference phenomenon predicted about a decade ago by Thomas *et al.* on the basis of numerical calculations. Our motivation to study the current echo originates from the fact that a simple physical picture explaining its appearance so far has been missing. It is shown that all characteristic features of Thomas’ current echo can be explained resorting to the well known phenomenon of weak localization in disordered systems. In view of recent technological progress in the creation of voltage pulses on a pico-second time scale, the experimental verification of the current echo should be feasible. The echo phenomenon may become a useful tool to determine dephasing rates in weakly disordered systems.

The second topic is titled “Dephasing by Kondo impurities”. In this part of the thesis we derive an analytical expression for the dephasing rate of non-interacting electrons propagating in a weakly disordered environment and scattering from very low concentrations of magnetic impurities. The motivation to study dephasing due to Kondo impurities traces back to a series of experiments performed over the last decade which show an unexpected saturation of the dephasing rate at lowest temperatures. The observed saturation clearly deviates from theoretical predictions based on the assumption that inelastic scattering due to electron-electron interactions is the dominant mechanism for dephasing. Therefore, it was suggested, that inelastic scattering from low concentrations of magnetic impurities may be responsible for the observed excess of dephasing. So far these speculations could not be quantitatively tested, since the dephasing rate due to diluted magnetic impurities in the experimentally probed range of temperature was unknown. Based on our results a quantitative comparison between theoretically predicted and experimentally measured dephasing rate was done. This allowed for a critical examination of the relevance of low concentrations of magnetic impurities for the observed behaviour of the dephasing rate. Moreover, this part of the thesis analyzes the magnetic field dependence of the dephasing rate due to magnetic impurities and generalizes the results for the dephasing rate from magnetic to arbitrary diluted dynamical impurities.

The third topic of this thesis relates to quantum interference and dephasing in a disordered Luttinger liquid. The standard approach to describe interacting one-dimensional systems is the bosonization method, which, however, becomes very intransparent when in addition disorder comes into play. Therefore, quantum interference phenomena and dephasing in a *disordered* Luttinger liquid remained unaddressed for a long time. In this part of the thesis we follow a new road and derive an effective field theory for the disordered Luttinger liquid. This model allows to systematically explore interference phenomena in disordered Luttinger liquids. As an application of the model we discuss for the first time the persistent current in a weakly disordered Luttinger liquid.

Zusammenfassung

Die vorliegende Arbeit beschäftigt sich mit drei verschiedenen Themengebieten, in deren Mittelpunkt quantenmechanische Interferenzphänomene und der Verlust von Phasenkohärenz (Dephasierung) in schwach ungeordneten mesoskopischen Systemen stehen.

Im ersten Abschnitt der Arbeit diskutieren wir sogenannte “Stromechos”, ein quantenmechanisches Interferenzphänomen, welches vor einem Jahrzehnt von Thomas *et al.* aufgrund numerischer Rechnungen vorhergesagt wurde. Die Motivation, uns mit den Stromechos zu beschäftigen, resultiert aus der Tatsache, dass eine einfache physikalische Erklärung dieses Phänomens fehlte. In der Tat kann gezeigt werden, dass alle in den numerischen Rechnungen gefundenen Eigenschaften des Echos mit derselben Physik erklärt werden können, welche der schwachen Lokalisierung in ungeordneten Systemen zugrundeliegt. Angesichts des rasanten technischen Fortschrittes in der Erzeugung von Spannungspulsen auf Zeitskalen von Pikosekunden, scheint eine experimentelle Verifizierung des Stromechos realisierbar. Praktische Bedeutung können die Stromechos in der Bestimmung von Dephasierungsraten erhalten.

Im zweiten Abschnitt, dem Themengebiet “Dephasing due to Kondo impurities”, berechnen wir die Dephasierungsrate von Elektronen, die durch ein ungeordnetes System propagieren und an einer geringen Konzentration magnetischer Unreinheiten streuen. Unser Interesse an diesem Problem geht auf zahlreiche Experimente zurück, welche im Laufe des letzten Jahrzehnts durchgeführt wurden und eine unerwartete Sättigung der Dephasierungsrate bei tiefsten Temperaturen zeigen. Die beobachtete Sättigung weicht von theoretischen Vorhersagen ab, welche auf der Annahme basieren, dass die Dephasierung allein durch Elektron-Elektron-Wechselwirkung verursacht wird. Daher wurde vermutet, dass inelastische Streuung an stark verdünnten magnetischen Verunreinigungen den wesentlichen Beitrag zur Dephasierung bei tiefen Temperaturen liefert. Diese Vermutung konnte jedoch bisher nicht quantitativ überprüft werden, da die Dephasierungsrate, welche von inelastischer Streuung an magnetischen Verunreinigungen herrührt, in dem experimentell untersuchten Temperaturbereich nicht bekannt war. Basierend auf unserem Ergebnis konnte nun erstmals die Vermutung, dass geringe Konzentrationen von magnetischen Unreinheiten verantwortlich für die experimentell beobachtete Sättigung der Dephasierungsrate bei tiefen Temperaturen sind, kritisch überprüft werden. Weiterhin diskutieren wir in diesem Abschnitt der Arbeit die Magnetfeldabhängigkeit der Dephasierungsrate, und verallgemeinern unsere Ergebnisse von magnetischen auf beliebige, verdünnte dynamische Verunreinigungen.

Im dritten Abschnitt der Arbeit diskutieren wir quantenmechanische Interferenz und Dephasierung in Luttinger-Flüssigkeiten. Eine sehr effiziente Methode zur Beschreibung wechselwirkender, eindimensionaler Systeme ist das Bosonisierungs-Verfahren. Kommt jedoch zusätzlich Unordnung ins Spiel, wird diese Methode sehr undurchsichtig. Deshalb wurden quantenmechanische Interferenz und Dephasierung in *ungeordneten* Luttinger-Flüssigkeiten für lange Zeit nicht untersucht. In diesem Abschnitt der Arbeit leiten wir eine effektive Feldtheorie für ungeordnete Luttinger-Flüssigkeiten ab, welche eine systematische Untersuchung quantenmechanischer Interferenzphänomene erlaubt. Als Anwendung unseres Modells diskutieren wir erstmals Dauerströme in einer ungeordneten Luttinger Flüssigkeit.

Contents

1	Current-Echoes in Metals and Semiconductors	11
1.1	Keldysh σ -model for systems with time-reversal invariance	12
1.2	Current in linear response to a pulsed electrical field	16
1.3	Cooperon in a pulsed electric field	17
1.4	Semiclassical analysis of the current-echo	20
1.5	Current-echo in semiconductors	22
1.6	Summary and outlook	26
2	Dephasing by Kondo Impurities	29
2.1	Replica NL σ M for disordered electron gas containing diluted magnetic impurities	30
2.2	Dephasing by static magnetic impurities	35
2.3	Dephasing due to dynamical magnetic impurities	37
2.3.1	Introduction of elastic and inelastic vertices	37
2.4	Dephasing-rate measured from the magnetoresistance	39
2.4.1	The dephasing rate measured in WL experiments	39
2.4.2	1. Contributions from inelastic vertex	41
2.4.3	2. Contributions from mixed diagrams	45
2.4.4	3. Contributions from higher-order corrections in n_S	46
2.4.5	Interplay: Kondo effect and electron-electron interactions	46
2.5	Summary	46
2.6	Generalizations	47
2.7	Dephasing-rate measured from universal conductance fluctuations and Aharonov-Bohm oscillations	49
2.8	Dephasing-rate measured from the current echo	54
2.9	Comparison to recent experiments and outlook	54
3	Disordered Luttinger Liquid	59
3.1	The model	60
3.2	Bosonization of non-interacting electrons in a clean wire: three equivalent approaches .	61
3.2.1	Standard bosonization	61
3.2.2	Functional bosonization	62
3.2.3	σ -Model bosonization	63
3.2.4	Higher loop corrections to the Gaussian propagator	71
3.2.5	Summary of this section and outlook	72
3.3	Interacting electrons in a clean wire: Equivalence of the three approaches	72
3.3.1	Standard bosonization	72
3.3.2	Functional bosonization	73
3.3.3	σ -model bosonization	74
3.3.4	Summary of this section	74
3.4	Inelastic scattering rate in a clean Luttinger liquid	75
3.4.1	Screening the Coulomb-interactions	76
3.4.2	The inelastic scattering rate	76
3.4.3	Summary of this section	78

3.5	Electrons in a disordered one-dimensional system	78
3.5.1	Localization in a disordered 1d system	79
3.5.2	Drude conductivity and weak localization in a disordered 1d system	80
3.5.3	Summary of this section	81
3.6	Interacting electrons in a disordered 1d system	82
3.6.1	RPA screening in a disordered system	83
3.6.2	"Renormalization" of disorder by electron-electron interactions	84
3.6.3	Summary of this section and outlook	86
3.7	An Application: Persistent current in a Luttinger liquid	86
3.7.1	Persistent current in a clean Luttinger liquid	86
3.7.2	Persistent current in a weakly disordered Luttinger liquid	90
3.7.3	Summary of this section	98
3.8	Summary and outlook	98
A	Appendix (Dephasing by Kondo impurities)	101
A.1	Gradient expansion	101
A.2	Spin-singlet and spin-triplet channels	103
A.2.1	Spin-singlet channels	103
A.2.2	Spin-triplet channels	104
A.3	Response kernels in Gaussian approximation	106
A.3.1	Response kernel for weak localization experiment	106
A.3.2	Response kernel for Aharonov-Bohm oscillations	107
A.4	Some details	109
A.5	Some more details	110
A.6	Renormalized perturbation theory for the Anderson model	110
A.7	Fluctuations of the Kondo-temperature	111
A.8	Limits of applicability: Cross-over temperatures for the dephasing-rate	112
A.8.1	Evaluation of the diagrams	114
A.9	Analytical continuation	114
A.9.1	Self-energy corrections $\Delta\sigma_1$	114
A.9.2	Vertex corrections $\Delta\sigma_2$	116
A.10	Lehmann representation	117
A.10.1	Self-energy	117
A.10.2	Two-vertex	117
A.10.3	Three-vertex	118
A.10.4	Four-vertex	119
B	Appendix (Disordered Luttinger Liquid)	127
B.1	l_0 -independent contributions from the "tr ln"-expansion	127
B.2	Diagrammatic evaluation of the density/density correlation function	130
B.3	Regularization of the propagator	131
B.4	Equivalence of Eq.(3.68) and Eq.(3.72)	132
B.5	Equivalence of Eq.(3.72) and Eq.(3.74)	133
B.6	Dephasing rates	134
B.7	Inclusion of back-scattering disorder	135
B.8	Some details	136
B.8.1	Analytical continuation of $S_\chi[c^{fb}c^{bf}]$	136
B.8.2	Poisson summation	137
B.8.3	Performing the y -integral	137
B.8.4	Coulomb field propagator	138

Introduction

The quantum mechanical wave-nature of matter not only appears on microscopic scales, but also can be studied in systems with macroscopic numbers of degree of freedom, as e.g. mesoscopic metals and semiconductors at low temperatures. The electron's wave nature manifests itself in its ability to interfere. Interference effects play an important role in *disordered* systems: Electrons scatter from impurities and form a complicated interference pattern, giving rise, on the one hand, to measurable deviations from classically expected values of observables, such as the conductivity, and, on the other hand, leading to new, classically not expected phenomena.

A new "interference-phenomenon", the so-called current echo, has been predicted by Thomas *et al.* about a decade ago. The predictions are based on numerical calculations and a simple physical interpretation for the current echo has been missing so far. In the first chapter of this thesis we will discuss this phenomenon and suggest an explanation which resorts only to the well-established theory of weak localization in disordered metals of non-interacting electrons.

In real physical systems the particles are, however, always exposed to *interactions*, which can be intrinsic (such as electron-electron interactions) or extrinsic due to interactions with an environment (such as dynamical impurities). Inelastic interaction processes lead to the destruction of the electron's phase coherence and therefore suppress interference phenomena. Phase space arguments lead to the expectation that dephasing of electrons in a Fermi sea becomes ineffective when the temperature is lowered. At lowest temperatures the electrons phase coherence should be fully re-established. Irritatingly, however, several experiments performed over the last decade, indicate a saturation of the dephasing rate at lowest temperatures. It was suggested that this excess of dephasing results from scattering of electrons at extremely low concentrations of magnetic impurities, which are inevitably contained in the probes. In the second chapter of this thesis we will tackle this problem with the aim to derive an analytical expression for the dephasing rate of electrons interacting with low concentrations of magnetic impurities.

Interactions not only cause dephasing but may also drastically change the systems properties. Arbitrary weak electron-electron interactions in one-dimensional systems are known to turn the system into a non-Fermi liquid state, the so-called Luttinger liquid. The Luttinger liquid is e.g. characterized by power-laws for the temperature and bias-voltage dependence of the tunneling current, which has been experimentally verified e.g. in carbon nanotubes. The standard approach to interacting one-dimensional systems is the bosonization method. This method, however, becomes very intransparent when disorder comes into play. Therefore, quantum interference phenomena and dephasing in a Luttinger liquid remained unaddressed for a long time. In the third chapter of this thesis we use a different approach to analyze disordered interacting one-dimensional systems. This approach leads to a field theory which is the single-channel limit of an "universal" model for disordered interacting systems, known from higher dimensions and which allows for a transparent description of interference phenomena. A practical application of this model will be the analysis of the persistent current in a disordered single-channel ring of (weakly) interacting electrons.

As indicated in the title we employ field theoretical methods to address the above mentioned problems. More precisely we use the nonlinear σ -model and the closely related diagrammatic perturbation theory in terms of Greens functions.

Chapter 1

Current-Echoes in Metals and Semiconductors

Introduction: Based on numerical calculations within the Anderson impurity model of non-interacting electrons Thomas *et al.* suggested about a decade ago the existence of current-echoes in disordered metals [1]. Experimentally, the generation of such current-echos is highly non-trivial, as it requires voltage pulses on time scales shorter than the dephasing time, which is typically of the order or less than nano seconds. Indeed, an experimental verification of their existence is so far lacking. Therefore, having in mind the feasibility to optically generate ultra-short current pulses in semiconductors on a femto- to picosecond time scale (by use of coherent control techniques, see e.g. [2, 3, 4]) numerical analysis of the echo scenario was extended to semiconductors [5, 6]. However, we do not know of any experiments probing the echo in semiconductors. Also, in later works the influence of electron-electron interactions on the echo has been studied [7]. The features characterizing the echo phenomenon in metals and semiconductors as found by numerical studies can be summarized as follows (the interested reader can find more details in [1, 5, 6]):

1. *Current-echo in metals:* A disordered conductor exposed to a short voltage pulse at time $t = 0$ generates a current pulse, which decays within the elastic scattering time. For a system without Coulomb interaction and in the absence of other dephasing mechanism, a second voltage pulse at $t = t_0$ leads to the reconstruction of a macroscopic current burst at $t = 2t_0$, opposite in sign to the original current pulses. Inclusion of Coulomb interactions (exponentially) reduces the amplitude of the echo.
2. *Current-echo in semiconductors:* In a two-band semiconductor with correlated disorder (for a definition of correlated disorder see section 1.5 “*Current-Echo in Semiconductors*” below) and different masses of the charge carriers in conduction and valence band the application of coherent control schemes at time $t = 0$ optically generates short inter- and intraband current pulses decaying due to elastic scattering from disorder. A second pulse applied at time $t = t_0$ again leads to the appearance of a current-echo. Three main findings characterize the current-echo in semiconductors:
 - (a) The echo only appears in the model with correlated disorder.
 - (b) In the case of correlated disorder, the echo even shows up for a simplified excitation sequence, where only the first light-pulse creates inter- and intraband current pulses whereas the second pulse is a simple full-gap pulse causing inversion of the band charges. That is, only one current pulse — which has to be the first pulse — is necessary to generate the echo. Reversing the order of pulses does not obtain an echo.
 - (c) Most surprisingly, for different masses, $m_c < m_v$, of the charge carriers in the conduction and valence band, respectively, the intraband current-echo splits into two separate contributions: a conduction band response at the advanced time $t_c = \left(1 + \frac{m_c}{m_v}\right) t_0$ and a delayed response in the valence band at the retarded time $t_v = \left(1 + \frac{m_v}{m_c}\right) t_0$. The interband echo, on the other hand, always appears at $t = 2t_0$

Interestingly to us, a simple picture explaining the physics behind the current echo so far has been missing. Therefore we found it challenging to look for a microscopic mechanism explaining the diversity of features characterizing the current-echo in metals and semiconductors. An explanation based on the constructive interference of time-reversed paths is given in the following sections.

Outline: The outline of the rest of the chapter is the following: In order to make this text self-contained we derive in the first section the basic equations (two particle- or “Cooperon”-equation) lying at the heart of our explanation of the current-echo. These equations can be found in textbooks (e.g. [16]) but we here use a different derivation within the Keldysh σ -model. Rather technical in nature, this section can be skipped as it does not give any new results.

In the second section we repeat [9] that in response to a pulsed electric field, the weak localization corrections to the conductivity (which can be described in terms of the two particle propagator “Cooperon”) give rise to a negative current, decaying algebraically in time (if perfect phase coherence is assumed). This observation leads us to study in the third section the fate of the Cooperon in the presence of an external electric field, or, more specifically, when a second voltage pulse is applied. Indeed, we show that due to breaking of time-reversal symmetry by the second pulse, the Cooperon becomes suppressed — except for a short moment $T = 2t_0$ when time reversal symmetry is re-established. In this way we can understand the current-echo as a sudden re-appearance of the weak localization contribution to the current. In the fourth section we re-derive the results of the third section from a semiclassical approach, and, finally, in the fifth section employ the semiclassical approach to explain the current-echo in semiconductors.

1.1 Keldysh σ -model for systems with time-reversal invariance

Consider a d -dimensional weakly disordered metal described by the Lagrangian

$$L[\bar{\psi}\psi, \phi, \mathbf{A}] = \int d^d \mathbf{x} \bar{\psi}(\mathbf{x}, t) \left\{ i\partial_t + e\phi(\mathbf{x}, t) + \mu + \frac{1}{2m} [\partial - ie\mathbf{A}(\mathbf{x}, t)]^2 - U_{\text{dis}}(\mathbf{x}) \right\} \psi(\mathbf{x}, t), \quad (1.1)$$

where $\bar{\psi}$, ψ are the electron and hole fields, U_{dis} is a white noise disorder potential, described by its second moment,

$$\langle U_{\text{dis}}(\mathbf{x}) U_{\text{dis}}(\mathbf{x}') \rangle_{\text{dis}} = \frac{1}{2\pi\nu\tau} \delta(\mathbf{x} - \mathbf{x}'), \quad (1.2)$$

and ϕ and \mathbf{A} denote some scalar and vector potentials. Within the Keldysh approach the time evolution of the system is considered along the Keldysh contour \mathcal{C} going from $t = -\infty$ to $t = +\infty$ and then back to $-\infty$ (see Fig. 1.1). At the initial time, $t = -\infty$, the system is supposed to be in thermal equilibrium, with all external fields and the disorder potential turned off. The partition function describes the evolution along the contour \mathcal{C} and can be written in terms of the functional integral over the fermionic fields $\bar{\psi}$, ψ as a function of the external fields ϕ and \mathbf{A} ,

$$\mathcal{Z}[\phi, \mathbf{A}] = \int \mathcal{D}[\bar{\psi}, \psi] \langle \exp \{ iS[\bar{\psi}\psi, \phi, \mathbf{A}] \} \rangle_{\text{dis}}, \quad (1.3)$$

with the action given by $S[\bar{\psi}\psi, \phi, \mathbf{A}] = \int_{\mathcal{C}} dt L$. If all external fields are classical — that is identical on the forward and backward branch of the time contour — then the Keldysh contour brings the system back to the initial state. In this case the partition function is automatically normalized to unity, i.e. $\mathcal{Z} = 1$. To get non-trivial results one has to introduce external fields with quantum components. Expectation values of operators are then given by functional derivatives of the free energy with respect to the quantum component of the field coupling to the operator.

Following the strategy outlined in [10] we resemble the fields living on the forward and backward component of the time contour in a single vector (matrix)

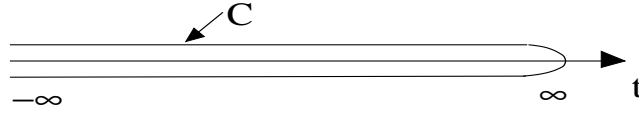


Figure 1.1: Schematic representation of the time contour C used in Keldysh formalism.

$$\bar{\psi} = (\bar{\psi}_1 \quad \bar{\psi}_2)_K, \quad \psi = \begin{pmatrix} \psi_1 \\ \psi_2 \end{pmatrix}_K, \quad \phi = \begin{pmatrix} \phi_1 & \\ & \phi_2 \end{pmatrix}_K, \quad \mathbf{A} = \begin{pmatrix} \mathbf{A}_1 & \\ & \mathbf{A}_2 \end{pmatrix}_K. \quad (1.4)$$

Here 1, 2 labels the Keldysh components for the fields residing on the forward/backward branch of the time contour. In this new fields the action reads $S = \int_{-\infty}^{\infty} dt L$, where

$$L = \int d^d \mathbf{x} \bar{\psi} \left\{ i\partial_t + e\phi + \mu + \frac{1}{2m} [\partial - ie\mathbf{A}]^2 - U_{\text{dis}} \right\} \sigma_3^K \psi. \quad (1.5)$$

Employing that the partition function is normalized for vanishing external quantum fields (notice that U_{dis} is a classical field), expectation values of operators can as well be written as functional derivatives of the partition function \mathcal{Z} itself instead of the free energy $\ln \mathcal{Z}$. The average of \mathcal{Z} over disorder configurations is readily done. It generates a four-fermion term local in space but non-local in time,

$$S_{\text{int}}[\bar{\psi}\psi] = \frac{i}{4\pi\nu\tau} \int_{-\infty}^{\infty} dt \int_{-\infty}^{\infty} dt' \int d^d \mathbf{x} \bar{\psi}(\mathbf{x}, t) \sigma_3^K \psi(\mathbf{x}, t) \bar{\psi}(\mathbf{x}, t') \sigma_3^K \psi(\mathbf{x}, t'), \quad (1.6)$$

reflecting the fact that the impurity scattering considered here is elastic. Separation into slow momenta $|\mathbf{q}| \ll p_F$ and fast momenta $|\mathbf{p}|, |\mathbf{p}'| \sim p_F$ we neglect the contribution from the density channel as it only constitutes renormalization of the chemical potential, μ , and, thus, only retain the Cooper and the exchange channels,

$$S_{\text{int}}[\bar{\psi}\psi] \approx \frac{i}{4\pi\nu\tau} \int_{-\infty}^{\infty} dt \int_{-\infty}^{\infty} dt' \sum_{q \ll p, p' \sim p_F} \left\{ \bar{\psi}_{\mathbf{p}+\mathbf{q}}(t) \sigma_3^K \psi_{\mathbf{p}'}(t) \bar{\psi}_{\mathbf{p}'+\mathbf{q}}(t') \sigma_3^K \psi_{\mathbf{p}}(t') + \bar{\psi}_{\mathbf{p}+\mathbf{q}}(t) \sigma_3^K \psi_{\mathbf{p}'+\mathbf{q}}(t) \bar{\psi}_{-\mathbf{p}}(t') \sigma_3^K \psi_{-\mathbf{p}'}(t') \right\}. \quad (1.7)$$

As pointed out e.g. in [11] among the four Keldysh sub-blocks of the Green's function only three are linearly independent. To make use of this property it is convenient to pass to a rotated basis in Keldysh space, where

$$\hat{\mathcal{G}}_{t,\mathbf{x}}^{-1} = \left\{ i\partial_t + \phi^i \gamma^i + \mu + \frac{1}{2m} [\partial - ie\mathbf{A}^i \gamma^i]^2 \right\}. \quad (1.8)$$

Here $\phi^i \gamma^i = \phi^{\text{cl}} \gamma^{\text{cl}} + \phi^{\text{q}} \gamma^{\text{q}}$ (as common we use $\gamma^1 = 1^K$ and $\gamma^2 = \sigma_1^K$) and correspondingly for \mathbf{A} . Notice though that Eq. (1.8) is a somewhat symbolical form as a more careful representation takes care of the fact that \mathcal{G} has off-diagonal structure in K-space, even in the case of vanishing external (quantum) fields ϕ^{q} . This results from the fact, that the forward and backward segments of the time-contour are connected at $t = \infty$. (For a discussion of this point see e.g. [12]). In this new basis, the quartic part of the action reads

$$S_{\text{int}}[\bar{\psi}\psi] = \frac{i}{4\pi\nu\tau} \int_{-\infty}^{\infty} dt \int_{-\infty}^{\infty} dt' \sum_{q \ll p, p' \sim p_F} \left\{ \bar{\psi}'_{\mathbf{p}+\mathbf{q}}(t) \psi'_{\mathbf{p}'}(t) \bar{\psi}'_{\mathbf{p}'+\mathbf{q}}(t') \psi'_{\mathbf{p}}(t') + \bar{\psi}'_{\mathbf{p}+\mathbf{q}}(t) \psi'_{\mathbf{p}'+\mathbf{q}}(t) \bar{\psi}'_{-\mathbf{p}}(t') \psi'_{-\mathbf{p}'}(t') \right\}. \quad (1.9)$$

In order to decouple in the two relevant channels (Cooper and exchange) simultaneously we introduce the two component spinors

$$\Psi(\mathbf{q}, t) = \frac{1}{\sqrt{2}} \begin{pmatrix} \psi(\mathbf{q}, t) \\ \bar{\psi}^\tau(\mathbf{q}, -t) \end{pmatrix}_T, \quad \bar{\Psi}(\mathbf{q}, t) = \frac{1}{\sqrt{2}} (\bar{\psi}(\mathbf{q}, t) \quad -\psi^t(\mathbf{q}, -t))_T. \quad (1.10)$$

Here τ refers to the transpose in K-space and T stands for time-reversal space. That is, we enlarge the internal field space from K to $K \otimes T$. With these definitions we rewrite the quadratic part of the action as

$$S = \int dt \int d^d \mathbf{x} \bar{\Psi}(t, \mathbf{x}) \begin{pmatrix} \hat{\mathcal{G}}_{t, \mathbf{x}}^{-1} \\ [\hat{\mathcal{G}}_{t, \mathbf{x}}^{-1}]^t \end{pmatrix}_T \Psi(t, \mathbf{x}). \quad (1.11)$$

The doubling of field space allows for summarizing the slow part of the four-fermion term in the form

$$S_{\text{int}} = \frac{i}{2\pi\nu\tau} \int dt dt' \sum_{q \ll p, p'} \bar{\Psi}_{\mathbf{p}+\mathbf{q}}(t) \Psi_{\mathbf{p}'}(t) \bar{\Psi}_{\mathbf{p}'+\mathbf{q}}(t') \Psi_{\mathbf{p}}(t'). \quad (1.12)$$

Notice that the presence of a Keldysh component in the propagator \mathcal{G} explicitly breaks time-reversal invariance. Furthermore external fields become matrices in T-space of the form

$$\mathbf{A}^i(t) = \begin{pmatrix} \mathbf{A}^i(t) & \\ & -\mathbf{A}^i(-t) \end{pmatrix}_T \quad \text{and} \quad \phi^i(t) = \begin{pmatrix} \phi^i(t) & \\ & \phi^i(-t) \end{pmatrix}_T. \quad (1.13)$$

Here the “ $-$ ” sign in the second component of the vector potential emerges due to partial integration. Finally, we mention that due to the field-doubling the electron-fields $\bar{\Psi}$ and Ψ are not independent variables anymore, but related by the symmetry-transformation

$$\bar{\Psi}_{\mathbf{q}}(t) = -\Psi_{\mathbf{q}}^\tau(-t) i\sigma_2^T. \quad (1.14)$$

We now follow the usual lines [10] to formulate an effective field-theory grasping the relevant physics. These steps consist in (a) introduction of new degrees of freedom (Hubbard-Stratonovich (HS) transformation), (b) integration over fermion fields, (c) mean-field approximation for HS-field, (d) gradient expansion around mean-field, and lead to the effective action

$$iS_\sigma[Q] = -\frac{\pi\nu}{4} \int dt dt' \int d^d \mathbf{x} \text{tr}_{K \otimes T} \left\{ 4\partial_t Q - 4i\phi^i \gamma^i Q - D (\partial Q - e [\mathbf{A}^i \gamma^i, Q])^2 \right\}, \quad (1.15)$$

where the HS-field $Q_{tt'}(\mathbf{x})$ is a matrix in space-time as well as in the product-space $K \otimes T$ -space; it is local in the coordinate-space (which is a hallmark of the δ -correlated disorder-potential considered here) and non-local in time. The symmetry relation of the electron-fields, Eq.(2.12), translates to the property

$$Q_{tt'}^\tau(\mathbf{q}) = \sigma_2^T Q_{-t', -t}(\mathbf{q}) \sigma_2^T, \quad (1.16)$$

where τ refers to transposition in $K \otimes T$ -space. Q describes fluctuations around the saddle point Λ , i.e. $Q = \Lambda e^W$, where

$$\Lambda = \begin{pmatrix} \lambda_{t-t'} & \\ & \lambda_{t-t'}^\tau \end{pmatrix}_T, \quad \text{and} \quad \lambda_{t-t'} = \begin{pmatrix} \delta_{t-t'-0} & 2F_{t-t'} \\ & -\delta_{t-t'+0} \end{pmatrix}_K. \quad (1.17)$$

$F_{t-t'} = -iT / \sinh[\pi T(t-t')]$ is the Fourier-transformed Fermi-distribution function and for a definition of $\delta_{t \pm 0}$ see e.g. [10]. Notice that the above representation of Q requires that the rotations generated

by W act on the saddle point fixed-point free, i.e. $[\Lambda, W] = 0$. Notice also that Λ fulfills the symmetry constraint Eq. (2.18). At this point it is convenient to introduce the self-inverse matrix (i.e. $\mathcal{F}^2 = 1$)

$$\mathcal{F}_{t-t'} \equiv \begin{pmatrix} f_{t-t'} & \\ & f_{t-t'}^t \end{pmatrix}_{\mathbf{T}}, \quad \text{where} \quad f_{t-t'} \equiv \begin{pmatrix} \delta_{t-t'-0} & F_{t-t'} \\ & -\delta_{t-t'+0} \end{pmatrix}_{\mathbf{K}}, \quad (1.18)$$

which allows the decompositions $\Lambda = \mathcal{F}\sigma_3^{\mathbf{K}}\mathcal{F}$ and $\mathcal{W} \equiv \mathcal{F}W\mathcal{F}$. Employing that $[\Lambda, W] = 0$ is equivalent to $[\sigma_3^{\mathbf{K}}, \mathcal{W}] = 0$, we parametrize the generators of the rotations by

$$\mathcal{W}_{\mathbf{C}} = \begin{pmatrix} & \bar{C} \\ C & \end{pmatrix}_{\mathbf{K}} \quad \text{and} \quad \mathcal{W}_{\mathbf{D}} = \begin{pmatrix} & \bar{D} \\ D & \end{pmatrix}_{\mathbf{K}}, \quad (1.19)$$

where we separated into a part diagonal in T-space (Diffuson) and a part off-diagonal in T-space (Cooperon), i.e.

$$\bar{C} = \begin{pmatrix} \bar{C}^{+-} & \\ & \bar{C}^{-+} \end{pmatrix}_{\mathbf{T}} \quad C = \begin{pmatrix} C^{+-} & \\ & C^{-+} \end{pmatrix}_{\mathbf{T}} \quad \bar{D} = \begin{pmatrix} \bar{D}^{++} & \\ & \bar{D}^{--} \end{pmatrix}_{\mathbf{T}} \quad D = \begin{pmatrix} D^{++} & \\ & D^{--} \end{pmatrix}_{\mathbf{T}}. \quad (1.20)$$

From an expansion to second order in the generators we get

$$iS_{\sigma}^2[\bar{C}C] = -\frac{\pi\nu}{2} \int dt dt' \int d^d \mathbf{x} \text{tr}_{\mathbf{T}} \left\{ (\partial_t + ie\phi(\mathbf{x}, t)) [\bar{C}_{tt'}(\mathbf{x}) C_{t't}(\mathbf{x}) - C_{tt'}(\mathbf{x}) \bar{C}_{t't}(\mathbf{x})] + D\partial^2 \bar{C}_{tt'}(\mathbf{x}) C_{t't}(\mathbf{x}) \right\}, \quad (1.21)$$

and correspondingly for the Diffuson. For convenience we only took into account a classical electrical potential ϕ , and dropped out the vector potential \mathbf{A} . We later reinstall the vector potential by gauge arguments. Next, we perform the trace over T-space and use that the symmetry relation for the matrix components are given by $C_{tt'}^{+-} = -\bar{C}_{-t-t'}^{+-}$ and $C_{tt'}^{++} = -\bar{C}_{-t-t'}^{++}$ for the off-diagonal components and $D_{tt'}^{++} = \bar{D}_{-t-t'}^{++}$ and $D_{tt'}^{--} = \bar{D}_{-t-t'}^{--}$ for the diagonal ones and get

$$iS_{\sigma}^2[\bar{C}C] = -\frac{\pi\nu}{2} \int dt dt' \int d^d \mathbf{x} \text{tr}_{\mathbf{T}} \left\{ (\partial_t - \partial_{t'} + ie[\phi(\mathbf{x}, t) - \phi(\mathbf{x}, t')]) \bar{C}_{t,-t'}^{+-}(\mathbf{x}) C_{-t',t}^{+-}(\mathbf{x}) \right\} \quad (1.22)$$

for the Cooperon and

$$iS_{\sigma}^2[\bar{D}D] = -\frac{\pi\nu}{2} \int dt dt' \int d^d \mathbf{x} \text{tr}_{\mathbf{T}} \left\{ (\partial_t + \partial_{t'} + ie[\phi(\mathbf{x}, t) - \phi(\mathbf{x}, t')]) \bar{D}_{tt'}^{++}(\mathbf{x}) D_{t't}^{--}(\mathbf{x}) \right\} \quad (1.23)$$

for the Diffuson. That is the $\langle \bar{C}^{+-} C^{-+} \rangle$ and $\langle \bar{D}^{++} D^{++} \rangle$ correlations solve the differential equations

$$\begin{aligned} \left\{ \partial_{t_1^+} - \partial_{t_1^-} - D\partial^2 - ie[\phi(t_1^+) - \phi(t_1^-)] \right\} \langle \bar{C}_{t_1^+ t_1^-}^{+-}(\mathbf{x}) C_{t_2^- t_2^+}^{-+}(\mathbf{x}') \rangle &= \frac{2}{\pi\nu} \delta(\mathbf{x} - \mathbf{x}') \delta(t_1^+ - t_2^+) \delta(t_1^- - t_2^-) \\ \left\{ \partial_{t_1^+} + \partial_{t_1^-} - D\partial^2 - ie[\phi(t_1^+) - \phi(t_1^-)] \right\} \langle \bar{D}_{t_1^+ t_1^-}^{++}(\mathbf{x}) D_{t_2^- t_2^+}^{--}(\mathbf{x}') \rangle &= \frac{2}{\pi\nu} \delta(\mathbf{x} - \mathbf{x}') \delta(t_1^+ - t_2^+) \delta(t_1^- - t_2^-). \end{aligned} \quad (1.24)$$

Finally, we introduce the center-of-mass and relative times, $T_{1/2} \equiv \frac{t_{1/2}^+ + t_{1/2}^-}{2}$ and $\eta_{1/2} \equiv t_{1/2}^+ - t_{1/2}^-$ and define the Diffuson and Cooperon respectively as

$$\langle \bar{C}_{t_1^+, -t_1^-}^{+-}(\mathbf{x}) C_{-t_2^+, t_2^-}^{-+}(\mathbf{x}') \rangle \equiv \frac{2\tau}{\pi\nu} C_{\eta_1 \eta_2}^{T_1}(\mathbf{x}, \mathbf{x}') \delta(T_1 - T_2) \quad (1.26)$$

$$\langle \bar{D}_{t_1^+, t_1^-}^{++}(\mathbf{x}) D_{t_2^+, t_2^-}^{++}(\mathbf{x}') \rangle \equiv \frac{2\tau}{\pi\nu} D_{T_1 T_2}^{\eta_1}(\mathbf{x}, \mathbf{x}') \delta(\eta_1 - \eta_2). \quad (1.27)$$

This leads us to the well-known differential equations for the Cooperon and Diffuson,

$$\left\{ 2\partial_{\eta_1} - D \left(\partial + ie \left[\mathbf{A}(T_1 + \frac{\eta_1}{2}) + \mathbf{A}(T_1 - \frac{\eta_1}{2}) \right] \right)^2 - ie \left[\phi \left(T + \frac{\eta_1}{2} \right) - \phi \left(T - \frac{\eta_1}{2} \right) \right] \right\} C_{\eta_1 \eta_2}^T(\mathbf{x}, \mathbf{x}') = \frac{2}{\tau} \delta(\eta_1 - \eta_2) \delta(\mathbf{x} - \mathbf{x}') \quad (1.28)$$

$$\left\{ \partial_{T_1} - D \left(\partial + ie \left[\mathbf{A}(T_1 + \frac{\eta_1}{2}) - \mathbf{A}(T_1 - \frac{\eta_1}{2}) \right] \right)^2 - ie \left[\phi \left(T_1 + \frac{\eta_1}{2} \right) - \phi \left(T_1 - \frac{\eta_1}{2} \right) \right] \right\} D_{T_1 T_2}^{\eta_1}(\mathbf{x}, \mathbf{x}') = \frac{1}{\tau} \delta(T_1 - T_2) \delta(\mathbf{x} - \mathbf{x}') \quad (1.29)$$

Here we re-introduced the (classical) vector potential \mathbf{A} by demanding invariance of the equations under the gauge transformation $\mathbf{A} \mapsto \mathbf{A} + \partial\chi$, $\phi \mapsto \phi + \partial_\eta\chi$ ($\phi \mapsto \phi + \partial_T\chi$) and

$$C_{\eta\eta'}^T(\mathbf{x}, \mathbf{x}') \mapsto e^{-ie[\chi(\mathbf{x}, T+\eta/2) + \chi(\mathbf{x}, T-\eta/2)]} C_{\eta\eta'}^T(\mathbf{x}, \mathbf{x}') e^{ie[\chi(\mathbf{x}', T+\eta'/2) + \chi(\mathbf{x}', T-\eta'/2)]}$$

$$D_{TT'}^\eta(\mathbf{x}, \mathbf{x}') \mapsto e^{-ie[\chi(\mathbf{x}, T+\eta/2) - \chi(\mathbf{x}, T-\eta/2)]} D_{TT'}^\eta(\mathbf{x}, \mathbf{x}') e^{ie[\chi(\mathbf{x}', T'+\eta/2) - \chi(\mathbf{x}', T'-\eta/2)]}.$$

The differential equation for the Cooperon, Eq. (1.28), are the starting point for our analysis of the echo scenario.

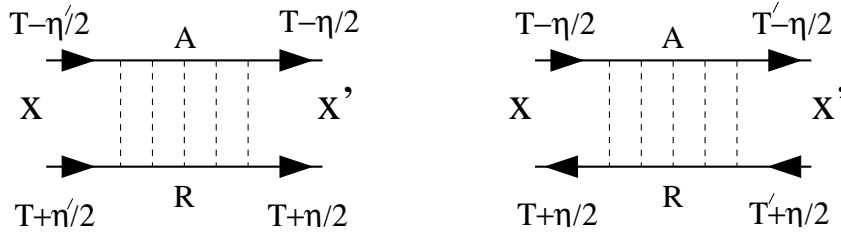


Figure 1.2: Cooperon (left) and Diffuson (right) in real-time representation. Dashed lines represent disorder scattering and R/A stands for retarded and advanced Green functions (i.e. for electron and hole lines). Notice that the propagation of the electron is denoted by an arrow, whereas the hole passes the line in opposite direction the arrow points to.

1.2 Current in linear response to a pulsed electrical field

Let us now turn to the response of a metal exposed to a voltage pulse. The electric current is calculated from the functional derivative of the free energy — or equivalently the partition function — with respect to the quantum component of the vector potential. Therefore the current in linear response to a homogeneous (classical) external field, $\mathbf{E}^{\text{cl}} = -\partial_t \mathbf{A}^{\text{cl}}$, is given by

$$\langle \mathbf{j}(t) \rangle = \int dt' \frac{\delta^2 \mathcal{Z}}{\delta \mathbf{A}^{\text{q}}(t) \delta \mathbf{A}^{\text{cl}}(t')} \mathbf{A}^{\text{cl}}(t').$$

Having done the two-fold derivative of the partition function Eq. (2.22) we expand the resulting expression in fluctuation matrices W around the saddle point value Λ . Each power W^{2k} corresponds to quantum corrections of the order $(k_F l)^{-k}$ to the classical value of the current, obtained from inserting

the saddle point, Λ . Up to second order in the fluctuation matrices one finds $\langle \mathbf{j}(t) \rangle = \mathbf{j}_0(t) + \Delta \mathbf{j}_{\text{WL}}(t)$, where

$$\mathbf{j}_0(t) = \int dt' \sigma^{\text{Drude}}(t, t') \mathbf{E}(t') \quad (1.30)$$

is the “classical” current proportional to the Drude conductivity, $\sigma^{\text{Drude}} = e^2 \nu D$, and the quantum corrections of order $1/(k_F l)$,

$$\Delta \mathbf{j}_{\text{WL}}(t) = -\frac{4\tau}{\pi \nu} \int_{\tau}^{\infty} d\eta C_{\eta, -\eta}^{t-\eta/2}(\mathbf{x}, \mathbf{x}) \mathbf{E}(t - \eta), \quad (1.31)$$

are proportional to the weak localization corrections to the conductivity. These leading order quantum corrections result from the constructive interference of an electron and a hole traveling along a closed loop in opposite direction, resulting in an enhanced return probability, i.e. in a negative correction to the classical conductivity (“coherent backscattering”, see Fig. 1.3).

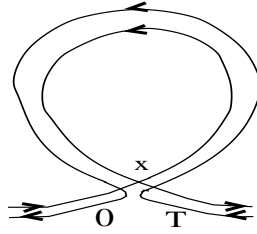


Figure 1.3: Interfering paths giving rise to weak localization contribution to the conductivity: Electron and hole meet at some space point \mathbf{x} at a time $t = 0$. They perform a collective propagation along a closed loop in opposite directions (electron follows the arrow, whereas the hole propagates in opposite direction the arrow points to, see Fig. 1.2), return to the space point \mathbf{x} at time $t = T$, where they split up again to follow their individual diffusive paths. In a time-reversal symmetric situation the phases acquired by the electron and the hole passing along the closed loop in opposite direction coincide and cancel each other. This leads to an enhanced return probability for the charge carriers, i.e. negative corrections to the conductivity.

It is interesting to remark that in (linear) response to a voltage pulse, $\mathbf{E}(t) = \mathbf{E}_0 \delta(t/\tau)$, the classical current decays exponentially on a scale given by the elastic scattering time τ , whereas the negative current wears off exponentially on a scale given by the dephasing time $\tau_\phi \gg \tau$ (and in an ideal situation of perfect coherence only decays algebraically), i.e.

$$\mathbf{j}_0(t) = \sigma \mathbf{E}_0 e^{-t/\tau} \quad (1.32)$$

$$\Delta \mathbf{j}_{\text{WL}}(t) = -\frac{2\sigma \tau \mathbf{E}_0}{\pi \nu} \frac{e^{-t/\tau_\phi}}{(4\pi D t)^{d/2}}. \quad (1.33)$$

This observation lies at the heart of our explanation of the current-echo, given in the next section. Let us, though, at this point repeat, that time reversal symmetry is essential for the phase cancellation of mutually time-reversed paths; breaking of the time reversal symmetry (e.g. by an external magnetic field) destroys this phase cancellation and leads to a suppression of coherent backscattering processes, that is, of the negative corrections to the conductivity.

1.3 Cooperon in a pulsed electric field

We are now going to study the echo scenario, i.e. a situation where after a time $t = t_0$ a second voltage pulse is applied to the metal. As we discussed in the last section, the (linear) response to a

single voltage pulse consists in two contributions: An exponentially decaying current pulse, which is the “classical” response, and negative quantum corrections — the “weak localization” contribution. We also pointed out that if all dephasing mechanisms are ignored (i.e. on time scales $t < \tau_\phi$) the latter decay algebraically. A first guess, assuming that the metal’s response to the echo scenario with two such contributions (consisting of the classical and the leading order quantum response), one at a time $t = 0$ and a second at $t = t_0$, is oversimplified, as the quantum corrections rely on the cancellation of the electron’s and the hole’s phases acquired during their propagation along a closed loop. This phase cancellation is very sensitive to external perturbations. Therefore, in order to find the right answer, we have to study the influence of the second voltage pulse on the collective propagation of the electron-hole pair constituting the Cooperon and giving rise to the negative current in response to the first voltage pulse. Once we found these, we add the classical response to the first voltage pulse as well as the classical and the quantum contributions from the second voltage pulse. The sum of these terms describes the leading order (i.e. $\sim 1/k_F l$) response to the echo scenario.

Considering time scales t_0 on which its life-time is long (i.e. $\tau_\phi > t_0$) the dynamics of the two-particle propagator (Cooperon) in the presence of external fields is described by Eq. (1.28). Specializing on the situation where the external field comes in form of a voltage pulse, the Cooperon equation takes the form

$$\left\{ 2 \frac{\partial}{\partial \eta} - D \partial^2 - ie\tau \mathbf{E}_0 \mathbf{x} \left[\delta \left(T - \frac{\eta}{2} - t_0 \right) - \delta \left(T + \frac{\eta}{2} - t_0 \right) \right] \right\} C_{\eta, \eta'}^T(\mathbf{x}, \mathbf{x}') = \frac{1}{\tau} \delta(\eta - \eta') \delta(\mathbf{x} - \mathbf{x}'). \quad (1.34)$$

Eq. (1.34) tells us that the second voltage pulse enters the Cooperon dynamics twice: Firstly, it acts on the electron at the time t_0 and, secondly, it acts on the “time-reversed” hole at the time $T - t_0$. Here T is the total time needed by the electron-hole pair to run along the closed path. A cartoon of the situation is depicted in Fig. 1.4. We thus notice, that in a generic situation the second voltage pulse breaks time-reversal, and only if the electron-hole pair spends a time $T = 2t_0$ to pass along the loop, this symmetry is re-established (see also Fig. 1.4). Mathematically, this observation is seen in the fact that, in the time-reversal symmetric situation (i.e. at $T = 2t_0$), the two contributions from the voltage pulse, entering Eq. (1.34) cancel; i.e. the external perturbation disappears from the differential equation. We now quantify these qualitative observations by explicitly solving the differential equation (1.34).



Figure 1.4: Constructive interference between electron traveling along closed path and hole transversing the same path in the opposite direction. A symmetric, i.e. time-reversal invariant situation arises only if $T = 2t_0$.

The equation of motion for the Cooperon in the presence of an external field, Eq. (1.28), is equivalent to the imaginary-time η Schrödinger equation for a particle of mass $1/2D$ in a scalar potential $\phi_T(\mathbf{x}, \eta) = \phi(\mathbf{x}, T - \frac{\eta}{2}) - \phi(\mathbf{x}, T + \frac{\eta}{2})$. Its solution can be written in the form of a path-integral [13]

$$C_{\eta, \eta'}^T(\mathbf{x}, \mathbf{x}') = \frac{1}{\tau} \int_{\mathbf{x}(\eta')=\mathbf{x}'}^{\mathbf{x}(\eta)=\mathbf{x}} \mathcal{D}[\mathbf{x}(t')] \exp \left\{ - \int_{\eta'}^{\eta} dt' \frac{1}{4D} \dot{\mathbf{x}}^2(t') + ie\phi_T(\mathbf{x}(t'), t') \right\}. \quad (1.35)$$

Therefore, in the situation, where the external potential is a pulsed electrical field the Cooperon has the Feynman path-integral representation

$$C_{T,-T}^{T/2}(\mathbf{x}, \mathbf{x}) = \frac{1}{\tau} \int_{\mathbf{x}(-T)=\mathbf{x}}^{\mathbf{x}(T)=\mathbf{x}} \mathcal{D}[\mathbf{x}(t')] \exp \left\{ - \int_{-T}^T dt' \frac{1}{4D} \dot{\mathbf{x}}^2(t') + ie\tau \mathbf{E}_0 \mathbf{x}(t') [\delta(T-2t_0-t') - \delta(T-2t_0+t')] \right\}. \quad (1.36)$$

Periodic in time we change to a Fourier-representation of the paths, $\mathbf{x}(t') = \frac{1}{\sqrt{2T}} \sum_n \mathbf{x}_n e^{-i\omega_n t'}$, where $\omega_n = \frac{\pi n}{T}$, with $n \in \mathbb{Z}$, and perform the functional-integral over the paths, resulting in

$$C_{T,-T}^{T/2}(\mathbf{x}, \mathbf{x}) = \mathcal{N} \exp \left\{ - \frac{4e^2 D \tau^2 \mathbf{E}_0^2}{T} \sum_{n \neq 0} \frac{\sin^2 [\omega_n (T-2t_0)]}{\omega_n^2} \right\}, \quad (1.37)$$

with the normalization constant $\mathcal{N} = \frac{1}{2\tau} \frac{1}{(4\pi DT)^{d/2}}$. Here we excluded the constant mode from the summation, as it does not contribute to the path-integral. Employing the identities

$$\sum_{k=1}^{\infty} \frac{1}{k^2} = \frac{\pi^2}{6} \quad \text{and} \quad \sum_{k=1}^{\infty} \frac{\cos(kx)}{k^2} = \frac{\pi^2}{6} - \frac{\pi|x|}{2} + \frac{|x|^2}{4}, \quad (1.38)$$

the summation over Matsubara-frequencies is calculated as follows

$$\sum_{n \neq 0} \frac{\sin^2 [\omega_n (T-2t_0)]}{\omega_n^2} = \sum_{n=1}^{\infty} \frac{1 - \cos [2\omega_n (T-2t_0)]}{\omega_n^2} = T|T-2t_0| - |T-2t_0|^2. \quad (1.39)$$

Concluding we find that

$$C_{T,-T}^{T/2}(\mathbf{x}, \mathbf{x}) = \frac{1}{2\tau} \frac{1}{(4\pi DT)^{d/2}} \exp \left\{ - \frac{4e^2 D \tau^2 \mathbf{E}_0^2}{T} (T|T-2t_0| - |T-2t_0|^2) \right\}, \quad (1.40)$$

and henceforth obtain for the current in response to a sequence of two voltage pulses $\langle \mathbf{j}(T) \rangle = \mathbf{j}_0(T) + \Delta \mathbf{j}_{\text{WL}}(T)$, where

$$\mathbf{j}_0(T) = \sigma \mathbf{E}_0 (e^{-T/\tau} + e^{-(T-t_0)/\tau} \Theta(T-t_0)), \quad (1.41)$$

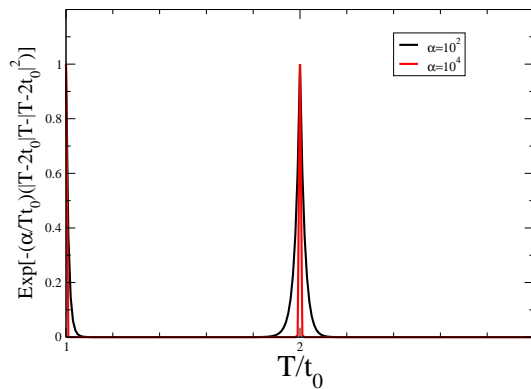


Figure 1.5: Shape of the einhuellende function $e^{-\frac{\alpha}{T t_0} (T|T-2t_0| - |T-2t_0|^2)}$ which gives the spatial profile of the echo for different values of $\alpha = e^2 \mathbf{E}_0^2 \tau^2 D t_0 \hbar^{-2}$.

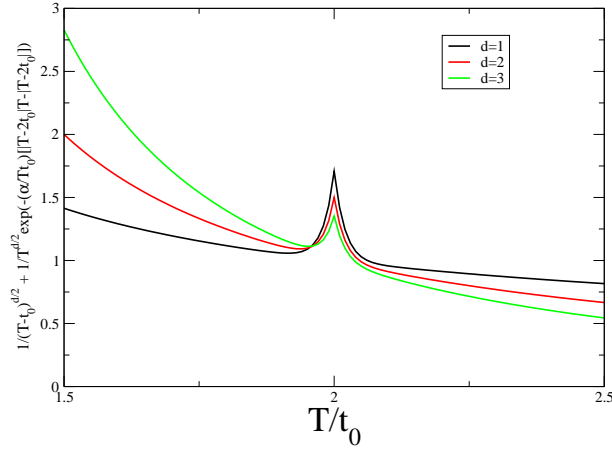


Figure 1.6: Echo contribution to the current in $d = 1, 2, 3$ for $\alpha = 100$.

and

$$\Delta j_{\text{WL}}(T) = -\frac{2\sigma\tau\mathbf{E}_0}{\pi\nu} \left(\frac{\Theta(t_0 - T)}{(4\pi DT)^{d/2}} + \frac{\Theta(T - t_0)}{(4\pi D(T - t_0))^{d/2}} + \frac{\Theta(T - t_0)}{(4\pi DT)^{d/2}} e^{-\frac{4e^2 D \tau^2 \mathbf{E}_0^2}{T} (T|T-2t_0| - |T-2t_0|^2)} \right). \quad (1.42)$$

The negative weak-localization contribution in response to the first voltage pulse is suppressed by the second voltage pulse (with a shape as shown in Fig. 1.5) as it destroys time-reversal invariance and, this way the phase cancelation between electron and hole-pair traveling along the closed loop in opposite directions. Only at a time $T = 2t_0$ time-reversal symmetry is re-established, causing a short re-appearance of the negative corrections. In an experimental situation (numerical simulation) this sudden re-appearance of the negative current is likely to be interpreted as a “current-echo”. Typical ranges of parameters are summarized in Table 1.1. The corresponding current profiles for $d = 1, 2, 3$ are shown in Fig. 1.6.

$e\mathbf{E}_0$	D	τ	t_0	\hbar	$\alpha = e^2 \mathbf{E}_0^2 \tau^2 D t_0 \hbar^{-2}$
1-100 eV/cm	1-100 cm/sec	10^{-12} sec	10^{-10} sec	10^{-15} eVsec	$10^2 - 10^6$

Table 1.1: Typical range of parameters entering the current-echo.

1.4 Semiclassical analysis of the current-echo

In this section we want to re-derive our main result, Eq. (1.42) of the last section, from a semiclassical approach. The semiclassical approach will then, in the next section, help us in the analysis of the echo scenario in semiconductors. With the aim of describing the current-echo from a semiclassical picture, we go back to the definition of the Cooperon as the disorder average of a pair of (retarded and advanced) electron Green’s functions [16], i.e.

$$C_{\mathbf{x}\mathbf{x}'}(t_1^+, t_2^+; t_1^-, t_2^-) = \frac{1}{(2\pi\nu\tau)^2} \langle \mathcal{G}^R(\mathbf{x}, \mathbf{x}'; t_1^+, t_2^+) \mathcal{G}^A(\mathbf{x}, \mathbf{x}'; t_1^-, t_2^-) \rangle. \quad (1.43)$$

A diagrammatic representation of the classical and the weak localization contributions to the current is given Fig. 1.7.



Figure 1.7: Classical (left), $\propto \langle G^R \rangle \langle G^A \rangle$, and weak localization (right), $\propto \langle G^R G^A \rangle$, contribution to the current. Again, the dashed lines represents scattering from static impurities and continuous lines the propagation of an electron (in direction of arrow) and a hole (opposite to direction indicated by the arrow). Wavy lines indicate the current operators.

As we are dealing with a non-interacting (i.e. single particle) theory we can represent the single particle Green's function in terms of a Feynman path-integral

$$\mathcal{G}^{R/A}(\mathbf{x}, t; \mathbf{x}', t') = \int_{\mathbf{x}(t)=\mathbf{x}}^{\mathbf{x}(t')=\mathbf{x}'} \mathcal{D}[\mathbf{x}(t)] e^{\pm i S(\mathbf{x}(t); t, t')}, \quad (1.44)$$

where the action

$$S(\mathbf{x}(t); t, t') = \int_t^{t'} dt \left\{ \frac{m}{2} \dot{\mathbf{x}}(t)^2 - V[\mathbf{x}(t)] - e\phi[\mathbf{x}(t)] \right\}, \quad (1.45)$$

describes the propagation of a particle in a disorder potential landscape V and an electrical potential ϕ from space-time point (\mathbf{x}, t) to space-time point (\mathbf{x}', t') along the path $\mathbf{x}(t)$. In the semiclassical limit ($\hbar \rightarrow 0$) we expect that the classical paths dominate the integral. Therefore we invoke the semiclassical approximation and substitute the sum over all paths in Eq. (1.44) by a sum over classical paths with quantum fluctuations superimposed, i.e.

$$\mathcal{G}^{R(A)}(\mathbf{x}, t; \mathbf{x}', t') = \sum_{\mathbf{x}_{cl}(t)} \mathcal{A}^{(*)}[\mathbf{x}_{cl}] e^{\pm i S(\mathbf{x}_{cl}(t); t, t')}, \quad (1.46)$$

where the sum runs over all classical paths \mathbf{x}_{cl} that start at \mathbf{x} and end at \mathbf{x}' . The prefactor $\mathcal{A}(\mathcal{A}^*)$ accounts for the inclusion of Gaussian quantum fluctuations around the classical path.

Turning to the Cooperon, defined in Eq. (1.43), we retain in the double sum only identical paths for the particle and the hole, as they give the dominant contribution. That is

$$C_{\mathbf{x}\mathbf{x}'}(t, t') = \sum_{\mathbf{x}_{cl}} \sum_{\mathbf{y}_{cl}} \mathcal{A}[\mathbf{x}_{cl}] \mathcal{A}^*[\mathbf{y}_{cl}] e^{i[S(\mathbf{x}_{cl}(t)) - S(\mathbf{y}_{cl}(t))]} \approx \sum_{\mathbf{x}_{cl}} \mathcal{A}[\mathbf{x}_{cl}] \mathcal{A}^*[\mathbf{x}_{cl}] e^{i[S(\mathbf{x}_{cl}(t)) - S(\mathbf{x}_{cl}(t'-t))]} \quad (1.47)$$

Notice, though, that particle and hole traverse these paths in opposite directions. In the absence of any external fields which might destroy the phase cancellation mechanism,

$$C_{\mathbf{x}-\mathbf{x}'}^0(t-t') \approx \sum_{\mathbf{x}_{cl}} \mathcal{A}[\mathbf{x}_{cl}] \mathcal{A}^*[\mathbf{x}_{cl}] = \frac{1}{(4\pi D|t-t'|)^{d/2}} e^{-|\mathbf{x}-\mathbf{x}'|^2/4D|t-t'|} \quad (1.48)$$

is just the probability for a particle to cover the distance $|\mathbf{x} - \mathbf{x}'|$ in the time $|t - t'|$ in a random-walk. Returning to the echo scenario, where a pulsed electrical field acts at a time t_0 after the electron-hole pair was created, we obtain for the Cooperon entering the weak localization contribution to the current

$$C_{\mathbf{x}\mathbf{x}}(0, T) \approx \int d^d \mathbf{x}_0 \int d^d \mathbf{x}_1 C_{\mathbf{x}\mathbf{x}_0}^0(t_0) e^{ie\tau \mathbf{E}_0 \mathbf{x}_0} C_{\mathbf{x}_0 \mathbf{x}_1}^0(T - 2t_0) e^{-ie\tau \mathbf{E}_0 \mathbf{x}_1} C_{\mathbf{x}_1 \mathbf{x}}^0(t_0), \quad (1.49)$$

where we introduced the notation $\mathbf{x}_0 = \mathbf{x}(t_0)$ and $\mathbf{x}_1 = \mathbf{x}(T - t_0)$. Notice that we employed that the weak localization corrections are given by contributions from closed paths, i.e. by paths with coinciding

start- and ending points. The diagrammatic representation of the current-echo is given in Fig. 1.8. Eq. (1.49) is easiest calculated in momentum representation,

$$C_{\mathbf{x}\mathbf{x}}(0, T) \approx \int d^d \mathbf{q} C_{\mathbf{q}}^0(t_0) C_{\mathbf{q}-\bar{\mathbf{q}}}^0(T-2t_0) C_{\mathbf{q}}^0(t_0) = \frac{1}{(4\pi DT)^{d/2}} e^{-D\bar{\mathbf{q}}^2|T-2t_0| \left(1 - \frac{|T-2t_0|}{T}\right)}, \quad (1.50)$$

where $\bar{\mathbf{q}} = 2e\tau\mathbf{E}_0$. Eq. (1.50) is in agreement with Eq. (1.42) and displays the exactness of the semiclassical approach for the above scenario. The semiclassical picture reviewed in this section is the starting point for our discussion of the echo scenario in semiconductors which we trace in the next section.

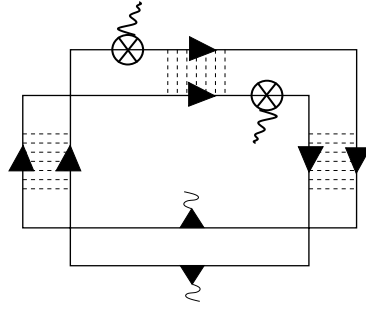


Figure 1.8: Diagrammatic representation of the echo. Diagrammatic code as in Fig. 1.7, the encircled crosses represent the electrical field pulse.

1.5 Current-echo in semiconductors

Following the lines given in [5, 6] we consider a disordered direct-gap semiconductor in the two-band approximation. This is described by the Hamiltonian

$$H = \int d^d \mathbf{x} \left\{ \sum_{\alpha=c,v} \bar{\psi}_{\alpha}(\mathbf{x}) \left[\frac{\mathbf{p}^2}{2m_{\alpha}} + \frac{1}{2} E_{\mathbf{g}}^{\alpha} + e\phi(\mathbf{x}) + V_{\alpha}(\mathbf{x}) \right] \psi_{\alpha}(\mathbf{x}) + e\phi(\mathbf{x}) [\bar{\psi}_v(\mathbf{x})\psi_c(\mathbf{x}) + \bar{\psi}_c(\mathbf{x})\psi_v(\mathbf{x})] \right\}, \quad (1.51)$$

where α is the band index with v, c referring to the valence- and conduction-band, respectively. Correspondingly, m_c and m_v denote the effective masses of the conduction- and valence-band charge carriers and V_{α} are the stochastic disorder potentials described by their second moments as in Eq. (1.2). $E_{\mathbf{g}}^{\alpha} = \pm E_{\mathbf{g}}$ is the band-gap energy. The electrical light field ϕ couples to the intra- and interband densities. Furthermore we assume that disorder is correlated in the sense that

$$\frac{V_c}{m_v} = \frac{V_v}{m_c}. \quad (1.52)$$

Schlichenmaier *et al.* point out that this assumption is not as restrictive as it might appear on first glance; it models, e.g., a disorder potential in a semiconductor heterostructure with effective dimensionality less than three, which is produced by local fluctuations in the confining potential [6].

We now explore the echo scenario, i.e. a sequence of two laser pulses, for a system described by the Hamiltonian Eq. (1.51): As in [6] we assume that the first pulse creates a large occupation of electrons (holes) in the conduction (valence) band. Furthermore, the first pulse, is designed in a refined scheme (so called “coherent control scheme”, see e.g. [2, 3, 4]) and generates short intra- and interband currents,

$$\mathbf{j}_{\text{intra}}^{\alpha} = \frac{e}{2m_{\alpha}} [\bar{\psi}_{\alpha} \partial \psi_{\alpha} - (\partial \bar{\psi}_{\alpha}) \psi_{\alpha}], \quad \alpha = \text{c}, \text{v} \quad (1.53)$$

$$\mathbf{j}_{\text{inter}} = \frac{e}{4} \frac{[m_{\text{c}} + m_{\text{v}}]}{m_{\text{c}} m_{\text{v}}} [\bar{\psi}_{\text{c}} \partial \psi_{\text{v}} - (\partial \bar{\psi}_{\text{c}}) \psi_{\text{v}}] + \text{c} \leftrightarrow \text{v}, \quad (1.54)$$

which — as in the metal-case studied above — due to the presence of disorder decay exponentially on time scales of the elastic scattering time. As we understood in the metal-case, weak localization corrections to the conductivity — suppressed by the second pulse and re-appearing for a short moment at the time $T = 2t_0$ — can be interpreted as a current-echo. Therefore, we have to understand how such weak localization corrections appear in semiconductors and how they are affected by the second pulse. To this end we resort to the semiclassical arguments established in the last section and study the fate of an electron-hole pair exposed to a second light-pulse. Doing so, we employ that the second pulse is a full-gap pulse, resonant in the terms proportional to the interband density (interband dipole matrix elements) and off-resonant in all terms proportional to the intraband density (intraband dipole matrix elements) and neglect — as it was done in [6] — the later. To keep the discussion simple, we first concentrate on the case of equal masses of charge carriers in conductance and valence bands (i.e. $m_{\text{c}} = m_{\text{v}}$), and rely on heuristic arguments as those given in the beginning of section 2. We then generalize to the case of interest, where $m_{\text{c}} < m_{\text{v}}$ and give (more) rigorous expressions.

The interband current consists of conduction-band electrons (c-electrons) and valence-band holes (v-holes) (c-holes and v-electrons, respectively), which are created by the first pulse-scheme, and by the action of the second, full-gap pulse pass over into the corresponding charge carriers in the opposite band. A schematic picture of the interband current is given in Fig. 1.9. The valence-band current, on the other hand, has its origin in an electron-hole pair in the conduction band, which by virtue of the second pulse is converted into an electron-hole pair in the valence band. Reversely, the conduction-band current is made up from an electron-hole pair in the valence-band being transferred into the conduction band by the second pulse. For schematic pictures see also Fig. 1.9. Notice, that we assume both types of charge carriers inside the valence and the conduction band after the first light-pulse has been applied, as stated above.

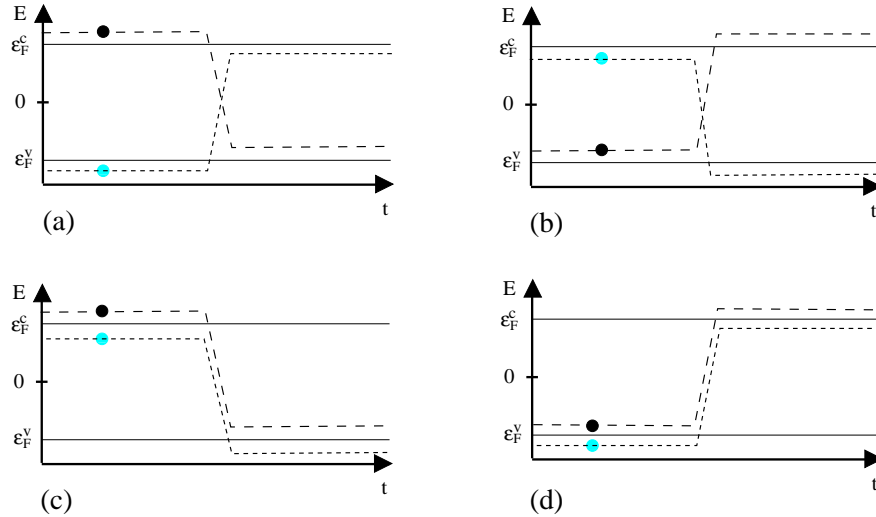


Figure 1.9: Schematic picture of interband current (a, b) and intraband current (c, d). The dark (light) circle represents an electron (hole) and $\epsilon_F^{c,v}$ denotes the Fermi-energy in the conduction and valence band respectively. A transition between the bands occurs at the time the second, full-gap pulse is applied.

An intra- (inter-) band-current-echo appears if the electron and hole running through the same loop in opposite direction interfere constructively and, this way enhance the back-scattering probability. Let us first look at the interband contribution; a real-space representation is given in Fig. 1.10: As the second pulse converts charge carriers from different bands into each other we can distinguish three

different path segments: Starting from the left (see Fig. 1.10 (a) and (b)), the first path-segment, I, comprises a c-electron and c-hole (again: electron and hole pass the loop in the opposite direction!) In the second path-segment, II, the c-electron was already transformed into a v-electron by the full-gap pulse, and therefore charge carriers from different bands interfere. Notice that the c-hole is affected by the full-gap pulse only at a time $T - t_0$ as it runs through the loop in the opposite direction. In the third segment, III, of the path both charge carriers have been stroken by the second, full-gap pulse and therefore belong to the valence band. In summary, only in the second path-segment, where the full-gap pulse already acted on the electron but not yet on the hole, the electron-hole pair comprises charge carriers of different bands. This segment has a duration of time $T - 2t_0$ and vanishes in the time-reversal symmetric moment $T = 2t_0$, as we discussed in sections 3 and 4. From this observation we may conclude that an echo always appears in the interband current.

Turning to the intraband-band current it is just the other way round; a real-space cartoon is given in Fig. 1.10 (c) and (d): Considering the current in the conduction band (Fig. 1.10 (c)), the first and third path-segments carry charge carriers from different bands, while in the middle segment electron and hole are both in the conduction band. It is important to observe, that the phase factors — i.e. the action — the charge carriers accumulate during the path, just depend on the kinetic energy and the disorder-potential energy. That is contributions from absolute energies, such as the band-gap energy, to the action of electron and hole exactly cancel, as can be seen from Fig. 1.9. We therefore expect that an echo also appears in the intraband current of the conduction band, provided that the valence- and conduction band charge carriers “see” the same disorder landscape. The same argument applies for the intraband current in the valence band, as shown in Fig. 1.10 (d).

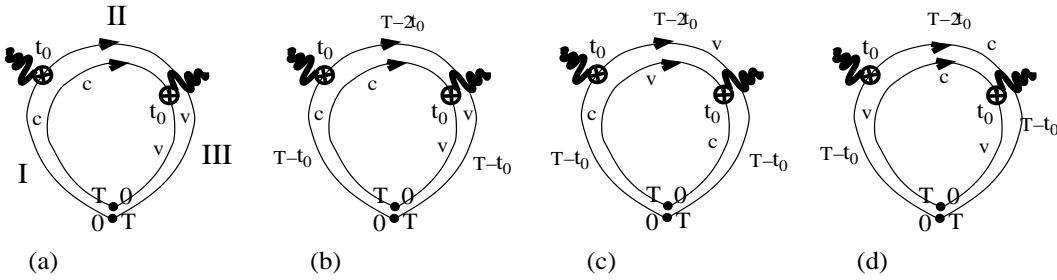


Figure 1.10: (a) Division of loop into three segments, corresponding to composition of electron-hole pair from different bands, (b) Interband-Cooperon, (c) Intraband-Cooperon in the conduction band and (d) Intraband-Cooperon in the valence band.

Summarizing, we find that for equal masses and disorder-landscapes for valence- and conduction-band charge carriers echoes appear in the intraband and interband currents. So let us now turn to the more interesting case of different masses. As electron and hole interfering along the same segment of the path are always from the same band (except for the short middle segment) for the intraband current we do not expect any changes for the intraband echo. In order to make this statement more rigorous we give the semiclassical representation of the weak localization contribution to the interband current in the echo scenario. The Cooperon comprises a valence-band Cooperon and a conduction-band Cooperon from the first and third path-segments respectively and single electron and hole propagators from the middle segment, i.e.

$$C_{\text{inter}} = \int d^d \mathbf{x}_0 \int d^d \mathbf{x}_1 \langle \mathcal{G}_{\mathbf{x}, \mathbf{x}_0}^{R, v}(t_0) \mathcal{G}_{\mathbf{x}, \mathbf{x}_0}^{A, v}(t_0) \rangle e^{ie \mathbf{E}_0 \mathbf{x}_0} \langle \mathcal{G}_{\mathbf{x}_0, \mathbf{x}_1}^{R, c}(T - 2t_0) \mathcal{G}_{\mathbf{x}_0, \mathbf{x}_1}^{A, v}(T - 2t_0) \rangle e^{ie \mathbf{E}_0 \mathbf{x}_1} \langle \mathcal{G}_{\mathbf{x}_1, \mathbf{x}}^{R, c}(t_0) \mathcal{G}_{\mathbf{x}_1, \mathbf{x}}^{A, c}(t_0) \rangle \propto e^{-|T-2t_0|/\tau}. \quad (1.55)$$

Here, in the last equality we used that the single-particle propagators decay exponentially on length scales of the order of the mean free path l , or equivalently — as motion on length-scales l is ballistic — on time scales of the mean elastic scattering time τ . That is, apart from the time $T = 2t_0$, the Cooperon is exponentially suppressed. The proportional constant (i.e. the contribution at time $T = 2t_0$) is just the backscattering probability as in Eq. (1.37).

The situation for the interband currents is more interesting: As we saw, in these cases interference occurs between electron-hole pairs made up from charge carriers of opposite bands. A phase cancellation

is thus unlikely to happen if we assume different effective masses for the charge carriers in conduction- and valence-band. Yet, we should take a closer look at the corresponding actions and remember the fact that the disorder considered here is *correlated* (Eq. (1.52)); the action for the valence-band hole from the first path-segment of the loop, for example, is given by

$$\begin{aligned} S^{\text{vh}}(t_0) &= \int_0^{t_0} dt' \left\{ \frac{m_v}{2} \dot{\mathbf{x}}^2 + V_v(\mathbf{x}) \right\} \\ &= \frac{m_c}{m_v} \int_0^{t_0} dt' \left\{ \left(\frac{m_v}{m_c} \right)^2 \frac{m_c}{2} \dot{\mathbf{x}}^2 + V_c(\mathbf{x}) \right\} \\ &= \int_0^{\frac{m_c}{m_v} t_0} d\tau \left\{ \frac{m_c}{2} \dot{\mathbf{x}}^2 + V_c(\mathbf{x}) \right\} = S^{\text{ch}} \left(\frac{m_c}{m_v} t_0 \right). \end{aligned} \quad (1.56)$$

That is, in the case of correlated disorder the dynamics of a hole in the valence-band correspond to those of a hole in the conduction-band if time is rescaled by the factor $\gamma \equiv \frac{m_c}{m_v} < 1$. Analogously for conduction and valence band electrons. (Notice that in Eq. (1.56) we left out contributions to the action from the energy E_g , as discussed above).

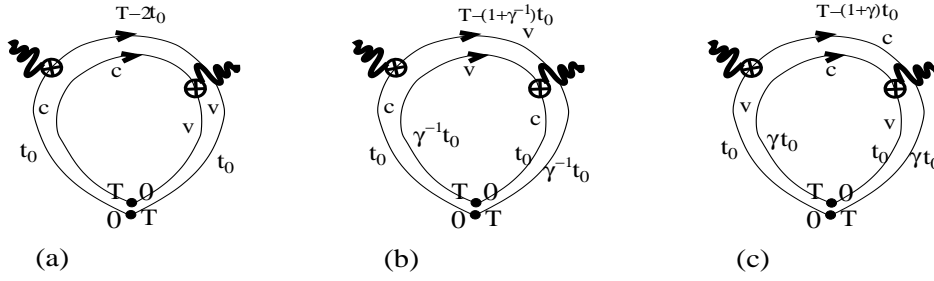


Figure 1.11: Echo condition for (a) interband current, (b) intraband current in the valence band, and (c) intraband current in the conduction-band

Turning back to Fig. 1.11 we may use that $\mathcal{G}^{\text{R/A},v}(t) = \mathcal{G}^{\text{R/A},c}(\gamma t)$ (which follows from Eq. (1.56)) to notice that constructive interference — i.e. a weak localization contribution to the conduction-band current — is achieved if the total traveling time is $T = (1 + \gamma)t_0$. In formulas

$$\begin{aligned} C_{\text{intra}}^c &= \int d^d \mathbf{x}_0 \int d^d \mathbf{x}_1 \langle \mathcal{G}_{\mathbf{x},\mathbf{x}_0}^{\text{R},v}(t_0) \mathcal{G}_{\mathbf{x},\mathbf{x}_0}^{\text{A},c}(\gamma t_0) \rangle e^{ie\mathbf{E}_0 \mathbf{x}_0} \langle \mathcal{G}_{\mathbf{x}_0,\mathbf{x}_1}^{\text{R},c}(T - (1 + \gamma)t_0) \mathcal{G}_{\mathbf{x}_0,\mathbf{x}_1}^{\text{A},c}(T - (1 + \gamma)t_0) \rangle \\ &\quad e^{ie\mathbf{E}_0 \mathbf{x}_1} \langle \mathcal{G}_{\mathbf{x}_1,\mathbf{x}}^{\text{R},c}(\gamma t_0) \mathcal{G}_{\mathbf{x}_1,\mathbf{x}}^{\text{A},v}(t_0) \rangle \\ &= \int d^d \mathbf{q} C_{\mathbf{q}}^c(\gamma t_0) C_{\mathbf{q}-\bar{\mathbf{q}}}^c(T - (1 + \gamma)t_0) C_{\mathbf{q}}^c(\gamma t_0) \\ &\propto e^{-D\bar{\mathbf{q}}|T-(1+\gamma)t_0| \left(1 - \frac{|T-(1+\gamma)t_0|}{T+(1-\gamma)t_0}\right)}, \end{aligned} \quad (1.57)$$

where $\bar{\mathbf{q}} = 2e\tau\mathbf{E}_0$ and the proportional constant is the probability to return to the starting point within the time T (see Eq. (1.37)). Interchanging masses, $m_v \leftrightarrow m_c$, the same argument holds for the valence-band intra-current,

$$C_{\text{intra}}^v \propto e^{-D\bar{\mathbf{q}}|T-(1+\gamma^{-1})t_0| \left(1 - \frac{|T-(1+\gamma^{-1})t_0|}{T+(1-\gamma^{-1})t_0}\right)}. \quad (1.58)$$

In summary we find that in the case of different masses for valence- and conduction-band charge carriers, the interband current-echo remains unchanged, whereas the intraband current-echo splits into an advanced c-band and a retarded v-band component at times $t_c = (1 + \gamma)t_0$ and $t_v = (1 + \gamma^{-1})t_0$, respectively. Crucial for the above analysis is the assumption of correlated disorder. The role of the second pulse is to achieve a band-inversion, i.e. it has to be a full-gap pulse but must not create a current pulse itself. These observations exactly cover the features characterizing the echo as found from numerical studies and as summarized in the introduction.

1.6 Summary and outlook

In this section we gave an explanation, based on the interference of time-reversed paths, for the current echo in metals and semiconductors as numerically studied by Thomas *et al.* Given the possibility to generate current pulses on femto- to picosecond time scales in semiconductors an experimental verification of the current echo in semiconductors should be feasible. An extension to metals depends on the technical realizability of voltage pulses on a pico-second time-scale. Only very recently experiments were reported using voltage pulses on such short time-scales [14]. As its amplitude is exponentially damped due to dephasing, the current echo may become a useful tool for measurements of the dephasing rate in weakly disordered metals. In order to check whether the interference of time-reversed paths really is the underlying mechanism of the echo found by Thomas *et al.* one could include a magnetic field in their numerical calculations and see whether this suppresses the echo.

Bibliography

- [1] W. Niggemeier, G. von Plessen, S. Sauter, and P. Thomas, Phys. Rev. Lett. **71**, 770 (1993).
- [2] R. Atanasov, A. Hach, J.L.P. Hughes, H.M. van Driel, and J.E. Sipe, Phys. Rev. Lett. **76**, 1703 (1996).
- [3] A. Hach, Y. Kostoulas, R. Atanasov, J.L.P. Hughes, J.E. Sipe, and H.M. van Driel, Phys. Rev. Lett. **78**, 306 (1997).
- [4] A. Hach, J.E. Sipe, and H.M. van Driel, IEEE J. Quantum Electron. **34**, 1144 (1998).
- [5] J. Stippler, C. Schlichenmaier, A. Knorr, T. Meier, M. Lindberg, P. Thomas, and S.W. Koch, Phys. Status Solidi B **221**, 379 (2000).
- [6] C. Schlichenmaier, I. Varga, T. Meier, P. Thomas, and S. W. Koch Phys. Rev. B **65**, 085306 (2002)
- [7] S. Sauter-Fischer, E. Runge, and R. Zimmermann, Phys. Rev. B **57**, 4299 (1998).
- [8] A. Altland and B. Simons, *Condensed Matter Field Theory*, (Cambridge Univ. Press 2006).
- [9] G. Bergman, Physics Reports **107**, 1 (1984).
- [10] A. Kamenev and A. Andreev, Phys. Rev. B **60**, 2218 (1999).
- [11] J. Ramer and H. Smith, Rev. Mod. Phys. **58**, 323359 (1986).
- [12] A. Kamenev, cond-mat/0412296 (Lectures notes for 2004 Les Houches Summer School on “Nano-scopic Quantum Transport”).
- [13] R. P. Feynman and A. R. Hibbs, *Quantum Mechanics and Path Integrals*, (New York: McGraw-Hill 1965).
- [14] B. Naser, J. Heeren, D. K. Ferry, and J. B. Bird, Rev. Sci. Instrum. **76**, 113905 (2005), and B. Naser, J. Heeren, D. K. Ferry, and J. B. Bird, Appl. Phys. Lett. **89**, 083103 (2006).

Chapter 2

Dephasing by Kondo Impurities

Introduction: Decoherence is the fundamental process leading to a suppression of quantum mechanical interference and therefore is indispensable for our understanding of the appearance of the classical world. The destruction of phase coherence in a quantum system occurs due to interactions with its environment and can be studied e.g. in mesoscopic metals and semiconductors where the quantum-mechanical wave nature of the electrons leads to a variety of novel transport phenomena observed at low temperatures.

Although the concrete definition of the dephasing rate, $1/\tau_\varphi$, depends on the experiment used to determine it, the electron-electron interactions is thought to become the dominating mechanism for the destruction of phase coherence in metals without dynamical impurities below about 1 K. The dephasing rate for interacting electrons in a diffusive environment was first calculated by Altshuler, Aronov and Khmelnitsky (AAK) and vanishes at low temperatures, T , with some power of T , depending on the dimensionality of the system [1].

In the late 90's several independent groups performed experiments [2, 3, 4, 5] to probe $1/\tau_\varphi$ of disordered metallic wires and surprisingly observed its saturation at lowest experimentally accessible temperatures. This observation has triggered an intense discussion on the mechanism responsible for the excess of dephasing [6, 7, 8]. By now consensus has been reached that the most promising candidates to explain the saturation of $1/\tau_\varphi$ are extremely low concentrations of dynamical impurities, such as atomic two-level systems or magnetic impurities.

Theoretically the effect of dynamic magnetic impurities on $1/\tau_\varphi$ has first been considered by Ohkawa, Fukuyama and Yosida [9] (the static case was first treated by Ref. [10]) using perturbation theory (generalized to renormalized perturbation theory in Refs. [4, 11]) which limits the range of applicability to temperatures larger than the Kondo temperature, $T \gg T_K$. For $T \ll T_K$, a quadratic T dependence, $1/\tau_\varphi \propto T^2$ has been predicted [11] based on Fermi liquid arguments.

A closed expression for the dephasing rate due to Kondo impurities, however, has so far been missing, and, therefore, a quantitative analysis of the role played by magnetic impurities in the saturation of the dephasing rate (by performing e.g. implantation experiments) was not feasible. This observation motivated us to study the role of Kondo impurities on dephasing in weakly disordered metals in the *full temperature regime* probed in the experiments. We derived a closed expression for the dephasing rate due to diluted Kondo impurities valid for all experimentally realized temperatures and its numerical evaluation was done by Theo Costi [12]. Recent experiments on Ag wires doped with small concentrations of Fe impurities allow for a critical discussion of our results.

Outlook: The outline of this chapter is the following: In a first section we derive an effective field theory (the so-called nonlinear σ -model, NL σ M) for a metallic system containing low concentrations of magnetic impurities. We then use this model to calculate the dephasing rate as measured (1) in weak localization experiments, (2) from Aharonov-Bohm oscillations, and (3) from the current-echo. Finally we discuss recent doping experiments performed separately by Mallet *et al.* [14] and Alzoubi *et al.* [15] which measure the dephasing rate in Ag wires containing known concentrations of dilute Fe impurities. Details of the calculations can be found in the appendices.

2.1 Replica NL σ M for disordered electron gas containing diluted magnetic impurities

In this section we derive an effective field theory for a metallic system containing static disorder and a low concentration of dynamical magnetic impurities. We start our analysis of such a system from the Hamiltonian $H = H_0 + H_S$, where

$$H_0 = \int d^d \mathbf{x} c_{\sigma}^{\dagger}(\mathbf{x}) \left[\frac{\hat{\mathbf{p}}^2}{2m} - \mu + V(\mathbf{x}) \right] c_{\sigma}(\mathbf{x}) \quad (2.1)$$

describes the dynamics of the conduction band electrons in a disorder potential V and

$$H_S = J \sum_i \hat{\mathbf{S}}(\mathbf{x}_i) c_{\sigma}^{\dagger}(\mathbf{x}_i) \sigma_{\sigma\sigma'} c_{\sigma'}(\mathbf{x}_i) \quad (2.2)$$

accounts for the coupling of the electrons to local magnetic moments situated at some space-points $\{\mathbf{x}_i\}$. As usual, we take V to be δ -correlated white noise, described by its second moment

$$\langle V(\mathbf{x})V(\mathbf{x}') \rangle_V = \frac{1}{2\pi\nu\tau} \delta(\mathbf{x} - \mathbf{x}'). \quad (2.3)$$

Here ν denotes the density of states per spin at the Fermi energy and τ is the mean scattering time corresponding to a mean free path $l = v_F \tau$. We account for the randomness in the distribution of the magnetic impurities by averaging over their location $\langle \dots \rangle_S = n_S \sum_i \int d^d \mathbf{x}_i (\dots)$, with n_S being the concentration of the magnetic impurities.

The derivation of the effective theory includes the following steps: We represent the quantum partition function in terms of a coherent state path integral employing the replica trick (see e.g. [16]) in order to ease the ensemble average over (static) disorder configurations. The resulting theory is then mapped to an effective field theory, the so-called nonlinear σ -model (NL σ M). This mapping consists in: (a) Hubbard-Stratonovich transformation, (b) mean-field analysis, (c) expansion around mean-field in fluctuation matrices. The gradient-expansion (i.e. part (c)) employed here deviates from the usual lines (see e.g. [16, 17]). This lies in the fact that studying the impact of magnetic impurities we want to keep in our model the *full* T-matrix describing the scattering from magnetic impurities to *all orders* in the coupling constant J . We give a detailed description of the gradient expansion in Appendix A.1.

Replica Trick: The replicated quantum partition function in the coherent-state path-integral formulation is given by

$$\mathcal{Z}^r = \int \prod_{\alpha} \mathcal{D}[\bar{\psi}_{\alpha} \psi_{\alpha}] e^{-S[\bar{\psi} \psi]}, \quad (2.4)$$

where $\bar{\psi} = \{\bar{\psi}_{\alpha}\}$ and $\psi = \{\psi_{\alpha}\}$ represent sets of r copies of the original electron fields and the replicated imaginary-time action S is given by

$$S[\bar{\psi} \psi] = \sum_{\alpha=1}^r S[\bar{\psi}_{\alpha} \psi_{\alpha}], \quad (2.5)$$

with the action of the α -th copy of the form

$$S[\bar{\psi}_{\alpha} \psi_{\alpha}] = \int_0^{\beta} d\tau \left\{ \bar{\psi}_{\alpha}(\tau) \partial_{\tau} \psi_{\alpha}(\tau) - H[\bar{\psi}_{\alpha} \psi_{\alpha}] \right\}. \quad (2.6)$$

Here and in the following we avoid writing out explicitly replica indices.

Symmetry doubling by introduction of T-space: As usual we want to incorporate time-reversal symmetry into our model. Later on this procedure will help us to decouple the two relevant channels (Cooper and exchange) of the disorder induced “interaction” simultaneously. We introduce the two component spinors

$$\Psi(\mathbf{x}, \tau) = \frac{1}{\sqrt{2}} \begin{pmatrix} \psi(\mathbf{x}, \tau) \\ -i\sigma_2^S \bar{\psi}^t(\mathbf{x}, -\tau) \end{pmatrix}_T, \quad \bar{\Psi}(\mathbf{x}, \tau) = \frac{1}{\sqrt{2}} (\bar{\psi}(\mathbf{x}, \tau), \quad -i\psi^t(\mathbf{x}, -\tau)\sigma_2^S)_T \quad (2.7)$$

and their Fourier-representation

$$\Psi_n(\mathbf{q}) = \frac{1}{\sqrt{2}} \begin{pmatrix} \psi_n(\mathbf{q}) \\ -i\sigma_2^S \bar{\psi}_n^t(\mathbf{q}) \end{pmatrix}_T, \quad \bar{\Psi}_n(\mathbf{q}) = \frac{1}{\sqrt{2}} (\bar{\psi}_n(\mathbf{q}), \quad -i\psi_n^t(\mathbf{q})\sigma_2^S)_T. \quad (2.8)$$

Here t refers to the transpose in replica-space (R) and spin-space (S) and T denotes the “time-reversal”-space. The electron-fields $\bar{\psi} = (\bar{\psi}_\uparrow, \bar{\psi}_\downarrow)_S$, $\psi = (\psi_\uparrow, \psi_\downarrow)_S^t$ are two-component spinors with entries in spin-space (S-space). Consequently, σ_i^S refers to the i -th Pauli-matrix in S-space. With the above definition we may write

$$S_0 = \int_0^\beta d\tau \int d^d \mathbf{x} \bar{\Psi}(\mathbf{x}, \tau) \left\{ \partial_\tau + \mu + \frac{1}{2m} (\partial - ie\mathbf{a}(\mathbf{x}, \tau)\sigma_3^T)^2 - U_{\text{dis}}(\mathbf{x}) \right\} \Psi(\mathbf{x}, \tau), \quad (2.9)$$

and

$$S_S = J \sum_i \int_0^\beta d\tau \mathbf{S}(\mathbf{x}_i, \tau) \bar{\Psi}(\mathbf{x}_i, \tau) \sigma_3^S \sigma_3^T \Psi(\mathbf{x}_i, \tau). \quad (2.10)$$

We mention that the external fields become matrices in T-space of the form

$$\mathbf{a}(\tau) = \begin{pmatrix} \mathbf{a}(\tau) & \\ & \mathbf{a}(-\tau) \end{pmatrix}_T \equiv \begin{pmatrix} \mathbf{a}^1(\tau) & \\ & \mathbf{a}^2(\tau) \end{pmatrix}_T, \quad \mathbf{S}(\tau) = \begin{pmatrix} \mathbf{S}(\tau) & \\ & \mathbf{S}(-\tau) \end{pmatrix}_T \equiv \begin{pmatrix} \mathbf{S}^1(\tau) & \\ & \mathbf{S}^2(\tau) \end{pmatrix}_T. \quad (2.11)$$

Finally, we emphasize that due to the symmetry-doubling of the field space the electron-fields $\bar{\Psi}$ and Ψ are not independent variables anymore, but related by the transformation

$$\bar{\Psi}_n(\mathbf{x}) = -\Psi_n^t(\mathbf{x}) i\sigma_2^S \otimes \sigma_1^T. \quad (2.12)$$

Disorder-average: The replica trick allows us to use the replicated partition function \mathcal{Z}^r instead of the free energy $\ln \mathcal{Z}$ as a generating functional in order to calculate the expectation values of operators. To be specific, in subsequent sections we will calculate the electrical conductivity by differentiating the partition function with respect to the vector potential \mathbf{a} . (Notice that in Eq. (2.9) we minimally coupled to the vector potential.) Using the replicated partition function and not its logarithm has the advantage that the disorder-average is easily done:

$$\langle \mathcal{Z}^r \rangle_V = \int \mathcal{D}V \mathcal{Z}^r[V] = \int \mathcal{D}[\bar{\psi}, \psi] e^{-S_0[\bar{\psi}, \psi] + S_{\text{int}}[\bar{\psi}, \psi]}, \quad (2.13)$$

with the interaction term

$$S_{\text{int}}[\bar{\Psi}, \Psi] = \frac{1}{4\pi\nu\tau} \int_0^\beta d\tau \int_0^\beta d\tau' \int d^d \mathbf{x} \bar{\Psi}(\mathbf{x}, \tau) \Psi(\mathbf{x}, \tau) \bar{\Psi}(\mathbf{x}, \tau') \Psi(\mathbf{x}, \tau'), \quad (2.14)$$

which is local in space but non-local in time, reflecting the fact that we consider only elastic impurity-scattering. Separation into slow momenta $\mathbf{q} \ll p_F$ and fast momenta $\mathbf{p} \sim p_F$ we neglect the contribution from the density channel as it only leads to a renormalization of the chemical potential μ and, thus, only retain the Cooper- and the Diffuson-channel, i.e.

$$S_{\text{int}}[\bar{\Psi}\Psi] = \frac{1}{4\pi\nu\tau} \int_0^\beta d\tau \int_0^\beta d\tau' \sum_{q \ll p, p' \sim p_F} \left\{ \bar{\Psi}_{\mathbf{p}+\mathbf{q}}(\tau) \Psi_{\mathbf{p}'}(\tau) \bar{\Psi}_{\mathbf{p}'+\mathbf{q}}(\tau') \Psi_{\mathbf{p}}(\tau') + \bar{\Psi}_{\mathbf{p}+\mathbf{q}}(\tau) \Psi_{\mathbf{p}'+\mathbf{q}}(\tau) \bar{\Psi}_{-\mathbf{p}}(\tau') \Psi_{-\mathbf{p}'}(\tau') \right\}. \quad (2.15)$$

At this point we benefit from the symmetry-doubling of the field-space and summarize the slow part of the four-Fermion term in a single contribution

$$S_{\text{int}} = \frac{1}{2\pi\nu\tau} \int_0^\beta d\tau \int_0^\beta d\tau' \sum_{q \ll p, p'} \bar{\Psi}_{\mathbf{p}+\mathbf{q}}(\tau) \Psi_{\mathbf{p}'}(\tau) \bar{\Psi}_{\mathbf{p}'+\mathbf{q}}(\tau') \Psi_{\mathbf{p}}(\tau'). \quad (2.16)$$

Hubbard-Stratonovich decoupling and mean-field analysis: In the following steps we distill an effective field-theory from Eqs. (2.9) and (2.16). The plan is to introduce a new degree of freedom which grasps all relevant physics and is described by a low-energy theory (the nonlinear σ -model). To this end we decouple the quartic part of the action, Eq. (2.16), by the Hubbard-Stratonovich (HS) matrix-field Q ,

$$e^{-S_{\text{int}}[\bar{\Psi}\Psi]} = \int \mathcal{D}Q e^{-\frac{\pi\nu}{8\tau} \int d\tau \int d\tau' \sum_{\mathbf{q}} \text{Tr} Q_{\mathbf{q}}(\tau, \tau') Q_{-\mathbf{q}}(\tau', \tau) - \frac{i}{2\tau} \int d\tau \int d\tau' \sum_{\mathbf{p}, \mathbf{p}'} \bar{\Psi}_{\mathbf{p}}(\tau) Q_{\mathbf{p}'-\mathbf{p}}(\tau, \tau') \Psi_{\mathbf{p}'}(\tau)}. \quad (2.17)$$

Notice that $Q_{\tau\tau'}(\mathbf{x})$ is a matrix in space-time as well as in the product space $\mathbb{R} \otimes \mathbb{S} \otimes \mathbb{T}$; it is local in coordinate space (which is a hallmark of the δ -correlated disorder potential considered here) and non-local in time. In the following we denote the trace in $\mathbb{R} \otimes \mathbb{S} \otimes \mathbb{T}$ -space by $\text{tr}(\dots)$, whereas the complete operator trace involving integration over space and time indices will be indicated as $\text{Tr}(\dots)$. It is important to observe that the symmetry relation of the electron-fields, Eq.(2.12), restricts the HS-fields Q , to matrices obeying the relation

$$Q_{nn'}^t(\mathbf{x}) = \sigma_2^S \otimes \sigma_1^T Q_{n'n}(\mathbf{x}) \sigma_1^T \otimes \sigma_2^S, \quad (2.18)$$

where t refers to transposition in $\mathbb{S} \otimes \mathbb{T}$ -space. Here and in the following we will use the Q -matrices defined in the energy domain according to the relation

$$Q_{nn'} = \frac{1}{\beta} \int_0^\beta d\tau \int_0^\beta d\tau' e^{i\epsilon_n \tau - i\epsilon_{n'} \tau'} Q_{\tau\tau'}. \quad (2.19)$$

After the HS transformation, Eq.(2.17), the fermionic part of the action becomes quadratic,

$$S_e = \text{Tr} \bar{\Psi} \left[\mathcal{G}^{-1} + \frac{i}{2\tau} Q \right] \Psi \equiv \text{Tr} \bar{\Psi} \mathcal{G}_Q^{-1} \Psi, \quad (2.20)$$

with the inverse Green's function $\mathcal{G}^{-1} \equiv \partial_\tau + \mu + \frac{1}{2m} (\partial - i e a \sigma_3^T)^2 - J \sum_i \sigma_3^S \sigma_3^T \mathbf{S}(\mathbf{x}_i) \delta(\mathbf{x} - \mathbf{x}_i)$. Gaussian integration over Ψ can therefore readily be done, resulting in

$$S_e = -\frac{1}{2} \text{Tr} \ln \mathcal{G}_Q^{-1}. \quad (2.21)$$

We thus succeeded in exchanging the microscopic degree of freedom, i.e. the electron/hole-fields, for the effective degree of freedom Q . Q describes the joined, coherent dynamics of electron-hole and electron-electron pairs. At this point we continue with a mean-field analysis of the action-functional

$$S[Q] = \frac{\pi\nu}{8\tau} \text{Tr} Q^2 - \frac{1}{2} \text{Tr} \ln \mathcal{G}_Q^{-1}. \quad (2.22)$$

Searching for an adequate starting point to formulate the low energy effective theory, we neglect contributions from the external fields \mathbf{a} and \mathbf{S} for the moment. Variation of Eq. (2.22) with respect to Q gives the mean-field equation

$$\bar{Q}_{nn'}(\mathbf{x}) = \frac{i}{\pi\nu} \left[g^{-1} + \frac{i}{2\tau} Q \right]^{-1} \Big|_{\mathbf{x}\mathbf{x}, nn'}, \quad (2.23)$$

which has the homogeneous, Matsubara-diagonal solution

$$\Lambda_{nn'} = \text{sgn}(n) \delta_{nn'}. \quad (2.24)$$

Our last remark before we continue with the construction of the effective model is the observation that Λ , indeed, satisfies the symmetry-constraint, Eq.(2.18).

Gradient-Expansion: Starting out from the action in Eq. (2.22), we parametrize the Q -fields in rotations around the saddle point in a way that fulfills the constriction $Q^2 = 1$. This way we obtain an action in the low energy modes denoted by g ,

$$S_{\text{eff}}[g] = \frac{1}{2} \text{Tr} \ln \left\{ \partial_\tau + \mu + \frac{1}{2m} \nabla^2 + \frac{i}{2\tau} g \Lambda g^{-1} - J \sum_i \sigma^S \sigma_3^T \mathbf{S}(\mathbf{x}_i) \right\}. \quad (2.25)$$

In a next step we expand the “tr ln”, making use of the small parameters $\omega\tau, D\mathbf{q}^2\tau \ll 1$ (“gradient expansion”, see Appendix A.1). As we are interested in all ranges of temperature, including the Kondo temperature T_K , we have to account for all orders in coupling constant the J . The expansion is rather technical and can be found in Appendix A.1. At this point we merely state that we use an expansion of the rotations, $g = e^W$, to second order (Gaussian approximation) in the generators, W . Also we may employ the fact that we are interested in experimental situations where only low concentrations of magnetic impurities are present and keep only the leading, i.e. the linear terms in n_S . We find $S^2[W] = S_\sigma^2[W] + S_S^2[W]$, where

$$S_\sigma^2[W] = \frac{\pi\nu}{8} \sum_{n_1 n_2} \int d^d \mathbf{q} \text{tr} \left\{ (D\mathbf{q}^2 + 2\hat{\epsilon}\Lambda) W_{n_1 n_2}(\mathbf{q}) W_{n_2 n_1}(-\mathbf{q}) \right\} \quad (2.26)$$

$$S_S^2[W] = \frac{i\pi\nu}{4} \sum_{n_1, n_2, n_3, n_4} \sum_i \text{tr} \left\{ T_{n_1 n_2}(\mathbf{x}_i) \Lambda_{n_2} W_{n_2 n_3}(\mathbf{x}_i) W_{n_3 n_1}(\mathbf{x}_i) \right. \\ \left. + i\pi\nu T_{n_1 n_2}(\mathbf{x}_i) \Lambda_{n_2} W_{n_2 n_3}(\mathbf{x}_i) T_{n_3 n_4}(\mathbf{x}_i) \Lambda_{n_4} W_{n_4 n_1}(\mathbf{x}_i) \right\}. \quad (2.27)$$

Here

$$T(\mathbf{x}_i) \equiv J\sigma^S \sigma_3^T \mathbf{S}(\mathbf{x}_i) + J\sigma^S \sigma_3^T \mathbf{S}(\mathbf{x}_i) \mathcal{G}_0^S(\mathbf{x}_i, \mathbf{x}_i) J\sigma^S \sigma_3^T \mathbf{S}(\mathbf{x}_i) \quad (2.28)$$

denotes the T -matrix (see Fig. 2.1) for the scattering at a single magnetic impurity located at some space-point \mathbf{x}_i and $\mathcal{G}_0^S = \left(-\frac{\mathbf{p}^2}{2m} + \mu + \frac{i}{2\tau} \Lambda - J\sigma^S \sigma_3^T \mathbf{S} \right)^{-1}$ is the Green's function for an electron moving in a static disorder potential (i.e. the electron has acquired a finite life-time τ) and scattering from diluted magnetic impurities, as contained in the part proportional to J . Notice that we used

that in leading order in the impurity concentration, n_S , T is diagonal in the location of the magnetic impurities, i.e. for low concentrations repeated scattering from a *single* magnetic impurity dominates. A more generic expression would contain T -matrices describing scattering at several different magnetic impurities; yet these terms are negligible for diluted concentrations of magnetic scatterers. We estimate their contribution to the dephasing rate below. In field-theoretical language, the first term in S_5^2 is the self-energy contribution (with scattering taking place only on one single electron line), whereas the second contribution represents vertex corrections (describing interactions between two electron lines); the diagrammatic representation is given in Fig. 2.2.

$$\begin{aligned}
 T &= \text{⊗} + \text{⊗} \rightarrow \text{⊗} + \text{⊗} \rightarrow \text{⊗} \rightarrow \text{⊗} + \dots \\
 &= \text{⊗} + \text{⊗} \rightleftarrows \text{⊗} \\
 &=: \text{⊗}
 \end{aligned}$$

Figure 2.1: Diagrammatic representation of the T -matrix. Crosses denote scattering from magnetic impurities, single lines the free Greens function \mathcal{G}_0 and double line the Greens function in presence of magnetic impurities \mathcal{G}_0^S .

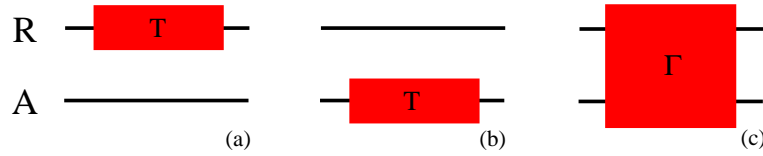


Figure 2.2: Diagrammatic representation of self-energy and vertex: (a) is the retarded self-energy Σ^R , (b) its advanced version Σ^A and (c) denotes the vertex Γ containing all scattering processes which subsumes scattering processes of retarded and advanced electron lines from magnetic impurities to all orders in J .

We now continue by separating the dynamics of coherent particle-hole pairs (“Diffuson”) from those of particle-particle pairs (“Cooperon”). Technically speaking, we divide the generators W into diagonal and off-diagonal contributions in T -space, i.e.

$$W_C = \begin{pmatrix} \mathcal{C}^{+-} & \mathcal{C}^{++} \\ \mathcal{C}^{-+} & \mathcal{C}^{--} \end{pmatrix}_T, \quad \text{and} \quad W_D = \begin{pmatrix} \mathcal{D}^{++} & \\ & \mathcal{D}^{--} \end{pmatrix}_T \quad (2.29)$$

with $2r \times 2r$ -matrices \mathcal{C}^{+-} , \mathcal{C}^{-+} , \mathcal{D}^{++} , \mathcal{D}^{--} in $S \otimes R$ -space. Notice that in quadratic order in the generators, diagonal and off-diagonal contributions do not couple since the actions Eq. (2.26), (2.27) are diagonal in T -space. Higher order terms in the generators describe interactions between the Cooperon and Diffuson modes. Since our parametrization uses that $[\Lambda, W] = 0$ (this was explicitly used in the gradient expansion, see Appendix A.1), \mathcal{C}^{+-} , \mathcal{C}^{-+} , \mathcal{D}^{++} and \mathcal{D}^{--} are off-diagonal in Matsubara-space. The symmetry constraint for the Q -fields, Eq.(2.18), imposes the following constraint for the generators W

$$W_{nn'}^t(\mathbf{q}) = -\sigma_2^S \otimes \sigma_1^T W_{n'n}(\mathbf{q}) \sigma_1^T \otimes \sigma_2^S, \quad (2.30)$$

which itself establishes the following relation between the matrices \mathcal{C}^{+-} , \mathcal{C}^{-+} , \mathcal{D}^{++} , \mathcal{D}^{--}

$$[\mathcal{C}_{nn'}^{+-}]^\tau(\mathbf{q}) = -\mathcal{C}_{n'n}^{+-}(\mathbf{q}), \quad (2.31)$$

$$[\mathcal{C}_{nn'}^{-+}]^\tau(\mathbf{q}) = -\mathcal{C}_{n'n}^{-+}(\mathbf{q}), \quad (2.32)$$

$$[\mathcal{D}_{nn'}^{++}]^\tau(\mathbf{q}) = -\mathcal{D}_{n'n}^{--}(\mathbf{q}), \quad (2.33)$$

with the generalized transpose τ defined as $X^\tau \equiv \sigma_2^S X^t \sigma_2^S$, where the transpose t acts in $S \otimes R$ -space. In terms of the \mathcal{C}, \mathcal{D} -fields the action Eq. (2.26) and Eq. (2.27) takes the form

$$S_\sigma[\mathcal{C}, \mathcal{D}] = \frac{\pi\nu}{4} \sum_{n_1 n_2} \int d^d \mathbf{q} (D\mathbf{q}^2 + 2|\epsilon_{n_1}|) \text{tr}_{R \otimes S} \{ \mathcal{C}_{n_1 n_2}^{+-}(\mathbf{q}) \mathcal{C}_{n_2 n_1}^{-+}(-\mathbf{q}) + \mathcal{D}_{n_1 n_2}^{++}(\mathbf{q}) \mathcal{D}_{n_2 n_1}^{++}(-\mathbf{q}) \}, \quad (2.34)$$

and

$$\begin{aligned} S_S[\mathcal{C}, \mathcal{D}] = \frac{i\pi\nu}{4} \sum_{n_1 n_2} \sum_i \text{tr}_{R \otimes S} \{ & (T_{n_1 n_2}^1 + [T_{n_2 n_1}^2]^\tau) \text{sgn}(n_2) [\mathcal{D}_{n_2 n_3}^{++}(\mathbf{x}_i) \mathcal{D}_{n_3 n_1}^{++}(\mathbf{x}_i) + \mathcal{C}_{n_2 n_3}^{+-}(\mathbf{x}_i) \mathcal{C}_{n_3 n_1}^{-+}(\mathbf{x}_i)] \\ & + i\pi\nu [T_{n_1 n_2}^1 \text{sgn}(n_2) \mathcal{D}_{n_2 n_3}^{++}(\mathbf{x}_i) T_{n_3 n_4}^1 \text{sgn}(n_4) \mathcal{D}_{n_4 n_1}^{++}(\mathbf{x}_i) \\ & + [T_{n_2 n_1}^2]^\tau \text{sgn}(n_2) \mathcal{D}_{n_2 n_3}^{++}(\mathbf{x}_i) [T_{n_4 n_3}^2]^\tau \text{sgn}(n_4) \mathcal{D}_{n_4 n_1}^{++}(\mathbf{x}_i) \\ & + T_{n_1 n_2}^1 \text{sgn}(n_2) \mathcal{C}_{n_2 n_3}^{+-}(\mathbf{x}_i) T_{n_3 n_4}^2 \text{sgn}(n_4) \mathcal{C}_{n_4 n_1}^{-+}(\mathbf{x}_i) \\ & + [T_{n_2 n_1}^2]^\tau \text{sgn}(n_2) \mathcal{C}_{n_2 n_3}^{+-}(\mathbf{x}_i) [T_{n_4 n_3}^1]^\tau \text{sgn}(n_4) \mathcal{C}_{n_4 n_1}^{-+}(\mathbf{x}_i)] \}. \end{aligned} \quad (2.35)$$

Here the indices 1, 2 denote the first and second component in T-space, the generalized transpose τ acts in S-space and we employed the symmetry relation Eq. (2.31) to express everything in the variables $\mathcal{D}^{++}, \mathcal{C}^{+-}$ and \mathcal{C}^{-+} .

To summarize this section, the particle-hole dynamics for disordered systems containing diluted concentrations of magnetic impurities is described by the nonlinear σ -model action,

$$\begin{aligned} S[\mathcal{D}^{++}] = \frac{\pi\nu}{4} \sum_{n_1 n_2} \int d^d \mathbf{q} \text{tr}_{R \otimes S} \{ & [D\mathbf{q}^2 + 2|\epsilon_{n_1}|] \mathcal{D}_{n_1 n_2}^{++}(\mathbf{q}) \mathcal{D}_{n_2 n_1}^{++}(-\mathbf{q}) \} \\ & + 2 \sum_i \text{tr}_{R \otimes S} \{ T_{n_1 n_2} \text{sgn}(n_2) \mathcal{D}_{n_2 n_3}^{++}(\mathbf{x}_i) \mathcal{D}_{n_3 n_1}^{++}(\mathbf{x}_i) \\ & + i\pi\nu T_{n_1 n_2} \text{sgn}(n_2) \mathcal{D}_{n_2 n_3}^{++}(\mathbf{x}_i) T_{n_3 n_4} \text{sgn}(n_4) \mathcal{D}_{n_4 n_1}^{++}(\mathbf{x}_i) \}, \end{aligned} \quad (2.36)$$

and the particle-particle dynamics are governed by the action

$$\begin{aligned} S[\mathcal{C}^{+-} \mathcal{C}^{-+}] = \frac{\pi\nu}{2} \sum_{n_1 n_2} \int d^d \mathbf{q} \text{tr}_{R \otimes S} \{ & [D\mathbf{q}^2 + 2|\epsilon_{n_1}|] \mathcal{C}_{n_1 n_2}^{+-}(\mathbf{q}) \mathcal{C}_{n_2 n_1}^{-+}(-\mathbf{q}) \} \\ & + 2 \sum_i \text{tr}_{R \otimes S} \{ T_{n_1 n_2} \text{sgn}(n_2) \mathcal{C}_{n_2 n_3}^{+-}(\mathbf{x}_i) \mathcal{C}_{n_3 n_1}^{-+}(\mathbf{x}_i) \\ & + i\pi\nu T_{n_1 n_2} \text{sgn}(n_2) \mathcal{C}_{n_2 n_3}^{+-}(\mathbf{x}_i) [T_{n_4 n_3}]^\tau \text{sgn}(n_4) \mathcal{C}_{n_4 n_1}^{-+}(\mathbf{x}_i) \}. \end{aligned} \quad (2.37)$$

Here we used that $[T_{nn'}^2]^\tau = T_{n'n}^1$ and denoted $T \equiv T^1$. The two-particle propagators of the spin-1/2 particles may be further divided into its singlet and triplet components. This is done in detail in Appendix A.2.

As a first application of the effective action Eq. (2.36)-(2.37) we re-derive [10] the dephasing rates resulting from scattering at static magnetic impurities (that is in the limit where the Korringa relaxation time is very large, see below). We then proceed with a discussion of the dephasing rate extracted from various experiments in the full range of temperatures including the strong coupling regime $T \sim T_K$.

2.2 Dephasing by static magnetic impurities

The impact of static magnetic impurities on the dephasing rate measured in weak localization experiments was first studied by Larkin *et al.* [10]. For sake of completeness we describe their findings within the nonlinear σ -model. The separation of the Diffuson and Cooperon into its spin-singlet and

spin-triplet components is given in Appendix A.2. For static magnetic impurities, that is in the limit of high temperatures, $T \gg T_K$, performing a perturbative expansion in the coupling J is a well-defined procedure. One can use that the spin-spin correlation functions takes the form

$$\langle S^i S^j \rangle = \frac{1}{3} S(S+1) \delta_{ij}, \quad (2.38)$$

in order to find for the singlet-Diffuson (to second order in J)

$$\begin{aligned} S_S[\mathcal{D}_{S=0}^{++}] &= \frac{i\pi\nu}{2} \sum_{n_1 n_2} \sum_i \text{tr}_{\mathbf{R} \otimes \mathbf{S}} \{ \langle T \rangle \mathcal{D}_{S=0}^{++}(\mathbf{x}_i) \mathcal{D}_{S=0}^{++}(\mathbf{x}_i) + i\pi\nu \langle T \mathcal{D}_{S=0}^{++}(\mathbf{x}_i) T \rangle \mathcal{D}_{S=0}^{++}(\mathbf{x}_i) \} \\ &= \frac{i\pi\nu}{2} \langle S^i S^j \rangle \sum_{n_1 n_2} \sum_i \text{tr}_{\mathbf{R} \otimes \mathbf{S}} \{ -i\pi\nu J^2 \sigma_i^S \sigma_j^S \mathcal{D}_{S=0}^{++}(\mathbf{x}_i) \mathcal{D}_{S=0}^{++}(\mathbf{x}_i) + i\pi\nu J^2 \sigma_i^S \mathcal{D}_{S=0}^{++}(\mathbf{x}_i) \sigma_j^S \mathcal{D}_{S=0}^{++}(\mathbf{x}_i) \} \\ &= \frac{i\pi\nu}{2} \langle S^i S^j \rangle \sum_{n_1 n_2} \sum_i \text{tr}_{\mathbf{R} \otimes \mathbf{S}} \{ -i\pi\nu J^2 \sigma_i^S \sigma_j^S \mathcal{D}_{S=0}^{++}(\mathbf{x}_i) \mathcal{D}_{S=0}^{++}(\mathbf{x}_i) + i\pi\nu J^2 \sigma_i^S \mathcal{D}_{S=0}^{++}(\mathbf{x}_i) \sigma_j^S \mathcal{D}_{S=0}^{++}(\mathbf{x}_i) \} \\ &= 0. \end{aligned} \quad (2.39)$$

The triplet channels, on the other hand, give e.g. in the $m = 0$ channel

$$\begin{aligned} S_S[\mathcal{D}_{S=1,0}^{++}] &= \frac{i\pi\nu}{2} \langle S^i S^j \rangle \sum_{n_1 n_2} \sum_i \text{tr}_{\mathbf{R} \otimes \mathbf{S}} \{ -i\pi\nu J^2 \sigma_i^S \sigma_j^S \mathcal{D}_{S=1,0}^{++}(\mathbf{x}_i) \mathcal{D}_{S=1,0}^{++}(\mathbf{x}_i) + i\pi\nu J^2 \sigma_i^S \mathcal{D}_{S=1,0}^{++}(\mathbf{x}_i) \sigma_j^S \mathcal{D}_{S=1,0}^{++}(\mathbf{x}_i) \} \\ &= i\pi\nu J^2 \langle S_x S_x + S_y S_y \rangle \sum_{n_1 n_2} \sum_i \text{tr}_{\mathbf{R} \otimes \mathbf{S}} \{ -i\pi\nu \mathcal{D}_{S=0}^{++}(\mathbf{x}_i) \mathcal{D}_{S=0}^{++}(\mathbf{x}_i) \} \\ &= \frac{\pi\nu}{4} \frac{8\pi\nu J^2}{3} S(S+1) \sum_{n_1 n_2} \sum_i \text{tr}_{\mathbf{R} \otimes \mathbf{S}} \{ \mathcal{D}_{S=1}^{++}(\mathbf{x}_i) \mathcal{D}_{S=1}^{++}(\mathbf{x}_i) \}. \end{aligned} \quad (2.40)$$

and correspondingly for the $m = -1, 1$ components. For the Cooperon we employ that $[\sigma_i^S]^\tau = -\sigma_i^S$, to write for its singlet contribution

$$\begin{aligned} S_S[\mathcal{C}_{S=0}^{+-} \mathcal{C}_{S=0}^{-+}] &= \frac{i\pi\nu}{2} \sum_{n_1 n_2} \sum_i \text{tr}_{\mathbf{R} \otimes \mathbf{S}} \{ T \mathcal{C}_{S=0}^{+-}(\mathbf{x}_i) \mathcal{C}_{S=0}^{-+}(\mathbf{x}_i) + i\pi\nu T \mathcal{C}_{S=0}^{+-}(\mathbf{x}_i) T^\tau \mathcal{C}_{S=0}^{-+}(\mathbf{x}_i) \} \\ &= \frac{i\pi\nu}{2} \langle S^i S^j \rangle \sum_{n_1 n_2} \sum_i \text{tr}_{\mathbf{R} \otimes \mathbf{S}} \{ -i\pi\nu J^2 \sigma_i^S \sigma_j^S \mathcal{C}_{S=0}^{++}(\mathbf{x}_i) \mathcal{C}_{S=0}^{++}(\mathbf{x}_i) - i\pi\nu J^2 \sigma_i^S \mathcal{C}_{S=0}^{++}(\mathbf{x}_i) \sigma_j^S \mathcal{C}_{S=0}^{++}(\mathbf{x}_i) \} \\ &= i\pi\nu \langle S^i S^j \rangle \sum_{n_1 n_2} \sum_i \text{tr}_{\mathbf{R} \otimes \mathbf{S}} \{ -i\pi\nu J^2 \sigma_i^S \sigma_j^S \mathcal{C}_{S=0}^{++}(\mathbf{x}_i) \mathcal{C}_{S=0}^{++}(\mathbf{x}_i) \} \\ &= \frac{\pi\nu}{4} 4\pi\nu J^2 S(S+1) \sum_{n_1 n_2} \sum_i \text{tr}_{\mathbf{R} \otimes \mathbf{S}} \{ \mathcal{C}_{S=0}^{++}(\mathbf{x}_i) \mathcal{C}_{S=0}^{++}(\mathbf{x}_i) \}, \end{aligned} \quad (2.41)$$

and for the triplet channels (e.g. the $m = 0$ component)

$$\begin{aligned} S_S[\mathcal{C}_{S=1,0}^{+-} \mathcal{C}_{S=1,0}^{-+}] &= \frac{i\pi\nu}{2} \sum_{n_1 n_2} \sum_i \text{tr}_{\mathbf{R} \otimes \mathbf{S}} \{ T \mathcal{C}_{S=0}^{+-}(\mathbf{x}_i) \mathcal{C}_{S=0}^{-+}(\mathbf{x}_i) + i\pi\nu T \mathcal{C}_{S=0}^{+-}(\mathbf{x}_i) T^\tau \mathcal{C}_{S=0}^{-+}(\mathbf{x}_i) \} \\ &= \frac{i\pi\nu}{2} \sum_{n_1 n_2} J^2 2 \langle S_z S_z \rangle \sum_i \text{tr}_{\mathbf{R} \otimes \mathbf{S}} \{ -i\pi\nu \mathcal{C}_{S=0,1}^{+-}(\mathbf{x}_i) \mathcal{C}_{S=0,1}^{-+}(\mathbf{x}_i) \} \\ &= \frac{i\pi\nu}{4} \frac{4\pi\nu J^2}{3} S(S+1) \sum_{n_1 n_2} \sum_i \text{tr}_{\mathbf{R} \otimes \mathbf{S}} \{ \mathcal{C}_{S=1}^{++}(\mathbf{x}_i) \mathcal{C}_{S=1}^{++}(\mathbf{x}_i) \}, \end{aligned} \quad (2.42)$$

and correspondingly for the $m = -1, 1$ components. In summary, we recover for static magnetic impurities the known [10] dephasing rates for Diffuson and Cooperon, respectively, summarized in Table 2.1.

	singlet	triplet
Diffuson	0	$\frac{4}{3\tau_S}$
Cooperon	$\frac{2}{\tau_S}$	$\frac{2}{3\tau_S}$

Table 2.1: Dephasing rates for static magnetic impurities after averaging over impurity sites, with $1/\tau_S = 2\pi\nu n_S J^2 S(S+1)$

2.3 Dephasing due to dynamical magnetic impurities

Having set the stage, the rest of this chapter discusses the dephasing rates due to dynamical magnetic impurities as measured from the weak localization corrections to the Drude-conductivity, the universal conductance fluctuations (and more specific the Aharonov-Bohm oscillations) and the current echo.

The strategy to be followed is as follows: In a first paragraph we introduce the notion of the *elastic* and *inelastic* vertices. We derive an expression for the dephasing rate, τ_ϕ , resulting from contributions described by self-energy and elastic vertex diagrams. We then discuss corrections to the dephasing rate resulting from processes encoded in the inelastic vertex, from mixed diagrams containing scattering from static and the dynamical, magnetic impurities and from diagrams describing the scattering off different magnetic impurities. While the first part (introduction of the elastic and inelastic vertices) is kept general the second part specializes to the particular experiment used to extract the dephasing rate.

2.3.1 Introduction of elastic and inelastic vertices

We already mentioned that we are interested in experimental situations where only low concentrations of magnetic impurities are present. Therefore we only kept the leading (i.e. linear order) contributions in the impurity concentration n_S . Contributions from higher orders in n_S are considered later on. Performing the average over locations of magnetic impurities in the action Eqs. (2.36), (2.37) we find

$$\langle S_S[\mathcal{D}^{++}] \rangle = -\frac{n_S \pi \nu}{4} \sum_{n_1 n_2} \text{tr}_{\mathbf{R} \otimes \mathbf{S}} \left\{ T_{n_1 n_1} \text{sgn}(n_1) \mathcal{D}_{n_1 n_2}^{++}(\mathbf{q}) \mathcal{D}_{n_2 n_1}^{++}(-\mathbf{q}) \right. \\ \left. + i\pi \nu T_{n_1 n_2} \text{sgn}(n_2) \mathcal{D}_{n_2 n_3}^{++}(\mathbf{q}) T_{n_3 n_4} \text{sgn}(n_4) \mathcal{D}_{n_4 n_1}^{++}(-\mathbf{q}) \right\} \quad (2.43)$$

$$\langle S_S[\mathcal{C}^{+-}] \rangle = -\frac{n_S \pi \nu}{4} \sum_{n_1 n_2} \text{tr}_{\mathbf{R} \otimes \mathbf{S}} \left\{ T_{n_1 n_1} \text{sgn}(n_1) \mathcal{C}_{n_1 n_2}^{+-}(\mathbf{q}) \mathcal{C}_{n_2 n_1}^{+-}(-\mathbf{q}) \right. \\ \left. + i\pi \nu T_{n_1 n_2} \text{sgn}(n_2) \mathcal{C}_{n_2 n_3}^{+-}(\mathbf{q}) T_{-n_3, -n_4}^T \text{sgn}(n_4) \mathcal{C}_{n_4 n_1}^{+-}(-\mathbf{q}) \right\}, \quad (2.44)$$

where T denotes the T -matrix describing the scattering from a *single* magnetic impurity. In a next step we split up the vertex contribution into its elastic and inelastic contributions with the former taking into account only scattering processes from the magnetic impurities, where no energy is exchanged between the electron and hole lines (diagrammatically: no interaction lines are drawn between electron and hole lines), whereas the later allows for energy exchange between electron and hole lines (diagrammatically: interaction lines between electron and hole lines), see Fig. 2.3. Notice that the elastic vertex is just the product of the single-particle T -matrices for the electron and the hole.

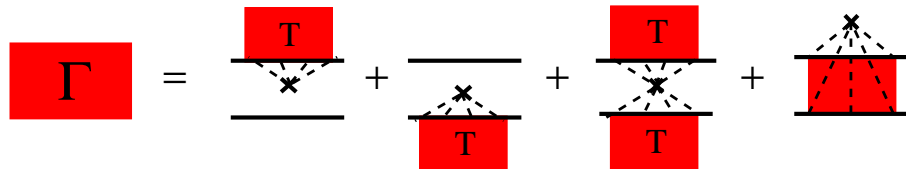


Figure 2.3: Separation of interaction vertex into its self-energy (first two), elastic vertex (third) and inelastic vertex (fourth) components, as defined in the text. All scattering processes take place at a single impurity.

The elastic + self-energy (S_{el}) and inelastic (S_{in}) contributions are given by

$$S_{\text{el}}[\mathcal{D}^{++}] = -\frac{n_S \pi \nu}{4} \sum_{n_1 n_2} \text{tr}_{\text{R} \otimes \text{S}} \left\{ T_{n_1 n_1} \text{sgn}(n_1) \mathcal{D}_{n_1 n_2}^{++}(\mathbf{q}) \mathcal{D}_{n_2 n_1}^{++}(-\mathbf{q}) \right. \\ \left. + i \pi \nu T_{n_1 n_1} \text{sgn}(n_1) \mathcal{D}_{n_1 n_2}^{++}(\mathbf{q}) T_{n_2 n_2} \text{sgn}(n_2) \mathcal{D}_{n_2 n_1}^{++}(-\mathbf{q}) \right\} \quad (2.45)$$

$$S_{\text{el}}[\mathcal{C}^{+-}] = -\frac{n_S \pi \nu}{4} \sum_{n_1 n_2} \text{tr}_{\text{R} \otimes \text{S}} \left\{ T_{n_1 n_1} \text{sgn}(n_1) \mathcal{C}_{n_1 n_2}^{+-}(\mathbf{q}) \mathcal{C}_{n_2 n_1}^{+-}(-\mathbf{q}) \right. \\ \left. + i \pi \nu T_{n_1 n_1} \text{sgn}(n_1) \mathcal{C}_{n_1 n_2}^{+-}(\mathbf{q}) T_{-n_2, -n_2}^\tau \text{sgn}(n_2) \mathcal{C}_{n_2 n_1}^{+-}(-\mathbf{q}) \right\}, \quad (2.46)$$

and

$$S_{\text{in}}[\mathcal{D}^{++}] = -\frac{n_S \pi \nu}{4} \sum_{n_1 n_2} \text{tr}_{\text{R} \otimes \text{S}} \left\{ i \pi \nu T_{n_1 n_2} \text{sgn}(n_2) \mathcal{D}_{n_2 n_3}^{++}(\mathbf{q}) T_{n_3 n_4} \text{sgn}(n_4) \mathcal{D}_{n_4 n_1}^{++}(-\mathbf{q}) \right\} \quad (2.47)$$

$$S_{\text{in}}[\mathcal{C}^{+-}] = -\frac{n_S \pi \nu}{4} \sum_{n_1 n_2} \text{tr}_{\text{R} \otimes \text{S}} \left\{ i \pi \nu T_{n_1 n_2} \text{sgn}(n_2) \mathcal{C}_{n_2 n_3}^{+-}(\mathbf{q}) T_{-n_3, -n_4}^\tau \text{sgn}(n_4) \mathcal{C}_{n_4 n_1}^{+-}(-\mathbf{q}) \right\}. \quad (2.48)$$

We proceed by restricting ourselves to study the impact of the self-energy and elastic vertex contributions (S_{el}) on dephasing, i.e. we neglect the last contribution in Fig. 2.3 (S_{in}) for the moment. Later on we analyze the impact of physical processes described by the inelastic vertex on dephasing (see below). We introduce the notation $\mathcal{C}_{n < 0, n' > 0}^{+-} = \bar{\mathcal{C}}_{nn'}^{+-}$, $\mathcal{C}_{n > 0, n' < 0}^{+-} = C_{nn'}^{+-}$, and correspondingly for \mathcal{C}^{+-} , \mathcal{D}^{++} and briefly mention that the symmetry-relation for the \mathcal{C}^{+-} (and correspondingly for the \mathcal{C}^{-+}) field reads $[\bar{\mathcal{C}}_{nn'}^{+-}]^\tau = -C_{n'n}^{+-}$ and $[\mathcal{C}_{nn'}^{+-}]^\tau = -\bar{C}_{n'n}^{+-}$. Furthermore, we employ that the single T-matrix, $\langle T \rangle$, is diagonal in S-space and that $\langle T_{-n, -n}^\tau \rangle = \langle T_{nn} \rangle$ and bring the standard σ -model action and the elastic vertex part to the form

$$S[\bar{\mathcal{D}}^{++} \mathcal{D}^{++}] = -\frac{\pi \nu}{2} \sum_{n_1 n_2} \int d^d \mathbf{q} (D \mathbf{q}^2 + \epsilon_{n_2} - \epsilon_{n_1} + \tau_\varphi^{-1}(n_1, n_2)) \text{tr}_{\text{S} \otimes \text{R}} \left\{ \bar{\mathcal{D}}_{n_1 n_1}^{++}(\mathbf{q}) \mathcal{D}_{n_2 n_1}^{++}(-\mathbf{q}) \right\} \quad (2.49)$$

$$S[\bar{\mathcal{C}}^{+-} \mathcal{C}^{+-}] = -\frac{\pi \nu}{2} \sum_{n_1 n_2} \int d^d \mathbf{q} (D \mathbf{q}^2 + \epsilon_{n_2} - \epsilon_{n_1} + \tau_\varphi^{-1}(n_1, n_2)) \text{tr}_{\text{S} \otimes \text{R}} \left\{ \bar{\mathcal{C}}_{n_1 n_2}^{+-}(\mathbf{q}) \mathcal{C}_{n_2 n_1}^{+-}(-\mathbf{q}) \right\}, \quad (2.50)$$

where ($n_1 < 0$, $n_2 > 0$)

$$\frac{1}{\tau_\varphi(n_1, n_2)} = \frac{2n_S}{\pi \nu} \left(\frac{\pi \nu}{2i} [T(\epsilon_{n_1}) - T(\epsilon_{n_2})] - (\pi \nu)^2 T(\epsilon_{n_1}) T(\epsilon_{n_2}) \right). \quad (2.51)$$

That is for $n_2 \rightarrow n_1$ and $q \rightarrow 0$, the standard σ -model action, S_σ , becomes massive; self-energy and elastic vertex contributions dress the bare propagator Eq. 2.34 with the mass (we analytically continue)

$$\frac{1}{\tau_\varphi(\epsilon)} = \frac{2n_S}{\pi \nu} [\pi \nu \text{Im} T^A(\epsilon) - |\pi \nu T^R(\epsilon)|^2]. \quad (2.52)$$

Notice, however, that for the Diffuson Eq. (2.52) is exactly canceled by inelastic vertex contributions. In fact, we will analyze in the following sections in what limits Eq. (2.49) is the dephasing rate for systems containing low concentrations of magnetic impurities as measured in WL, AB and current-echo experiments. Notice, that in the diagrammatic Greens function approach the massive propagators are given by the diagrams depicted in Fig 2.4. Since single particle lines conserve energy, the second term on the right hand side of the diagrammatic equation, depicted in Fig. 2.4(a), splits into a product of the single constituents, bare Cooperon, interaction vertex and massive Cooperon. Therefore the equation is easily solved and the massive Cooperon is obtained from summing up a geometric series.

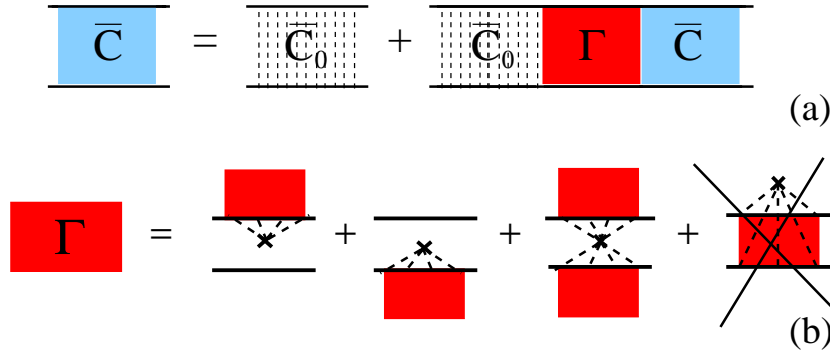


Figure 2.4: (a) Diagrammatic definition of the massive Cooperon given in Eq. (2.50). Here C_0 denotes the bare Cooperon and Γ is the interaction vertex containing self-energy and elastic vertex contributions, as defined in (b).

2.4 Dephasing-rate measured from the magnetoresistance

2.4.1 The dephasing rate measured in WL experiments

As already mentioned in the beginning of this section, the precise definition of the dephasing rate, and its experimental determination vary from context to context. In this paragraph we resort to the weak localization (WL) experiment to determine the dephasing rate. We already discussed that fitting the magnetoresistivity to WL theory allows to determine the dephasing rate with a high precision. As we specialize to the dephasing rate measured in WL experiments we may restrict ourselves to the Cooperon-contribution, as it constitutes the relevant degree of freedom for describing the physics of WL.

We start out from repeating the definition of the (homogeneous) dc-conductivity in the linear-response approximation, $\sigma = -\frac{K(\omega)}{i\omega}|_{\omega \rightarrow 0}$, where

$$K(\omega) \equiv \frac{1}{d} \sum_{i=1}^d \frac{\delta^2 F[\mathbf{a}]}{\delta \mathbf{a}_0^i(\omega_m) \delta \mathbf{a}_0^i(-\omega_m)} \Big|_{i\omega_m \rightarrow \omega + i0} \quad (2.53)$$

is the response kernel and \mathbf{a}_0 denotes the homogeneous component, $\mathbf{a}(\mathbf{q} = 0)$, of the vector potential. Performing the two-fold derivative of the partition function with respect to the vector potential we expand the obtained expression in fluctuation matrices $\bar{C}C$ around the saddle point Λ . Each power $(\bar{C}C)^k$ corresponds to quantum corrections of the order $(k_F l)^{-k}$ to the 0^{th} order classical value,

$$K_{mf}(\omega) = \frac{e^2 \pi \nu D}{\beta} \text{tr} \{ 2_{n_1} - \Lambda_{n_1} (\Lambda_{n_1+m} + \Lambda_{n_1-m}) \} = -2e^2 \nu D i\omega. \quad (2.54)$$

Eq 2.54 leads to the Drude conductivity $\sigma_{\text{Drude}} = 2e^2 \nu D$. In Appendix A.3 we work out the the response kernel up to quadratic order in the fluctuation matrices $\bar{C}C$. We show that the lowest order quantum corrections are given by $K(\omega) = \langle K_1(\omega) + K_2(\omega) \rangle_{\bar{C}C}$, where the average is taken with respect to the Gaussian action Eq. (2.49), i.e. $\langle \dots \rangle_{\bar{C}C} \equiv \int \mathcal{D}[\bar{C}C] e^{-S_o^2[\bar{C}C] - S_s^2[\bar{C}C]} (\dots)$ and

$$K_1(\omega) = \frac{e^2 \pi \nu D}{\beta} \text{tr} \{ \bar{C}_{n_1 n_2+m}^i(\mathbf{q}) C_{n_2 n_1+m}^i(-\mathbf{q}) \} \quad (2.55)$$

$$K_2(\omega) = \pm \frac{e^2 \pi \nu D}{2\beta} \text{tr} \{ \bar{C}_{n_1 n_2}^i(\mathbf{q}) C_{n_2 n_1}^i(-\mathbf{q}) |_{n_1 > -m} + \bar{C}_{n_1 n_2}^i(\mathbf{q}) C_{n_2 n_1}^i(-\mathbf{q}) |_{n_2 < m} \}, \quad m > 0. \quad (2.56)$$

The strategy to be followed is dictated by our previous calculations: We perform the average over the fluctuation matrices with respect to the massive σ -model action in Gaussian approximation. The

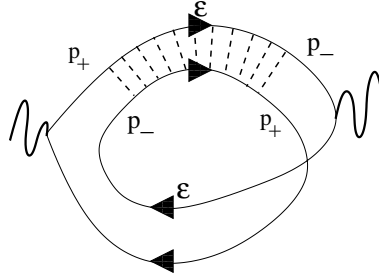


Figure 2.5: Diagrammatic representation of the weak localization corrections to the conductivity. Here $p_{\pm} = q/2 \pm p$ and curly lines denote current vertices.

contribution from the inelastic vertices on the other hand is accounted for by a perturbative treatment, i.e.

$$\langle \dots \rangle_{\bar{C}C} = \int \mathcal{D}[\bar{C}C] e^{-S^2[\bar{C}C]} \left(\dots \left[1 - S_{\text{in}}[\bar{C}C] + \frac{1}{2} S_{\text{in}}^2[\bar{C}C] + \dots \right] \right). \quad (2.57)$$

Corrections to the Drude conductivity zeroth order in the inelastic vertex are given by $\langle K_1 \rangle$, or more precisely

$$K_{\text{WL}}(\omega) = \frac{e^2 \pi \nu D}{\beta} \sum_{-m < n_1 < 0} \int (dq) \int \mathcal{D}[\bar{C}C] e^{-S[\bar{C}C]} \bar{C}_{n_1 n_1 + m}^i(\mathbf{q}) \bar{C}_{n_1 n_1 + m}^i(-\mathbf{q}). \quad (2.58)$$

Analytical continuation of Eq. (2.58) gives the WL corrections,

$$\Delta \sigma_{\text{WL}} = -\frac{2e^2 D}{\pi} \int d\epsilon f'(\epsilon) \int d^d \mathbf{q} \frac{1}{D \mathbf{q}^2 + 1/\tau_{\varphi}(\epsilon)}, \quad (2.59)$$

which are diagrammatically depicted in Fig. 2.5. For a concrete comparison with experiment we recall that the dephasing rate in Eq. (2.49) is still energy and temperature dependent. In order to find the energy-independent dephasing rate, $1/\tau_{\varphi}(T)$, measured in the experiment, we have to answer the question, which energy-independent $1/\tau_{\varphi}(T)$ gives the same WL correction as the $1/\tau_{\varphi}(\epsilon, T)$. Answering this question leads to

$$\frac{1}{\tau_{\varphi}(T)} = \begin{cases} \left[-\int d\epsilon f'(\epsilon) \tau_{\varphi}(\epsilon, T)^{\frac{2-d}{2}} \right]^{\frac{2}{d-2}} & d = 1, 3 \\ \exp \left[\int d\epsilon f'(\epsilon) \frac{1}{\tau} \ln \frac{\tau_{\varphi}(\epsilon, T)}{\tau} \right] & d = 2 \\ -\int d\epsilon f'(\epsilon) / \tau_{\varphi}(\epsilon, T) & \omega_B \tau_{\varphi} \gg 1, \end{cases} \quad (2.60)$$

where the last line is valid for all dimensions d in the presence of a sufficiently large magnetic field B which allows an expansion of the Cooperon in $1/(\omega_B \tau_{\varphi})$ (ω_B being the "cyclotron" frequency of the Cooperon).

Eq. (2.60) is the main result of this section. In order to find its range of applicability we have to estimate corrections arising from inelastic vertex contributions. Furthermore we have to estimate corrections arising from diagrams mixing interaction and impurity scattering processes. Finally we also have to analyze to what extent the approximation, to keep only linear contributions in n_S , is justified. Technically, the last two corrections are given by higher than 2^{nd} order contributions in \mathcal{CC} to the σ -model action. Working out and estimating the correction from these three classes of contributions will absorb the next three subsections. In order to illustrate the three classes of corrections we depict some diagrams making up the different corrections

1. Contributions from the inelastic vertex

$$\Gamma_{\text{inel.}} = \text{[diagram 1]} + \text{[diagram 2]} + \text{[diagram 3]} + \text{[diagram 4]} + \dots$$

2. Mixed interaction-disorder diagrams

$$\text{[diagram 1]} + \text{[diagram 2]} + \text{[diagram 3]} + \text{[diagram 4]} + \dots$$

3. Higher-order corrections in n_S

$$\text{[diagram 1]} + \text{[diagram 2]} + \text{[diagram 3]} + \text{[diagram 4]} + \dots$$

We start with a discussion of the contributions from the inelastic vertices.

2.4.2 1. Contributions from inelastic vertex

We start with the lowest order inelastic vertex corrections,

$$\langle K_1 + K_2 \rangle_{\bar{C}C} = \int \mathcal{D}[\bar{C}C] e^{-S^2[\bar{C}C]} [(K_1 + K_2) S_{\text{in}}[\bar{C}C]].$$

Performing the contractions gives a sum of two terms,

$$\Delta\sigma = \Delta\sigma_1 + \Delta\sigma_2, \quad (2.61)$$

where

$$\Delta\sigma_1 = \frac{\text{const.}}{i\omega} \left(\sum_{-m < n_1 < 0, n_2 > 0} + \sum_{n_1 < 0, 0 < n_2 < m} \right) \int (dq) \Pi_{n_1 n_2}^C(\mathbf{q}) \Pi_{n_1 n_2}^C(\mathbf{q}) \Gamma_{\text{inel}}(n_1, n_2) \quad (2.62)$$

$$\Delta\sigma_2 = \frac{\text{const.}}{i\omega} \sum_{-m < n_1 n_2 < 0} \int (dq) \Pi_{n_1 n_2 + m}^C(\mathbf{q}) \Pi_{n_2 n_1 + m}^C(\mathbf{q}) \Gamma_{\text{inel}}(n_1, n_2, m). \quad (2.63)$$

Here we introduced the inelastic vertex,

$$\Gamma_{\text{inel}}(n_1, n_2, m) = \Gamma^{(2)}(n_1, n_2, m) - J\Gamma^{(3)}(n_1, n_2, m) + J^2\Gamma^{(4)}(n_1, n_2, m),$$

with

$$\Gamma^{(2)}(n_1, n_2, m) \equiv 2 \langle S_{n_1 - n_2}^\alpha S_{n_2 - n_1}^\alpha \rangle \quad (2.64)$$

$$\Gamma^{(3)}(n_1, n_2, m) \equiv \langle S_{n_1 - n_2}^{\alpha\beta} (Sc)_{n_2}^\beta (c^\dagger S)_{n_1}^\alpha + S_{n_2 - n_1}^{\alpha\beta} (Sc)_{n_1 + m}^\beta (c^\dagger S)_{n_2 + m}^\alpha \rangle \quad (2.65)$$

$$\Gamma^{(4)}(n_1, n_2, m) \equiv \langle (Sc)_{n_1 + m}^\alpha (c^\dagger S)_{n_2 + m}^\beta (Sc)_{n_2}^\beta (c^\dagger S)_{n_1}^\alpha \rangle. \quad (2.66)$$

The analytical continuation of Eqs. (2.62) is done in detail in Appendix A.9, with the result

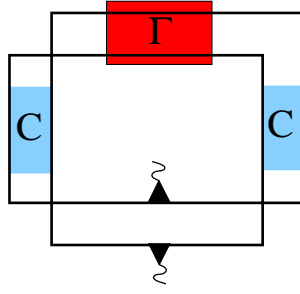


Figure 2.6: Lowest order correction to WL contributions due to inelastic vertex (denoted $\Delta\sigma_2$ in the text). Notice that this diagram only accounts for processes where the analytical structure of the single-particle propagators is *conserved* during the interaction processes. The Cooperon \bar{C} is dressed with the mass $1/\tau_\varphi$. Diagrams of this type become important for dephasing if the typical energy transfer ΔE is smaller than $1/\tau_\varphi$.

$$\Delta\sigma_1 = \text{const.} \int d\epsilon d\Omega \int (dq) \Pi_\Omega^C(\mathbf{q}) \Pi_\Omega^C(\mathbf{q}) \left(\frac{d}{d\epsilon} \tanh \left[\frac{\epsilon}{2T} \right] \right) \tanh \left[\frac{\epsilon + \Omega}{2T} \right] \Gamma_B(\epsilon, \Omega) \quad (2.67)$$

$$\Delta\sigma_2 = \text{const.} \int d\epsilon d\Omega \int (dq) \Pi_\Omega^C(\mathbf{q}) \Pi_{-\Omega}^C(\mathbf{q}) \left(\frac{d}{d\epsilon} \tanh \left[\frac{\epsilon}{2T} \right] \right) \left[\left(\coth \left[\frac{\Omega}{2T} \right] - \tanh \left[\frac{\epsilon + \Omega}{2T} \right] \right) \right. \\ \left. (\Gamma^2 - J\Gamma^3 + J^2\Gamma^4)(\epsilon, \Omega) + \left(\coth \left[\frac{2\epsilon + \Omega}{2T} \right] - \tanh \left[\frac{\epsilon + \Omega}{2T} \right] \right) J^2\Gamma^4(2\epsilon + \Omega, \Omega) \right]. \quad (2.68)$$

For a precise definition of the functions Γ^2 , Γ^3 , Γ^4 and Γ_B see Appendices A.9 and A.10. A diagrammatic representation of these two contributions is given in Fig.2.6 and Fig.2.7. We first turn to the contribution $\Delta\sigma_1$. We perform the momentum-integral over the two Cooperon-propagators and find

$$\Delta\sigma_1 = \text{const.} \int d\epsilon d\Omega \tanh \left[\frac{\epsilon + \Omega}{2T} \right] f^+(\epsilon, \Omega),$$

where

$$f^+(\epsilon, \Omega) = \left(\frac{d}{d\epsilon} \tanh \left[\frac{\epsilon}{2T} \right] \right) \frac{1}{(-i\Omega + 1/\tau_\varphi)^{(4-d)/2}} \Gamma_B(\epsilon, \Omega)$$

is an analytic function in the upper half-plane $\text{Im } \Omega > 0$. Employing the analytic structure of the above expression the Ω -integration can be done by summing up the poles at integer multiples of the temperature T . Therefore its contribution can be estimated as

$$\frac{\Delta\sigma_1}{\Delta\sigma_{\text{WL}}} \sim \left(\frac{1}{T\tau_\varphi} \right)^{(4-d)/2} \ll 1, \quad (2.69)$$

where the last inequality holds, since in the limit of small concentrations of magnetic impurities $T\tau_\varphi \gg 1$. Notice that the corrections $\Delta\sigma_1$ are always negligible as long as $T\tau_\varphi \gg 1$, independently of the nature of the interaction considered. That is, the function Γ_B does not enter the argument as the analytical structure is just determined by the diagram itself; no assumptions concerning the typical energy-transfer in the interaction process has to be made. In fact, we here just repeated an argument given by Aleiner *et al.* [7] in the context of dephasing due to Coulomb interactions in disordered metals.

Next, we turn to the second type of corrections, $\Delta\sigma_2$, arising from linear order inelastic vertex contributions,

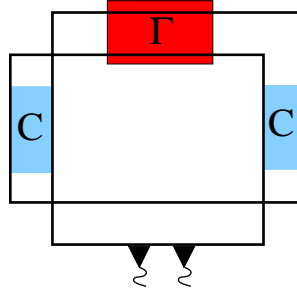


Figure 2.7: Different type of lowest order interaction correction to WL (denoted $\Delta\sigma_1$ in the text). This diagram contains only processes where the single particle lines *change* their analytical structure after the interaction process. The diagram describes self-energy corrections to the single particle propagator due to interactions (dressed with Cooperons) and is always irrelevant for dephasing. Again the Cooperon C is dressed with the mass $1/\tau_\varphi$.

$$\Delta\sigma_2 = \text{const.} \int d\epsilon d\Omega \left(\frac{d}{d\epsilon} \tanh \left[\frac{\epsilon}{2T} \right] \right) I_d(\Omega, \tau_\varphi) \left[\left(\coth \left[\frac{\Omega}{2T} \right] - \tanh \left[\frac{\epsilon + \Omega}{2T} \right] \right) (\Gamma^2 + J\Gamma^3 + J^2\Gamma_1^4)(\epsilon, \Omega) \right. \\ \left. + \left(\coth \left[\frac{2\epsilon + \Omega}{2T} \right] - \tanh \left[\frac{\epsilon + \Omega}{2T} \right] \right) J^2\Gamma_2^4(2\epsilon + \Omega, \Omega) \right],$$

where the function $I_d(\Omega, \tau_\varphi)$ results from the momentum-integral over the two Cooperons in a d -dimensional system. More interesting than its precise form, the structure of this term is given by

$$\Delta\sigma_2 = \int d\epsilon \int d\Omega \tilde{f}(\epsilon, \Omega) \Gamma_{\text{in}}(\epsilon, \Omega) I_d(\Omega), \quad (2.70)$$

where \tilde{f} denotes some thermal function restricting ϵ and Ω to values smaller than T , Γ_{in} is the inelastic vertex and in Appendix A.4 we show that $I_d(\Omega, \tau_\varphi) \sim [(1/\tau_\varphi)^2 + \Omega^2]^{\frac{d-4}{4}}$. Obviously the behavior of this integral depends on whether the typical energy transfer $\Delta E \sim \Omega$ is smaller or larger than $1/\tau_\varphi$. If $\Delta E \lesssim 1/\tau_\varphi$ then $\Delta\sigma_2$ is of the same order as $\Delta\sigma_{\text{WL}}$. However (see Appendix A.5), in the opposite limit one obtains

$$\frac{\Delta\sigma_2}{\Delta\sigma_{\text{WL}}} \sim \max \left\{ \left(\frac{1}{\Delta E \tau_\varphi} \right)^{(4-d)/2}, (\Delta E \tau_\varphi)^{-1} \right\} \lesssim \max \left\{ \left(\frac{n_S}{\nu T_K} \right)^{(4-d)/2}, \frac{n_S}{\nu T_K} \right\} \ll 1. \quad (2.71)$$

The typical energy transfer for interactions transmitted by Kondo impurities in the Fermi liquid regime $T \ll T_K$ is $\Delta E \approx T$ while for $T \gg T_K$ it is given by the life-time of the spin, i.e. $\Delta E \approx T / \ln^2[T/T_K]$. The precise values do, however, not matter. The main observation is that $1/\tau_\varphi$ vanishes linearly with n_S while ΔE is independent of n_S . Therefore the criterion $\Delta E \tau_\varphi \gg 1$ is always fulfilled if n_S is sufficiently small, or more precisely for $n_S \ll \nu T_K$ where we used that at $T \approx T_K$ one has $\Delta E \sim T_K$ and $1/\tau_\varphi \sim n_S/\nu$, see below. In conclusion, whether the corrections $\Delta\sigma_2$ become important or not depends — in contrast to the corrections $\Delta\sigma_1$ — on the physical nature of the interaction under consideration. In the case of interactions transmitted by diluted Kondo impurities, their contribution is negligible.

The observation that inelastic vertex corrections are only relevant for processes with energy transfer smaller than $1/\tau_\varphi$ has been made before by several authors (e.g. [1]) in the context of Coulomb interaction and can be easily understood using semi-classical arguments: Inelastic vertex corrections describe the interference of two (time-reversed) electrons undergoing the same interaction process (see Fig. 2.8). As energy is transferred, the two electrons collect after time t a phase factor of the order of $e^{i\Delta E t}$. Since the typical time-scale of a weak localization experiment is τ_φ , no interference will take place if $\Delta E \gg 1/\tau_\varphi$, while quasi-static processes with $\Delta E \ll 1/\tau_\varphi$ do not lead to dephasing. Put

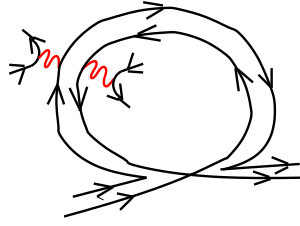


Figure 2.8: Illustration of second order inelastic vertex process. Electron and hole undergo the same interaction process and pick up a phase difference $e^{i\Delta E t}$, where ΔE denotes the amount of energy exchanged in the interaction process and $t \sim \tau_\varphi$ is the time needed to traverse the closed loop. Interference effects are destroyed if $\Delta E \gg 1/\tau_\varphi$.

differently, interactions with energy transfer smaller than the dephasing rate correspond to fluctuations of the bath on time-scales exceeding the typical propagation time of the electron-hole pair, i.e. to fluctuations which are static from the Cooperon's point of view. Such fluctuations, therefore, cannot cause dephasing and have to be extracted from the inelastic scattering rate. Precisely this is achieved by the inelastic vertex contributions. Dephasing by Coulomb interactions in $d \leq 2$, for example, is dominated by low-energy transfers, and inelastic vertex corrections are important to control the infrared divergences [1]. This, however, is not the case for diluted Kondo impurities and therefore the inelastic vertex corrections may be neglected.

The above argument readily generalizes from the lowest, i.e. linear order to arbitrary orders in the number of inelastic vertices. As the typical width of the inelastic vertex is always large, the integrals over the transferred energy always smear out the sharp structures due to Cooperons with a width given by $1/\tau_\varphi$ leading to a suppression in some (positive) powers of $1/(T\tau_\varphi)$ or $1/(\Delta E\tau_\varphi)$.

Note on Korringa relaxation rate: The typical energy transfer ΔE is also known as the Korringa relaxation rate, which for high temperatures $T \gg T_K$ takes the form

$$\Delta E = \frac{1}{\tau_K} \sim \nu n_e J^2 \frac{T}{E_F}, \quad (2.72)$$

where n_e is the electron density. Meyer *et al.* argued in [18] that, in order to study the influence of magnetic impurities on the WL, one has to distinguish two different limits, corresponding to whether $\frac{1}{\tau_K}$ is smaller or bigger than the spin flip rate,

$$\frac{1}{\tau_S} \sim \nu n_S J^2 S(S+1). \quad (2.73)$$

In the former case (realized at temperatures above T_S , where Eq. (2.72) equals Eq. (2.73), i.e. $1/\tau_K(T_S) = 1/\tau_S$) the impurity states seen by electrons propagating in opposite directions are uncorrelated and the Cooperon acquires the mass $\frac{1}{\tau_S}$. In the later case (realized at temperatures $T < T_S$) a single spin-flip does not completely destroy coherence between clock- and anti-clockwise paths and decoherence in the spin singlet and spin triplet channels are different (decoherence in the triplet channel takes three times longer than in the singlet). The temperature discriminating the two regimes is $T_S \sim \frac{n_S}{n_e} E_F$. As we study the case of diluted magnetic impurities we are always in the limit $T \gg T_S$, or equivalently $\frac{1}{\tau_K} \gg \frac{1}{\tau_S}$.

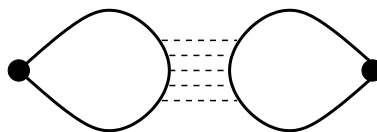


Figure 2.9: Diagrammatic representation of the fluctuations of the LDOS leading to fluctuations in the Kondo temperature. The evaluation of the diagram can be found in Appendix A.7.

2.4.3 2. Contributions from mixed diagrams

We next turn to the discussion of the second class of corrections arising due to the interplay of disorder and interaction processes, as e.g. shown in Fig. 2.10(a). These type of corrections arise from higher than second order in the fluctuation matrices \mathcal{C} . The diagram in Fig 2.10(a), for example, represents a “disorder-dressed” interaction process, which in the σ -model approach results from a contraction (symbolically) of the form

$$n_S \langle \text{tr} \{ T \mathcal{C}(\mathbf{q}) \mathcal{C}(-\mathbf{q}) \} \text{tr} \{ T \mathcal{C}(\mathbf{q}) \mathcal{C}(-\mathbf{q}) \} \rangle_{S_\sigma^2[\mathcal{C}]} \sim n_S \langle \text{tr} \{ T \Pi^{\mathcal{C}} T \mathcal{C}(\mathbf{q}) \mathcal{C}(-\mathbf{q}) \} \rangle \quad (2.74)$$

Here $T \Pi^{\mathcal{C}} T$ is just the T -matrix dressed by a Cooperon, as entering in Fig. 2.10(a). We are only interested in parametric dependencies (i.e. in orders of magnitudes) and resort to diagrammatic perturbation theory for the estimation of such corrections. A preliminary indication as to the relevance of such contributions may already be obtained by estimating the sample-to-sample fluctuations of the Kondo temperature, T_K . For details we refer to Appendix A.7, and here merely state that

$$\left(\frac{\delta T_K}{T_K} \right)^2 = \frac{1}{\nu^2} \int_{T_K}^{E_F} d\omega \int_{T_K}^{E_F} d\omega' \frac{\langle \delta \nu(\omega) \delta \nu(\omega') \rangle_V}{\omega \omega'}. \quad (2.75)$$

Substituting the results for the fluctuations of the local density of states $\delta \nu$ (see Fig. 2.9) in weakly disordered d -dimensional metals (which is calculated in Appendix A.7) we obtain

$$\left(\frac{\delta T_K}{T_K} \right)^2 \sim \begin{cases} \frac{1}{(k_F L_\perp)^2} \frac{1}{\sqrt{\tau} T_K} & \text{in (quasi) } d = 1, \\ \frac{1}{k_F l} \frac{1}{(J\nu)^3} & \text{in } d = 2, \\ \frac{1}{(k_F l)^2} \frac{1}{(J\nu)^2} & \text{in } d = 3, \end{cases} \quad (2.76)$$

where L_\perp is the transversal extension of a quasi one-dimensional wire. In the following we will always assume that $k_F l$ is sufficiently large, such that $\delta T_K \ll T_K$. While this condition seems to be fairly restrictive in quasi-1d, it turns out to be always met in the WL regime, $\Delta \sigma^{\text{WL}} \ll \sigma^{\text{Drude}}$, realized in experiments (and assumed in this work).

As already stated, more formally the role of correlations disorder/interactions may be explored in terms of the diagrams shown in Fig. 2.10(a). On the face of it, these diagrams are smaller by factors of $1/(k_F l)$ than the leading contributions considered above (as quantum interference maintained across the impurity limits the momentum exchanged to values $\lesssim l^{-1}$ much smaller than k_F). However, for very low T the enhanced infrared singularity caused by the presence of extra diffusion modes may over-compensate this phase space suppression factor. Using that for $T \ll T_K$, the bare interaction may be described by Fermi liquid theory [19], we find that only in (quasi-) one dimensional systems these diagrams ($\propto T^{(d+2)/2} + T^2$) lead to contributions of anomalously strong singularity. Specifically, for a quasi-one dimensional system we obtain a correction to the dephasing rate, $1/\tau_{\varphi,c} \sim n_S T^{3/2} / [\nu T_K^2 \sqrt{\tau} (k_F L_\perp)^2]$. Therefore, for temperatures

$$T \lesssim \frac{1}{(k_F L_\perp)^4} \frac{1}{\tau T_K} T_K \ll T_K \quad (2.77)$$



Figure 2.10: Diagrammatic representation of (a) corrections from mixed diagrams and (b) corrections from higher orders in n_S . The evaluation of the diagrams is given in Appendices A.7 and A.8.

the separation disorder/interactions used above becomes invalid in $d = 1$. Notice that the cross-over temperature is proportional to the Kondo-temperature, with the proportionality constant just given by the (square of) the same small number that we found from estimations of the Kondo-temperature fluctuations. In order to get an idea of the order of magnitude of the cross-over temperature, we give its values for the experiments on (quasi)-1d wires recently performed by Mallet *et al.* [14] in the summary of this section.

2.4.4 3. Contributions from higher-order corrections in n_S

At very low T , yet another type of corrections begins to play a role: The diluted Kondo impurities become indistinguishable from a conventional disordered Fermi liquid with short-range momentum-conserving interactions [20] and the dephasing rate is determined by Altshuler-Aronov-Khmelnitsky [1, 20] type processes which, in our context, are encapsulated in the third family of diagrams shown in Fig. 2.10(b). Technically, the σ -model expression are of similar form as those considered in the analysis of the interplay between disorder and interaction processes, i.e. (symbolically)

$$n_S^2 \langle \text{tr} \{TC(\mathbf{q})\mathcal{C}(-\mathbf{q})\} \text{tr} \{TC(\mathbf{q})\mathcal{C}(-\mathbf{q})\} \rangle_{S^2[C]} \sim n_S^2 \langle \text{tr} \{TII TC(\mathbf{q})\mathcal{C}(-\mathbf{q})\} \rangle. \quad (2.78)$$

Yet, involving spin correlation functions for spins situated at different places, the momentum conserving short-ranged interaction is screened, see Appendix A.8 for details. Contributing only at order n_S^2 these contributions generate corrections scaling as $T^{2/3}$, T , and $T^{3/2}$ in $d = 1, 2, 3$, respectively. Evaluating the prefactor again in Fermi liquid theory (see Appendices A.8) we find that these contributions become sizable at temperatures below

$$T \lesssim \begin{cases} \frac{1}{(k_{\text{F}l})^4} \left(\frac{n_S}{\nu T_K} \right)^2 \tau T_K^2 & d = 3 \\ \frac{1}{k_{\text{F}l}} \frac{n_S}{\nu T_K} T_K & d = 2 \\ \frac{1}{k_{\text{F}l\perp}} \frac{1}{(\tau T_K)^{1/4}} \left(\frac{n_S}{\nu T_K} \right)^{1/4} T_K & d = 1. \end{cases} \quad (2.79)$$

In all cases the crossover scale is well below T_K and may arguably be neglected in all relevant experiments. Further corrections to $1/\tau_\varphi$ of order n_S^2 and higher arise from clusters of two and more magnetic impurities which are sufficiently close such that the inter-impurity coupling dominates over the Kondo effect [21]. Typical values (using the data from experiments by Mallet *et al.* [14]) for the cross-over temperature, indicating when n_S^2 -corrections become important, can be found in the summary of the section.

2.4.5 Interplay: Kondo effect and electron-electron interactions

In passing to the next section, we notice that in the comparison to concrete experiments one needs to account for the interplay of dephasing due to magnetic impurities and due to Coulomb interactions [1]. Since the latter are controlled by infrared divergences in $d \leq 2$, the respective rates do not simply add. Instead one needs to solve, e.g. in quasi one-dimensional systems, the equation

$$\frac{1}{\tau_\varphi} = \kappa T \sqrt{\tau_\varphi} + \frac{1}{\tau_{\varphi,S}} \approx \begin{cases} (\kappa T)^{2/3} + 2/(3\tau_{\varphi,S}) \\ 1/\tau_{\varphi,S} + \kappa T \sqrt{\tau_{\varphi,S}}, \end{cases} \quad (2.80)$$

where the first term describes the self-consistently calculated effects of Coulomb interactions while $1/\tau_{\varphi,S}$ is the dephasing rate due to the magnetic impurities. The first (second) line holds when the Coulomb dephasing (Kondo dephasing) dominates.

2.5 Summary

In this section we established

$$\frac{1}{\tau_\varphi(\epsilon, T)} = \frac{2n_S}{\pi\nu} (\pi\nu \operatorname{Im} T^A(\epsilon) - |\pi\nu T^R(\epsilon)|^2) \quad (2.81)$$

(and its energy averaged version, Eq. (2.60)) as the dephasing rate due to diluted Kondo impurities as measured in the WL experiment. Since $\pi\nu \operatorname{Im} T^A$ is proportional to the *total* cross section, while $|\pi\nu T^R|^2$ describes the *elastic* cross section their difference is just the *inelastic* cross section. The vanishing of the inelastic cross section for static impurities is guaranteed by the optical theorem. The factor $\tau_{\text{hit}} = \frac{\pi\nu}{2n_S}$ denotes the typical time the electron needs to scatter from a magnetic impurity, see next section.

Universality of τ_φ : In order to discuss universality of our result Eq. (2.81) one should be more precise and distinguish between local and thermodynamic DOS. To be precise, Eq. (2.81) reads

$$\frac{1}{\tau_\varphi(\epsilon, T)} = \frac{2n_i}{\pi\nu} \left[\pi\nu^{\text{loc}} \operatorname{Im} [T^A(\epsilon)] - |\pi\nu^{\text{loc}} T^R(\epsilon)|^2 \right], \quad (2.82)$$

where ν^{loc} is the *local* density of states at the Fermi energy at the site of the impurity which can differ from the thermodynamic density of states entering the prefactor. In the case of Kondo impurities, the combination $\nu^{\text{loc}} T^{R/A}(\epsilon) = f(\epsilon/T_K, T/T_K, B/T_K)$ is an *universal* dimensionless function of the ratios $\epsilon/T_K, T/T_K, B/T_K$. If the assumptions underlying the derivation of Eq. (2.82) are valid, one therefore can predict, *without* any free parameter, the dephasing rate if the concentration of spin-1/2 impurities, the Kondo temperature and the thermodynamic density of states are known. However, one of the assumptions underlying the derivation of the prefactor of Eq. (2.82) may not be valid in realistic materials: we assumed that the static impurities are completely uncorrelated and local such that electrons are scattered uniformly over the Fermi surface. While this should be a good assumption in doped semiconductors, this may not be valid in metals with complex Fermi surfaces and strongly varying Fermi velocities. Under the latter conditions, we expect that the prefactor of Eq. (2.82) becomes non-universal, obtaining temperature-independent corrections of order unity, which may be important for the interpretation of the high-precision experiments discussed below.

Some orders of magnitude: In order to provide an idea below which temperatures Eq. (2.81) loses its applicability table 2.3 gives some typical values for the crossover temperatures. These values were calculated for the system parameters summarized in table 2.2 and belong to (quasi)-1 dimensional wires on which Mallet *et al.* [14] recently measured the dephasing rate due to diluted Kondo impurities. Notice that for DOS of the order $\nu \sim 10^{41} \text{ J}^{-1} \text{ cm}^{-3}$ a measured dephasing rate of order $1/\tau_\varphi \sim 10 \text{ ns}$ corresponds to concentrations $n_S \sim 10^{16} \text{ cm}^{-3}$ which is of the order of parts per million (ppm).

Sample	n_S (ppm)	τ (10^{-14} s)	D (cm^3/s)
AgFe1	2.7	2.2	429
AgFe2	27	2.1	400
AgFe3	67.5	1.9	360

Table 2.2: Material parameters for three Ag wires on which Mallet *et al.* [14] recently performed WL experiments to extract $1/\tau_\varphi$ due to diluted Kondo impurities (see also the end of this chapter, “Comparison to recent experiments and outlook”). Here we used the Fermi velocity for the free electron gas, $v_F = 1.39 \times 10^8 \text{ cm/s}$, in order to obtain the value for the mean scattering time τ .

2.6 Generalizations

In this section we generalize formula Eq. (2.52) for the dephasing rate due to Kondo impurities as measured in the WL experiment to account for dephasing due to scattering from *arbitrary* diluted

Sample	$n_S/(\nu T_K)$	$T^{(1)} (T_K)$	$T^{(2)} (T_K)$
AgFe1	0.04	$\lesssim 10^{-10}$	0.03
AgFe2	0.4	$\lesssim 10^{-10}$	0.02
AgFe3	0.9	$\lesssim 10^{-10}$	0.02

Table 2.3: Values for the parameter $n_S/(\nu T_K)$ and temperatures limiting the applicability of Eq. (2.81) as obtained from the values summarized in Table 2.2. Here $T^{(1)} = \frac{1}{(k_F L_\perp)^4} \frac{1}{\tau T_K} T_K$ and $T^{(2)} = \frac{1}{k_F L_\perp} \left(\frac{1}{\tau T_K} \right)^{1/4} \left(\frac{n_S}{\nu T_K} \right)^{1/4} T_K$. Furthermore we use the values $L_\perp = 90$ nm [14], $\nu_F^{\text{Ag}} = 1.03 \times 10^{41}$ J $^{-1}$ cm $^{-3}$ [5], and a Kondo temperature $T_K = 4$ K [14]. Notice that for high concentrations, $n_S = 67.5$ ppm, $n_S/(\nu T_K)$ becomes of the order of 1.

dynamical impurities (for which the typical energy transfer is larger than $1/\tau_\varphi$) as measured from WL. To be specific we consider a Hamiltonian of the general form

$$H_{\text{imp}} = H_{\text{imp}}^0 + \sum_i c_{\mathbf{k}\sigma}^\dagger c_{\mathbf{k}'\sigma'} f_{\mathbf{k}\mathbf{k}'\sigma\sigma'}^\alpha \hat{X}_\alpha e^{i(\mathbf{k}-\mathbf{k}')\mathbf{x}_i}, \quad (2.83)$$

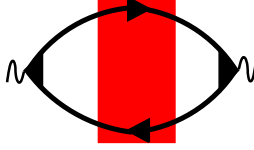
where H_{imp}^0 is the Hamiltonian of the isolated impurity, c^\dagger, c are creation and annihilation operators of conduction band electrons, \mathbf{x}_i denotes the position of the impurities, and the momentum and spin dependent function f^α parametrizes the coupling to some operator \hat{X}_α describing transitions of the internal states of the dynamical impurity. Eq. (2.83), e.g., describes the coupling of the conduction band electrons to Kondo impurities, two-level systems, etc. We use the strategy of the last section, in order to find the dephasing rate generated by the operator of Eq. (2.83). As argued above, diagrams mixing scattering from dynamical and static impurities are suppressed by factors of a/l or $1/(k_F l)$ for $a < 1/k_F$ where a is the typical diameter of the dynamical impurity. For small concentrations, n_i , one can furthermore restrict the analysis of the irreducible vertex Γ to terms linear in n_i and neglect contributions from the inelastic vertex (see Fig. 2.4). The latter can be neglected, since $\Delta E \tau_\varphi \gg 1$ always holds for sufficiently small n_i , as $1/\tau_\varphi$ scales with the concentration. Summing up a geometric series, as in the last section, one finds for the energy-dependent dephasing rate, $1/\tau_\varphi(\epsilon, T)$,

$$\begin{aligned} \frac{1}{\tau_\varphi(\epsilon, T)} = \frac{2n_i}{\pi\nu} & \left[\int \frac{d^3\mathbf{p}}{(2\pi)^3} g_\epsilon(\mathbf{p}) \frac{1}{2i} [T_{-\mathbf{p}, -\mathbf{p}}^{\text{A}}(\epsilon) - T_{\mathbf{p}\mathbf{p}}^{\text{R}}(\epsilon)] \right. \\ & \left. - \int \frac{d^3\mathbf{p}}{(2\pi)^3} \int \frac{d^3\mathbf{p}'}{(2\pi)^3} g_\epsilon(\mathbf{p}) g_\epsilon(\mathbf{p}') T_{\mathbf{p}\mathbf{p}'}^{\text{R}}(\epsilon) T_{-\mathbf{p}, -\mathbf{p}'}^{\text{A}}(\epsilon) \right]. \end{aligned} \quad (2.84)$$

Here $g_\epsilon(\mathbf{p}) = \frac{\pi/2\tau}{[\epsilon(\mathbf{p}) - \epsilon]^2 + \frac{1}{4\tau^2}}$ restricts the electrons momenta, \mathbf{p} , and energies, ϵ , to the Fermi-surface, $\epsilon(\mathbf{p})$ is the dispersion relation of the conduction band, $T^{\text{A},\text{R}}$ are the advanced/retarded T-matrices and ν denotes the density of states per spin. Eq. (2.84) generalizes the result for Kondo impurities to arbitrarily shaped diluted impurities (for which the typical energy transfer exceeds the dephasing rate). Notice that also forward scattering processes enter $1/\tau_\varphi$, which do not contribute to the transport scattering rate (see Fig. 2.11). We stress that Eq. (2.84) is the general result for the dephasing rate for a weakly disordered metal due to a low concentration of *generic* dynamical impurities for which the condition $\Delta E \gg 1/\tau_\varphi$ holds. As we assumed that $a \ll l$, Eq. (2.84) can be further simplified,

$$\frac{1}{\tau_\varphi(\epsilon, T)} = \frac{2n_i}{\pi\nu} \left[\int_{S_F^\epsilon} \frac{d^2\mathbf{p}}{(2\pi)^3} \frac{1}{|v_F(\mathbf{p})|} \text{Im} [\pi T_{\mathbf{p}\mathbf{p}}^{\text{A}}(\epsilon)] - \int_{S_F^\epsilon} \frac{d^2\mathbf{p}}{(2\pi)^3} \int_{S_F^\epsilon} \frac{d^2\mathbf{p}'}{(2\pi)^3} \frac{1}{|v_F(\mathbf{p})|} \frac{1}{|v_F(\mathbf{p}')|} |\pi T_{\mathbf{p}\mathbf{p}'}^{\text{R}}(\epsilon)|^2 \right], \quad (2.85)$$

where S_F^ϵ is the Fermi-surface (or more precisely the surface with $\epsilon_k = \epsilon$). Here we also assumed a time-reversal invariant system with $T_{\mathbf{p}\mathbf{p}'}^{\text{R}}(\epsilon) = T_{-\mathbf{p}', -\mathbf{p}}^{\text{R}}(\epsilon)$ and employed the identity $[T_{\mathbf{p}\mathbf{p}'}^{\text{R}}(\epsilon)]^* = T_{\mathbf{p}'\mathbf{p}}^{\text{A}}(\epsilon)$. Again, we notice that the dephasing rate given in Eq. (2.85) is proportional to the *inelastic* cross section,



$$\sim n_i \sigma^{\text{Drude}} \int d\epsilon [f'_F(\epsilon)] \left(\int d^d \mathbf{p} \frac{1}{2i} g_{E_F}(\mathbf{p}) [T_{\mathbf{p}\mathbf{p}}^R - T_{-\mathbf{p}, -\mathbf{p}}^A] \right. \\ \left. - \int d^d \mathbf{p} \int d^d \mathbf{p}' \cos \theta g_{E_F}(\mathbf{p}) g_{E_F}(\mathbf{p}') T_{\mathbf{p}\mathbf{p}'}^R T_{-\mathbf{p}, -\mathbf{p}'}^A \right)$$

Figure 2.11: Corrections to the Drude conductivity σ^{Drude} due to diluted dynamical impurities with concentration n_i . The vertex contribution contains a dependence on the angle θ between \mathbf{p} and \mathbf{p}' . Notice that for static impurities only forward scattering processes do not contribute to the corrections.

σ_{inel} , i.e. Eq. (2.85) can be rewritten in the form

$$\frac{1}{\tau_\varphi(\epsilon)} = n_i \langle v_F(\mathbf{p}) \sigma_{\text{inel}}(\mathbf{p}, \epsilon) \rangle, \quad (2.86)$$

where $\langle \dots \rangle$ denotes an angular average weighted by $1/v_F(\mathbf{p})$ to take into account that fast electrons are scattered more frequently from elastic impurities. According to Eq. (2.86), τ_φ is nothing but the average time needed (in a semiclassical picture) to scatter from an impurity with cross section σ_{inel} . Notice that the vanishing of $1/\tau_\varphi$ for static impurities is, again, guaranteed by the optical theorem.

It is instructive to rewrite Eq. (2.86) in the following way

$$\frac{1}{\tau_\varphi} = \frac{1}{\tau_{\text{hit}}} \frac{\langle \sigma_{\text{inel}} \rangle}{\sigma_{\text{max}}}, \quad (2.87)$$

where $\sigma_{\text{max}} = 4\pi/k_F^2$ is the cross section of a unitary scatterer, $\sigma_{\text{inel}}/\sigma_{\text{max}}$ is the conditional probability of *inelastic* scattering if an electron hits the impurity and

$$\frac{1}{\tau_{\text{hit}}} = \frac{2n_i}{\pi\nu} \quad (2.88)$$

describes the typical 'hitting rate'. The estimates of sub-leading corrections presented in the last section can be generalized to extended dynamical impurities by replacing $1/(k_F l)$ by a/l for $k_F a > 1$.

2.7 Dephasing-rate measured from universal conductance fluctuations and Aharonov-Bohm oscillations

Introduction: An obvious possibility to study the influence of magnetic impurities on the dephasing rate is to measure its dependence on an externally applied magnetic field. The application of sufficiently large magnetic fields freezes out inelastic spin-flip processes and therefore one expects the dephasing rate to return to the value predicted by AAK for dephasing induced by Coulomb interactions in a diffusive environment [1]. Methods to extract the dephasing rate apart from the WL experiment discussed above include measurements of the universal conductance fluctuations (UCF) of metals and the determination of the Aharonov-Bohm (AB) oscillations in the magneto-conductance of metallic rings. (We propose a further theoretical procedure relying on the current echo, see below.) Measuring the magnetic field dependence of $1/\tau_\varphi$ in such experiments, however, one carefully has to separate direct from indirect magnetic field effects. That is, application of an external magnetic field B directly influences the interference effect probed while the B -dependence of the dephasing rate due to the presence of diluted magnetic impurities is only an indirect effect. Indeed, we mentioned that the WL base on the constructive interference occurring during the joined propagation of an electron and a hole along *time-reversed* trajectories (the Cooperon), which requires time-reversal symmetry in the system and therefore is heavily disturbed by external magnetic fields: The orbital contribution of the magnetic field destroys the weak-localization (WL) contribution to the magneto-resistance, as the joined propagation of an electron and a hole along time-reversed trajectories picks up extra (random) Aharonov-Bohm phases. Measuring the B -dependent dephasing rate in a WL experiment is therefore only possible in strictly one- or two-dimensional systems using magnetic fields almost exactly parallel to such a structure, requiring an accurate alignment of magnetic fields.

The UCF and AB oscillations, on the other hand, rely on the constructive interference occurring in the joined propagation of electrons and holes traveling along the *same* path (the Diffuson). These are robust against the breaking of time-reversal invariance. The external magnetic field enters the metal and changes the pattern of the electrons wave functions. It therefore effectively acts as an ensemble average leading to fluctuations in the conductance of the system as a function of B , and provides a characteristic signature (“magneto fingerprint”). In the AB experiment these sample fluctuations are further modulated by periodic \hbar/e -oscillations resulting from the change of the boundary conditions, due to magnetic flux lines piercing the ring. In [13], we discussed the magnetic field dependence of $1/\tau_\varphi$ as measured in AB experiments. This section briefly summarizes the main points.

Dephasing Rate from Universal Conductance Fluctuations: In the following we concentrate on wires, i.e. on quasi 1-dimensional geometries. We include the effect of an external magnetic field, B , by accounting for the Zeeman splitting, ϵ_z , of the conduction band electron spin states,

$$\epsilon_z = g_e \mu_B B, \quad (2.89)$$

and by coupling the impurity spins to the external field according to

$$H_B = g_S \mu_B B \sum_i \hat{S}_i^z. \quad (2.90)$$

g_e , g_S are the electrons and the magnetic impurities gyromagnetic factors, respectively. The static conductance g of the wire is related to the conductivity $\sigma(\mathbf{x}_1, \mathbf{x}_2)$ as

$$g = \frac{1}{L^2} \int d\mathbf{x}_1 d\mathbf{x}_2 \sigma(\mathbf{x}_1, \mathbf{x}_2). \quad (2.91)$$

The calculation of the sample-to-sample fluctuations,

$$\text{var } g = \langle g^2 \rangle - \langle g \rangle^2, \quad (2.92)$$

within the field theoretical approach is most comfortably done by enlarging the field space of the starting electron fields by a two-dimensional fluctuation sector F (see e.g. [16]) The source (vectorpotential) becomes a matrix in F -space, $\mathbf{a} = \begin{pmatrix} \mathbf{a}^1 & \\ & \mathbf{a}^2 \end{pmatrix}_F$, and one obtains the fluctuations by means of a functional derivative of the free energy,

$$\text{var } \sigma = \frac{1}{\omega_{m_1} \omega_{m_2}} \frac{\delta^4 F[\mathbf{a}]}{\delta \mathbf{a}_{m_1}^1 \delta \mathbf{a}_{-m_1}^1 \delta \mathbf{a}_{m_2}^2 \delta \mathbf{a}_{-m_2}^2} \Big|_{i\omega_{m_1}, i\omega_{m_2} \rightarrow i0}. \quad (2.93)$$

Connected diagrams contain only components of the generators W , which are off-diagonal in F -space. In Appendix A.3 we elaborate the expression given in Eq. (2.93) and rederive (see e.g. [32]) that

$$\text{var } \sigma = K_\nu + K_D, \quad (2.94)$$

where

$$K_\nu = \frac{(e^2 \pi \nu D)^2}{\beta^2 \omega_{m_1} \omega_{m_2}} \sum_{-m_1 < n_1 < 0} \sum_{-m_2 < n_2 < 0} \text{tr}_{\mathbf{R} \otimes \mathbf{S}} \{ \bar{D}_{n_1+m_2, n_2}^{12}(\mathbf{q}) D_{n_2, n_1+m_1}^{21}(-\mathbf{q}) \} \text{tr}_{\mathbf{R} \otimes \mathbf{S}} \{ \bar{D}_{n'_1+m'_2, n'_2}^{12}(\mathbf{q}) D_{n'_2, n'_1+m'_1}^{21}(-\mathbf{q}) \} \quad (2.95)$$

and

$$K_D = \frac{(e^2 \pi \nu D)^2}{\beta^2 \omega_{m_1} \omega_{m_2}} \sum_{-m_1 < n_1 < 0} \sum_{-m_2 < n_2 < 0} \text{tr}_{\mathbf{R} \otimes \mathbf{S}} \{ \bar{D}_{n_1, n_2+m_2}^{12}(\mathbf{q}) \bar{D}_{n_2, n_1+m_1}^{21}(-\mathbf{q}) \} \text{tr}_{\mathbf{R} \otimes \mathbf{S}} \{ D_{n'_1, n'_2+m'_2}^{12}(\mathbf{q}) D_{n'_2, n'_1+m'_1}^{21}(-\mathbf{q}) \} \quad (2.96)$$

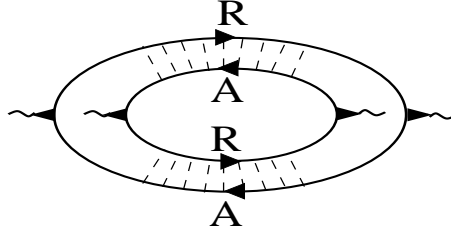


Figure 2.12: Diagrammatic representation of K_D which gives the main contribution to the UCF. Dashed lines represent coherent impurity scattering of electron (R) hole (A) pair, i.e. the bare Diffuson where interaction due to scattering from magnetic impurities is not yet taken into account.

arise due to ensemble fluctuations of the density of states, ν , and diffusion constant, D , respectively [32]. The indices 1, 2 refer to the F-space components and for notational convenience we did not write out the T-space indices $+/ -$. For wires of length $L \gg L_\varphi = \sqrt{D\tau_\varphi} \gg L_T = \sqrt{D/T}$ the conductance fluctuations are determined by the fluctuations of the diffusion constant, i.e. by K_D . A diagrammatic representation of K_D is given in Fig. 2.12.

Notice that generally there is also a contribution from the Cooperon. Yet, suppressed by a factor τ_B/τ_φ , this is negligible already for weak magnetic fields $B \gtrsim \left(\frac{n_S}{\vartheta(\mathbf{n})e^2\nu DA}\right)^{1/2}$. Here [11] $1/\tau_B = \vartheta(\mathbf{n})e^2 DAB^2$ is the dephasing rate of the Cooperon due to the external magnetic field, B , applied in direction \mathbf{n} . The function $\vartheta(\mathbf{n})$ is of order unity, A is the area of the wire cross-section and we estimated $1/\tau_\varphi \gtrsim n_S/\nu$, see below.

The Diffuson propagator is given by Eq. (2.49), with Zeeman spitting and spin-orbit scattering rate included. Most conveniently it is separated into its spin-singlet and spin triplet components, such that (we define $\Pi^{(i)} = \pi\nu\langle\bar{D}^{(i)}D^{(i)}\rangle$)

$$\Pi_{\epsilon_1\epsilon_2}^{(i)}(\mathbf{q}) = \frac{1}{D\mathbf{q}^2 + i(\epsilon_1 - \epsilon_2 + \zeta_i\epsilon_z) + \gamma_{SO}^{(i)} + 1/\tau_{\varphi,S}^{(i)}(\epsilon_1, \epsilon_2, B)}. \quad (2.97)$$

The modes $i = 1, 2, 3$ describe the spin triplet state with S_z component equal to 1, -1 and 0, respectively. $i = 4$ denotes the spin singlet channel. The Zeeman splitting enters only the triplet-Diffuson with non-vanishing projection $S_z = \pm 1$, i.e. $\zeta_i = \pm 1$ for $i = 1, 2$ and zero otherwise. $1/\tau_{SO}^{(i)}$ is the spin-orbit scattering rate. $1/\tau_{SO}^{(i)}$ is identical for the three spin triplet-Diffuson ($i = 1, 2, 3$) and zero for the spin singlet mode ($i = 4$). For strong spin-orbit scattering only the singlet Diffuson contributes (otherwise $1/\tau_{SO}^{(i)}$ is an additional fitting parameter). Finally $1/\tau_{\varphi,S}^{(i)}$ is the dephasing rate for the i -th Diffuson mode due to the presence of diluted magnetic impurities and has the structure

$$\frac{1}{\tau_{\varphi,S}^{(i)}(\epsilon_1, \epsilon_2)} = \frac{2n_i}{\pi\nu} \left(\frac{\pi\nu}{2i} [T^{(i,a)}(\epsilon_2, B) - T^{(i,b)}(\epsilon_1, B)] - (\pi\nu)^2 T^{(i,c)}(\epsilon_1, B) T^{(i,d)}(\epsilon_2, B) \right), \quad (2.98)$$

where the proper combination of T -matrices for the various channels can be read off by comparison with Table 2.4. Eq. (2.98) is evaluated from summing up self-energy and elastic vertex contributions. Notice that in contrast to the WL experiment the electron and hole lines (i.e. the inner and outer rings) in Fig. 2.12 represent different measurements. Therefore there are no correlations between dynamical impurities residing on different rings and interaction lines may only be drawn within the same ring. Consequently the inelastic vertex contributions do not enter the Bethe-Salpeter equation for the Diffuson, see Fig. 2.13. However, there are inelastic vertex contributions, as e.g. depicted in Fig. 2.14, which become important in the context of electron-electron interactions [24]. It is instructive to compare those to the inelastic vertex corrections relevant for WL depicted in Fig. 2.6. In the latter case, the sum of the incoming momenta of the vertex is small due to the Cooperon in Fig. 2.6. Consequently, the inelastic vertex corrections to the WL dephasing rate are *not* suppressed by powers of $1/(k_F l)$ but only by powers of $1/(\Delta E \tau_\varphi)$. In contrast, the relevant momenta in Fig. 2.14 are uncorrelated (i.e. particle and hole are far apart), leading to an suppression both by powers of $1/(k_F l)$ and of $1/(\Delta E \tau_\varphi)$. Notice

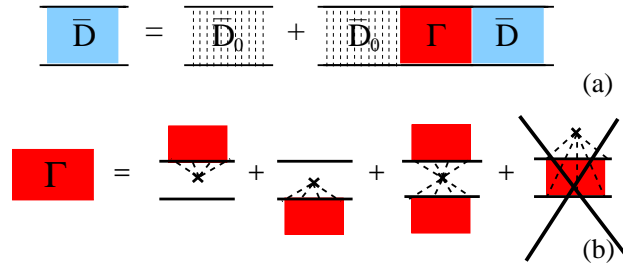


Figure 2.13: (a) Bethe-Salpeter equation for the Diffuson, \bar{D} , in the presence of (dilute) magnetic impurities to linear order in n_i . \bar{D}_0 is the bare Diffuson in the absence of interactions. (b) Diagrammatic representation of the irreducible interaction vertex, Γ , consisting of the self-energy (represented by the first two contributions), the elastic vertex (third contribution). The inelastic vertex (the fourth contribution) does not enter the Diffuson as measured in the UCF.

that in the AB experiment considered below the suppression of inelastic vertex contributions is even larger and proportional to [23] $1/(\Delta E t_D)^2 \ll 1$, where $t_D = L^2/D \gg \tau_\varphi$ and L is the ring length. This is due to the fact that in this case the typical time scale of interfering electrons is t_D rather than τ_φ as electrons contributing the AB oscillations have to circle the ring at least once.

i	$ S, M\rangle$	Combinations of T -matrices
1	$S = 1, M = 1$	$T^1 = \frac{1}{2i} (T_\downarrow^A - T_\uparrow^R) - T_\downarrow^R T_\uparrow^A$
2	$S = 1, M = -1$	$T^2 = \frac{1}{2i} (T_\uparrow^A - T_\downarrow^R) - T_\uparrow^R T_\downarrow^A$
3	$S = 1, M = 0$	$T^3 = \frac{1}{2} \text{Im} (T_\uparrow^A + T_\downarrow^A) - \frac{1}{2} (T_\uparrow^R T_\uparrow^A + T_\downarrow^R T_\downarrow^A)$
4	$S = 0$	$T^4 = \frac{1}{2} \text{Im} (T_\uparrow^A + T_\downarrow^A) - \frac{1}{2} (T_\uparrow^R T_\uparrow^A + T_\downarrow^R T_\downarrow^A)$

Table 2.4: Combination of T -matrices entering the dephasing rates for spin-triplet and spin-singlet Diffusons. S denotes the total spin and M its z component. T_\uparrow, T_\downarrow denotes the T -matrix for spin-up and spin-down electrons, respectively.

We point out the following differences for $1/\tau_{\varphi,S}$ measured from the UCF experiment, Eq. (2.98), compared to that found from the WL, Eq. (2.82). Firstly, the T -matrices entering Eq. (2.98) depend on the spin configuration of the Diffuson-mode and have acquired a B -dependence due to the coupling of the impurity spin to B , Eq. (2.90). Secondly, $1/\tau_{\varphi,S}$ depends on two energies. This results from the fact, that in the UCF experiment electron and hole lines constituting the Diffuson are produced in different measurements of the conductance (see Fig. 2.12). Therefore their energies are individually averaged as can be seen in Eq. (2.99) below.

From Eqs. (2.96) and (2.97) the amplitude of the UCFs is obtained to be proportional to $\sqrt{\tau_{\varphi,S}}$ (e.g. [32]). Especially compared to the AB oscillations, discussed below, the $1/\tau_{\varphi,S}$ dependence of the UCFs is rather weak. In the following we will therefore focus our discussion on AB experiments.

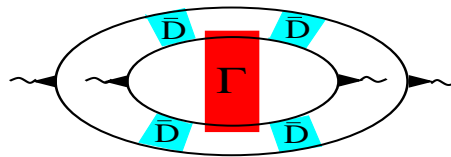


Figure 2.14: Diagrammatic representation of lowest order corrections to UCF due to inelastic vertex contributions. Notice that for a local interaction these are not only suppressed by powers of $1/(\Delta E \tau_\varphi)$ but also small in powers $1/(k_F l)$.

Dephasing rate measured from AB oscillations: Aharonov-Bohm oscillations are measured in a ring geometry [29, 25], where the conductance oscillates periodically as a function of B piercing the ring, and the amplitude of these AB-oscillations decrease exponentially with $1/\tau_{\varphi,S}$. The periodic oscillations result from the change of boundary conditions, due to flux lines piercing the ring and can be calculated from Eq. (2.95) by performing the twofold contractions in \bar{D}, D , i.e.

$$\langle \delta g(\phi) \delta g(\phi + \Delta\phi) \rangle = \frac{(2e^2 D)^2}{3\pi T L^4} \int d\epsilon_1 d\epsilon_2 f'_F(\epsilon_1) f'_F(\epsilon_2) \int d\mathbf{x}_1 d\mathbf{x}_2 |\Pi_{\epsilon_1, \epsilon_2}^{\Delta\phi}(\mathbf{x}_1, \mathbf{x}_2)|^2. \quad (2.99)$$

Here $\Pi^{\Delta\phi}$ is as given in Eq. (2.97) but now with discrete momenta, $\mathbf{q} = \mathbf{q}_m(\Delta\phi) = \frac{2\pi}{L}(m + \frac{\Delta\phi}{\phi_0})$, depending on the difference of the magnetic fields during the individual measurements of g . The fluctuations are a periodic function in $\Delta\phi/\phi_0$, where $\phi_0 = 2\pi/e$ is the elementary flux-quantum and $\Delta\phi = \Delta B L^2/(4\pi)$. Therefore an expansion in its harmonics can be done [26],

$$\langle \delta g(\phi) \delta g(\phi + \Delta\phi) \rangle = \frac{C e^4}{\pi^2} \sum_{k=0}^{\infty} \mathcal{A}_k(B) \cos \left[2\pi k \frac{\Delta\phi}{\phi_0} \right], \quad (2.100)$$

where C is a factor of order 1, depending on the sample geometry in the vicinity of the ring. In the case of strong spin-orbit scattering [28] the spin singlet-Diffuson gives the leading contributes to Eq. (2.99), and one finds that [26]

$$\mathcal{A}_k(\mathbf{B}) = \frac{(2\pi)^3 D^{3/2}}{T^2 L^3} \int d\epsilon_+ \frac{e^{-\frac{kL}{\sqrt{D\tau_{\varphi,S}^{(4)}(\epsilon_+)}}}}{\cosh^4(\epsilon_+/2T)} \sqrt{\tau_{\varphi,S}^{(4)}(\epsilon_+)}, \quad (2.101)$$

where

$$\frac{1}{\tau_{\varphi,S}^{(4)}(\epsilon_+, T, B)} \frac{2n_S}{\pi\nu} \left(\pi\nu \text{Im} \left[T_{(4)}^A(\epsilon_+, B) \right] - |(\pi\nu) T_{(4)}^R(\epsilon_+, B)|^2 \right). \quad (2.102)$$

Here $\epsilon_+ = \epsilon_1 + \epsilon_2$ and we used that relevant contributions to the integral over energy differences, $\epsilon_- = \epsilon_1 - \epsilon_2$, result from energies $\epsilon_- \ll 1/\tau_{\varphi,S}^{(4)}$. Notice that such a reduction to a single energy-integral can only be done in a one-dimensional system. In a two-dimensional system, e.g., relevant energies extend up to $\epsilon_- \sim T$.

Finally, for a comparison with experiment we have to give the ϵ -independent dephasing rate which for $k = 1$ follows from solving the equation

$$\frac{L_{\varphi}^{(4)}(T, B, L)}{L} e^{-\frac{L}{L_{\varphi}^{(4)}(T, B, L)}} = \frac{3}{8T} \int d\epsilon \frac{e^{-\frac{L}{L_{\varphi}^{(4)}(\epsilon, T, B)}}}{\cosh^4(\epsilon/2T)} \frac{L_{\varphi}^{(4)}(\epsilon, T, B)}{L}, \quad (2.103)$$

where $L_{\varphi}^{(4)} = \sqrt{D\tau_{\varphi,S}^{(4)}}$ is the dephasing length. Notice that the actually measured dephasing rate depends on the length of the ring.

The numerical evaluation of $1/\tau_{\varphi,S}(T, B, L)$ was done by Theo Costi and is given in [13]. In Ref. [13] we also discuss the B, L and T dependence of the Aharonov-Bohm amplitude and the dephasing rate extracted from the amplitude. As a side remark we here only mention that in the limit of long ring lengths $L \gg L_{\varphi}$ the integral on the right hand side of Eq. (2.103) (for fixed T and B) is dominated by the saddle points of the function

$$f(\epsilon) = \frac{L}{L_{\varphi}^{(4)}(\epsilon)} - \ln \left[\frac{L_{\varphi}^{(4)}(\epsilon)}{L} \right] + 4 \ln \left[\cosh \left(\frac{\epsilon}{2T} \right) \right].$$

For temperatures $T \lesssim \max\{B, T_K\}$ f has a saddle point at $\epsilon = 0$, which for temperatures $T \gtrsim T_K$ becomes unstable. At very large ring diameters $L/L_{\text{hit}} \gg 10^2$, a second saddle point at $\epsilon =$

$\frac{L}{2L_{\text{hit}} \ln^2 \left[\frac{L}{2L_{\text{hit}}} \right]} T$ starts to dominate the integral for $T \gtrsim T_K$. Here $L_{\text{hit}} = \sqrt{D\tau_{\text{hit}}}$ is the diffusive length scale corresponding to the time $\tau_{\text{hit}} = \frac{\pi\nu}{2n_i}$ and introduced above. Although this limit is rather academic it is interesting that for such large rings dephasing is dominated by rare events of highly excited thermal electrons scattering from the magnetic impurities. Inserting this second saddle point into Eq. (2.103) one finds that the length dependence of $1/\tau_\varphi$ for high temperatures follows

$$\frac{1}{\tau_\varphi(T, L)} \sim \frac{1}{\ln^2 \left[\frac{L}{2L_{\text{hit}} \ln^2 \left[\frac{L}{2L_{\text{hit}}} \right]} \right]}. \quad (2.104)$$

2.8 Dephasing-rate measured from the current echo

To build a bridge to the first part of the thesis we give the dephasing rate as measured from the current echo experiment. Since the current echo is just a manifestation of the WL corrections, the energy resolved dephasing rate is given by Eq. (2.81). A difference to the WL dephasing rate merely arises in the experimentally measured rate due to the different energy averaging procedures. Since dephasing due to Kondo impurities is purely exponential in time, the current echo for metals containing low concentrations of magnetic impurities takes the form

$$\Delta j(t) = \Delta \tilde{j}(t) \int d\epsilon [-f'_F(\epsilon)] e^{-t/\tau_\varphi(\epsilon)}, \quad (2.105)$$

where $\Delta \tilde{j}(t)$ is the current echo in the absence of dephasing, as given in Eq. (1.42), and f_F denotes the Fermi distribution function. Therefore, the experimentally measured energy averaged dephasing rate is given by

$$\frac{1}{\tau_\varphi(T, t)} = -\frac{1}{t} \ln \left[\int d\epsilon [-f'_F(\epsilon)] e^{-t/\tau_\varphi(\epsilon, T)} \right]. \quad (2.106)$$

As in the AB-experiment, the energy resolved rate enters exponentially into the averaging procedure. For long time differences between the applied voltage pulses, $t \gg \tau_{\text{hit}}$, the experimentally measured dephasing rate is therefore dominated by the saddle points of the function

$$f(\epsilon) = \frac{t}{\tau_\varphi(\epsilon)} + \ln \cosh \left[\frac{\epsilon}{2T} \right]. \quad (2.107)$$

In the limit of long times, $t/\tau_\varphi \gg 1$, and for temperatures $T \gtrsim T_K$, this function has a second saddle point at high energies $\epsilon = \frac{4t}{\tau_{\text{hit}}} \ln \left[\frac{4t}{\tau_{\text{hit}}} \right] T$, which describes rare events of highly excited electrons scattering from the magnetic impurities. In contrast to the AB oscillations, however, the exponentially suppressed long-time echo amplitude may be possibly still be observable due to its sharp temporal shape.

2.9 Comparison to recent experiments and outlook

Two independent experimental groups, Mallet *et al.* [14] and Alzoubi *et al.* [15], recently performed phase coherence time measurements in quasi-one-dimensional Ag wires doped with Fe Kondo impurities of different concentrations. Due to the relatively high Kondo temperature of this system, $T_K = 2 - 4K$, the temperature regime from $T \gtrsim T_K$ down to $0.01T_K$ could be explored. The main findings of these experiments can be summarized as follows:

- Both experiments show that the dephasing rate per magnetic impurity, plotted as a function of T/T_K , is a universal function (Mallet *et al.* included data from earlier experiments on AgFe-wires which have a different Kondo temperature in order to show the scaling).
- Both experiments are fitted well by Eq. (2.60) down to temperatures $T = 0.1T_K$.

- Both, the concentration and the Kondo temperature obtained from fitting $1/\tau_\varphi$ deviate from the values obtained from resistivity measurements [14] and high field magnetoresistance measurements [15] by a factor ~ 2 in one experiment and a factor $\sim 1/2$ in the other experiment.
- At temperatures $T \lesssim 0.1T_K$ strong deviation from the theory is observed.

Both groups conclude that the theory for spin-1/2 Kondo impurities describes well the experiment down to temperatures of $0.1T_K$ and state that the mismatch in the values for the concentration and Kondo temperature may possibly be explained by the higher spin ($S = 2$) for Fe impurities. Whereas Alzoubi *et al.* speculate about an incomplete screening of the impurity spin, Mallet *et al.* definitely rule out an under-screened scenario from comparison with theory for $S > 1/2$ models. This is due to the observation that in the under-screened scenario $1/\tau_\varphi$ displays a much broader maximum around T_K and the resistivity has a much smaller temperature dependence than those observed in experiments. They also rule out the over-screened scenario, as this would lead to even larger values for $1/\tau_\varphi$. Therefore they conclude that the Ag electrons couple via various channels to the Fe atoms, such that a perfect screening of the $S = 2$ is obtained. Both groups conclude that further theoretical work on realistic spin-2 systems is needed to resolve this issue. Furthermore, Mallet *et al.* point out that $1/\tau_\varphi$ perfectly scales with the doping even for $T < 0.1T_K$, implying that the derivation at lowest temperatures cannot be explained by extrinsic effects. They therefore conclude that the curious temperature dependence of $1/\tau_\varphi$ has to originate from the magnetic impurities themselves (e.g. a small fraction of implanted Fe impurities which end up close to lattice defects) or from the implantation process (e.g. the creation of additional dynamical defects, such as two-level systems). In order to investigate the latter scenario they propose ion implantation experiments of non-magnetic impurities.

Outlook: As already mentioned, further progress may be obtained from additional theoretical work on realistic spin-2 systems. Such models have to account for the orbital degree of freedom of the impurity atom, spin-orbit coupling, crystal field effects and the position of the impurity atom within the host metal crystal structure.

Concerning the dephasing rate measured from the Aharonov-Bohm amplitude, such experiments using samples doped with a known concentration of magnetic impurities are not available. For a comparison to our results, experiments on AB rings, doped with magnetic impurities with a higher Kondo temperature, would be highly desirable.

Bibliography

- [1] B. L. Altshuler, A. G. Aronov and D. E. Khmel'nitsky, J. Phys. C: Solid State Phys., **15**, 7367-7386 (1982).
- [2] P. Mohanty, E. M. Q. Jariwala and R. A. Webb, Phys. Rev. Lett. **78**, 3366-3369 (1997); P. Mohanty and R. A. Webb, Phys. Rev. B **55**, R13452 (1997).
- [3] F. Schopfer, Ch. Bäuerle, W. Rabaud and L. Saminadayar, Phys. Rev. Lett. **90**, 056801 (2003).
- [4] C. Van Haesendonck, J. Vranken and Y. Bruynseraede Phys. Rev. Lett. **58**, 1968-1971 (1987).
- [5] F. Pierre, A. B. Gougam, A. Anthore, H. Pothier, D. Esteve and N. O. Birge, Phys. Rev. B **68**, 085413 (2003).
- [6] D. S. Golubev and A. D. Zaikin, Phys. Rev. Lett. **81**, 1074 (1998).
- [7] I. L. Aleiner, B. L. Altshuler and M. E. Gershenson, Waves in Random Media **9**, 201 (1999).
- [8] J. v. Delft, J. Phys. Soc. Jpn., Suppl. A, **72**, 24 (2003).
- [9] F. J. Ohkawa, H. Fukuyama and K. Yosida, J. Phys. Soc. Jpn. **52**, 1701-1709 (1983); F. J. Ohkawa, Prog. Th. Phys. Suppl. **84**, 166 (1985).
- [10] S. Hikami, A.I. Larkin, and Y. Nagaoka, Progr. Theor. Phys. **63**, 707 (1980).
- [11] M. G. Vavilov and L. I. Glazman, Phys. Rev. B **67**, 115310 (2003); M. G. Vavilov, L. I. Glazman, A. I. Larkin, Phys. Rev. B **68**, 075119 (2003).
- [12] T. Micklitz, T. A. Costi, A. Altland and A. Rosch, Phys. Rev. Lett. **96**, 226601 (2006).
- [13] T. Micklitz, T. A. Costi, A. Altland and A. Rosch, cond-mat/0610304.
- [14] F. Mallet *et al.*, Phys. Rev. Lett. **97**, 226804 (2006).
- [15] G. M. Alzoubi and N. O. Birge, Phys. Rev. Lett. **97**, 226803 (2006).
- [16] A. Altland and B. Simons, *Condensed Matter Field Theory*, (Cambridge Univ. Press 2006).
- [17] A. Kamenev and A. Andreev, Phys. Rev. B **60**, 2218 (1999).
- [18] J. S. Meyer, V. I. Fal'ko, B.L. Altshuler, Nato Science Series II, Vol. 72, edited by I.V. Lerner, B.L. Altshuler, V.I. Fal'ko, and T. Giamarchi (Kluwer Academic Publishers, Dordrecht, 2002) [cond-mat/0206024].
- [19] A. C. Hewson, *The Kondo Problem to Heavy Fermions* (Cambridge University Press, 1993).
- [20] B. N. Narozhny, Gábor Zala and I. L. Aleiner, Phys. Rev. B **65**, 180202(R) (2002).
- [21] G. Frossati, J.L. Tholence, D. Thoulouze, and R. Tournier, Physica B **84**, 33 (1976).
- [22] B. L. Altshuler and A. G. Aronov, in *Electron-Electron Interaction in Disordered Systems*, edited by A. L. Efros and M. Pollak (North-Holland, Amsterdam, 1985).

- [23] G. Zaránd, L. Borda, J. v. Delft and N. Andrei, Phys. Rev. Lett. **93**, 107204 (2004).
- [24] I. L. Aleiner and Ya. M. Blanter, Phys. Rev. B **65**, 115317 (2004).
- [25] F. Pierre and N. O. Birge, Phys. Rev. Lett. **89**, 206804 (2002); F. Pierre and N. O. Birge, J. Phys. Soc. Jpn. Vol. **72** (2003) Suppl. A pp. 19-23.
- [26] A.G. Aronov and Y.V. Sharvin, Rev. Mod. Phys. **59**, 755 (1987).
- [27] T. Ludwig and A. D. Mirlin, Phys. Ref. B **69**, 193306 (2004).
- [28] In their experiments F. Pierre *et al.* [25] measured spin-orbit lengths of order $\sim 1\mu\text{m}$ much smaller than L_φ .
- [29] R. A. Webb *et al.*, Phys. Rev. Lett. **54**, 2696 (1985).
- [30] A. Zawadowski, J. v. Delft and D.C. Ralph, Phys. Rev. Lett. **83**, 2632 (1999).
- [31] H. Pothier, S. Guron, Norman O. Birge, D. Esteve, and M. H. Devoret, Phys. Rev. Lett. **79**, 3490 (1997)
- [32] B. L. Altshuler and B.I. Shklovskii, Sov Phys JETP 64 (1), 127-135
- [33] P. Mohanty, R. Webb, Phys. Rev. Lett. **84**, 4481 (2000).
- [34] We define and determine the Kondo temperature T_K from the $T = 0$ susceptibility $\chi = (g\mu_B)^2/(4T_K)$.
- [35] J. Korringa, Physica **16**, 601 (1959).
- [36] K. G. Wilson, Rev. Mod. Phys. **47**, 773 (1975); H. B. Krishna-murthy, J. W. Wilkins and K. G. Wilson, Phys. Rev. **B21**, 1003 (1980).
- [37] T. A. Costi, A. C. Hewson and V. Zlatić, J. Phys. Cond. Matt. **6** 2519 (1994).
- [38] T. A. Costi, Phys. Rev. Lett. **85**, 1504 (2000); A. Rosch, J. Paaske, T. A. Costi and P. Wölfle, Phys. Rev. B **68**, 014430, (2003).
- [39] W. Hofstetter, Phys. Rev. Lett. **85**, 1508 (2000).
- [40] G. M. Eliashberg, Soviet Phys. JETP **14**, 886-892 (1962); G. M. Eliashberg, Soviet Phys. JETP **15**, 1151-1157 (1962).
- [41] A. Oguri, cond-mat/0309420; A. Oguri, cond-mat/0106033.

Chapter 3

Disordered Luttinger Liquid

Introduction: The coalescence of ideas from mesoscopic, weakly disordered systems and strongly correlated systems has emerged as a growing field of research interest. One example for a physical system which requires the expertise from both communities is that of interacting disordered electrons in a strictly one dimensional geometry. For such systems *disorder* as well as electron-electron *interactions* (even if they are weak) drastically change the large-scale, low-energy physics. Arbitrary weak disorder, on one hand, drives the 1d system into an Anderson insulator (provided phase coherence is not destroyed) and electron-electron interactions in a clean 1d system, on the other hand, lead to the formation of a non Fermi-liquid state, the so-called Luttinger liquid.

From a conceptual point of view it is interesting to note that different theoretical techniques are applied in the investigation of 1d systems, on the one hand, and their higher dimensional relatives on the other hand. Whereas for higher dimensions the diffusive nonlinear σ -model proves useful in the description of the weak disorder [1], weak interaction [2, 3] limit, the (clean) interacting 1d system is successfully treated within bosonization methods [4]. However powerful in the clean case, inclusion of (arbitrary weak) disorder renders the bosonization method disparate more complicated, such that key notions of mesoscopic disordered systems, such as quantum interference phenomena and dephasing, remained unaddressed for a long time.

Only very recently Gornyi *et al.* [5, 6] addressed the disordered Luttinger liquid within a new approach combining bosonization methods and Fermi-liquid perturbation theory for weakly disordered systems. In a first step bosonization methods were used in order to describe the renormalization of disorder by interactions (and to account for the typical Luttinger liquid singularities). In a second step, the authors re-fermionized the theory in order to describe low energy quantum interference effects by diagrammatic perturbation theory. In this way it was shown that notions such as weak localization and dephasing, familiar from higher dimensional analogues, are also meaningful concepts in the disordered Luttinger liquid. In fact, Gornyi *et al.* were able to calculate the weak localization corrections to the Drude conductivity in the limit of high temperatures, where dephasing impedes Anderson localization to become strong and derived an explicit expression for the dephasing rate due to electron-electron interactions.

In view of this recent development one may wonder if there is an “universal” model for the disordered interacting systems interpolating between the single channel limit and its higher dimensional counterparts and accounting for quantum interference effects in the Luttinger liquid in a transparent way. Such a model in terms of a coupled ballistic nonlinear σ -model is suggested in the following sections.

Outline: The outline of this chapter is the following: In the first section we introduce the model for interacting electrons in a strictly one dimensional disordered system. In the second section we briefly repeat two established bosonization methods, in order to derive a generating functional (for density/current correlation functions) for the clean, non-interacting system. The central issues of this second section is, however, to show how this generating functional may be obtained within a third “bosonization method” (“ σ -model bosonization”). In the third section we show how the derivation of the generating functional has to be changed in order to account for electron-electron interaction. We then discuss in a fourth section the notion of an inelastic scattering rate for the clean Luttinger liquid. In the fifth section we show how the σ -model bosonization may be employed to derive an effective

theory for non-interacting electrons in a disordered single channel system. We briefly discuss within the σ -model approach the recently analyzed regime of temperatures [5, 6], where the conductivity of the disordered single-channel wire is given by the Drude conductivity and weak localization corrections can be organized in a systematic expansion in powers of the small parameter $\tau_\varphi v_F/l_1$, where τ_φ is the dephasing rate due to electron-electron interactions.

The following, sixth section combines interactions and disorder. In this section we introduce the coupled ballistic σ -model for the interacting disordered Luttinger liquid, which has a multi-channel (i.e. higher dimensional) generalization, that was recently introduced by Mora *et al.* [7]. As an brief application, illustrating the interplay between disorder and interactions, we discuss the RPA screening of the Coulomb interactions in a disordered system and the renormalization of the disorder scattering length due to electron-electron interactions. The last, seventh section shows for the prominent example of the persistent current in a ring shaped geometry, how the model accounts for interference effects in the disordered Luttinger. I want to point out, however, that at some points this chapter presents more a collection of ideas than a closed theory; some questions still need to be clarified.

3.1 The model

In the following we want to study a single-channel infinite wire at temperatures much lower than the bandwidth and the Fermi energy. The low-energy properties of such a system are contained within the Luttinger model [12, 4] which accounts only for electrons and holes in the vicinity of the Fermi-points $\pm k_F$ where a linearization of the spectrum, $\epsilon_{p\pm p_F} - \epsilon_F = \pm v_F p$, is justified. The two species of excitations in the vicinity of the Fermi-points $\pm k_F$ are labeled by $s = \pm$ and referred to as left-(+) and right (-) moving fields ("left"/"right-movers"). Furthermore, we restrict to the case of spin polarized electrons, interacting via a weak, finite range (screened) pairwise e-e interaction potential $V(x-x')$ and moving in stochastic disorder potentials, $u(x)$ and $v(x)$, describing forward and backward scattering processes, respectively. Keeping only the forward and backward e-e scattering amplitudes, $V(q=0)$ and $V(q=\pm k_F)$ (as commonly done [10]), the (imaginary-time) action for the one-dimensional, disordered interacting electron gas takes the form

$$S[\bar{\chi}\chi] = S_0[\bar{\chi}\chi] + S_u[\bar{\chi}\chi] + S_v[\bar{\chi}\chi] + S_{\text{int.}}[\bar{\chi}\chi] + S_{\text{sou.}}[\bar{\chi}\chi], \quad (3.1)$$

where

$$S_0[\bar{\chi}\chi] = - \int d^2x \bar{\chi} \hat{\partial} \chi \quad (3.2)$$

$$S_u[\bar{\chi}\chi] = - \int d^2x \bar{\chi} u \sigma_1 \chi \quad (3.3)$$

$$S_v[\bar{\chi}\chi] = - \int d^2x \bar{\chi} v \chi \quad (3.4)$$

$$S_{\text{int.}}[\bar{\chi}\chi] = \frac{1}{2} \int d^2x (\rho_+ \quad \rho_-) \hat{g} \begin{pmatrix} \rho_+ \\ \rho_- \end{pmatrix} \quad (3.5)$$

$$S_{\text{sou.}}[\bar{\chi}\chi] = - \int d^2x [\mu \bar{\chi} \sigma_1 \chi + a \bar{\chi} \sigma_2 \chi], \quad (3.6)$$

and we use the short notation $d^2x = d\tau dx$, $\bar{\chi} = (\bar{\chi}_- \quad \bar{\chi}_+)$, $\chi = \begin{pmatrix} \chi_+ \\ \chi_- \end{pmatrix}$, $\hat{\partial} = \begin{pmatrix} \partial_+ & \partial_- \end{pmatrix}$, $\partial_\pm = \partial_\tau \pm i v_F \partial_x$. The interaction matrix $\hat{g} = \begin{pmatrix} g_4 & g_2 \\ g_2 & g_4 \end{pmatrix}$ relates to the Fourier components of the interaction potential in the following way: g_4 is the forward scattering amplitude of right- (left-) movers on right- (left-) movers, i.e. $g_4 = V(q=0)$, and g_2 is a combination of the forward scattering amplitude between fields of opposite chirality (i.e. scattering between + and - densities) and the backscattering amplitude (i.e. right-movers scattering into left-moving states and vice verse). In formulas $g_2 = V(q=0) - V(q=\pm k_F)$. Naively, one could think that the matrix element g_4 has to vanish due to the Pauli principle as it describes a local interaction between identical fermions. However, as pointed out (e.g. in [6]), although

this term does not generate any interaction between densities of the same chirality it shifts the velocity according to

$$v_F \rightarrow v_F + \frac{g_4}{2\pi}. \quad (3.7)$$

Therefore, remembering that the Fermi velocity is shifted according to Eq.(3.7), we may work with a model that accounts only for interactions between densities of opposite chirality and set $g_4 = 0$ in $S_{\text{int.}}$. The stochastic forward and backward scattering potentials are (for convenience) modeled by δ -distributed white noise, described by the forward and backward scattering lengths l_0 and l_1 , i.e.

$$\begin{aligned} \langle u(x)u(x') \rangle_u &= 2v_F l_0^{-1} \delta(x - x') \\ \langle v(x)v(x') \rangle_v &= v_F l_1^{-1} \delta(x - x'). \end{aligned}$$

Finally, the source term, $S_{\text{sou.}}$, describes the coupling of the density, $\rho = \rho_+ + \rho_-$, to a (time-dependent) chemical potential, μ , and that of the current, $j = ie v_F (\rho_+ - \rho_-)$ to a vector potential, a . Here $\rho_s = \bar{\chi}_s \chi_s$, $s = \pm$. For convenience we set $e = 1$ and $v_F = 1$ in the following.

3.2 Bosonization of non-interacting electrons in a clean wire: three equivalent approaches

In this section we want to prepare the ground for the latter sections, where we discuss interacting electrons in a disordered system, and show how a generating functional for current/density correlation functions for the non-interacting clean system may be obtained within the “ σ -model bosonization”. In the subsequent sections we then generalize this approach in order to include interactions and disorder. Let us, however, firstly repeat how to derive the generating functional within the two established bosonization methods (“standard” and “functional” bosonization).

So let us start out from the action for the non-interacting, clean system,

$$S[\bar{\chi}\chi] = S_0[\bar{\chi}\chi] + S_u[\bar{\chi}\chi] + S_{\text{sou.}}[\bar{\chi}\chi]. \quad (3.8)$$

Notice that we speak of a *clean* system although we included forward scattering disorder. This is due to the fact that forward scattering merely effects the phase of wave functions and therefore decouples from all gauge invariant observables. That is, for the analysis of current/density correlations, Eq.(3.8) is equivalent to the clean model and the second term in action Eq.(3.8) may equally be dropped out. Whereas the standard and the functional bosonization methods are most comfortably derived without introduction of forward scattering disorder, the σ -model approach employs the forward scattering in order to introduce a bosonic field, which describes the joined propagation of electrons and holes. Let us start with a recapitulation of the standard bosonization scheme.

3.2.1 Standard bosonization

Free fermions $\bar{\chi}, \chi$ may be bosonized in the “standard way” [4, 12] with the help of two bosonic fields θ, ϕ . In the Hamiltonian language these fields are related to the canonical momenta and coordinate and the commutation relation are $[\phi(x), \theta(x')] = \delta(x - x')$. The bosonization rules are

$$\chi_{\pm} \propto \exp \{i(\theta \pm \phi)\}. \quad (3.9)$$

With help of these rules, bosonization of the free electron action, Eq.(3.8), one obtains

$$S_0[\theta, \phi] = \frac{1}{2\pi} \int d^2x [(\partial_x \theta)^2 + (\partial_x \phi)^2 - 2i\partial_\tau \theta \partial_x \phi]. \quad (3.10)$$

In terms of the bosonic degrees of freedom the left- and right-moving densities read $\rho_{\pm} = \frac{1}{2\pi} (\partial_x \theta \mp \partial_x \phi)$. Therefore the source term of action Eq.(3.8) in terms of the bosonic degrees of freedom takes the form

$$S_{\text{sou.}}[\theta, \phi] = \frac{1}{\pi} \int d^2x [\mu \partial_x \theta + i a \partial_x \phi]. \quad (3.11)$$

Changing to a frequency/momentum representation the free action and the source term take the form

$$S_0[\theta, \phi] = \frac{1}{2\pi} \sum_{km} \left\{ \begin{pmatrix} \theta_{mk} & \phi_{mk} \end{pmatrix} \begin{pmatrix} k^2 & i\omega_m k \\ i\omega_m k & k^2 \end{pmatrix} \begin{pmatrix} \theta_{-m,-k} \\ \phi_{-m,-k} \end{pmatrix} \right\} \quad (3.12)$$

and

$$S_{\text{sou.}}[\theta, \phi] = \frac{1}{2\pi} \sum_{km} \left\{ \begin{pmatrix} ik\mu_{mk} & ka_{mk} \end{pmatrix} \begin{pmatrix} \theta_{-m,-k} \\ \phi_{-m,-k} \end{pmatrix} + \begin{pmatrix} \theta_{mk} & \phi_{mk} \end{pmatrix} \begin{pmatrix} -ik\mu_{-m,-k} \\ -ka_{-m,-k} \end{pmatrix} \right\}. \quad (3.13)$$

Integration over the bosonic fields θ, ϕ we finally obtain

$$S[a, \mu] = \frac{1}{2\pi} \sum_{m,q} \left\{ \frac{q^2}{q^2 + \omega_m^2} [\mu_{mq} \mu_{-m,-q} - a_{mq} a_{-m,-q}] - \frac{\omega_m q}{q^2 + \omega_m^2} [\mu_{mq} a_{-m,-q} + a_{mq} \mu_{-m,-q}] \right\}. \quad (3.14)$$

As the bosonized theory is an exact representation of the fermionic theory, Eq.(3.8), Eq. (3.14) contains all density/current correlation functions.

3.2.2 Functional bosonization

Working directly with the electron-fields, one may perform the Gaussian integral to obtain

$$\begin{aligned} & \int d^2x \bar{\chi} [\hat{\partial} + \mu\sigma_1 + a\sigma_2] \chi \\ & \rightarrow \text{tr} \ln \{ \hat{\partial} + \mu\sigma_1 + a\sigma_2 \} = \text{tr} \ln \{ \hat{\partial} \} + \text{tr} \ln \{ 1 + \mathcal{G}^0 [\mu\sigma_1 + a\sigma_2] \}, \end{aligned}$$

where $\mathcal{G}^0 = \hat{\partial}^{-1}$, which in momentum/frequency representation takes the form

$$\mathcal{G}_n^0(k) = \begin{pmatrix} g_n^-(k) & g_n^+(k) \end{pmatrix} = \begin{pmatrix} -1 & \frac{1}{k - i\epsilon_n} \\ k + i\epsilon_n & \end{pmatrix}. \quad (3.15)$$

Expansion of the “tr ln” reveals that all contributions from higher than second order vanish [13] (“loop-cancellation”). The linear order contribution vanishes in a charge neutral system and therefore the “tr ln” is equal to

$$\begin{aligned} & \text{tr} \ln \{ 1 + \mathcal{G}^0 [\mu\sigma_1 + a\sigma_2] \} \\ & = -\frac{T}{2L} \sum_{n,m} \sum_{k,q} \text{tr} \{ \mathcal{G}_n^0(k) [\mu_{mq}\sigma_1 + a_{mq}\sigma_2] \mathcal{G}_{n+m}^0(k+q) [\mu_{-m,-q}\sigma_1 + a_{-m,-q}\sigma_2] \} \\ & = -\frac{T}{2L} \sum_{n,m} \sum_{k,q} \text{tr} \{ [g_n^+(k)g_{n+m}^+(k+q) + g_n^-(k)g_{n+m}^-(k+q)] [\mu_{mq}\mu_{-m,-q} - a_{mq}a_{-m,-q}] \\ & \quad + i [g_n^+(k)g_{n+m}^+(k+q) - g_n^-(k)g_{n+m}^-(k+q)] [\mu_{mq}a_{-m,-q} + a_{mq}\mu_{-m,-q}] \}. \end{aligned}$$

We may now evaluate the sums by employing a non-relativistic momentum-regularization (which accounts for the fact that the model applies only for length scales exceeding the lattice constant, a_0), i.e.

$$\begin{aligned} \frac{T}{L} \sum_p \sum_n g_n^+(p) g_{n+m}^+(p+q) &= \int_{-\Lambda}^{\Lambda} \frac{dp}{2\pi} \int \frac{d\epsilon}{2\pi} \frac{1}{p - i\epsilon_n} \frac{1}{p+q - i\epsilon_{n+m}} \\ &= \frac{1}{q - i\omega_m} \int_{-\Lambda}^{\Lambda} \frac{dp}{2\pi} \int \frac{d\epsilon}{2\pi} \left[\frac{1}{p - i\epsilon} - \frac{1}{p+q - i\epsilon - i\omega_m} \right] \\ &= \frac{1}{q - i\omega_m} \int_{-\Lambda}^{\Lambda} \frac{dp}{2\pi} \frac{1}{2} [\text{sgn}(p) - \text{sgn}(p+q)] \\ &= -\frac{1}{2\pi} \frac{q}{q - i\omega_m}, \end{aligned}$$

where $\Lambda = a_0^{-1}$ and we approximated $\frac{1}{L} \sum_k = \int \frac{dp}{2\pi}$ and $T \sum_n = \int \frac{d\epsilon}{2\pi}$. Correspondingly

$$\frac{T}{L} \sum_p \sum_n g_n^-(p) g_{n+m}^-(p+q) = -\frac{1}{2\pi} \frac{q}{q + i\omega_m},$$

and therefore

$$\begin{aligned} S[a, \mu] &= \text{tr} \ln \left\{ \hat{\partial} \right\} \\ &+ \frac{1}{2\pi} \sum_{m,q} \left\{ \frac{q^2}{q^2 + \omega_m^2} [\mu_{mq} \mu_{-m,-q} - a_{mq} a_{-m,-q}] + \frac{\omega_m q}{q^2 + \omega_m^2} [\mu_{mq} a_{-m,-q} + a_{mq} \mu_{-m,-q}] \right\}, \end{aligned} \quad (3.16)$$

which coincides with Eq. (3.14). Notice also, that keeping the (static) forward scattering potential, one simply has to substitute $\mu_m \rightarrow \mu_m + u_m \delta_{m0}$. This leads to the additional contribution,

$$S[u] = \frac{1}{2} \sum_q \left[\frac{l_0}{L} + \frac{1}{\pi} \right] u_q u_{-q}, \quad (3.17)$$

and shows that the (gauge-invariant) observables, μ, j , decouple from the elastic forward scattering disorder.

3.2.3 σ -Model bosonization

Let us finally turn to the central issue of this section which is the “ σ -model bosonization”. We already mentioned that the physically irrelevant forward scattering disorder is essential to this approach. Notice, however, that the resulting model has to be independent from the forward scattering length, l_0 .

In this subsection we find it more convenient to work in a rotated basis, where

$$S[\bar{\chi}\chi] = - \int dx d\tau \bar{\chi} \left\{ \begin{pmatrix} \partial_+ & \\ & \partial_- \end{pmatrix} + u + \mu + ia\sigma_3 \right\} \chi \quad (3.18)$$

and, as before, $\chi = \begin{pmatrix} \chi_+ \\ \chi_- \end{pmatrix}$, but $\bar{\chi} = (\bar{\chi}_+ \quad \bar{\chi}_-)$. The steps which follow are standard in the context of higher dimensional disordered systems and here are only adapted to the situation of chiral Dirac fermions.

Time-reversal symmetry: In a first step we incorporate time-reversal symmetry into the model. This allows us to take into account the joined propagation of particles and holes along the same path in *parallel* and in *opposite* directions. The latter is essential for the understanding of certain interference phenomena such as the $h/2e$ Aharonov-Bohm oscillations in mesoscopic rings, which are discussed in section 7. In order to incorporate time-reversal symmetry we double the field space by introduction of a time-reversed component. In the following this component is denoted as the “backward”-component in time-reversal (T) space. To be precise, time-reversal symmetry implies that

$$\begin{aligned} S[\bar{\chi}\chi] &= - \int dx d\tau \bar{\chi}(\tau) \left\{ \begin{pmatrix} \partial_+ & \\ & \partial_- \end{pmatrix} + u + \mu + ia\sigma_3 \right\} \chi(\tau) \\ &= \int dx d\tau \chi^t(-\tau) \left\{ \begin{pmatrix} \partial_- & \\ & \partial_+ \end{pmatrix} + u + \mu + ia\sigma_3 \right\} \bar{\chi}^t(-\tau) \\ &= \int dx d\tau \chi^t(-\tau) \sigma_1 \left\{ \begin{pmatrix} \partial_+ & \\ & \partial_- \end{pmatrix} + u + \mu - ia\sigma_3 \right\} \sigma_1 \bar{\chi}^t(-\tau). \end{aligned}$$

Introducing the four-component vectors,

$$\bar{\psi}(x, \tau) = \frac{1}{\sqrt{2}} (\bar{\chi}(x, \tau), -\chi^t(x, -\tau)\sigma_1)_T \quad (3.19)$$

$$\psi(x, \tau) = -i\sigma_2^T \sigma_1 \bar{\psi}^t(x, -\tau), \quad (3.20)$$

allows for a reformulation of action Eq. (3.18) in the form

$$S[\bar{\psi}\psi] = - \int dx d\tau \bar{\psi} [\partial + u + \hat{\mu} + i\hat{a}\sigma_3\sigma_3^T] \psi. \quad (3.21)$$

Notice that due to this “doubling procedure” the time-dependent sources have become matrices in T-space of the form

$$\hat{a}(\tau) = \begin{pmatrix} a(\tau) & \\ & a(-\tau) \end{pmatrix}_T, \quad \hat{\mu}(\tau) = \begin{pmatrix} \mu(\tau) & \\ & \mu(-\tau) \end{pmatrix}_T. \quad (3.22)$$

Disorder-average: We start out from a replicated version of action Eq. (3.21) and perform the average over forward-scattering disorder, i.e.

$$- \int d^2x w \bar{\psi}\psi \rightarrow S_V = \frac{1}{2l_0} \int dx d\tau d\tau' \bar{\psi}(x, \tau) \psi(x, \tau) \bar{\psi}(x, \tau') \psi(x, \tau'). \quad (3.23)$$

In a next step we perform a Hubbard-Stratonovich transformation in order to decouple the “interaction” term, S_V , in the two relevant channels (exchange- and Cooper-channel). This results in

$$S_V = \int dx d\tau d\tau' \left[\frac{l_0}{4} \text{tr} \{Q^2\} - i\bar{\psi}Q\psi \right]. \quad (3.24)$$

Integration over the fermionic degrees of freedom leads us to the action

$$S[\bar{\chi}\chi] = - \int d^2\bar{\chi} [\partial - iQ + \hat{\mu} + i\hat{a}\sigma_3\sigma_3^T] \chi \rightarrow \frac{1}{2} \text{tr} \ln \{ \partial - iQ + \hat{\mu} + i\hat{a}\sigma_3\sigma_3^T \}. \quad (3.25)$$

That is, we end up with a theory in the bosonic Q -fields

$$S[Q] = \frac{l_0}{4} \text{tr} \{Q^2\} - \frac{1}{2} \text{tr} \ln \left\{ \underbrace{\partial - iQ}_{\mathcal{G}_Q^{-1}} + \hat{\mu} + i\hat{a}\sigma_3\sigma_3^T \right\}. \quad (3.26)$$

Notice that due to the linear dependence of $\bar{\psi}$ and ψ the matrix-field Q obeys the symmetry relation,

$$Q_{nn'}(q) = \sigma_2^T \sigma_1 Q_{n'n}^t(q) \sigma_1 \sigma_2^T, \quad (3.27)$$

where the transpose, t , acts in the replica and \pm -sectors.

Saddle-point analysis: We proceed by exposing action Eq.(3.26) to a stationary phase analysis. Variation of action Eq.(3.26) one obtains the saddle-point equation

$$Q(x) = \frac{-i}{l_0} \mathcal{G}_Q(x, x), \quad (3.28)$$

which has a homogeneous, Matsubara-, Replica- and \pm -diagonal solution,

$$Q_{nn'} = \begin{pmatrix} q_{nn'}^+ & \\ & q_{nn'}^- \end{pmatrix} = \frac{1}{2l_0} \text{sgn}(n) \delta_{nn'}. \quad (3.29)$$

Eq.(3.29) is a solution of Eq.(3.28), which may be checked with help of the identity

$$q_{nn'}^\pm = \frac{-i}{l_0} \int \frac{dp}{2\pi} \frac{1}{p \mp i\epsilon_n \mp \frac{1}{2l_0} \text{sgn}(n)} = \frac{1}{2l_0} \text{sgn}(n). \quad (3.30)$$

Notice that there are no \pm -off-diagonal solutions to the saddle-point equation [9].

Goldstone-modes and Wess-Zumino action: Since the action

$$S[Q] = \frac{l_0}{2} \text{tr} \{Q^2\} - \frac{1}{2} \text{tr} \ln \left\{ \partial - iQ + \hat{\mu} + i\hat{a}\sigma_3\sigma_3^T \right\} \quad (3.31)$$

is invariant under rotations TQT^{-1} , where T is some constant matrix which is diagonal in the \pm sector, it establishes Goldstone-modes $T\Lambda T^{-1}$, with $T = \text{diag}(T_+, T_-)_\pm$. Substituting the general expression $Q = \frac{1}{2l_0} T\Lambda T^{-1}$ into Eq.(3.31), we obtain

$$\begin{aligned} S[T] &= -\frac{1}{2} \text{tr} \ln \left\{ \partial - \frac{i}{2l_0} T\Lambda T^{-1} + \hat{\mu} + i\hat{a}\sigma_3\sigma_3^T \right\} \\ &= -\frac{1}{2} \text{tr} \ln \left\{ \underbrace{\partial - \frac{i}{2l_0} \Lambda}_{\mathcal{G}_\Lambda^{-1}} + \underbrace{T^{-1}(\partial T)}_{X_1} + \underbrace{T^{-1} [\hat{\mu} + i\hat{a}\sigma_3\sigma_3^T] T}_{X_2} \right\} \\ &= -\frac{1}{2} \text{tr} \ln \{ \mathcal{G}_\Lambda^{-1} \} - \frac{1}{2} \text{tr} \ln \{ 1 + \mathcal{G}_\Lambda [X_1 + X_2] \}, \end{aligned}$$

where, in the second line we used the cyclic invariance of the trace. We now proceed with a straightforward expansion of the logarithm,

$$S[T, X_1, X_2] = -\frac{1}{2} \text{tr} \ln \{ 1 + \mathcal{G}_\Lambda [X_1 + X_2] \} = \frac{1}{2} \sum_{k=1} \frac{(-1)^k}{k} \text{tr} \{ \mathcal{G}_\Lambda [X_1 + X_2] \}^k = \sum_{k=1} S^{(k)}[T], \quad (3.32)$$

where in the momentum/frequency representation

$$\mathcal{G}_n^\Lambda(k) = \begin{pmatrix} g_n^+(k) & \\ & g_n^-(k) \end{pmatrix} = \begin{pmatrix} \frac{1}{-i\epsilon_n + k - \frac{i}{2l_0} \text{sgn}(n)} & \\ & \frac{1}{-i\epsilon_n - k - \frac{i}{2l_0} \text{sgn}(n)} \end{pmatrix} \quad (3.33)$$

$$\begin{aligned} X_{nn'}^1(q) &= [T^{-1}(\partial T)]_{nn'}(q) \\ &= \frac{1}{\sqrt{L}} \sum_{m,k} T_{n,n+m}^{-1}(k) [i\epsilon_{n+m} - (k-q)\sigma_3] T_{n+mn'}(q-k) \end{aligned} \quad (3.34)$$

$$\begin{aligned} X_{nn'}^2(q) &= [T^{-1} [\mu + ia\sigma_3\sigma_3^\top] T]_{nn'}(q) \\ &= \frac{\sqrt{T}}{L} \sum_{n'',m,k',k} T_{nn''}^{-1}(k') [\hat{\mu}_m(k) + i\hat{a}_m(k)\sigma_3\sigma_3^\top] T_{n''+m,n'}(-k'-k+q). \end{aligned} \quad (3.35)$$

Here we use Fourier-transformations according to

$$X_{\tau\tau'}^i = T \sum_{nn'} X_{nn'}^i e^{i\epsilon_n \tau - i\epsilon_{n'} \tau'} \quad \text{and} \quad X^i(x) = \frac{1}{\sqrt{L}} \sum_k X^i(k) e^{-ikx}. \quad (3.36)$$

The first order contribution to the “tr ln”-expansion takes the form

$$S^{(1)}[T] = -\frac{1}{2} \text{tr} \{ \mathcal{G}_\Lambda [X_1 + X_2] \} = -\frac{1}{2\sqrt{L}} \sum_{n,k} \text{tr} \{ \mathcal{G}_{n,k}^\Lambda [X_{nn}^1(q=0) + X_{nn}^2(q=0)] \}, \quad (3.37)$$

where, more explicitly,

$$\text{tr} \{ \mathcal{G}_\Lambda X_1 \} = \frac{1}{L} \sum_{n,p} \sum_{m,k} \text{tr} \{ \mathcal{G}_{n,p}^\Lambda T_{n,n+m}^{-1}(k) [i\epsilon_{n+m} - k\sigma_3] T_{n+m,n}(-k) \} \quad (3.38)$$

$$\text{tr} \{ \mathcal{G}_\Lambda X_2 \} = \frac{\sqrt{T}}{L^{3/2}} \sum_{n,p} \sum_{n',m,k,q} \text{tr} \{ \mathcal{G}_{n,p}^\Lambda T_{nn'}^{-1}(k) [\hat{\mu}_m(q) + i\hat{a}_m(q)\sigma_3\sigma_3^\top] T_{n'+m,n}(-k-q) \}. \quad (3.39)$$

Using that $\frac{1}{L} \sum_p \mathcal{G}_{n,p}^\Lambda = \frac{i}{2} \Lambda_n$ one obtains

$$S^{(1)}[T] = S_+^0[T] + S_+^{\text{sou.}}[T] + S_-^0[T] + S_-^{\text{sou.}}[T], \quad (3.40)$$

with

$$S_\pm^0[T] = -\frac{1}{4} \sum_{nm,q} \text{tr} \{ \Lambda_n T_{\pm,nn+m}^{-1}(q) [\epsilon_{n+m} \pm iq] T_{\pm,n+mn}(-q) \} \quad (3.41)$$

$$S_\pm^{\text{sou.}}[T] = -\frac{1}{4} \left(\frac{T}{L} \right)^{1/2} \sum_{nn'm} \sum_{q,k} \text{tr} \{ \Lambda_n T_{\pm,nn'}^{-1}(q) [-i\hat{\mu}_m(k) \pm \hat{a}_m(k)\sigma_3^\top] T_{\pm,n'+mn}(-q-k) \}. \quad (3.42)$$

In Appendix B.1 we show that the “tr ln”-expansion has merely one more non-vanishing contribution. This comes from the second order and is

$$\begin{aligned} S^{(2)}[T] &= \frac{1}{4} \text{tr} \{ \mathcal{G} [\hat{\mu} + i\hat{a}\sigma_3\sigma_3^\top] \mathcal{G} [\hat{\mu} + i\hat{a}\sigma_3\sigma_3^\top] \} \\ &= \frac{T}{4L} \sum_{n,m} \sum_{k,q} \text{tr} \{ \mathcal{G}_n(k) [\mu_{mq} + ia_{mq}\sigma_3\sigma_3^\top] \mathcal{G}_{n+m}(k+q) [\mu_{-m,-q} + ia_{-m,-q}\sigma_3\sigma_3^\top] \} \\ &= \frac{T}{4L} \sum_{n,m} \sum_{k,q} \text{tr} \{ [g_n^+(k)g_{n+m}^+(k+q) + g_n^-(k)g_{n+m}^-(k+q)] [\mu_{mq}\mu_{-m,-q} - a_{mq}\sigma_3^\top a_{-m,-q}\sigma_3^\top] \\ &\quad + i [g_n^+(k)g_{n+m}^+(k+q) - g_n^-(k)g_{n+m}^-(k+q)] [\mu_{mq}a_{-m,-q}\sigma_3^\top + a_{mq}\sigma_3^\top \mu_{-m,-q}] \}. \end{aligned}$$

Dividing the range of frequency-summation, this term can be separated into its “para”- and “diamagnetic” contributions. Starting with the former one finds, e.g. for ($m > 0$)

$$\begin{aligned} \frac{T}{L} \sum_p \sum_{-m < n < 0} g_n^+(p) g_{n+m}^+(p+q) &= \int \frac{dp}{2\pi} \sum_{-m < n < 0} \frac{1}{p+q - i\epsilon_{n+m} - \frac{i}{2l_0}} \frac{1}{p - i\epsilon_n + \frac{i}{2l_0}} \\ &= T \sum_{-m < n < 0} \frac{1}{\omega_m + iq + \frac{1}{l_0}} = \frac{1}{2\pi} \frac{\omega_m l_0}{1 + \omega_m l_0 + iql_0}, \end{aligned}$$

which depends on the mean forward-scattering length, l_0 . We already stated that such l_0 -dependent contributions have to decouple from all gauge invariant observables. Below we demonstrate for the example of the density/density correlation function that, taking into account all contributions depending on l_0 , the final expression, indeed, becomes independent from l_0 and is equal to what is obtained from setting l_0 to zero right in the beginning. Turning to the diamagnetic contribution one finds

$$\frac{T}{L} \sum_p \sum_n g_n^+(p) g_n^+(p) = 2 \operatorname{Re} \int \frac{dp}{2\pi} \int_0^\infty \frac{d\epsilon}{2\pi} \frac{1}{[p - i\epsilon - \frac{i}{2l_0}]^2} = \frac{1}{\pi} \operatorname{Im} \int \frac{dp}{2\pi} \frac{1}{p - \frac{i}{2l_0}} = -\frac{1}{2\pi}.$$

Accordingly, there is a diamagnetic contribution proportional to $g^- g^-$ which gives $-\frac{1}{2\pi}$. Therefore,

$$\begin{aligned} \frac{1}{4} \operatorname{tr} \{ \mathcal{G} [\hat{\mu} + i\hat{a}\sigma_3\sigma_3^T] \mathcal{G} [\hat{\mu} + i\hat{a}\sigma_3\sigma_3^T] \} &= -\frac{1}{4\pi} \sum_{m,q} [\hat{\mu}_{mq}\hat{\mu}_{-m,-q} - \hat{a}_{mq}\sigma_3^T \hat{a}_{-m,-q}\sigma_3^T] \\ &= -\frac{1}{2\pi} \sum_{m,q} [\mu_{mq}\mu_{-m,-q} - a_{mq}a_{-m,-q}], \end{aligned}$$

where in the last line we traced over the T-sector. As already mentioned, there are no further contributions to the “tr ln”-expansion (see Appendix B.1). Collecting everything we thus end up with the following Goldstone-mode action,

$$S[T] = S^{(1)}[T] + S^{(2)}[T], \quad (3.43)$$

where

$$\begin{aligned} S[T_+, T_-, \hat{a}, \hat{\mu}] &= -\frac{1}{4} \sum_{s=\pm} \left\{ \sum_{nm,q} \operatorname{tr} \{ \Lambda_n T_{s,nn+m}^{-1}(q) [\epsilon_{n+m} + siq] T_{s,n+mn}(-q) \} \right. \\ &\quad \left. + \left(\frac{T}{L} \right)^{1/2} \sum_{nn'm} \sum_{q,k} \operatorname{tr} \{ \Lambda_n T_{s,nn'}^{-1}(q) [-i\hat{\mu}_m(k) + s\hat{a}_m(k)\sigma_3^T] T_{s,n'+mn}(-q-k) \} \right\} \\ &\quad - \frac{1}{2\pi} \sum_{m,q} [\mu_{mq}\mu_{-m,-q} - a_{mq}a_{-m,-q}]. \end{aligned} \quad (3.44)$$

That is, the action is given by a sum of three terms: (i) Ballistic σ -model actions [?] for left- and right-moving particle-hole excitations, (ii) a source-term accounting for the coupling of particle-hole excitations to the vector- and chemical potentials and (iii) a “pure” source term resulting from a loop with diamagnetic particle-particle (hole-hole) excitations, see Fig. 3.1.

Expansion in generators: As we will show in section 6, inclusion of backscattering disorder leads to a coupling of the ballistic σ -model actions for left and right moving fields. However, in the “clean” situation considered here, the actions for left- and right-moving particle-hole excitations remain uncoupled. As we momentarily will see this leads to the nice property that an expansion of the rotation-matrices T to second order in its generators, $T = e^W = 1 + W + \frac{1}{2}W^2$, is exact. So let us start out from a parametrization of the Goldstone-modes, T , by generators, W , which anticommute with the saddle-point Λ and fulfill the symmetry constraint Eq.(3.27)

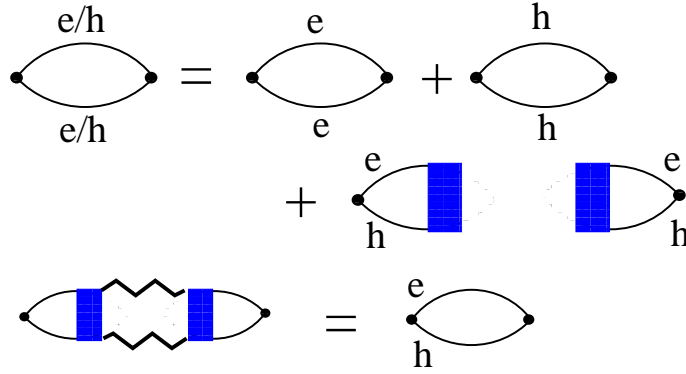


Figure 3.1: Diagrammatic illustration how the source/source correlation function is obtained within the σ -model: The source/source correlation function is separated into its dia- (first line on right side) and paramagnetic (second line on right side) contributions. The diamagnetic contribution is given by the third line of Eq.(3.44) and the paramagnetic contribution is obtained by integration over the particle-hole excitation, T , (second line of Eq.(3.44)) with respect to the action given in the first line of Eq.(3.44). Technically this is achieved by performing one contraction in the Diffuson propagator and is indicated in the third line of the Figure. The introduction of the bosonic field, T , accounting for the particle-hole excitations allows for a transparent description of interference effects, when disorder comes into play.

$$W_{nn'}^t(q) = -\sigma_2^T \sigma_1 W_{n'n}(q) \sigma_1 \sigma_2^T. \quad (3.45)$$

Here t is the transpose in replica, \pm and time-reversal sectors. As usual we separate the generators into contributions diagonal and off-diagonal in the T-sector, corresponding to particle-hole excitations where particle and hole follow the same trajectory in the *same* (Diffuson) and in *opposite* (Cooperon) directions, respectively, i.e.

$$W_D = \begin{pmatrix} \mathcal{D}^{ff} & \\ & \mathcal{D}^{bb} \end{pmatrix} \quad (\text{Diffuson}) \quad W_C = \begin{pmatrix} & \mathcal{C}^{fb} \\ \mathcal{C}^{bf} & \end{pmatrix} \quad (\text{Cooperon}). \quad (3.46)$$

The symmetry-relation for Diffuson and Cooperon reads

$$\mathcal{D}_{nn'}^{ff}(q) = -[\mathcal{D}_{n'n}^{bb}]^T(q) \quad (3.47)$$

$$\mathcal{C}_{nn'}^{fb}(q) = [\mathcal{C}_{n'n}^{bf}]^T(q), \quad (3.48)$$

where we introduced the generalized transpose $A^T = \sigma_1 A^t \sigma_1$. More explicitly

$$\mathcal{D}_{+,nn'}^{ff}(q) = -[\mathcal{D}_{-,n'n}^{bb}]^t(q) \quad (3.49)$$

$$\mathcal{C}_{+,nn'}^{fb}(q) = [\mathcal{C}_{-,n'n}^{bf}]^t(q) \quad (3.50)$$

$$\mathcal{C}_{+,nn'}^{bf}(q) = [\mathcal{C}_{-,n'n}^{fb}]^t(q). \quad (3.51)$$

Accounting for the condition that the generators anti-commute with the saddle point, we introduce the following parametrization of the above matrices in Matsubara-space

$$\begin{aligned} \mathcal{D}_{nn'}^{ff} &= \begin{pmatrix} \bar{D}_{nn'}^{ff} \\ D_{nn'}^{ff} \end{pmatrix}, \quad \mathcal{D}_{nn'}^{bb} = \begin{pmatrix} D_{nn'}^{bb} & \bar{D}_{nn'}^{bb} \end{pmatrix}, \\ \mathcal{C}_{nn'}^{fb} &= \begin{pmatrix} \bar{C}_{nn'}^{fb} \\ C_{nn'}^{fb} \end{pmatrix}, \quad \mathcal{C}_{nn'}^{bf} = \begin{pmatrix} C_{nn'}^{bf} & \bar{C}_{nn'}^{bf} \end{pmatrix}, \end{aligned} \quad (3.52)$$

where $\bar{X}_{n<0,n'>0}$ and $X_{n>0,n'<0}$. Employing the symmetry relation for the Diffuson one finds, that the Diffuson-action in second order in the generators (Gaussian approximation) takes the form ($s = \pm$)

$$S_s^0[\mathcal{D}] = - \sum_{m>0} \sum_{-m<n<0} \sum_q \text{tr} \left\{ \bar{D}_{s,nn+m}^{\text{ff}}(q) [\omega_m + siq] D_{s,n+mn}^{\text{ff}}(-q) \right\} \quad (3.53)$$

$$S_s^{\text{SOU.}}[\mathcal{D}, \hat{\mu}, \hat{a}] = -T^{1/2} \sum_{m>0} \sum_{-m<n<0} \sum_q \text{tr} \left\{ \bar{D}_{s,nn+m}^{\text{ff}}(q) [-i\mu_{-m}(-q) + sa_{-m}(-q)] \right. \\ \left. + [i\mu_m(q) - sa_m(q)] D_{s,n+mn}^{\text{ff}}(-q) \right\}. \quad (3.54)$$

Accordingly the Cooperon-action in Gaussian approximation is given by

$$S_s^0[\mathcal{C}] = - \sum_{m>0} \sum_{-m<n<0} \sum_q \text{tr} \left\{ \bar{C}_{s,nn+m}^{\text{fb}}(q) [\omega_m + siq] C_{s,n+mn}^{\text{bf}}(-q) \right\}. \quad (3.55)$$

As the Cooperon is off-diagonal in T-space, there are no linear contributions coupling the particle-hole excitation to the sources. We will argue below that the Gaussian approximation (for the clean system considered here) is exact. That is all contributions from higher than second order in the generators do not give any contribution to the density/current generating functional. Therefore Eq. (3.53) - Eq.(3.55) is yet another representation of the starting action Eq.(3.1). That Eq. (3.53) - Eq.(3.55) leads to the generating functional Eq.(3.14) can be seen as follows:

Integration over the Diffuson \bar{D}, D we find

$$S[\mu, a] = T \sum_{s=\pm} \sum_{m>0} \sum_{-m<n<0} \sum_q \left\{ \frac{1}{\omega_m + siq} [i\mu_m(q) - sa_m(q)] [-i\mu_{-m}(-q) + sa_{-m}(-q)] \right\} \\ = T \sum_{m>0} m \sum_q \left\{ \left[\frac{1}{\omega_m + iq} + \frac{1}{\omega_m - iq} \right] [\mu_m(q)\mu_{-m}(-q) - a_m(q)a_{-m}(-q)] \right. \\ \left. + \left[\frac{i}{\omega_m + iq} - \frac{i}{\omega_m - iq} \right] [\mu_m(q)a_{-m}(-q) + a_m(q)\mu_{-m}(-q)] \right\} \\ = \frac{1}{\pi} \sum_{m>0} \sum_q \left\{ \frac{\omega_m^2}{\omega_m^2 + q^2} [\mu_m(q)\mu_{-m}(-q) - a_m(q)a_{-m}(-q)] \right. \\ \left. + \frac{\omega_m q}{\omega_m^2 + q^2} [\mu_m(q)a_{-m}(-q) + a_m(q)\mu_{-m}(-q)] \right\} \\ = \frac{1}{2\pi} \sum_m \sum_q \left\{ \frac{\omega_m^2}{\omega_m^2 + q^2} [\mu_m(q)\mu_{-m}(-q) - a_m(q)a_{-m}(-q)] \right. \\ \left. + \frac{\omega_m q}{\omega_m^2 + q^2} [\mu_m(q)a_{-m}(-q) + a_m(q)\mu_{-m}(-q)] \right\}.$$

Adding the diamagnetic contribution from the second order “tr ln” expansion finally gives

$$S[\mu, a] = \frac{1}{2\pi} \sum_{m>0} \sum_q \left\{ \frac{q^2}{q^2 + \omega_m^2} [\mu_m(q)\mu_m(-q) - a_m(q)a_m(-q)] \right. \\ \left. + \frac{\omega_m q}{q^2 + \omega_m^2} [\mu_m(q)a_m(-q) + a_m(q)\mu_m(-q)] \right\}, \quad (3.56)$$

which is the generating functional obtained from the standard and the functional bosonization methods, see Eq.(3.14).

A few remarks at this point: In order to establish the “ σ -model bosonization” as an equivalent method to derive the density/current generating functional we still owe the argument that higher orders in the “ tr ln ” expansion as well as higher orders in the generator expansion do not contribute.

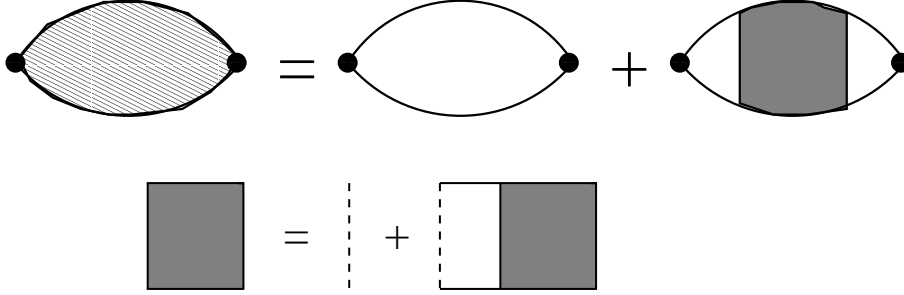


Figure 3.2: Diagrammatic representation of the “paramagnetic” contribution to the density-density correlation function. Solid lines represent advanced and retarded Green’s functions and dashed line represents forward scattering from disorder. The explicit evaluation of the diagrams can be found in Appendix B.2.

- Starting with the former we here merely repeat the main argument and refer for the technicalities to Appendix B.1. Our argument is based on the observation, that forward scattering decouples from all (gauge invariant) observables, and therefore the effective theory has to be independent of the forward scattering length l_0 . In Appendix B.1 we show that only the first and second order in the “ tr ln ”-expansion contain l_0 -independent contributions, and consequently these are the only contributions from the “ tr ln ”-expansion that have to be taken into account. We may exemplify the strategy of keeping only l_0 -independent expressions on the following example:

Take the density-density correlation function for a non-interacting clean system. The Green’s function for left- and right-moving electrons is given by

$$g_n^\pm(p) = \frac{1}{-i\epsilon_n \pm p - \frac{i}{2l_0} \text{sgn}(n)}, \quad (3.57)$$

and from the generating functional derived above, we know that the paramagnetic contribution to the density-density correlation function is given by

$$\langle \rho_m^+(q) \rho_{-m}^+(-q) \rangle_{\text{para.}} = -\frac{1}{2\pi} \frac{\omega_m^2}{\omega_m^2 + q^2}. \quad (3.58)$$

Using, on the other hand, a diagrammatic approach the density/density correlation function may be calculated from summing up the diagrams depicted in Fig.3.2. The explicit calculation of the diagrams can be found in Appendix B.2 and here we merely state that

$$\text{Diagram 1} = \frac{1}{2\pi} \text{Im} \left\{ \frac{\omega_m}{q + i\omega_m + i/l_0} \right\} \quad (3.59)$$

$$\text{Diagram 2} = \frac{1}{2\pi} \text{Im} \left\{ \frac{\omega_m}{(\omega_m l_0 - iql_0)(q + i\omega_m + i/l_0)} \right\} \quad (3.60)$$

Summing up both contributions one finds

$$\text{Eq. (3.59)} + \text{Eq. (3.60)} = \frac{1}{2\pi} \text{Im} \left\{ \frac{\omega_m}{q + i\omega_m} \right\}, \quad (3.61)$$

i.e. Eq. (3.58). Instead of summing up both contributions, however, we may equally take a “short-cut” and set l_0 to zero, which gives

$$\begin{aligned} \text{Eq. (3.59)} &= \frac{-1}{2\pi} \text{Re} \left\{ \frac{\omega_m l_0}{1 - iql_0 + \omega_m l_0} \right\} = 0 \\ \text{Eq. (3.60)} &= \frac{1}{2\pi} \text{Im} \left\{ \frac{\omega_m}{(\omega_m - iq)(ql_0 + i\omega_m l_0 + i)} \right\} = \frac{1}{2\pi} \text{Im} \left\{ \frac{\omega_m}{i\omega_m + q} \right\}, \end{aligned}$$

i.e. the right result. We may thus take the short cut and set $l_0 = 0$ right in the beginning; this is somewhat the strategy of keeping only l_0 -independent contributions from the “tr ln”-expansion.

- This leads us to the second remark concerning contributions from higher orders in the generators (“higher loop corrections” to the Gaussian propagator). In Appendix B.3 we argue that due to the finite space-resolution set by the cut-off, Λ , used to regularize the momentum integrals, one should instead of using δ -distributed disorder better work with finite correlated Gaussian disorder, where the correlation length is given by Λ^{-1} . Doing so one finds (see Appendix B.3) that the Gaussian propagator is modified according to

$$\langle \bar{D}_{s,nn+m}^{\text{ff}}(x) D_{s,n+mn}^{\text{ff}}(x') \rangle_{S_{\text{reg}}^0} = \begin{cases} \langle \bar{D}_{s,nn+m}^{\text{ff}}(x) D_{s,n+mn}^{\text{ff}}(x') \rangle_{S^0}, & s(x - x') > \Lambda^{-1} \\ 0, & s(x - x') < \Lambda^{-1}. \end{cases} \quad (3.62)$$

That is the propagator is unchanged on scales where the particle-hole excitation travels at least the distance Λ^{-1} , but vanishes on smaller length scales. With this remark in mind we turn to the higher loop corrections to the Gaussian propagator.

3.2.4 Higher loop corrections to the Gaussian propagator

We may now turn to the discussion of contributions from higher than second order in the generators. This point still needs further elaboration, and here I merely indicate a line of arguments which might show that all higher loop corrections to the Gaussian propagator vanish. Contributions from higher than second order in the generators can be treated perturbatively with respect to the propagator from the Gaussian approximation, Eq.(3.62). These terms can be organized in a loop expansion where the loop order is given by the number of free momentum integrals. The lowest order corrections to the Gaussian approximation result from terms which are fourth order in the generators, i.e. of the form $S^4[\bar{D}D] = \text{tr} \{O\bar{D}D\bar{D}D\}$, where O denotes the operator a , μ , ∂_x , ∂_τ , etc. For an operator which is local in space, all fields \bar{D}, D under a trace sit at the same space point and therefore no contractions can be performed within one trace. Consider for example the contribution

$$\langle \text{tr} \{O\bar{D}D\bar{D}D\} \text{tr} \{O\bar{D}D\bar{D}D\} \rangle_{S_{\text{reg}}^0} \quad (3.63)$$

Performing Wick contraction on ends up with expressions

$$\left(\langle \bar{D}_{s,nn+m}^{\text{ff}}(x) D_{s,n+mn}^{\text{ff}}(x') \rangle_{S_{\text{reg}}^0} \right)^2 \langle \bar{D}_{s,nn+m}^{\text{ff}}(x') D_{s,n+mn}^{\text{ff}}(x) \rangle_{S_{\text{reg}}^0} \quad (3.64)$$

which vanishes as it contains the product of propagators from x to x' and from x' to x . A systematic analysis however still needs to be done in order to see if this argument generalizes to all contributions from higher than second order in the generators. Especially a discussion of the lowest order corrections, $\langle \text{tr} \{O\bar{D}D\} \text{tr} \{O\bar{D}D\bar{D}D\} \rangle_{S_{\text{reg}}^0}$ and $\langle \text{tr} \{O\bar{D}D\bar{D}D\} \text{tr} \{O\bar{D}D\} \text{tr} \{O\bar{D}D\bar{D}D\} \rangle_{S_{\text{reg}}^0}$ is still needed.

3.2.5 Summary of this section and outlook

In this section we showed that besides the well established standard and functional bosonization schemes one might apply a third method, the “ σ -model bosonization”, in order to derive a generating functional for density/current correlation functions of the non-interacting, clean system. As already mentioned, the argument concerning the vanishing of higher loop corrections to the Gaussian propagators may need a critical revision. In the next section we show that even in the presence of e-e interactions the σ -model approach is equivalent to the former two approaches. The advantage of the “ σ -model bosonization” shows up when we introduce the stochastic backscattering disorder into the model. This will be discussed in the subsequent sections. Before proceeding, however, we may summarize the three bosonization procedures discussed in this section in the following way:

1. The “standard bosonization approach” represents generating functional with help of a bosonic field, i.e.

$$\int d^2x J^t \Pi_J J = \int d^2x \Theta^t \Pi_J^{-1} \Theta + J^t \Theta + \Theta^t J,$$

2. the functional bosonization method uses the loop-cancellation in order to obtain from the “ $\text{tr} \ln$ ”-expansion the generating functional

$$\int d^2x J^t \Pi_J J = \text{tr} \ln \{ \hat{\partial} + J \},$$

3. the “ σ -model approach” uses the identity $\Pi_m^J(q) = 1 - \frac{\omega_m}{q} \Pi_m^J(q) = 1 - i\omega_m \Pi_m^\sigma(q)$ in order to express the generating functional in terms of a matrix field, i.e.

$$\int d^2x J^t \Pi_J J = \int d^2x \text{tr} \{ \bar{\mathcal{D}} q \Pi_{\sigma,m}^{-1}(q) \mathcal{D} + J^t \mathcal{D} + \bar{\mathcal{D}} J \} + J^t J.$$

Here $J^t = (\mu + ia, \mu - ia)$, $\Pi_m^J(q) = \text{diag} \left(\frac{q}{q + i\omega_m}, \frac{q}{q - i\omega_m} \right)$ and $\Pi_m^\sigma(q) = \text{diag} \left(\frac{1}{|\omega_m| + iq}, \frac{1}{|\omega_m| - iq} \right)$.

3.3 Interacting electrons in a clean wire: Equivalence of the three approaches

Having exposed the σ -model bosonization for the clean non-interacting case we now want to show that the method also works for clean *interacting* systems. As our main focus, however, lies in disordered systems we merely give a brief sketch of the strategy followed in the case of clean interacting systems and relegate more detailed calculations to Appendices B.4 and B.5. So let us start from the action given in Eq.(3.8) and include Coulomb-interactions,

$$S_{\text{int.}}[\bar{\chi}\chi] = \frac{1}{2} \int d^2x (\rho_+ \quad \rho_-) \hat{g} \begin{pmatrix} \rho_+ \\ \rho_- \end{pmatrix}. \quad (3.65)$$

As discussed in section 1 we keep only the interaction between densities of opposite chirality and account for the interaction described by g_4 by considering the renormalized Fermi-velocity, see Eq.(3.7). The interaction term is treated in the different bosonization schemes as follows:

3.3.1 Standard bosonization

In the standard bosonization scheme one employs that $\rho_\pm = \frac{1}{2\pi} (\partial_x \theta \mp \partial_x \phi)$, in order to rewrite $S_{\text{int.}}$ in terms of the bosonic degrees of freedom,

$$S_{\text{int.}}[\bar{\chi}\chi] = \frac{g_2}{4\pi^2} \int d^2x \{ (\partial_x \theta)^2 - (\partial_x \phi)^2 \}. \quad (3.66)$$

The bosonic action for the clean interacting system is therefore purely Gaussian in the bosonic fields,

$$S_0[\theta, \phi] + S_{\text{int.}}[\theta, \phi] = \frac{1}{2\pi} \sum_{km} \left\{ \begin{pmatrix} \theta_{mk} & \phi_{mk} \end{pmatrix} \begin{pmatrix} (1 + \frac{g_2}{2\pi})k^2 & i\omega_m k \\ i\omega_m k & (1 - \frac{g_2}{2\pi})k^2 \end{pmatrix} \begin{pmatrix} \theta_{-m, -k} \\ \phi_{-m, -k} \end{pmatrix} \right\}. \quad (3.67)$$

Adding the source term, $S_{\text{sou.}}$, given in Eq.(3.13) and integrating over the bosonic fields θ, ϕ one finds

$$S[a, \mu] = \frac{1}{2\pi} \sum_{m,q} \left\{ \frac{vq^2}{v^2q^2 + \omega_m^2} [g\mu_{mq}\mu_{-m,-q} - g^{-1}a_{mq}a_{-m,-q}] + \frac{\omega_m q}{v^2q^2 + \omega_m^2} [\mu_{mq}a_{-m,-q} + a_{mq}\mu_{-m,-q}] \right\}, \quad (3.68)$$

where we introduced $g = \sqrt{\frac{1 - \frac{g_2}{2\pi}}{1 + \frac{g_2}{2\pi}}}$ and $v = \sqrt{(1 + \frac{g_2}{2\pi})(1 - \frac{g_2}{2\pi})}$.

3.3.2 Functional bosonization

Working with the fermions, one decouples the interaction term with help of a Hubbard-Stratonovich transformation. To this end one introduces the bosonic Hubbard-Stratonovich field $\varphi^t = (\varphi^+ \ \varphi^-)$, with action

$$S[\varphi] = \frac{1}{2} \int d^2x \varphi^t \hat{g}^{-1} \varphi \quad (3.69)$$

and shifts the field $\varphi \rightarrow \varphi + i\hat{g} \begin{pmatrix} \rho_+ \\ \rho_- \end{pmatrix}$ in order to obtain

$$S[\varphi] = \frac{1}{2} \int d^2x \left\{ \varphi^t \hat{g}^{-1} \varphi - (\rho_+ \ \rho_-) \hat{g} \begin{pmatrix} \rho_+ \\ \rho_- \end{pmatrix} - 2i\bar{\chi}\hat{\varphi}\chi \right\},$$

where $\hat{\varphi} = \begin{pmatrix} \varphi_+ & \varphi_- \end{pmatrix}$. Combining the free and the interaction contributions one finds

$$S_0[\bar{\chi}\chi] + S_{\text{int.}}[\bar{\chi}\chi] \rightarrow S[\varphi] + S_0[\bar{\chi}\chi, \varphi] = \frac{1}{2} \int d^2x \left\{ \varphi^t \hat{g}^{-1} \varphi - \int d^2x \bar{\chi} [\partial + i\hat{\varphi}] \chi \right\}, \quad (3.70)$$

which after integration over the fermionic fields leads to

$$S[\varphi] + S_{\text{sou.}}[\mu, a] = \frac{1}{2} \int d^2x \varphi^t \hat{g}^{-1} \varphi + \text{tr} \ln \{\partial\} + \text{tr} \ln \{1 + \mathcal{G}^0 [\mu\sigma_1 + a\sigma_2 + i\hat{\varphi}]\}. \quad (3.71)$$

Expansion of the “tr ln” (as in section 3) one simply has to shift the sources by the Hubbard-Stratonovich fields, i.e. $J \rightarrow J + \varphi$, and finds

$$S[\varphi] + S_{\text{sou.}}[\mu, a] = \frac{1}{2} \int d^2x \varphi^t \hat{g}^{-1} \varphi + \text{tr} \ln \{\partial\} + \frac{1}{2\pi} \int d^2x (J + \varphi)^t \Pi (J + \varphi), \quad (3.72)$$

where we introduced the notation

$$J = \begin{pmatrix} \mu + ia \\ \mu - ia \end{pmatrix} \quad \text{and} \quad \Pi_m(q) = \begin{pmatrix} \Pi_m^+(q) & \\ & \Pi_m^-(q) \end{pmatrix} \quad \text{with} \quad \Pi_m^\pm(q) = \frac{q}{q \pm i\omega_m}. \quad (3.73)$$

One can now show that Eq.(3.72) is equivalent to Eq.(3.68). This may be done by introduction of a further bosonic field and, as it is rather technical, is postponed to Appendix B.4. At this point, however,

we want to mention that one can derive Eq.(3.72) also in a different manner: Instead of accounting for the Hubbard-Stratonovich field in the “tr ln”-expansion one may also employ a gauge transformation, $\bar{\chi}_s \rightarrow \bar{\chi}_s e^{i(\theta_1 + s\theta_2)}$ and $\chi_s \rightarrow e^{-i(\theta_1 + s\theta_2)} \chi_s$ in order to remove the Hubbard-Stratonovich field from the action. Whereas the global (charge) U(1) gauge transformation (described by setting $\theta_2 = 0$) is unproblematic, the chiral U(1) gauge transformation (described by setting $\theta_1 = 0$) can only be implemented by costs of an anomaly term (“chiral anomaly”, see e.g. [14]). This anomaly is exactly given by the polarization operator [14], $S_{\text{anomaly}} = \frac{1}{2\pi} \int d^2x \varphi^t \Pi \varphi$.

3.3.3 σ -model bosonization

Proceeding as in the last subsection (i.e. decoupling the interaction by means of a Hubbard-Stratonovich transformation) and following the same steps as in the clean case (we simply have to substitute $J \rightarrow J + \varphi$ in every step), one obtains after integration over the Diffusons

$$S[\varphi] + S_{\text{sou.}}[\mu, a] = \frac{1}{2} \int d^2x \varphi^t \hat{g}^{-1} \varphi + \text{tr} \ln \{ \mathcal{G}_\Lambda^{-1} \} + \frac{1}{2\pi} \int d^2x (J + \varphi)^t \Pi (J + \varphi). \quad (3.74)$$

In order to show the equivalence to the functional bosonization method we therefore simply have to show that $\text{tr} \ln \{ \mathcal{G}_\Lambda^{-1} \} = \text{tr} \ln \{ \partial \}$. Again, this rather technical step is postponed to the appendices (see Appendix B.5).

3.3.4 Summary of this section

In this section we showed that interacting electrons in a clean 1d system can be described by the action

$$S = S[\phi] + S_\sigma[T] + S_{\text{coup}}[T, \phi, J] + S_{\text{sou}}[J], \quad (3.75)$$

where

$$S[\phi] = \frac{1}{2} \sum_{m,q} \phi_m^t(q) \left(\hat{g}^{-1} - \frac{1}{2\pi} \right) \phi_{-m}(-q) \quad (3.76)$$

$$S_\sigma[T] = -\frac{1}{4} \sum_{nm,q} \text{tr} \{ \Lambda_n T_{nn+m}^{-1}(q) \Pi_{n+m}^\sigma(q) T_{n+mn}(-q) \} \quad (3.77)$$

$$S_{\text{coup}}[T, \phi, J] = -i \left(\frac{T}{L} \right)^{1/2} \sum_{nn'm} \sum_{q,k} \text{tr} \{ \Lambda_n T_{nn'}^{-1}(q) [\hat{\phi}_m(k) + \hat{J}_m(k)] T_{n'+mn}(-q-k) \} \quad (3.78)$$

$$S_{\text{sou}}[J] = -\frac{1}{4\pi} \sum_{m,q} J_m^t(q) J_{-m}(-q). \quad (3.79)$$

Notice that the “tr” includes the trace over the \pm -sector and we introduced the matrices $T = \begin{pmatrix} T_+ & \\ & T_- \end{pmatrix}_\pm$ and $\Pi_{n+m}^\sigma(q) = \begin{pmatrix} \epsilon_{n+m} + iq & \\ & \epsilon_{n+m} - iq \end{pmatrix}_\pm$. The bosonic fields have the following structure in $T \otimes \pm$ -space

$$\hat{J}(t) = \begin{pmatrix} J^+(t) & & & \\ & J^-(t) & & \\ & & J^-(-t) & \\ & & & J^+(-t) \end{pmatrix}_{T \otimes \pm}, \quad \hat{\phi}(t) = \begin{pmatrix} \phi^+(t) & & & \\ & \phi^-(t) & & \\ & & \phi^-(-t) & \\ & & & \phi^+(-t) \end{pmatrix}_{T \otimes \pm}, \quad (3.80)$$

where $J^\pm = \mu \pm ia$ and correspondingly the vectors

$$J^t(t) = (J^+(t) \quad J^-(t) \quad J^-(-t) \quad J^+(-t))_{T \otimes \pm} \quad \phi^t(t) = (\phi^+(t) \quad \phi^-(t) \quad \phi^-(-t) \quad \phi^+(-t))_{T \otimes \pm}. \quad (3.81)$$

3.4 Inelastic scattering rate in a clean Luttinger liquid

In a recent paper Gornyi *et al.* [5, 6] pointed out that, contrary to what one might expect due to the non-Fermi liquid character of the Luttinger liquid, the notion of an inelastic scattering rate is finite and meaningful even in the weakly interacting 1d system. The inelastic scattering rate is proportional to the imaginary part of the interaction induced self-energy, which is dominated by *real inelastic* processes, i.e. interaction processes involving real electron excitations, $|\epsilon| \lesssim T$, and characteristic frequencies $|\omega| \lesssim T$. To be precise, a second order (Golden Rule) calculation of the inelastic scattering-rate gives (see [5, 6] and below, Eq.(3.94))

$$\frac{1}{\tau_{ee}} = \frac{g_2^2}{4\pi} T. \quad (3.82)$$

Gornyi *et al.* compared the perturbative inelastic scattering rate, Eq.(3.82), to the damping of the exact single-particle Green's function and found that the temporal decay for $t \rightarrow \infty$ agrees with the Golden Rule expression [6]. That is, the temporal decay of the Green's function is determined by the processes of inelastic scattering of right-movers on left-movers. Notice also that in the case of weak interactions ($g_2 \ll 1$) $1/\tau_{ee}$ is much smaller than temperature, i.e. $T\tau_{ee} \gg 1$. Gornyi *et al.* point out that the fact that the quasiparticle's characteristic energy ($|\epsilon| \lesssim T$) is much larger than its lifetime, τ_{ee} , is one of the conditions for the existence of the Fermi-liquid state. "In this respect", the authors conclude, "the weakly interacting Luttinger liquid, while being a canonical example of a non-Fermi liquid, reveals the typical Fermi liquid property" [6]. The self-energy's real part, on the other hand, is determined by high energy transfers $|\omega| \gtrsim T$, which is characteristic for *elastic virtual* processes. It is pointed out by Gornyi *et al.* that it is specific to the 1d system that the real part of the self-energy is UV-divergent (it is logarithmically divergent in the ultraviolet and cut off by Λ) and the non-Fermi liquid physics of the Luttinger liquid is encoded in the singular *real* part of the (perturbative) self-energy.

In order to see how the σ -model for the clean interacting system works we briefly show how Eq.(3.82) can be obtained from Eq.(3.75). The Golden Rule calculation corresponds in the σ -model approach to an expansion to second order in generators. The second order expansion leads to the Diffuson action

$$\begin{aligned} S_\sigma[\mathcal{D}] &= -\frac{1}{2} \sum_{n,m} \sum_q \text{tr} \left\{ \mathcal{D}_{nn+m}^{\text{ff}}(q) \Pi_{|m|}^\sigma(q) \mathcal{D}_{n+mn}^{\text{ff}}(-q) \right\} \theta(-n(n+m)) \\ S_{\text{coup}}[\mathcal{D}, \phi] &= iT^{1/2} \sum_{nm} \sum_q \text{tr} \left\{ \Lambda_n \mathcal{D}_{nn+m}^{\text{ff}}(q) \hat{\phi}_{-m}^{\text{f}}(-q) \right\} \theta(-n(n+m)) \\ &\quad + 2i \left(\frac{T}{L} \right)^{1/2} \sum_{mnn'} \sum_{pq} \text{tr} \left\{ \Lambda_n \mathcal{D}_{nn'}^{\text{ff}}(p) \mathcal{D}_{n'n+m}^{\text{ff}}(-p-q) \hat{\phi}_m^{\text{f}}(q) \right\} \theta(-nn') \theta(-n'(n+m)), \end{aligned} \quad (3.84)$$

where $\mathcal{D}^{\text{ff}} = \text{diag}(\mathcal{D}^{+, \text{ff}}, \mathcal{D}^{-, \text{ff}})_\pm$ and $\Pi_{|m|}^\sigma(q) = \text{diag}(|\omega_m| + iq \text{sgn}(m), |\omega_m| - iq \text{sgn}(m))_\pm$. The Cooperon action, on the other hand, is given by

$$\begin{aligned} S_\sigma[\mathcal{C}] &= -\frac{1}{2} \sum_{mn} \sum_q \text{tr} \left\{ \mathcal{C}_{nn+m}^{\text{fb}}(q) \Pi_{|m|}^\sigma(q) \mathcal{C}_{n+mn}^{\text{bf}}(-q) \right\} \theta(-n(n+m)) \\ S_{\text{coup}}[\mathcal{C}, \phi] &= 2i \left(\frac{T}{L} \right)^{1/2} \sum_{mnn'} \sum_{pq} \text{tr} \left\{ \Lambda_n \mathcal{C}_{nn'}^{\text{fb}}(p) \mathcal{C}_{n'n+m}^{\text{bf}}(-p-q) \hat{\phi}_m^{\text{f}}(q) \right\} \theta(-nn') \theta(-n'(n+m)). \end{aligned} \quad (3.86)$$

Notice again, that since the Cooperon is off-diagonal in T-space, it does not couple linearly to the Coulomb-field, ϕ . Notice also that in Eq. (3.83) - Eq. (3.85), the bosonic fields are those on the forward time-branch (the first component in T-space). In the following we will suppress the T-space index, i.e. $\phi = \phi^{\text{f}}$.

3.4.1 Screening the Coulomb-interactions

The peculiarity of a clean Luttinger liquid is that the RPA approximation for the dynamically screened interaction is exact (we already mentioned the cancelation of higher loop contributions in the “tr ln” expansion in section 3.2.2). We briefly show how the RPA screening is obtained from Eq.(3.84). With the RPA screened Coulomb propagator we then derive Eq.(3.82).

The Coulomb interactions are screened by virtual particle-hole excitations. This effect is contained in the coupling of the photon-field, ϕ , to the “linear” particle-hole excitation, i.e. the “linear” Diffuson, \mathcal{D} (first line in Eq.(3.84)). Performing the integral over the linear \mathcal{D} with respect to the Gaussian action we obtain

$$\begin{aligned}
& \langle S_{\text{coup}}[\mathcal{D}, \phi] S_{\text{coup}}[\mathcal{D}, \phi] \rangle \\
&= -T \sum_{nmn'm'} \sum_{qq'} \langle \text{tr} \left\{ \Lambda_n \mathcal{D}_{nn+m}^{\text{ff}}(q) \hat{\phi}_{-m}(-q) \right\} \text{tr} \left\{ \Lambda_{n'} \mathcal{D}_{n'n'+m'}^{\text{ff}}(q') \hat{\phi}_{-m'}(-q') \right\} \rangle \\
& \quad \theta(-n(n+m)) \theta(-n'(n'+m')) \\
&= \frac{1}{2\pi} \sum_{s=\pm} \sum_m \sum_q \frac{|\omega_m|}{|\omega_m| + isq \text{sgn}(m)} \phi_m^s(q) \phi_{-m}^s(-q) \\
&= \frac{1}{2\pi} \sum_{s=\pm} \sum_m \sum_q \phi_m^t(q) \left(\frac{|\omega_m|}{|\omega_m| + iq \text{sgn}(m)} \quad \frac{|\omega_m|}{|\omega_m| - iq \text{sgn}(m)} \right) \phi_{-m}(-q).
\end{aligned}$$

Adding $\frac{1}{2} \langle S_{\text{coup}} S_{\text{coup}} \rangle$ to the photon action, $S[\phi]$, one finds the screened photon propagator,

$$S[\phi] = \frac{1}{2} \sum_{m,q} \phi_m^t(q) \left(g^{-1} - \frac{1}{2\pi} \Pi_m^\phi(q) \right) \phi_{-m}(-q), \quad (3.87)$$

with the polarization matrix

$$\Pi_m^\phi(q) = \begin{pmatrix} \frac{iq \text{sgn}(m)}{|\omega_m| + iq \text{sgn}(m)} & \\ & \frac{-iq \text{sgn}(m)}{|\omega_m| - iq \text{sgn}(m)} \end{pmatrix} = \begin{pmatrix} \frac{q}{q - i\omega_m} & \\ & \frac{q}{q + i\omega_m} \end{pmatrix}. \quad (3.88)$$

As we restrict our analysis to weak interactions we may perform an expansion in $g_2 \ll 1$ to find the photon propagators (again $\phi = \phi^{\text{f}}$)

$$\langle \phi_m^+(q) \phi_{-m}^+(-q) \rangle = \frac{g_2^2}{2\pi} \frac{q}{q + i\omega_m} \left\{ 1 + \frac{g_2^2}{4\pi^2} \frac{q^2}{q^2 + \omega_m^2} + \dots \right\} \quad (3.89)$$

$$\langle \phi_m^-(q) \phi_{-m}^-(-q) \rangle = \frac{g_2^2}{2\pi} \frac{q}{q - i\omega_m} \left\{ 1 + \frac{g_2^2}{4\pi^2} \frac{q^2}{q^2 + \omega_m^2} + \dots \right\} \quad (3.90)$$

$$\langle \phi_m^+(q) \phi_{-m}^-(-q) \rangle = g_2 \left\{ 1 + \frac{g_2^2}{2\pi} \frac{q^2}{q^2 + \omega_m^2} + \dots \right\}. \quad (3.91)$$

3.4.2 The inelastic scattering rate

The Coulomb interaction causes inelastic scattering between electrons, and leads to a finite life-time of the quasi-particles. As mentioned in the introduction the concept of a quasi-particle life time makes also sense for the Luttinger liquid and, for the weakly interacting case, may be obtained from a perturbative calculation of the self-energy. In the σ -model approach the lowest order contribution to the self-energy is obtained from an expansion of the quadratic (in \mathcal{D} , \mathcal{C} respectively) coupling term (first line in Eq.(3.84))

and Eq.(3.86)) to second order followed by a contraction in \mathcal{D} , \mathcal{C} respectively; i.e.

$$\begin{aligned}
& \frac{1}{2} \langle S_{\text{coup}}[\mathcal{D}, \phi] S_{\text{coup}}[\mathcal{D}, \phi] \rangle \\
&= \frac{2T}{L} \sum_{mm' n_1, \dots, n_4} \sum_{pp' qq'} \\
& \quad \langle \text{tr} \left\{ \Lambda_{n_1} \mathcal{D}_{n_1 n_2}^{\text{ff}}(p) \mathcal{D}_{n_2 n_1+m}^{\text{ff}}(-p-q) \hat{\phi}_m(q) \right\} \text{tr} \left\{ \Lambda_{n_3} \mathcal{D}_{n_3 n_4}^{\text{ff}}(p') \mathcal{D}_{n_4 n_3+m'}^{\text{ff}}(-p'-q') \hat{\phi}_{m'}(q') \right\} \rangle_{S_\sigma} \\
&= \frac{4T}{L} \sum_{s=\pm} \sum_{mn_1 n_2} \sum_{qp} \\
& \quad \left\{ \frac{\phi_m^s(p) \phi_{-m}^s(-p)}{|\omega_m| + \text{sign}(m)} [\theta(n_1(n_1+m)) + \theta(n_1(n_1-m)) + 2\delta_{m,0}] \text{tr} \left\{ \mathcal{D}_{n_1 n_2}^{\text{s,ff}}(q) \mathcal{D}_{n_2 n_1}^{\text{s,ff}}(-q) \right\} \right. \\
& \quad - \frac{\phi_m^s(p) \phi_{-m}^s(-p)}{|\omega_m| + \text{sign}(m)} \left[\theta(n_1(n_1+m)) \theta(n_2(n_2+m)) \text{tr} \left\{ \mathcal{D}_{n_1 n_2}^{\text{s,ff}}(q) \mathcal{D}_{n_2+m n_1+m}^{\text{s,ff}}(-q) \right\} \right. \\
& \quad \left. \left. + 2\delta_{m,0} \text{tr} \left\{ \mathcal{D}_{n_1 n_2}^{\text{s,ff}}(q) \mathcal{D}_{n_2 n_1}^{\text{s,ff}}(-q) \right\} \right] \right\}.
\end{aligned}$$

Here we set the Diffuson frequency ($\omega_m = \epsilon_{n_1-n_2}$) and momentum ($q = p - p'$) to zero since the inelastic scattering rate is, by definition, the mass term, i.e. the self-energy at zero momentum and frequency. Expansion of the self-energy in powers of ω_m and q , one finds quantum corrections to the diffusion constant, the density of states, and the frequency [15, 16]. The bosonic frequency summation, m , is restricted to values such that the interaction process only involves electron-hole pairs. The first line contains the “pure” self-energy contribution and the second line contains the vertex contributions (see also Chapter 2 “Dephasing due to magnetic impurities”).

For the Cooperon, one obtains similarly

$$\begin{aligned}
& \frac{1}{2} \langle S_{\text{coup}}[\mathcal{C}, \phi] S_{\text{coup}}[\mathcal{C}, \phi] \rangle \\
&= \frac{2T}{L} \sum_{mm' n_1, \dots, n_4} \sum_{pp' qq'} \\
& \quad \langle \text{tr} \left\{ \Lambda_{n_1} \mathcal{C}_{n_1 n_2}^{\text{fb}}(p) \mathcal{C}_{n_2 n_1+m}^{\text{bf}}(-p-q) \hat{\phi}_m(q) \right\} \text{tr} \left\{ \Lambda_{n_3} \mathcal{C}_{n_3 n_4}^{\text{fb}}(p') \mathcal{C}_{n_4 n_3+m'}^{\text{bf}}(-p'-q') \hat{\phi}_{m'}(q') \right\} \rangle_{S_\sigma} \\
&= \frac{4T}{L} \sum_{s=\pm} \sum_{mn_1 n_2} \sum_{qp} \\
& \quad \left\{ \frac{\phi_m^s(p) \phi_{-m}^s(-p)}{|\omega_m| + \text{sign}(m)} [\theta(n_1(n_1+m)) + \theta(n_1(n_1-m)) + 2\delta_{m,0}] \text{tr} \left\{ \mathcal{C}_{n_1 n_2}^{\text{s,fb}}(q) \mathcal{C}_{n_2 n_1}^{\text{s,bf}}(-q) \right\} \right. \\
& \quad - \frac{\phi_m^s(p) \phi_{-m}^s(-p)}{|\omega_m| + \text{sign}(m)} \left[\theta(n_1(n_1+m)) \theta(n_2(n_2+m)) \text{tr} \left\{ \mathcal{C}_{n_1 n_2+m}^{\text{s,fb}}(q) \mathcal{C}_{n_2 n_1+m}^{\text{s,bf}}(-q) \right\} \right. \\
& \quad \left. \left. + 2\delta_{m,0} \text{tr} \left\{ \mathcal{C}_{n_1 n_2}^{\text{s,fb}}(q) \mathcal{C}_{n_2 n_1}^{\text{s,bf}}(-q) \right\} \right] \right\}.
\end{aligned}$$

Again, the first line gives the “pure” self-energy and the second line the vertex contributions. Notice that the energy-structure of the vertex-contribution is different for the Diffuson and Cooperon. Indeed, the energy structure for the Diffuson is such, that self-energy and vertex contributions exactly cancel (no dephasing in one loop), whereas for the Cooperon vertex contributions cancel only interaction processes from the self-energy involving small energies, $\omega \lesssim 1/\tau_\varphi$, see Appendix B.6 and Chapter 2 (“Dephasing due to magnetic impurities”).

As already mentioned, the inelastic scattering rate is obtained from the self-energy contribution only. It is (for Diffuson and Cooperon) given by

$$\frac{1}{\tau_{\text{inel}}^s(\epsilon_n)} = \frac{4T}{L} \sum_m \sum_q \Pi_m^s(q) V_m^s(q) [\theta(n(n+m)) + \theta(n(n-m))],$$

where $\Pi_m^s(q) = \frac{1}{\omega_m + sip \operatorname{sgn}(m)}$ and we introduced $V_m^s(q) = \langle \phi_m^s(p) \phi_{-m}^s(-p) \rangle$. The analytical continuation gives

$$\begin{aligned} & \sum_m \Pi_m^s(q) V_m^s(q) [\theta(n(n+m)) + \theta(n(n-m))] \\ &= -\frac{2}{\pi T} \int d\Omega \left(\coth \left[\frac{\Omega}{2T} \right] \operatorname{Im} V_\Omega^{\text{R},s}(q) + \frac{1}{2i} \tanh \left[\frac{\epsilon - \Omega}{2T} \right] V_\Omega^{\text{R},s}(q) + \frac{1}{2i} \tanh \left[\frac{\epsilon + \Omega}{2T} \right] V_\Omega^{\text{A},s}(q) \right) \Pi_\Omega^{\text{R},s}(q) \\ &+ \frac{1}{\pi T} \int d\Omega \left(\frac{1}{2i} \tanh \left[\frac{\epsilon - \Omega}{2T} \right] V_\Omega^{\text{R},s}(q) + \frac{1}{2i} \tanh \left[\frac{\epsilon + \Omega}{2T} \right] V_\Omega^{\text{A},s}(q) \right) \Pi_\Omega^{\text{R},s}(q), \end{aligned} \quad (3.92)$$

where we also analytically continued $i\epsilon_n \rightarrow \epsilon$. The contribution in the second line describes high-energy $\epsilon, \Omega \gtrsim T$ processes with *virtual* electrons involved (see discussion of the beginning of this section). These combine with diagrams where the analytical structure of a single particle line is changed due to the interaction process (i.e. with diagrams not considered here) to describe corrections to the diffusion constant, see e.g. [17]. That is, they are not relevant for inelastic scattering processes which only include *real* electrons (i.e. electrons with energy $\epsilon \lesssim T$) and will be dropped out in the following. The remaining term involves only processes with energy transfer $\Omega \lesssim T$ (i.e. *real inelastic* processes). This is guaranteed by the combination of thermal functions. Notice also, that, since only the imaginary part of the screened Coulomb interaction, $\operatorname{Im} V$, enters the inelastic scattering rate, the diamagnetic contribution from the polarization operator vanishes and only its paramagnetic part contributes. Taking into account only electrons at the Fermi energy ($\epsilon = 0$) and using that $\coth \left[\frac{\Omega}{2T} \right] - \tanh \left[\frac{\Omega}{2T} \right] = 2 \sinh^{-1} \left[\frac{\Omega}{T} \right]$ and $\Pi_{-\Omega}^{\text{R},s}(q) = \Pi_\Omega^{\text{A},s}(q)$ and $V_{-\Omega}^{\text{R},s}(q) = V_\Omega^{\text{A},s}(q)$ one finds

$$\frac{1}{\tau_{\text{inel.}}(\epsilon = 0)} = -\frac{2}{L\pi} \sum_q \int d\Omega \frac{1}{\sinh \left[\frac{\Omega}{T} \right]} \operatorname{Im} V_\Omega^{\text{R},s}(q) \operatorname{Re} \Pi_\Omega^{\text{R},s}(q). \quad (3.93)$$

With the RPA screened propagator, Eq.(3.89) - Eq.(3.91), analytically continued to real frequencies, $V_\Omega^{\text{R},s}(q) = \frac{g_2^2}{2\pi} \frac{q}{q + s\Omega + si0}$ and $\Pi_\Omega^{\text{R},s}(q) = \frac{-i}{sq - \Omega - i0}$ one finds the inelastic scattering rate

$$\begin{aligned} \frac{1}{\tau_{\text{inel.}}^s(\epsilon = 0)} &= \frac{g_2^2}{\pi^2} \int \frac{dq}{2\pi} \int d\Omega \frac{1}{\sinh \left[\frac{\Omega}{T} \right]} \operatorname{Im} \frac{q}{q + s\Omega + si0} \operatorname{Im} \frac{1}{sq - \Omega - i0} \\ &= -\frac{sg_2^2}{2\pi} \int dq \int d\Omega \frac{q}{\sinh \left[\frac{\Omega}{T} \right]} \delta(q + s\Omega) \delta(sq - \Omega) \\ &= \frac{g_2^2 T}{2\pi} \int dq \int d\Omega \delta(q + s\Omega) \delta(q - s\Omega) \\ &= \frac{g_2^2}{4\pi} T. \end{aligned} \quad (3.94)$$

3.4.3 Summary of this section

In this section we showed how the σ -model works at the example of the inelastic dephasing rate in a clean Luttinger liquid. More important, we repeated the observations of Gornyi *et al.* [5, 6] that it is the *elastic virtual* processes, which are determined by interaction processes with high energies $\Omega \gtrsim T$, which lead to the non-Fermi liquid singularities typical for the Luttinger liquid. The *inelastic real* processes, on the other hand, (involving interaction processes with energy transfer $\Omega \lesssim T$) lead to finite and meaningful results, as e.g. for the quasi-particle life-time. We will come back to the Golden Rule calculation of the inelastic scattering rate when we interpret the dephasing rate which governs the decay of the persistent current in a disordered Luttinger liquid, see section 3.7.2.

3.5 Electrons in a disordered one-dimensional system

As stated in the introduction, our main focus lies on disordered one-dimensional systems. We already mentioned that including arbitrary weak (stochastic) disorder in the “standard” or the “functional” bosonization schemes leads to theories disparate more complicated. In this section we want to show

how stochastic disorder can be treated within the σ -model bosonization. To this end we restrict ourselves in this section to the non-interacting case. That is we start out from the action Eq.(3.8) and include back-scattering disorder described by

$$S_v[\bar{\chi}\chi] = - \int d^2x \bar{\chi} v \sigma_1 \chi, \quad \langle v(x)v(x') \rangle = l_1^{-1}. \quad (3.95)$$

Notice that compared to Eq. (3.6) we work in the rotated basis, as introduced in section 3. Going through the steps of section 3. integrating out the electrons leads to (compare with Eq.(3.32))

$$S[T] = -\frac{1}{2} \text{tr} \ln \{1 + \mathcal{G}_\Lambda[X_1 + X_2 + X_3]\}, \quad (3.96)$$

where $X_{nn'}^3(x) = [T^{-1}v\sigma_1 T]_{nn'}(x)$. In Appendix B.7 we show that expansion of the “ $\text{tr} \ln$ ” gives only one contribution involving X_3 , which comes from the second order “ $\text{tr} \ln$ ”-expansion, i.e. $S^{(2)}[T] = S_{\text{bs}}[T]$, where

$$S_{\text{bs}}[T] = -\frac{1}{16l_1} \sum_{nn'} \text{tr} \{ [T\Lambda T^{-1}]_{nn'}(q) \sigma_1 [T\Lambda T^{-1}]_{n'n}(-q) \sigma_1 \}. \quad (3.97)$$

Therefore, non-interacting electrons in a disordered wire are described by the action

$$S = S_\sigma[T] + S_{\text{bs}}[T] + S_{\text{coup}}[T, J] + S_{\text{sou}}[J], \quad (3.98)$$

where

$$S_\sigma[T] = -\frac{1}{4} \sum_{nm,q} \text{tr} \{ \Lambda_n T_{nm+m}^{-1}(q) \Pi_m^\sigma(q) T_{n+mn}(-q) \} \quad (3.99)$$

$$S_{\text{bs}}[T] = -\frac{1}{16l_1} \sum_{nn'} \text{tr} \{ \sigma_1 [T\Lambda_n T^{-1}]_{nn'}(q) \sigma_1 [T\Lambda T^{-1}]_{n'n}(-q) \} \quad (3.100)$$

$$S_{\text{coup}}[T, J] = -i \left(\frac{T}{L} \right)^{1/2} \sum_{nn'm} \sum_{q,k} \text{tr} \{ \Lambda_n T_{nn'}^{-1}(q) \hat{J}_m(k) T_{n'+mn}(-q-k) \} \quad (3.101)$$

$$S_{\text{sou}}[J] = -\frac{1}{4\pi} \sum_{m,q} J_m^t(q) J_{-m}(-q), \quad (3.102)$$

with T , $\Pi_m^\sigma(q)$, \hat{J} and J as in the last section. That is, the inclusion of backscattering disorder leads to a coupling of the ballistic σ -model actions for the left- and right -moving particle-hole excitations (i.e. for the $+$ - and $-$ -branches). As we will see below this innocent looking coupling renders the model much more complicated, since e.g. in a perturbative evaluation one has to account for contributions from higher than second order.

3.5.1 Localization in a disordered 1d system

The model Eq.(3.97) shows nicely that in a non-interacting system (i.e. where phase coherence is not destroyed by inelastic scattering processes) the ballistic motion on short scales crosses over directly into the localization regime, with no diffusive dynamics on intermediate length scale. This may be seen as follows: We parametrize rotations by a massless “center-of-mass”- and a massive “relative”-coordinate, $T_\pm = e^{\pm K} T_0$, and perform an expansion to second order in the “relative”-coordinate, K ,

$$S = S_\sigma[K, T_0] + S_{\text{bs}}[K] + S_{\text{coup}}[K, T_0, \hat{a}, \hat{\mu}] + S_{\text{sou}}[J], \quad (3.103)$$

where

$$S_\sigma[K, T_0] = \frac{1}{2} \int d\tau d\tau' dx \operatorname{tr} \{ (1 - 2K^2) \Lambda T_0^{-1} i \partial_\tau T_0 - K \Lambda T_0^{-1} \partial_x T_0 \} \quad (3.104)$$

$$S_{\text{bs}}[K] = -l_1^{-1} \int d\tau d\tau' dx \operatorname{tr} \{ K^2 \} \quad (3.105)$$

$$S_{\text{coup}}[K, T_0, \hat{\mu}, \hat{a}] = -2i \int d\tau d\tau' dx \operatorname{tr} \{ (1 - 2K^2) \Lambda T_0^{-1} \hat{\mu} T_0 - 2i K \Lambda T_0^{-1} \hat{a} \sigma_3^T T_0 \} \quad (3.106)$$

$$S_{\text{sou}}[J] = -\frac{1}{4\pi} \int d^2x J^t J. \quad (3.107)$$

Integration over the massive quadratic K fluctuations one finds (For strong disorder $l_1 \rightarrow 0$ the K -action is governed by its saddle-point $K = 0$ and small fluctuations around it)

$$\begin{aligned} S_{\text{bs}}[K] + S_\sigma[K, T_0] + S_{\text{coup}}[K, T_0, \hat{\mu}, \hat{a}] \\ \approx -l_1^{-1} \int d\tau d\tau' dx \operatorname{tr} \{ K^2 \} - \frac{1}{2} \int d\tau d\tau' dx \operatorname{tr} \{ K \Lambda T_0^{-1} [\partial_x + 8\hat{a} \sigma_3^T] T_0 \} \\ \rightarrow \frac{l_1}{2} \int d\tau d\tau' dx \operatorname{tr} \{ (\Lambda T_0^{-1} [\partial_x - 8\hat{a} \sigma_3^T] T_0)^2 \}. \end{aligned}$$

Adding the K -independent terms we end up with the diffusive σ -model in the “center-of-mass” coordinate T_0 ,

$$S\sigma[Q, a, \mu] = \frac{1}{2} \int d\tau d\tau' dx \operatorname{tr} \{ (i\partial_\tau + \mu) Q - l_1 (\partial_x + i[a\sigma_3^T, \cdot]Q)^2 \}, \quad (3.108)$$

where $Q = T_0^{-1} \Lambda T_0$. Notice that while in higher dimension the derivation of the diffusive σ -model relies on a gradient expansion, which makes use of the small parameters $\omega_m \tau, D\mathbf{q}^2 \tau \ll 1$ (see Chapters 1 and 2), the above derivation does not make any use of this presumption.

Even more important, the higher dimensional σ -model has a regime of “weak disorder” in which the largeness of the parameter $\epsilon_F \tau \gg 1$ (weak disorder) allows for a perturbative expansion in generators. This allows for a systematic organization of quantum corrections to e.g. the classical Drude conductivity (to be more precise, in 2d and quasi 1d systems one also has to assume that quantum corrections are cut-off by some dephasing mechanism, see Chapters 1 and 2). In contrast to this, Eq.(3.108) lacks of a global large parameter allowing for a perturbative expansion in the generators. Therefore, large fluctuations of the Q -field (describing the proliferation of particle-hole excitations) are not suppressed and cause Anderson localization [1]. The ballistic motion on short length scales crosses over into the localized regime, without diffusive intermediate regime.

3.5.2 Drude conductivity and weak localization in a disordered 1d system

In their recent work Gornyi *et al.* [5, 6] showed that key notions of mesoscopic physics, such as weak localization and dephasing are also applicable to disordered (interacting) one-dimensional systems. To be precise, the authors showed that in the regime of relatively high temperatures, where the dephasing-time, τ_φ , due to e-e interactions is much smaller than the mean free path, l_1 , of the forward scattering disorder interference corrections to the Drude conductivity (signaling the onset of Anderson localization) can be organized in a perturbative expansion with expansion parameter τ_φ/l_1 . In this subsection we briefly indicate how this may be seen within the σ -model without presenting a more careful analysis.

Drude conductivity: The Drude conductivity, $\sigma_D = \frac{l_1}{\pi}$, is obtained from Eq.(3.108) by insertion of the saddle point value $Q = \Lambda$ (see Chapters 1 and 2). In section 3.6.2 we show that *virtual elastic* e-e interaction processes renormalize the backscattering length, l_1 , leading to a temperature dependent Drude conductivity (see Eq.(3.144)). At moderately high temperatures it is however the weak localization corrections to the Drude conductivity that govern the temperature dependence of the conductivity for the case of weak e-e interactions (compare Eq.(3.112) and Eq.(3.143)) and, with lowering the temperature, eventually drive the system into the strong localization regime. So let us briefly discuss the interference corrections to the Drude conductivity.

Interference corrections to the Drude conductivity: arise due to coherent backscattering processes and in the higher dimensional systems can be obtained from Eq.(3.108) by a systematic expansion in generators, $Q = \Lambda(1 + W + \dots)$ (as discussed in Chapters 1 and 2) We already mentioned that, in contrast to its higher dimensional relatives, such a perturbative expansion in generators is not justified in the noninteracting one-dimensional system. Assuming however strong dephasing, such that $\tau_\varphi \ll l_1$, quantum corrections to the Drude conductivity are strongly suppressed. Weak localization corrections are then given by a minimal loop consisting of three scattering events [5, 6].

Technically, one may introduce a dephasing rate $1/\tau_\varphi \gg 1/l_1$, and expand action Eq.(3.98) to second order in the generators. This leads to the ballistic \pm -Cooperon propagator

$$\Pi_{|m|}^{\sigma, l_1}(q) = \begin{pmatrix} |\omega_m| + iq \operatorname{sgn}(m) + l_1^{-1} + \tau_\varphi^{-1} & 1/l_1 \\ 1/l_1 & |\omega_m| + iq \operatorname{sgn}(m) + l_1^{-1} + \tau_\varphi^{-1} \end{pmatrix}. \quad (3.109)$$

A systematic expansion in the off-diagonal coupling term amounts to an expansion in the parameter τ_φ/l_1 . In the limit of strong dephasing, $\tau_\varphi \ll l_1$ the weak localization corrections to the Drude conductivity are dominated by a loop consisting of three scattering events, which is the minimal number to form a loop [5, 6], i.e.

$$\Delta\sigma_{WL}^3 \propto \sigma^D l_1^{-2} \sum_{-m < n < 0} \int dq \frac{1}{q + i/\tau_\varphi} \frac{1}{q - i/\tau_\varphi} \frac{1}{q + i/\tau_\varphi}, \quad (3.110)$$

and leads to

$$\Delta\sigma_{WL}^3 \propto \sigma^D \left(\frac{\tau_\varphi}{l_1} \right)^2. \quad (3.111)$$

Accordingly, a k^{th} -order scattering processes (the “ k -Cooperon”) gives interference corrections to the Drude conductivity of the order $\Delta\sigma_{WL}^k \propto \sigma^D \left(\frac{\tau_\varphi}{l_1} \right)^k$. Notice however, that in the case where dephasing is due to electron-electron interactions, a more careful analysis, reveals that WL corrections are dominated by contributions of rare configurations in which two of the three impurities are anomalously close to each other [5, 6]. In these configurations the dephasing is strongly suppressed (since the impurities are close to each other) and [5, 6] $\Delta\sigma_{WL} \propto \left(\frac{\tau_\varphi}{l_1} \right)^2 \ln \frac{l_1}{\tau_\varphi}$. In any case, lowering the temperature decreases the dephasing rate (for e-e interactions this happens more rapidly than the renormalization of the backscattering length), such that finally $\tau_\varphi \sim l_1$ marks the cross over temperature where strong localization sets in. Let us briefly mention that for weak electron-electron interactions the dephasing rate measured in the weak localization experiment is given by [5, 6]

$$\frac{1}{\tau_\varphi} = \frac{g_2}{2} \sqrt{\frac{T}{\pi l_1}}. \quad (3.112)$$

3.5.3 Summary of this section

In this section we derived an effective field theory for the non-interacting disordered 1d system. We showed how in the absence of any interactions (leading to dephasing due to inelastic processes), the ballistic propagation of electron-hole pairs on short scales crosses over directly into the localization regime, with no diffusive dynamics on intermediate length scales. Technically, considering length scales greater than l_1 scattering between the \pm -branches becomes effectual and the field theory for the two independent branches gets locked into a single copy. We repeated recent arguments by Gornyi that for interacting systems there exists a regime (of moderate high temperatures) where the conductivity is dominated by the Drude conductivity (with temperature-dependent renormalized backscattering length) and interference corrections, which can be organized in an perturbative expansion. Introducing *phenomenologically* a dephasing rate we indicated how these results can be obtained within the σ -model.

3.6 Interacting electrons in a disordered 1d system

So let us finally turn to interacting electrons in a disordered 1d system. Including interactions, Eq.(3.65), into the model, Eq.(3.75), we proceed as in section 4 and decouple the interaction by means of a Hubbard-Stratonovich transformation. We may now proceed in the two ways described in section 4. Following the first way, we keep the Hubbard-Stratonovich field in all calculations (i.e. simply shift $J \rightarrow J + \phi$ in all calculations) and obtain

$$S = S[\phi] + S_\sigma[T] + S_{\text{bs}}[T] + S_{\text{coup}}[T, \phi, J] + S_{\text{sou}}[J], \quad (3.113)$$

where

$$S[\phi] = \frac{1}{2} \sum_{m,q} \phi_m^t(q) \left(\hat{g}^{-1} - \frac{1}{2\pi} \right) \phi_{-m}(-q) \quad (3.114)$$

$$S_\sigma[T] = -\frac{1}{4} \sum_{nm,q} \text{tr} \left\{ \Lambda_n T_{nn+m}^{-1}(q) \Pi_m^\sigma(q) T_{n+mn}(-q) \right\} \quad (3.115)$$

$$S_{\text{bs}}[T] = -\frac{1}{16l_1} \sum_{nn',q} \text{tr} \left\{ \sigma_1 [T \Lambda T^{-1}]_{nn'}(q) \sigma_1 [T \Lambda T^{-1}]_{n'n}(-q) \right\} \quad (3.116)$$

$$S_{\text{coup}}[T, \phi, J] = -i \left(\frac{T}{L} \right)^{1/2} \sum_{nn'm} \sum_{q,k} \text{tr} \left\{ \Lambda_n T_{nn'}^{-1}(q) \left[\hat{\phi}_m(k) + \hat{J}_m(k) \right] T_{n'+mn}(-q-k) \right\} \quad (3.117)$$

$$S_{\text{sou}}[J] = -\frac{1}{4\pi} \sum_{m,q} J_m^t(q) J_{-m}(-q), \quad (3.118)$$

with T , Π^σ , J and ϕ as before. The second way to proceed is to use the global $U(1)$ -symmetry of the model to eliminate one component of the Hubbard-Stratonovich field and to move the remaining chiral $U(1)$ -field from the ballistic σ -model actions to the back-scattering term by means of the chiral gauge transformation. That is, $\bar{\chi}_s \rightarrow \bar{\chi}_s e^{i(\theta+s\chi)}$ and $\chi_s \rightarrow e^{-i(\theta+s\chi)} \chi_s$ removes the Hubbard-Stratonovich field from the “clean action” (see section 4) but dresses the back-scattering term with the Hubbard-Stratonovich field. Furthermore the chiral gauge transformation leads (due to the anomaly) to the polarization operator, i.e. the RPA screened Coulomb interaction (see also section 4). Following this second road, one finds Eq.(3.113), with

$$S[\phi] = \frac{1}{2} \sum_{m,q} \phi_m^t(q) \left(\hat{g}^{-1} - \frac{1}{2\pi} \Pi_m^\phi(q) \right) \phi_{-m}(-q) \quad (3.119)$$

$$S_\sigma[T] = -\frac{1}{4} \sum_{nm,q} \text{tr} \left\{ \Lambda_n T_{nn+m}^{-1}(q) \Pi_m^\sigma(q) T_{n+mn}(-q) \right\} \quad (3.120)$$

$$S_{\text{bs}}[T, \chi] = -\frac{1}{8l_1} \sum_{nn',q} \text{tr} \left\{ Q_+ e^{i\chi} Q_- e^{-i\chi} \right\} \quad (3.121)$$

$$S_{\text{coup}}[T, J] = -i \left(\frac{T}{L} \right)^{1/2} \sum_{nn'm} \sum_{q,k} \text{tr} \left\{ \Lambda_n T_{nn'}^{-1}(q) \hat{J}_m(k) T_{n'+mn}(-q-k) \right\} \quad (3.122)$$

$$S_{\text{sou}}[J] = -\frac{1}{4\pi} \sum_{m,q} J_m^t(q) J_{-m}(-q), \quad (3.123)$$

where $Q_\pm = T_\pm \Lambda T_\pm^{-1}$ and the Coulomb-fields, ϕ and χ , are connected by a linear transformation in the following way:

$$\begin{pmatrix} \phi_m^+(q) \\ \phi_m^-(q) \end{pmatrix} = \begin{pmatrix} q + i\omega_m & q + i\omega_m \\ -q + i\omega_m & q - i\omega_m \end{pmatrix} \begin{pmatrix} \chi_m(q) \\ \theta_m(q) \end{pmatrix}. \quad (3.124)$$

Depending on the situation it is more comfortable to work with either action. The above model is the single channel limit of a recently developed low-energy field theory of weakly disordered multi-channel conductors [7], which in the limit of small energies $\epsilon < \tau_0^{-1}$ (τ_0^{-1} being the bare elastic scattering rate) and a large number of transport channels recovers Finkel'stein's diffusive interacting σ -model [2] with all known consequences.

3.6.1 RPA screening in a disordered system

As a first application of Eq.(3.113) let us see how the RPA screening is changed due to disorder. These calculations show that the life-time of the particle-hole excitations responsible for the RPA screening of the Coulomb interactions becomes finite. This leads to non-vanishing dephasing rates determining the magnitude of the WL (see [5, 6]) and the amplitude of the persistent current (see end of section 3.7.2) in a disordered Luttinger liquid.

This is most conveniently done in the representation Eq.(3.114) - Eq.(3.118). We already saw (in section 4) that the RPA-screening is obtained from integrating over the expression in the action, where the "linear" Diffuson couples to the Coulomb field. Expansion of Eq.(3.114) - Eq.(3.118) to second order in the Diffusons we obtain

$$S[\mathcal{D}] = S_\sigma[\mathcal{D}] + S_{bs}[\mathcal{D}] + S_{\text{coup}}[\mathcal{D}, \phi], \quad (3.125)$$

where

$$S_\sigma[\mathcal{D}] + S_{bs}[\mathcal{D}] = -\frac{1}{2} \sum_{n,m} \sum_q \text{tr} \left\{ [\mathcal{D}^{\text{ff}}]_{nn+m}^t(q) \Pi_{|m|}^{\sigma, l_1}(q) \mathcal{D}_{n+mn}^{\text{ff}}(-q) \right\} \theta(-n(n+m)) \quad (3.126)$$

$$\begin{aligned} S_{\text{coup}}[\mathcal{D}, \phi] = & iT^{1/2} \sum_{nm} \sum_q \text{tr} \left\{ \Lambda_n \mathcal{D}_{nn+m}^{\text{ff}}(q) \hat{\phi}_{-m}(-q) \right\} \theta(-n(n+m)) \\ & + 2i \left(\frac{T}{L} \right)^{1/2} \sum_{mnn'} \sum_{pq} \text{tr} \left\{ \Lambda_n \mathcal{D}_{nn'}^{\text{ff}}(p) \mathcal{D}_{n'n+m}^{\text{ff}}(-p-q) \hat{\phi}_m(q) \right\} \theta(-nn') \theta(-n'(n+m)), \end{aligned} \quad (3.127)$$

with

$$\Pi_{|m|}^{\sigma, l_1}(q) = \begin{pmatrix} |\omega_m| + iq \text{sgn}(m) + l_1^{-1} & -l_1^{-1} \\ -l_1^{-1} & |\omega_m| - iq \text{sgn}(m) + l_1^{-1} \end{pmatrix}_{\pm} \quad \text{and} \quad \mathcal{D}^t = (\mathcal{D}^+ \quad \mathcal{D}^-)_{\pm}.$$

Proceeding as in section 4, the polarization operator, providing the RPA screening, is obtained in the following way:

$$\begin{aligned} & \langle S_{\text{coup}}[\mathcal{D}, \phi] S_{\text{coup}}[\mathcal{D}, \phi] \rangle \\ &= \frac{1}{2\pi} \sum_{s,s'=\pm} \sum_{nm} \sum_q [\Pi^{\sigma, l_1}]_{ss',m}^{-1}(q) \phi_m^s(q) \phi_{-m}^{s'}(-q) \theta(-n(n+m)) \\ &= \frac{1}{2\pi} \sum_{s=\pm} \sum_m \sum_q \phi_m^t(q) \frac{|\omega_m|}{(|\omega_m| + l_1^{-1})^2 + q^2 - l_1^{-2}} \begin{pmatrix} |\omega_m| - iq \text{sgn}(m) + l_1^{-1} & l_1^{-1} \\ l_1^{-1} & |\omega_m| + iq \text{sgn}(m) + l_1^{-1} \end{pmatrix} \phi_{-m}(-q) \\ &= \frac{1}{2\pi} \sum_{s=\pm} \sum_m \sum_q \phi_m^t(q) \frac{|\omega_m|}{|\omega_m|^2 + q^2 + 2|\omega_m|l_1^{-1}} \begin{pmatrix} |\omega_m| - iq \text{sgn}(m) + l_1^{-1} & l_1^{-1} \\ l_1^{-1} & |\omega_m| + iq \text{sgn}(m) + l_1^{-1} \end{pmatrix} \phi_{-m}(-q). \end{aligned}$$

Adding $\frac{1}{2} \langle S_{\text{coup}} S_{\text{coup}} \rangle$ to the photon action $S[\phi]$ therefore gives

$$S[\phi] = \frac{1}{2} \sum_{m,q} \phi_m^t(q) \left(\hat{g}^{-1} + \frac{1}{2\pi} - \frac{1}{2\pi} \Pi_m^\phi(q) \right) \phi_{-m}(-q), \quad (3.128)$$

with the polarization

$$\Pi_m^\phi(q) = \frac{|\omega_m|}{|\omega_m|^2 + q^2 + 2|\omega_m|l_1^{-1}} \begin{pmatrix} |\omega_m| - iq \operatorname{sgn}(m) + l_1^{-1} & l_1^{-1} \\ l_1^{-1} & |\omega_m| + iq \operatorname{sgn}(m) + l_1^{-1} \end{pmatrix}, \quad (3.129)$$

and

$$1 - \Pi_m^\phi(q) = \frac{1}{q^2 + |\omega_m|^2 + 2|\omega_m|l_1^{-1}} \begin{pmatrix} q^2 + |\omega_m|l_1^{-1} + i\omega_m q & |\omega_m|l_1^{-1} \\ |\omega_m|l_1^{-1} & q^2 + |\omega_m|l_1^{-1} + i\omega_m q \end{pmatrix}. \quad (3.130)$$

Notice that the polarization operator, Eq.(3.129), acquires Eq.(3.88) in the clean limit $l_1^{-1} \rightarrow 0$ and the conventional diffusion pole $1/(Dq^2 + |\omega_m|)$ in the limit $|\omega_m| \ll l_1^{-1}, q$, where the 1d diffusion constant $D = l_1/2$ (we use $v_F = 1$).

For weak interactions $g_2 \ll 1$ and we may expand,

$$\langle \phi_s \phi_{s'} \rangle = g_{ss'} - [g(1 - \Pi^\phi)g]_{ss'} + O(g_2^3) \quad (3.131)$$

leading to the photon propagators

$$\langle \phi_m^+(q) \phi_{-m}^+(-q) \rangle = \frac{g_2^2}{2\pi} \left(1 - \frac{i\omega_m}{q + i\omega_m + il_1^{-1} \operatorname{sgn}(m)} \right) + O(g_2^4) \quad (3.132)$$

$$\langle \phi_m^-(q) \phi_{-m}^-(-q) \rangle = \frac{g_2^2}{2\pi} \left(1 - \frac{-i\omega_m}{q - i\omega_m - il_1^{-1} \operatorname{sgn}(m)} \right) + O(g_2^4) \quad (3.133)$$

$$\langle \phi_m^+(q) \phi_{-m}^-(-q) \rangle = g_2 + \frac{g_2^2}{2\pi} \frac{l_1^{-1} |\omega_m|}{q^2 + (|\omega_m| + l_1^{-1})^2} + O(g_2^3). \quad (3.134)$$

3.6.2 “Renormalization” of disorder by electron-electron interactions

Let us now turn to the renormalization of the static disorder scattering length due to electron-electron interactions. The only peculiarity of the Luttinger liquid as compared to higher dimensions is that the renormalization of the (back-) scattering length is more singular and necessitates going beyond the Hartree-Fock approximation even in the case of weak interactions [5, 6]. The renormalization occurs due to *elastic virtual* electron-hole excitations involving virtual electron states with energies $|\epsilon| \gtrsim T$ and typical energy transfers $|\omega| \gtrsim T$. The underlying physics of the elastic renormalization of disorder can be described in terms of the T -dependent screening of individual impurities and scattering by slowly decaying in real space Friedel oscillations [18]. I want to point out, however, that a complete understanding of the renormalization of the backscattering length still requires an investigation of the role played by particle-hole fluctuations (Notice that in the standard bosonization scheme, also (bosonized) electrons renormalize the backscattering length. In the present approach a similar contribution may result from “high-energy” contributions of the Q -fields).

The renormalization of disorder is most conveniently treated within the representation Eq.(3.119) - Eq.(3.123). In a first step we represent the Coulomb-action, Eq.(3.119), in terms of the gauge fields θ and χ . Using Eq.(3.124) we find that

$$S[\theta, \chi] = \frac{1}{2} \sum_{m,q} \begin{pmatrix} \theta_m(q) & \chi_m(q) \end{pmatrix} \begin{pmatrix} \frac{1}{g_2}(q^2 + \omega_m^2) - \frac{1}{2\pi}q^2 & -\frac{1}{2\pi}i\omega_m q \\ -\frac{1}{2\pi}i\omega_m q & \frac{1}{g_2}(q^2 + \omega_m^2) - \frac{1}{2\pi}q^2 \end{pmatrix} \begin{pmatrix} \theta_{-m}(-q) \\ \chi_{-m}(-q) \end{pmatrix}. \quad (3.135)$$

Introducing $v_J = 1 - \frac{g_2}{2\pi}$ and $v_N = 1 + \frac{g_2}{2\pi}$ and integrating over θ gives

$$S[\chi] = \frac{1}{2g_2} \sum_{m,q} \chi_m(q) \left[\frac{(q^2 + \omega_m^2)(v_J v_N q^2 + \omega_m^2)}{v_J q^2 + \omega_m^2} \right] \chi_{-m}(-q). \quad (3.136)$$

Motivated by the observation that the renormalization of the static disorder occurs due to virtual electron-hole excitations we proceed by decomposing the Coulomb-field into its slow and fast fluctuating contributions, $\chi_\tau(q) = \chi_\tau^s(q) + \chi_\tau^f(q)$, where

$$\chi_\tau^s(q) = \frac{1}{2\pi T^{1/2}} \int_{|\omega| < T} d\omega e^{i\omega\tau} \chi_\omega(q), \quad (3.137)$$

$$\chi_\tau^f(q) = \frac{1}{2\pi T^{1/2}} \int_{T < |\omega| < \Lambda} d\omega e^{i\omega\tau} \chi_\omega(q). \quad (3.138)$$

Here we used the continuum approximation for frequencies (we want to study high energies $\omega \gtrsim T$), and substituted the discrete sums by integrals. In order to integrate out the fast fields we use a perturbative approach and approximate

$$e^{-S_{\text{bs}}^{\text{eff}}[T, \chi_s]} \approx e^{-S_{\text{bs}}[T, \chi_s]} e^{-\langle S_{\text{bs}}[T, \chi_s, \chi_f] \rangle_f},$$

with the average $\langle \dots \rangle_f$ taken with respect to fast Coulomb-field action,

$$S[\chi_f] = \frac{1}{2g_2} \sum_{m,q} \chi_m(q) \left[\frac{(q^2 + \omega_m^2)(v_J v_N q^2 + \omega_m^2)}{v_J q^2 + \omega_m^2} \right] \chi_{-m}(-q) \quad (3.139)$$

$$= \frac{L}{8\pi^2 T g_2} \int dq \int_{T < |\omega| < \Lambda} \chi_\omega^f(q) \left[\frac{(q^2 + \omega^2)(v_J v_N q^2 + \omega^2)}{v_J q^2 + \omega^2} \right] \chi_{-\omega}^f(-q) \quad (3.140)$$

$$\equiv \frac{1}{2} \int dq \int_{T < |\omega| < \Lambda} \chi_\omega^f(q) [\Pi^\chi]_\omega^{-1}(q) \chi_{-\omega}^f(-q). \quad (3.141)$$

For high energies $\epsilon_n, \epsilon_{n'} \gtrsim T$ slow and fast fields do not couple, i.e.

$$\begin{aligned} S_{\text{bs}}[T, \chi] &= -\frac{1}{8l_1} \int d\tau d\tau' dx \text{tr} \{ Q_+ e^{i\chi} Q_- e^{-i\chi} \} \\ &= -\frac{1}{8l_1} \int d\tau d\tau' dx \text{tr} \left\{ Q_{\tau\tau'}^+(x) e^{i\chi_\tau^s(x)} Q_{\tau'\tau}^-(x) e^{-i\chi_{\tau'}^s(x)} \right\} e^{i\chi_\tau^f(x) - i\chi_{\tau'}^f(x)}, \end{aligned}$$

and therefore $\langle S_{\text{bs}}[T, \chi_s, \chi_f] \rangle_f = \langle e^{i\chi_\tau^f(x) - i\chi_{\tau'}^f(x)} \rangle_f$. Using that

$$\begin{aligned} \ln \left[\langle e^{i\chi_\tau^f(x) - i\chi_{\tau'}^f(x)} \rangle_f \right] &= \frac{L}{16\pi^4 T} \int dq \int_{T < |\omega| < \Lambda} d\omega \Pi_\omega^\chi(q) [1 - \cos[\omega(\tau - \tau')]] \\ &= \frac{g_2}{4\pi^2} \int dq \int_{T < |\omega| < \Lambda} d\omega \frac{v_J q^2 + \omega^2}{(q^2 + \omega^2)(v_J v_N q^2 + \omega^2)} \\ &= \frac{g_2}{4\pi} \int_{T < |\omega| < \Lambda} d\omega \frac{1}{|\omega|} \left[\frac{1 - v_J}{1 - v_J v_N} + \sqrt{\frac{v_J}{v_N}} \frac{1 - v_N}{1 - v_J v_N} \right] \\ &= \frac{1}{2} \int_{T < |\omega| < \Lambda} d\omega \frac{1}{|\omega|} \left[1 - \sqrt{\frac{1 - \frac{g_2}{2\pi}}{1 + \frac{g_2}{2\pi}}} \right] \\ &= \alpha \ln \left[\frac{\Lambda}{T} \right], \end{aligned}$$

where $\alpha = 1 - \sqrt{\frac{1 - \frac{g_2}{2\pi}}{1 + \frac{g_2}{2\pi}}}$ and reexponentiating one finally finds $\langle S_{\text{bs}}[T, \chi_s, \chi_f] \rangle_f = \left(\frac{\Lambda}{T} \right)^\alpha$, i.e. the former back-scattering term,

$$S_{\text{bs}}^{\text{eff}}[T, \chi_s] = S_{\text{bs}}[T, \chi_s] \langle S_{\text{bs}}[T, \chi_f] \rangle_f = -\frac{1}{8l_1^{\text{eff}}} \int d\tau d\tau' dx \text{tr} \{ Q_+ e^{i\chi} Q_- e^{-i\chi} \}, \quad (3.142)$$

with the renormalized scattering length

$$\frac{1}{l_1^{\text{eff}}} = \frac{1}{l_1} \left(\frac{\Lambda}{T} \right)^\alpha, \quad \alpha = 1 - \sqrt{\frac{1 - \frac{g^2}{2\pi}}{1 + \frac{g^2}{2\pi}}}. \quad (3.143)$$

Taking into account the renormalization of disorder by virtual electron-hole pairs, the Drude conductivity, mentioned in section 3.5.2, shows the following temperature dependence,

$$\sigma^D \propto \left(\frac{\Lambda}{T} \right)^\alpha. \quad (3.144)$$

3.6.3 Summary of this section and outlook

In this section we introduced the σ -model for the interacting disordered 1d system. We showed, on the one hand, how the RPA screening is changed due to disorder and, on the other hand, how the back-scattering length is renormalized by interactions. The latter leads to a T -dependence of the Drude conductivity. We emphasized that the derived σ -model represents the single-channel version of a multi-channel model, recently given by Mora *et al.* [7], which describes the physics of quasi-1d and higher dimensional systems. Therefore, the coupled ballistic σ -model can be viewed as an “universal” model for interacting disordered systems. As already pointed out, the role of “high energy” fluctuations of the Q -matrices in the renormalization of the backscattering length still needs to be discussed.

3.7 An Application: Persistent current in a Luttinger liquid

We already mentioned at different points the work of Gornyi *et al.* [5, 6], showing that concepts from multi-channel disordered mesoscopic systems, also apply to the disordered Luttinger liquid. To be precise, the work of Gornyi *et al.* concentrates on the WL corrections to the Drude conductivity. In this section we want to discuss a further prominent example of an interference phenomenon, well known for disordered mesoscopic systems and, up to now, not analyzed in *single channel disordered* rings. This is the persistent equilibrium current produced by a Aharonov-Bohm (AB) flux piercing the ring. Before turning to the disordered case, let us, however, show how the result for a *clean* ring, obtained by D. Loss [21] within an extension of the standard bosonization scheme, may be derived within the functional bosonization (and the σ -model bosonization) approach.

3.7.1 Persistent current in a clean Luttinger liquid

The persistent current for a clean Luttinger liquid firstly has been derived by D. Loss [21] within an extension of the standard bosonization approach, in order to account for the so-called “zero-mode” contributions arising in a finite size system and the “topological excitations” arising due to the AB flux piercing the ring. In this subsection we want to propose a method how to incorporate the zero-mode and topological excitations into the functional (σ -model) bosonization. Since the zero-mode contributions are related to the discreteness of particles we turn to a description within the canonical ensemble. Technically this is achieved by introducing a chemical potential which, after being integrated over, ensures the particle discreteness. First, however, we briefly recapitulate how finite size effects are accounted for in the standard bosonization method. In this section we reintroduce the Fermi velocity, v_F .

Finite Size effects in the standard bosonization: Consider a Luttinger liquid on a ring of length L . According to Haldane (see Eq. (2.1) of [19]) taking into account finite size effects leads to the following Hamiltonian for the non-interacting system

$$H_0 = \sum_q v_F |q| b_q^\dagger b_q + \frac{\pi v_F}{2L} [(N - N_0)^2 + J^2]. \quad (3.145)$$

Here b, b^\dagger are the bosonic degrees of freedom describing particle-hole excitations and N, J are the total particle number and current, respectively, which have to be introduced in a finite size system in order to guarantee the right commutation relations. This second contribution is called the zero-mode contribution. N and J are integers, subject to selection rules, which (for periodic boundary conditions, see below) take the form

$$(-1)^{J+N} = -1. \quad (3.146)$$

Taking into account interactions changes the Hamiltonian, Eq.(3.145), according to (see Eq. (4.13) in [19])

$$H = \sum_q \omega_q b_q^\dagger b_q + \frac{\pi}{2L} [v_N(N - N_0)^2 + v_J J^2], \quad (3.147)$$

where $v_N = v_F + \frac{g_4 + g_2}{\pi}$ and $v_J = v_F + \frac{g_4 - g_2}{\pi}$.

Finite size effects in the functional bosonization method: We now want to show how Eqs. (3.145) and (3.147) may be obtained within the functional bosonization method (since the σ -model approach gives equivalent results after integration over the particle-hole excitations, it suffices to consider only the functional bosonization approach). Let us first consider the case of free, non-interacting electrons.

In order to account for discreteness of particles we follow [20] and write the grand canonical partition function according to

$$\mathcal{Z} = \sum_{M, J=0}^{\infty} \mathcal{Z}_{MJ}, \quad \mathcal{Z}_{MJ} = \text{tr} \left\{ e^{-\beta \hat{H}} \delta(\hat{N} - M) \delta(\hat{J} - J) \right\}, \quad (3.148)$$

and introduce 'chemical potentials' θ_M and θ_J in order to represent the δ -functions, i.e.

$$\mathcal{Z}_{MJ} = \oint \frac{d\theta_M}{2\pi} \oint \frac{d\theta_J}{2\pi} e^{-i\theta_M M} e^{-i\theta_J J} \mathcal{Z}[\theta_M, \theta_J], \quad (3.149)$$

with grand-canonical partition function

$$\mathcal{Z}[\theta_M, \theta_J] = \text{tr} \left\{ e^{-\beta \hat{H} + i\hat{N}\theta_M + i\hat{J}\theta_J} \right\}. \quad (3.150)$$

Turning to a path integral representation one has

$$\mathcal{Z}[\theta_M, \theta_J] = \int \mathcal{D}[\bar{\chi}\chi] e^{S[\bar{\chi}\chi, \theta_M, \theta_J]}, \quad (3.151)$$

with

$$S[\bar{\chi}\chi, \tilde{\theta}_M, \tilde{\theta}_J] = \int d^2x \bar{\chi} \left[\partial_\tau + iv_F \sigma_3 \partial_x + iT\tilde{\theta}_M + iT\sigma_3 \tilde{\theta}_J \right] \chi, \quad (3.152)$$

where the chemical potentials $\tilde{\theta}_M$ and $\tilde{\theta}_J$ are homogeneous, dynamical fields (In the construction of the field integral representation of the partition function the chemical potentials become dynamical fields in order to guarantee particle discreteness at every time step). We integrate out the fermions and expand the resulting "tr ln" to second order, i.e.

$$\begin{aligned} \mathcal{Z}[\theta_M, \theta_J] &= \det \left[\partial_\tau + iv_F \sigma_3 \partial_x + iT\tilde{\theta}_M + iT\sigma_3 \tilde{\theta}_J \right] \\ &= \exp \left\{ \text{tr} \ln \left[\partial_\tau + iv_F \sigma_3 \partial_x + iT\tilde{\theta}_M + iT\sigma_3 \tilde{\theta}_J \right] \right\} \\ &= \exp \left\{ \text{tr} \ln [\partial_\tau + iv_F \sigma_3 \partial_x] + \frac{TL}{2\pi v_F} (\theta_M^2 + \theta_J^2) \right\}. \end{aligned}$$

The first term, $\det[\partial_\tau + iv_F \sigma_3 \partial_x]$, gives the 'standard' bosonic term and in the second term we only kept the static components ("zero-modes"), $\theta_{M,J}$, of $\tilde{\theta}_{M,J}$. The partition function factorizes into the product

$$\mathcal{Z} = \tilde{\mathcal{Z}} \mathcal{Z}_0, \quad (3.153)$$

where $\tilde{\mathcal{Z}}$ is the 'standard' bosonic term describing particle-hole excitations and the zero-mode contribution is

$$\mathcal{Z}_0 = \sum_{MJ} \oint \frac{d\theta_M}{2\pi} \oint \frac{d\theta_J}{2\pi} e^{-i\theta_M M} e^{-i\theta_J J} e^{-\frac{\pi L}{2\pi v_F}(\theta_M^2 + \theta_J^2)} = \sum_{MJ} e^{-\frac{\pi v_F}{2TL}(M^2 + J^2)}. \quad (3.154)$$

This is the action one obtains starting from the Hamiltonian Eq.(3.145).

So let us now take into account electron-electron interactions. The interaction term is a sum of zero-mode and non-zero mode contributions. The partition function therefore factorizes into the 'standard' and the zero-mode contribution. (The non-zero-mode interaction changes the standard term in the known way, see section 3.4.) The zero-mode interaction is given by

$$S[M, J] = \frac{1}{2TL} [(g_4 + g_2) M^2 + (g_4 - g_2) J^2] \quad (3.155)$$

and, therefore, changes the zero-mode partition function by 'renormalizing' velocities

$$\mathcal{Z}_0 = \sum_{MJ} e^{-\frac{\pi}{2TL}(v_M M^2 + v_J J^2)}, \quad (3.156)$$

with v_M and v_J as in Eq.(3.147).

Topological excitations, etc.: We now undertake a more careful analysis taking into account topological constraints and parity effects [21]. To be specific we take a ring pierced by a flux $\phi = a_0 L$. The periodic boundary conditions for the electron-fields,

$$\psi(x) = e^{ik_F x} \chi_+(x) + e^{-ik_F x} \chi_-(x) \quad (3.157)$$

imply that

$$\chi_s(x + L) = e^{-sik_F L} \chi_s(x), \quad s = \pm. \quad (3.158)$$

Choosing $k_F = \frac{N_0}{2} \Delta k = \frac{\pi N_0}{L}$ as the linearization point for the spectrum, the boundary-conditions for right and left movers, Eq. (3.158), becomes parity dependent,

$$\chi_s(x + L) = (-1)^{N_0} \chi_s(x), \quad s = \pm. \quad (3.159)$$

Because N_+ and N_- are both integral numbers, allowed values for J and M are restricted by a selection rule [19, 21]. M is the number of particle excitations, i.e. number of particles left after the subtraction of the number of particles in the ground state, N_0 , and J is the current excitation. An odd number of particle excitations carries no current, while an even number of particles does (we take N_0 even). Therefore if M is even N is odd and vice versa, i.e.

$$(-1)^{J+M} = -1. \quad (3.160)$$

This holds for periodic boundary conditions. We may account for the boundary condition, Eq. (3.158), by adding half of an elementary flux to the physical flux piercing the ring in the case of odd particle numbers N_0 , i.e.

$$\phi \rightarrow \bar{\phi} = \phi + (1 - (-1)^{N_0}) \frac{\phi_0}{4}, \quad (3.161)$$

where $\phi_0 = \frac{2\pi}{e}$. One may equally incorporate the anti-periodic boundary conditions by demanding that instead of selection rule, Eq. (3.160), M and J have to fulfil the condition $(-1)^{J+M} = -(-1)^{N_0}$ (see below).

The external magnetic field (belonging to the flux piercing the ring) shifts the momenta according to $p \rightarrow p + ea$. Therefore the kinetic energy becomes

$$\begin{aligned} \frac{1}{2m} (p + ea)^2 \bar{\psi}\psi &\rightarrow \frac{1}{2m} \left[2p_F (q + ea) \bar{\chi}\sigma_3\chi + (ea)^2 N_0 \right] \\ &= v_F (q + ea) \bar{\chi}\sigma_3\chi + \frac{v_F L}{2\pi} (ea)^2 \\ &= v_F \left(q + \frac{2\pi}{L} \frac{\phi}{\phi_0} \right) \bar{\chi}\sigma_3\chi + \frac{v_F L}{2\pi} \left(\frac{2\pi}{L} \frac{\phi}{\phi_0} \right)^2, \end{aligned} \quad (3.162)$$

where we linearized around $k_F = \frac{\pi N_0}{L}$ and employed that $ea = \frac{2\pi}{L} \frac{\phi}{\phi_0}$. The magnetic flux, Eq. (3.161), therefore shifts the 'chemical potential' θ_J according to

$$\theta_J \rightarrow \theta_{J,\bar{\phi}} = \theta_J + \frac{i2\pi v_F}{TL} \frac{\bar{\phi}}{\phi_0}. \quad (3.163)$$

Following the steps of the last paragraph we end up with

$$\mathcal{Z}_0 = \sum_{M,J} \oint \frac{d\theta_M}{2\pi} \oint \frac{d\theta_J}{2\pi} e^{-i\theta_M M} e^{-i\theta_J J} e^{-\frac{TL}{2\pi v_F} (\theta_M^2 + \theta_{J,\bar{\phi}}^2) - \frac{2\pi v_F}{TL} \left(\frac{\bar{\phi}}{\phi_0} \right)^2}, \quad (3.164)$$

where the sum over M, J is restricted to fulfill the selection rule of Eq. (3.160). Using that

$$\frac{TL}{2\pi v_F} \theta_{J,\bar{\phi}}^2 + \frac{2\pi v_F}{TL} \left(\frac{\bar{\phi}}{\phi_0} \right)^2 = \frac{TL}{2\pi v_F} \theta_J^2 + i2\theta_J \frac{\bar{\phi}}{\phi_0} \quad (3.165)$$

we obtain

$$\mathcal{Z}_0 = \sum_{M,J} \oint \frac{d\theta_M}{2\pi} \oint \frac{d\theta_J}{2\pi} e^{-i\theta_M M} e^{-i\theta_J \left(J + \frac{2\bar{\phi}}{\phi_0} \right)} e^{-\frac{TL}{2\pi v_F} (\theta_M^2 + \theta_J^2)}. \quad (3.166)$$

Notice that the flux simply fixes the current J to

$$\delta(\hat{J} - J) \rightarrow \delta(\hat{J} - J - 2\bar{\phi}/\phi_0). \quad (3.167)$$

That is in the ground state, $J = 0$ ($J = 1$), the current is shifted due to the presence of the magnetic flux, i.e. $\langle \hat{J} \rangle = 2\bar{\phi}/\phi_0$ ($\langle \hat{J} \rangle = 1 + 2\bar{\phi}/\phi_0$). Adding the zero-mode interaction (notice that we have to substitute $(g_4 - g_2)\hat{J}^2 \rightarrow (g_4 - g_2)(J - 2\bar{\phi}/\phi_0)^2$) and performing the integral over the chemical potentials we obtain

$$\mathcal{Z}_0 = \sum_{M,J} e^{-\frac{\pi}{2TL} \left(v_M M^2 + v_J \left(J + \frac{2\bar{\phi}}{\phi_0} \right)^2 \right)}. \quad (3.168)$$

In order to compare the result, Eq. (3.168), with that obtained by D. Loss [21] we write the sums over integers M and J as sums over even integers and 'topological excitations' $\kappa_M, \kappa_J = 0, 1$ i.e.

$$\mathcal{Z}_0 = \sum_{\kappa_M, \kappa_J=0,1} \sum_{MJ} e^{-\frac{\pi v_M}{2TL}(2M+\kappa_M)^2} e^{-\frac{\pi TL}{2v_J}J^2 + i2\pi J\left(\frac{\kappa_J}{2} + \frac{[N_0]_2}{2} + \frac{\phi}{\phi_0}\right)}, \quad (3.169)$$

where we performed a Poisson summation over J and $[\dots]_2 \equiv \text{mod}_2(\dots)$ (we used that $\exp\{i\pi J(1 + (-1)^{N_0})\} = \exp\{i\pi J[N_0]_2\}$). The summation over the topological excitations has to be done with the constraint $(-1)^{\kappa_M + \kappa_J} = -1$. We may therefore write

$$\mathcal{Z}_0 = \sum_{\kappa_M, \kappa_J=0,1} \sum_{MJ} e^{-\frac{\pi v_M}{2TL}(2M+\kappa_M)^2} e^{-\frac{\pi TL}{2v_J}J^2 + i2\pi J\left(\frac{\kappa_J}{2} + \frac{\phi}{\phi_0}\right)}, \quad (3.170)$$

with $\kappa_M = \kappa_J$ if N_0 is odd and $\kappa_J = [\kappa_M + 1]_2$ if N_0 is even. Using further that $\kappa_M^2 = \kappa_M$ one may equally write

$$\begin{aligned} \mathcal{Z}_0 &= \sum_{\kappa_M, \kappa_J=0,1} \sum_{MJ} e^{-\frac{\pi v_M}{2TL}\kappa_M} e^{-\frac{2\pi v_M}{TL}M^2} e^{-\frac{2\pi v_M}{TL}M\kappa_M} e^{-\frac{\pi TL}{2v_J}J^2} e^{i2\pi J\left(\frac{\phi}{\phi_0} + \frac{\kappa_J}{2}\right)} \\ &= \sum_{\kappa_M, \kappa_J=0,1} \sum_{MJ} e^{-\frac{\pi v_M^* K^*}{TL}\kappa_M} e^{-\frac{4\pi v_M^* K^*}{TL}M^2} e^{-\frac{4\pi v_M^* K^*}{TL}M\kappa_M} e^{-\frac{\pi TL K^*}{v_M^*}J^2} e^{i2\pi J\left(\frac{\phi}{\phi_0} + \frac{\kappa_J}{2}\right)} \\ &= \sum_{\kappa_M, \kappa_J=0,1} e^{-\frac{\pi v_M^* K^*}{TL}\kappa_M} \theta_3(\kappa_M, z_M) \theta_3(\kappa_J, z_J), \end{aligned} \quad (3.171)$$

where in the second line $K^* v^* = \frac{v_M}{2}$, $\frac{v^*}{K^*} = 2v_J$ and in the last line $\theta_3(q, z) = \sum_n q^{n^2} e^{i2nz}$ is the Jacobi θ function and $z_J = \frac{\pi\theta_0}{2}$, $q_J = e^{-\pi TL K^*/v^*}$, $z_M = i2\pi\kappa_M K^* v^*/(TL)$, $q_M = e^{-4\pi K^* v^*/(TL)}$ and $\theta_0 = \kappa_J + \frac{2\phi}{\phi_0}$. This equals Eq. (13) of [21]. (Notice that instead of taking into account anti-periodic boundary conditions by working with Eq. (3.160) and adding half a flux quantum we could have equally worked with the selection rule $(-1)^{M+J} = -(-1)^{N_0}$.)

The persistent current is obtained from the free energy, $F = T \ln \mathcal{Z}$, according to

$$j = -\partial_\phi F. \quad (3.172)$$

Using Eq.(3.171) one obtains [21],

$$j = \frac{2\pi T}{\phi_0} \sum_{n=1}^{\infty} (-1)^{nN_0} \frac{\sin\left[\frac{2\pi n\phi}{\phi_0}\right]}{\sinh\left[\frac{n\pi TL K^*}{v_F^*}\right]}, \quad (3.173)$$

which oscillates with a period of an elementary flux quantum, $\phi_0 = h/e$. The amplitude of the current decreases exponentially with increasing size and temperature and decreasing (renormalized) Fermi velocity. Notice also that j is diamagnetic for odd N_0 and paramagnetic for even N_0 . In the next subsection we show that in *single channel disordered* wires one finds persistent currents oscillating with half period, $h/2e$.

3.7.2 Persistent current in a weakly disordered Luttinger liquid

We now turn to the Luttinger liquid in a weakly disordered ring. In this section we assume weak disorder and apply a grand-canonical calculation. To be precise we consider the action,

$$S = S^0[\chi] + S_\sigma[T] + S_{bs}[T, \phi], \quad (3.174)$$

where

$$S^0[\chi] = \frac{1}{2g_2} \sum_{m,q} \chi_m(q) [(v_F q)^2 + \omega_m^2] \chi_{-m}(-q) \quad (3.175)$$

$$S_\sigma[T] = -\frac{1}{4} \sum_{nm,q} \text{tr} \{ \Lambda_n T_{nn+m}^{-1}(q) \Pi_m^\sigma(q) T_{n+mn}(-q) \} \quad (3.176)$$

$$S_{\text{bs}}[T, \chi] = -\frac{v_F}{8l_1} \int d^2x \text{tr} \{ Q_+ e^{i\chi} Q_- e^{-i\chi} \}. \quad (3.177)$$

Here $Q_\pm = T_\pm \Lambda T_\pm^{-1}$, $S[\chi]$ is the Coulomb-field propagator to lowest order in g_2 and we assume a mean free path of the order of the ring length, i.e. $l_1 \sim L$.

The following considerations are analogous to those made by Gornyi *et al.* in the context of WL [5, 6]: We begin by identifying the leading contribution to the persistent current in the regime of strong dephasing, $\tau_\varphi v_F / l_1 \ll 1$. This regime takes place at sufficiently high temperatures (the precise condition is given below). Contributions to the persistent current result from electron and hole paths encircling the ring at least once and in opposite direction. We can organize all these paths by the number of backscattering events. In the absence of interactions, all order scattering processes (including non-Cooperon diagrams) are equally important. In the presence of interactions however, long paths are suppressed due to dephasing. In the regime of strong dephasing, $\tau_\varphi v_F / l_1 \ll 1$, the shortest path (i.e. the one containing the minimal number of backscattering processes) gives the leading contribution. All higher orders backscattering processes only give subleading corrections through a systematic expansion in powers of the small parameter $\tau_\varphi v_F / l_1$ [5, 6]. Up to here we only repeated the argument of Gornyi *et al.* In difference to the WL situation, where the minimal loop contains three backscattering processes, in the ring geometry the minimal loop contains only one backscattering process. (Notice that diagrams with no backscattering process due not contribute due to charge neutrality). Technically we therefore may expand the Q -fields to quadratic order in the generators and perform a perturbative expansion in the backscattering term. The leading contribution results from one contraction in the backscattering action (see below).

Expansion in generators: Expansion in the generators to quadratic order (Gaussian approximation) gives the Cooperon propagator

$$S_\sigma^0[C_s^{\text{fb}} C_s^{\text{bf}}] = \frac{1}{2} \sum_{n(n+m)<0} \sum_q \text{tr} \left\{ C_{nn+m}^{\text{fb},s}(q) [|\omega_m| + i s v_F q \text{sgn}(m)] C_{n+mn}^{\text{bf},s}(-q) \right\}. \quad (3.178)$$

The back-scattering term in Gaussian approximation is given by $S_{\text{bs}}[T, \chi] = S_\chi^1[\chi] + S_\chi[C_s^{\text{fb}} C_s^{\text{bf}}] + S_{\text{bs}}[C_s^{\text{fb}} C_{-s}^{\text{bf}}]$, where

$$S_\chi^1 = \frac{v_F}{4l_1} \int d^2x \text{tr} \{ \Lambda e^{i\chi} \Lambda e^{-i\chi} \} \quad (3.179)$$

$$S_\chi[C_s^{\text{fb}} C_s^{\text{bf}}] = \frac{v_F}{2l_1} \int d^2x \text{tr} \{ C_s^{\text{fb}} C_s^{\text{bf}} \Lambda e^{i\chi^f} \Lambda e^{-i\chi^f} \} \quad (3.180)$$

$$S_{\text{bs}}[C_s^{\text{fb}} C_{-s}^{\text{bf}}] = \frac{v_F}{4l_1} \int d^2x \text{tr} \{ C_+^{\text{fb}} \Lambda e^{i\chi^b} C_-^{\text{bf}} \Lambda e^{-i\chi^f} \}. \quad (3.181)$$

We regularize S_χ^1 by subtracting a constant (T here denotes the temperature),

$$S_\chi^1 = \frac{v_F}{4l_1} \int d^2x \text{tr} \{ \Lambda e^{i\chi} \Lambda e^{-i\chi} - T \} \quad (3.182)$$

$$= \frac{v_F}{4\pi l_1} \sum_m \int dx |\omega_m| \left(e^{-i\chi(x)} \right)_{-m} \left(e^{-i\chi(x)} \right)_m, \quad (3.183)$$

and keep S_χ^1 to quadratic order in χ , i.e.

$$S_\chi^1 = \frac{v_F}{4\pi l_1} \sum_{m,q} \chi_{-m}(q) |\omega_m| \chi_m(-q) = \frac{1}{2g_2} \sum_{m,q} \chi_{-m}(q) \kappa |\omega_m| \chi_m(-q), \quad (3.184)$$

where we introduced for later convenience $\kappa = \frac{g_2 v_F}{2\pi l_1}$. Eq.(3.184) describes the lowest order disorder corrections to the RPA screening as discussed in section 3.6.1.

$S_\chi[\mathcal{C}_s^{\text{fb}} \mathcal{C}_s^{\text{bf}}]$ changes the Gaussian propagator, S_σ^0 , of the right- (left-) moving particle-hole excitations. The high-energy Coulomb interaction processes (contained in the virtual fluctuations of the Coulomb field χ) renormalize the backscattering length, as discussed in section 3.6.2. Eq.(3.180) would be of further interest if it also described dephasing. However, this is not the case as may be seen by the following observation: Dephasing occurs due to real inelastic scattering processes, which in the Keldysh formalism is described by a classical interaction field (see Chapter 1, *Current-Echoes in Metals and Semiconductors*) and is given by a diagonal matrix in Keldysh-space. Using further that in the Keldysh formalism (see also Chapter 1) $\Lambda_\epsilon = \begin{pmatrix} 1 & 2F_\epsilon \\ & -1 \end{pmatrix}$ and $\mathcal{C}\mathcal{C}\Lambda = \begin{pmatrix} \bar{C}C & * \\ C\bar{C} & \end{pmatrix}$, where $*$ is some non-vanishing combinations of the thermal function F and the matrices \bar{C} , C , one may check, that a classical Coulomb field χ simply drops out of Eq.(3.180). That is, the Coulomb-field entering in Eq.(3.180) describes only high energy interaction processes (as in the Keldysh formalism contained within the quantum components of the Coulomb field χ) and therefore no dephasing. In the calculations for the persistent current we may therefore simply take

$$S_\chi[\mathcal{C}_s^{\text{fb}} \mathcal{C}_s^{\text{bf}}] = \frac{v_F}{2l_{\text{eff}}} \int d^2x \text{tr} \{ \mathcal{C}_s^{\text{fb}} \mathcal{C}_s^{\text{bf}} \}, \quad s = \pm, \quad (3.185)$$

where l_{eff} denotes the interaction renormalized back-scattering length. The statement that Eq.(3.180) contains only interaction processes with high energy transfers is confirmed within the Matsubara formalism by analytical calculation in Appendix B.8.

We may now calculate corrections to the free energy, F , arising from back-scattering processes. To first order back-scattering,

$$\Delta F = \frac{v_F T}{2l_1} \sum_{nm',q} \langle \text{tr} \{ \mathcal{C}_+^{\text{fb}} \Lambda e^{i\chi^b} \mathcal{C}_-^{\text{bf}} \Lambda e^{-i\chi^f} \} \rangle_{S_\chi, S_\sigma} + (+ \leftrightarrow -), \quad (3.186)$$

where $\langle \dots \rangle_{S_\chi, S_\sigma}$ is the average with respect to the Coulombfield propagator the Cooperon propagator $S_\chi = S_\chi^0 + S_\chi^1$ and $S_\sigma = S_\sigma^0 + S_\chi$. Performing the contraction in the Cooperon gives

$$\Delta F = \frac{4v_F T}{\pi l_1 L} \sum_{qq'} \sum_{m>0} \frac{\omega_m^2}{(iv_F q + \omega_m + v_F l_{\text{eff}}^{-1})(iv_F q - \omega_m - v_F l_{\text{eff}}^{-1})} \langle (e^{i\chi})_{-m, -q'} (e^{-i\chi})_{m, q'} \rangle_{S_\chi}, \quad (3.187)$$

Perturbation theory: In a first approximation we introduce a phenomenological dephasing time $\tau_\varphi \ll l_1^{-1}, l_{\text{eff}}^{-1}$ into the Cooperon propagator and treat the interaction term to lowest order in g_2 , i.e. (in lowest order g_2 : $S_\chi = S_\chi^0$),

$$\begin{aligned} \frac{T}{L} \sum_{q'} \langle (e^{i\chi})_{-m, q'} (e^{-i\chi})_{m, -q'} \rangle_{S_\chi} \\ = \frac{T}{L} \sum_{q'} \langle \chi_{-m}(q') \chi_m(q') \rangle_{S_\chi^0} = \frac{T}{L} \sum_{q'} \frac{g_2}{(v_F q')^2 + \omega_m^2} = \frac{g_2 T}{2v_F |\omega_m|}, \end{aligned} \quad (3.188)$$

and therefore

$$\begin{aligned}\Delta F &= \frac{2g_2 T}{\pi l_1} \sum_q \sum_{m>0} \frac{\omega_m}{(iv_F q + \omega_m + v_F l_{\text{eff}}^{-1} + \tau_\varphi^{-1})(iv_F q - \omega_m - v_F l_{\text{eff}}^{-1} - \tau_\varphi^{-1})} \\ &= \frac{2g_2 T}{\pi l_1} \frac{1}{i4\pi T} \int d\Omega \sum_q \frac{-i\Omega \coth[\frac{\Omega}{2T}]}{(v_F q + \Omega + i\tau_\varphi^{-1})(v_F q - \Omega - i\tau_\varphi^{-1})}.\end{aligned}$$

Notice that in the first line we introduced the *phenomenological* dephasing rate, $1/\tau_\varphi$, and in the second line we neglected $v_F/l_{\text{eff}} \ll 1/\tau_\varphi$. In a next step we perform a Poisson-summation over discrete momenta and (taking into account only the magnetic flux-dependent contributions, see Appendix B.8) obtain

$$\Delta F = \frac{g_2}{i\pi l_1} \sum_{m>0} \cos[2\pi m x] e^{-2\pi m \gamma} \int dy \frac{y \coth[\frac{y}{2\theta}] e^{i2\pi m y}}{y + i\gamma}, \quad (3.189)$$

where we introduced $y = \frac{L}{2\pi v_F} \Omega$, $x = \frac{2\phi}{\phi_0}$, $\gamma = \frac{L}{2\pi v_F \tau_\varphi}$ and $\theta = \frac{TL}{2\pi v_F}$. Performing the integral over y (see Appendix B.8) we find

$$\Delta F = \frac{g_2 TL}{\pi l_1 v_F} \sum_{m>0} \frac{\cos[2\pi m x] e^{-\frac{2\pi m TL}{v_F}} e^{-\frac{mL}{v_F \tau_\varphi}}}{\sinh[\frac{2\pi m TL}{v_F}]} + O(1/T\tau_\varphi). \quad (3.190)$$

This leads to the persistent current

$$j = \frac{4g_2 T t_b}{l_1 \phi_0} \sum_{m>0} \frac{m \sin[4\pi m \phi/\phi_0] e^{-2\pi m T t_b} e^{-\frac{m t_b}{\tau_\varphi}}}{\sinh[2\pi m T t_b]} + O(1/T\tau_\varphi), \quad (3.191)$$

where we introduced the time $t_b = L/v_F$ an electron needs to ballistically encircle the ring once. The persistent current oscillates as a function of the magnetic flux with a period of *half* of the elementary flux quantum and an amplitude, which is a factor $g_2 L/(\pi v_F l_1)$ smaller than in the clean case. The amplitude decreases exponentially with increasing ring length and temperature. Higher order scattering processes are suppressed by factors $\tau_\varphi v_F/l_1$ as is the case for the weak localization corrections to the Drude conductivity, discussed in section 3.5.2. Dephasing leads to an exponential damping, $j \propto e^{-m t_b/\tau_\varphi}$, where $m t_b$ is the time an electrons needs to (ballistically) transverse the ring m times. For a comparison with multi-channel rings we state that in the weakly disordered quasi-1d system [22] (we reintroduce the electron's charge e)

$$j = \frac{e^2/C\phi_0}{1 + e^2/(\Delta C)} \sum_{m>0} \sin\left[\frac{4\pi m \phi}{\phi_0}\right] e^{-\sqrt{2\pi T m t_D}} e^{-m\sqrt{\frac{t_D}{\tau_\varphi}}} \left(m^2 T t_D + m\sqrt{2\pi T t_D}\right) \quad (3.192)$$

where $t_D = \frac{L^2}{D}$ is the time an electron needs to diffusively encircle the ring once Δ is the mean DOS at the Fermi energy and e^2/C is the charging energy of the system $e^2/2C \sim v_F/L$. The amplitude $\frac{e^2/C}{1+e^2/(\Delta C)}$ results from an RPA approximation and the dephasing rate $1/\tau_\varphi$ is phenomenological introduced.

Higher orders – Renormalization of disorder, current-amplitude and dephasing: We are now more ambitious and try to identify the impact from different energy regimes of the Coulomb interaction on the persistent current. Moreover we want to identify the dephasing rate caused due to electron-electron interactions. We start out from

$$\Delta F = \frac{4v_F T}{\pi l_1 L} \sum_{qq'} \sum_{m>0} \frac{\omega_m^2}{(iv_F q + \omega_m + v_F l_{\text{eff}}^{-1})(iv_F q - \omega_m - v_F l_{\text{eff}}^{-1})} \langle (e^{i\chi})_{-m, -q'} (e^{-i\chi})_{m, q'} \rangle_{S_X}, \quad (3.193)$$

which we may write as

$$\Delta F = \frac{4v_F T}{\pi l_1} \int_0^{1/T} d\tau \sum_q \sum_{m>0} \frac{\omega_m^2 e^{i\omega_m \tau - S(\tau)}}{(iv_F q + \omega_m + v_F l_{\text{eff}}^{-1})(iv_F q - \omega_m - v_F l_{\text{eff}}^{-1})}, \quad (3.194)$$

where

$$S(\tau) = \frac{T}{2L} \sum_{mq} \langle \chi_{-m}(q) \chi_m(-q) \rangle_{S_\chi} (1 - \cos[\omega_m \tau]). \quad (3.195)$$

Performing the Poisson summation (as in the last subsection) we find (notice that latter on we take $\tau = \pm i t + \text{const.}$ and therefore the y -integral is convergent)

$$\Delta F = \frac{4v_F}{il_1 t_b} \sum_{m>0} \cos[2\pi m x] \int_0^{1/T} d\tau e^{-S(\tau)} e^{-2\pi m \gamma} \int dy \frac{-iy^2 e^{-\frac{2\pi\tau}{t_b} y} \coth\left[\frac{y}{2\theta}\right] e^{i2\pi m y}}{y + i\gamma}, \quad (3.196)$$

where we introduced $y = \frac{L}{2\pi v_F} \Omega$, $x = \frac{2\phi}{\phi_0}$, $\gamma = \frac{L}{2\pi v_F \tau_\varphi}$ and $\theta = \frac{TL}{2\pi v_F}$. Rewriting

$$\Delta F = \frac{-4v_F}{l_1 t_b} \sum_{m>0} \cos[2\pi m x] \int_0^{1/T} d\tau e^{-S(\tau)} \frac{t_b}{2\pi} d_\tau e^{-2\pi m \gamma} \int dy \frac{y \coth\left[\frac{y}{2\theta}\right] e^{(i2\pi m - \frac{2\pi\tau}{t_b})y}}{y + i\gamma}, \quad (3.197)$$

we may use again the result from the last subsection and obtain

$$\begin{aligned} \Delta F &= \frac{-2iT L}{\pi l_1} \sum_{m>0} \cos[2\pi m x] e^{-\frac{mL}{l_1}} \int_0^{1/T} d\tau e^{-S(\tau)} d_\tau \frac{e^{-2\pi(m + i\frac{\tau}{t_b})T t_b}}{\sinh\left[2\pi(m + i\frac{\tau}{t_b})T t_b\right]} + O(v_F/TL_1) \\ &= \frac{2T^2 L}{l_1} \sum_{m>0} \cos[2\pi m x] e^{-\frac{mL}{l_1}} \int_0^{1/T} d\tau e^{-S(\tau)} \frac{1}{\sinh^2\left[2\pi(m + i\frac{\tau}{t_b})T t_b\right]} + O(v_F/TL_1). \end{aligned} \quad (3.198)$$

In Appendix B.8 we show that $S(\tau)$ is given by a sum of four terms, each one resulting from a different range of energies of the Coulomb interaction,

$$S(\tau) = S^1(\tau) + S^2(\tau) + S^3(\tau) + S^4(\tau), \quad (3.199)$$

where ($\kappa = \frac{g_2 v_F}{2\pi l_1}$)

$$S^1(\tau) = \frac{g_2}{2\pi v_F} \ln\left[\frac{\Lambda}{T}\right] \quad \text{from energies } 1/\tau < |\Omega| < \Lambda, \quad (3.200)$$

$$S^2(\tau) = \frac{g_2}{2\pi v_F} \ln[\sin[2\pi T \tau + i0]] \quad \text{from energies } \kappa < |\Omega| < 1/\tau, \quad (3.201)$$

$$S^3(\tau) = -\frac{g_2 \kappa}{8v_F} |\tau| \quad \text{from energies } T < |\Omega| \ll 1/\tau, \quad (3.202)$$

$$S^4(\tau) = \frac{g_2 \kappa}{8v_F} T \tau^2 \quad \text{from energies } |\Omega| \ll T, \quad (3.203)$$

and therefore (up to $O(v_F/TL_1)$)

$$\Delta F = 2T^2 L \frac{1}{l_1} \left(\frac{\Lambda}{T}\right)^{\frac{g_2}{2\pi v_F}} \sum_{m>0} \cos[2\pi m x] e^{-\frac{mL}{l_1}} \int_0^{1/T} d\tau (\sin[2\pi T \tau + i0])^{\frac{g_2}{2\pi v_F}} \frac{e^{\frac{g_2 \kappa}{8v_F} (T \tau^2 - |\tau|)}}{\sinh^2\left[2\pi(m + i\frac{\tau}{t_b})T t_b\right]}. \quad (3.204)$$

This may be interpreted as follows:

- $P_m(\tau) = \frac{1}{\sinh^2 \left[2\pi(m + i\frac{\tau}{t_b})Tt_b \right]}$ is the probability that a particle-hole excitations encircles the ring m times within the time $i\tau$ (to be analytically continued). $P_m(\tau)$ has double poles in the upper half plane ($m > 0$) at the value $\tau_m = imt_b$.
- $\frac{1}{t_1} \left(\frac{\Delta}{T} \right)^{\frac{g_2}{2\pi v_F}}$ describes the renormalization of the back-scattering length due to virtual particle-hole excitations (as discussed in section 1.6.2) and described by S^1 .
- $A(\tau) = (\sin[2\pi T\tau + i0])^{\frac{g_2}{2\pi v_F}}$ determines the amplitude of the persistent current (see below). $A(\tau)$ results from S^2 . To lowest order in g_2 we may approximate

$$A(\tau) = A_-(\tau) + A_+(\tau) = (1 - e^{-i4\pi T\tau - 0})^{\frac{g_2}{4\pi v_F}} + (1 - e^{+i4\pi T\tau - 0})^{\frac{g_2}{4\pi v_F}}.$$

$A_{\pm}(\tau)$ has a branch cut due to the branch cut of the logarithm $\ln[1 - e^{\pm i4\pi T\tau - 0}]$. Notice that $A_+(\tau)$ can be analytically continued to values of τ from the upper half plane and $A_-(\tau)$ to values of τ from the lower half-plane.

- $e^{-\frac{g_2 \kappa}{8v_F} |\tau|}$ gives corrections $O(g_2)$ to the amplitude and is irrelevant in the following
- $e^{\frac{g_2 \kappa}{8v_F} T\tau^2}$ suppresses the “long-time” probability for particle hole excitations, i.e. leads to a damping of the particle-hole life-time (dephasing). This term results from interactions involving low energies, S^4 .

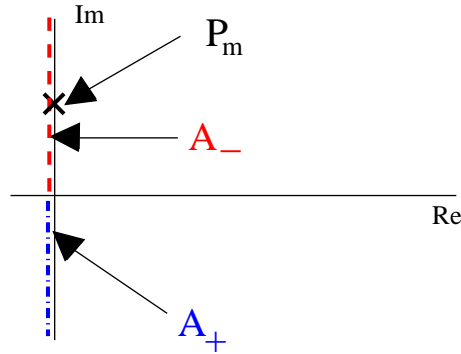


Figure 3.3: Analytical structure of the terms $P_m(\tau)$ and $A_{\pm}(\tau)$ discussed above. P_m has a single pole at $\tau_m = imt_b$ corresponding to the classical time an electron needs to encircle the ring m times. A_{\pm} have branch cuts from the logarithms.

Fig. 3.3 summarizes the analytical properties of the terms discussed. With these information on the analyticity of the various terms we may now perform the τ -integral (depicted in Fig. 3.4)

$$I_m^{\pm} = \int_0^{1/T} d\tau A_{\pm}(\tau) \frac{e^{\frac{g_2 \kappa}{8v_F} (T\tau^2 - |\tau|)}}{\sinh^2 \left[2\pi(m + i\frac{\tau}{t_b})Tt_b \right]} \quad (3.205)$$

Let us start our discussion with I^- : First we deform the τ -integration from the real axis to the complex half plane. As I^- has a branch cut at positive complex values this is done to the negative half plane, see Fig. 3.5. To be precise, we change from the integral along $\tau \in [+0, 1/T]$ to an integral along the axis $\tau = it + 0$ and $\tau = it + 1/T - 0$ with $t \in [0, -\infty]$. Next we use the periodicity of $S(\tau)$ in order to exchange the contour parametrized by $\tau = it + 1/T - 0$ to a contour parametrized by $\tau = it - 0$ (see again Fig. 3.5). These contours exactly cancel and therefore $I^- = 0$.

Turning to I^+ we proceed in the same manner, i.e. we deform the τ -integration from the real axis to the complex half plane. This is done to the positive half plane as I^+ has a branch cut in the negative half plane, see Fig. 3.6. To be precise, we change from the integral along $\tau \in [+0, 1/T]$ to an integral along the axis $\tau = it + 0$ and $\tau = it + 1/T - 0$ with $t \in [0, \infty]$. Now we use again the periodicity of

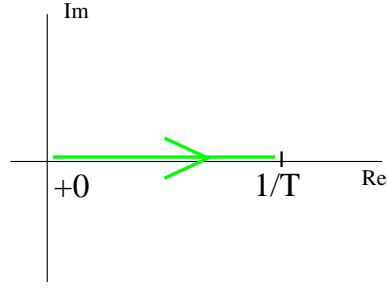


Figure 3.4: Original contour of integration, which is deformed as described below.

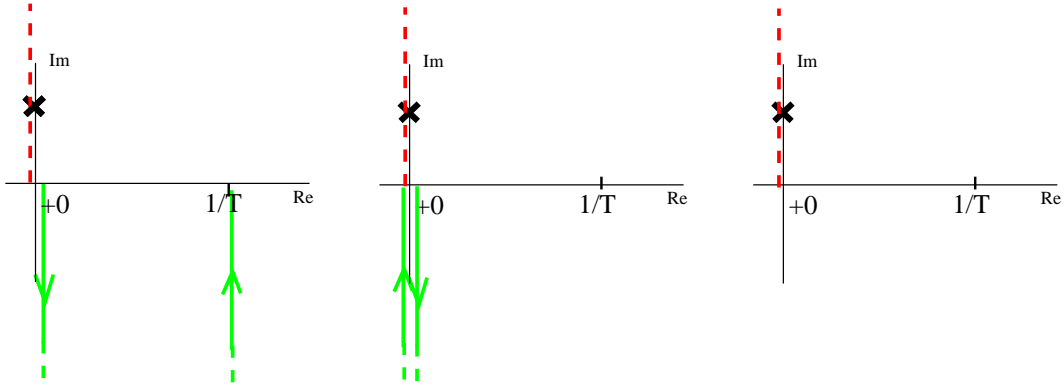


Figure 3.5: Deformation of the integration contour used to evaluate I^- and discussed in the text.

$S(\tau)$ in order to exchange the contour parametrized by $\tau = it + 1/T - 0$ to a contour parametrized by $\tau = it - 0$. These contours exactly cancel everywhere, apart from the region where $P_m(\tau = it)$ has its pole, i.e. at $t = mt_b$. Evaluating I^+ at the double pole, we obtain

$$I_m^+ = \int_0^{1/T} d\tau A_+(\tau) \frac{e^{-\frac{g_2 \kappa}{8v_F}(Tt^2 - it)}}{\sinh^2 \left[2\pi(m + i\frac{\tau}{t_b})Tt_b \right]} = \frac{2\pi}{(2\pi T)^2} \left(d_t \frac{e^{-\frac{g_2 \kappa}{8v_F}(Tt^2 - it)}}{(1 - e^{-4\pi Tt})^{\frac{-g_2}{4\pi v_F}}} \right)_{t=mt_b}. \quad (3.206)$$

Notice that in the non-interacting case $g_2 = 0$, where $A_{\pm} = 1$ the τ -integral vanishes, since one can always choose the contour in the negative half-plane. Indeed one would expect that $\Delta F = 0$ in the non-interacting case, since the persistent current is induced by density fluctuations due to the interaction.

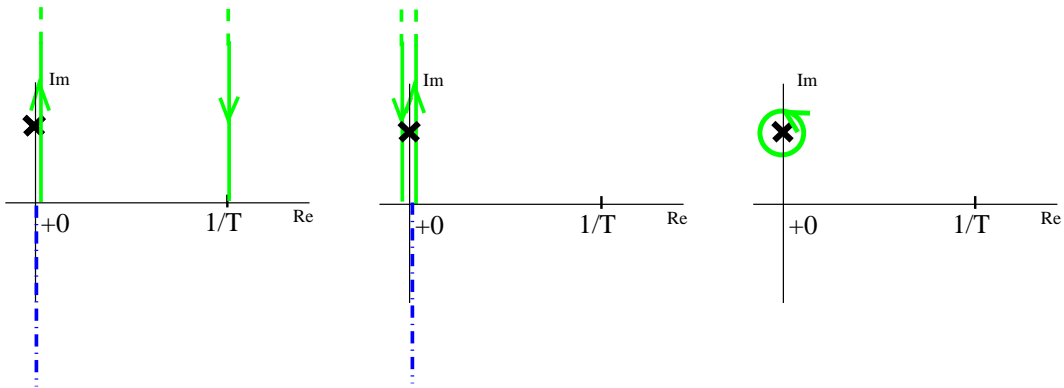


Figure 3.6: Deformation of the integration contour used to evaluate I^+ and discussed in the text.

The leading order contribution to I^+ in g_2 is given by

$$I_m^+ = \frac{g_2}{2\pi v_F T} \frac{e^{-4\pi m t_b T} e^{-\frac{g_2^2 \kappa T}{8v_F} (m t_b)^2}}{1 - e^{-4\pi m t_b T}}, \quad (3.207)$$

and therefore

$$\Delta F = \frac{g_2 T t_b}{\pi} \frac{1}{l_1} \left(\frac{\Lambda}{T} \right)^{\frac{g_2}{2\pi v_F}} \sum_{m>0} \cos[2\pi m x] \frac{e^{-\frac{mL}{l_1}} e^{-2\pi m t_b T} e^{-\frac{g_2^2 \kappa}{8v_F} (m t_b)^2}}{\sinh[2\pi m t_b T]} + O(v_F / T l_1). \quad (3.208)$$

This is what we obtained from the perturbative calculation, however with a renormalized backscattering length and the dephasing rate due to the electron-electron interactions

$$\frac{1}{\tau_\varphi^{\text{pc}}} = \frac{g_2^2 T m t_b}{16\pi l_1 v_F}. \quad (3.209)$$

This dephasing rate is in fact what one would expect [23] by the following argument:

In section 3.4.2 we discussed the inelastic scattering rate in the clean Luttinger liquid and found that it is given by

$$\frac{1}{\tau_{\text{ee}}} \propto \int dq \int d\Omega \delta(q + \Omega) \delta(q - \Omega). \quad (3.210)$$

Technically, the dephasing rate differs from the inelastic scattering rate in the fact that the Ω -integral is cut-off by some inverse time-scale. This is due to the fact, that very-low frequency interaction processes, corresponding to time-scales exceeding the typical traveling-time of the Cooperon do not contribute to dephasing as these correspond to *static* processes from the Cooperon's point of view (see also Chapter 2, *Dephasing by Kondo impurities*). Introducing such a frequency cut-off $1/t_{\text{typ}}$ one finds that the dephasing rate vanishes for the clean Luttinger liquid (see also [5, 6]). In fact we found above that the dephasing rate arises from interaction processes described by S^4 which involves corrections to the RPA screening due to disorder (i.e. which is proportional to κ).

Introducing disorder softens the δ -functions in Eq.(3.211) and leads to

$$\frac{1}{\tau_\varphi(t_{\text{typ}})} \propto \int dq \int_{1/t_{\text{typ}} < |\Omega|} d\Omega \delta_{l_1}(q + \Omega) \delta_{l_1}(q - \Omega) \propto \frac{g^2}{l_1 v_F} T t_{\text{typ}}, \quad (3.211)$$

where $\delta_{l_1}(x) = -i\pi \text{Im} \frac{1}{x + i/l_1}$. The typical traveling time for the electron-hole excitation (making up the Cooperon) in the context of weak localization corrections to the Drude conductivity is given by the dephasing time itself. This leads to (compare Eq.(3.112))

$$\frac{1}{\tau_\varphi^{\text{WL}}} \propto g_2 \sqrt{\frac{T}{l_1 v_F}}. \quad (3.212)$$

T. Ludwig and A. Mirlin first observed that in the AB experiment in a diffusive wire the typical traveling time for the Cooperon picking up a phase $m\phi/\phi_0$ is given by $t_{\text{typ}}^m = m t_D$ [23]. Correspondingly, in a nearly clean wire the typical traveling time of the Cooperon picking up the phase $m\phi/\phi_0$ is given by the ballistic time $t_{\text{typ}}^m = m t_b$. Therefore one would, indeed, expect

$$\frac{1}{\tau_\varphi^{\text{pc},m}} \propto \frac{g_2^2 T m t_b}{l_1 v_F}. \quad (3.213)$$

Finally we mention, that the condition $\tau_\varphi v_F / l_1$ holds for temperatures

$$T \gg \frac{16\pi v_F^2}{g_2^2 t_b}. \quad (3.214)$$

3.7.3 Summary of this section

In this section we studied the persistent current in a single-channel ring. In a first subsection we proposed a method how one can obtain the known results for the persistent current in a clean Luttinger liquid within the functional (σ -model) bosonization approach. The main idea was to introduce extra fields (“chemical potentials”) which fix the constraint that the number of particles is discrete. It is known that the persistent current for the *clean* Luttinger liquid oscillates as a function of the magnetic flux, piercing the ring, with a period given by the elementary flux quantum. In a second subsection we showed that the *disordered* Luttinger liquid establishes persistent currents oscillating as a function of the external magnetic flux with a period given by *half* of the elementary flux quantum. We also found that the amplitude is exponentially damped by a dephasing rate due to electron-electron interactions.

3.8 Summary and outlook

In this chapter a coupled ballistic σ -model is suggested as a low-energy field theory for the disordered Luttinger liquid. This model may be seen as the single-channel limit of an “universal” model for the disordered interacting electron gas. The model shows how in the absence of dephasing Anderson localization sets in. Moreover, it becomes very effective when it comes to the analysis of interference phenomena; as an example we calculated (in the limit where strong dephasing impedes Anderson localization) the persistent current in a disordered single channel ring with weakly interacting electrons. The model may also become useful in the localization regime. In the limit of strong localization it can be mapped on a model for granular chains, with the grains representing localization islands. This may serve as a starting point for the analysis of electron-electron interaction induced hopping between these islands. As already mentioned in the introduction of this chapter, some points resemble a collection of ideas and still need to be elaborated more carefully.

Bibliography

- [1] K. Efetov, *Supersymmetry in disorder and Chaos* (Cambridge University Press, 1997).
- [2] A. M. Finkel'stein, Zh. Eksp. Teor. Fiz. **84**, 168 (1983); [Sov. Phys. JETP **57**, 97 (1983)]; Z. Phys. B **56**, 189 (1984); A. M. Finkel'stein, *Electron Liquid in Disordered Conductors*, Vol. 14 of *Soviet Scientific Reviews*, ed. I. M. Khalatnikov. Harwood Academic Publisher, GmbH, London, 1990.
- [3] A. Kamenev and A. Andreev, Phys. Rev. B **60**, 2218 (1999).
- [4] H. J. Schulz, in *Mesoscopic Quantum Physics*, edited by E. Akkermans, G. Montambaux, J.-L. Pichard, and J. Zinn-Justin (North-Holland, Amsterdam, 1995); A. O. Gogolin, A. A. Nersisyan, and A. M. Tsvelik, *Bosonization and Strongly Correlated Systems* (Cambridge University, Cambridge, 1998); H. J. Schulz, G. Cuniberti, and P. Pieri, in *Field theories for Low-Dimensional Condensed Matter Systems*, edited by G. Morandi, P. Sodano, P. Tagliacozzo, and V. Tognetti (Springer, Berlin, 2000); T. Giamarchi, *Quantum Physics in One Dimension* (Oxford University Press, Oxford, 2004).
- [5] I. V. Gornyi, A. D. Mirlin and D. G. Polyakov, Phys. Rev. Lett. **95**, 206603 (2005).
- [6] I. V. Gornyi, A. D. Mirlin and D. G. Polyakov, cond-mat/0608590.
- [7] C. Mora, R. Egger, and A. Altland, cond-mat/0602411.
- [8] H.C.Frogedby, J. Phys. C **9**, 3757 (1976); D.K.K.Lee and Y.Chen, J. Phys. A **21**, 4155 (1988); I.V.Yurkevich, in *Strongly correlated fermions and bosons in low-dimensional disordered systems*, edited by I.V.Lerner, B.L.Altshuler, and V.I.Falko (Kluwer, Dordrecht, 2002), cond-mat/0606387; I.V.Lerner and I.V.Yurkevich, in *Impurity in the Tomonaga-Luttinger model: a functional integral approach*, to be published in Proc. LXXXI Les Houches School on Nanoscopic Quantum Transport, 2004, cond-mat/0508223.
- [9] J. Meyer private communication.
- [10] J. Solyom, Adv Phys. **28**, 201 (1979); J. Voit, Rep. Prog. Phys. **57**, 977 (1994); T.Giamarchi, *Quantum Physics in One Dimension* (Oxford University Press, Oxford, 2004).
- [11] A. V. Andreev, O. Agam, B. D. Simons, and B. L. Altshuler, Phys. Rev. Lett. **76**, 3947 (1996); A. V. Andreev, B. D. Simons, O. Agam, and B. L. Altshuler, Nucl. Phys. B **482**, 536 (1996).
- [12] F. D. M. Haldane, J. Phys. C **12** (1979) 4791; J. von Delft and H. Schoeller Annalen der Physik **7**, 225-306 (1998).
- [13] I. E. Dzyaloshinskii and K. B. Larkin, Sov. Phys. JETP **38**, 202 (1973); I.V.Yurkevich, in *Strongly correlated fermions and bosons in low-dimensional disordered systems*, edited by I.V.Lerner, B.L.Altshuler, and V.I.Falko (Kluwer, Dordrecht, 2002), cond-mat/0606387; I.V.Lerner and I.V.Yurkevich, in *Impurity in the Tomonaga-Luttinger model: a functional integral approach*, to be published in Proc. LXXXI Les Houches School on Nanoscopic Quantum Transport, 2004, cond-mat/0508223.
- [14] J. Zinn-Justin, *Quantum Field Theory and Critical Phenomena*, Oxford University Press UK (2002).
- [15] R. Raimondi, P. Schwab, C. Castellani, Phys. Rev. B **60**, 5818 (1999).

- [16] C. Castellani, C. Di Castro, P.A. Lee, and M. Ma, Phys. Rev. B **30**, 527 (1984).
- [17] I. L. Aleiner, B. L. Altshuler and M. E. Gershenson, Waves in Random Media **9**, 201 (1999).
- [18] A. M. Rudin, A. Aleiner, and L. I. Glazman, Phys. Rev. B **55**, 9322 (1997).
- [19] F. D. M. Haldane, J. Phys. C **14**, 2585-2609 (1981).
- [20] N. Sedlmayr, I. V. Yurkevich and I. V. Lerner, cond-mat/0607649.
- [21] D. Loss, Phys. Rev. Lett. **69**, 343-346 (1992).
- [22] U. Eckern, Phys. Rev. Lett. **70**, 3123 (1993).
- [23] T. Ludwig and A. D. Mirlin, Phys. Ref. B **69**, 193306 (2004).

Appendix A

Appendix (Dephasing by Kondo impurities)

A.1 Gradient expansion

In this appendix we perform the gradient expansion to obtain the effective action given in Eqs. (2.26), (2.27) and (2.28). The gradient expansion employs the fact that Q describes the low-energy/low-momentum sector of the theory, reflected in the dependency of Q only on small momenta, $Dq^2\tau \ll 1$, and small frequencies, $\omega_m\tau \ll 1$. Starting out from the action,

$$S[g] = \frac{1}{2} \text{Tr} \ln \left\{ i\partial_\tau + \frac{1}{2m}\partial^2 + \mu + \frac{i}{2\tau}g\Lambda g^{-1} - J \sum_i \sigma^S \sigma_3^T \mathbf{S}(\mathbf{x}_i) \right\},$$

the strategy is to express the rotation matrices, g , in generators and to expand the “Tr ln” in the generators as well as the small parameters $Dq^2\tau$, $\omega_m\tau \ll 1$ and $1/\epsilon_F\tau \ll 1$, keeping all orders in J . For notational convenience we introduce the following Green's functions

$$\begin{aligned} \mathcal{G}_0(\mathbf{p}) &\equiv \left(-\frac{\mathbf{p}^2}{2m} + \mu + \frac{i}{2\tau}\Lambda \right)^{-1} \\ \mathcal{G}_0^S(\mathbf{p}) &\equiv \left(-\frac{\mathbf{p}^2}{2m} + \mu + \frac{i}{2\tau}\Lambda - J\sigma^S \sigma_3^T \mathbf{S} \right)^{-1}, \end{aligned}$$

where we used the short notation $\sigma^S \sigma_3^T \mathbf{S} \equiv \sum_i \sigma^S \sigma_3^T \mathbf{S}(\mathbf{x}_i)$. Using that the rotation matrices, g , depend only on small momenta we decompose the momentum operator,

$$\hat{\mathbf{p}} \mapsto \mathbf{p} + \hat{\mathbf{q}},$$

where the large momenta \mathbf{p} enter through the global summation in the trace and the small momentum-operator $\hat{\mathbf{q}}$ acts on the effective degree of freedom g . As already mentioned we parametrize the rotation-matrix fields $g(\mathbf{x})_{\tau\tau'}$ by generators W ,

$$Q = g\Lambda g^{-1} = e^{-W/2}\Lambda e^{W/2} = \Lambda e^W,$$

where the second equality follows from the requirement that the Lie-algebra elements W generate rotations g that act on the saddle point fixed-point free, i.e. $[\Lambda, W] = 0$. We proceed by expanding g in W and expansion of the “Tr ln” to second order in W (Gaussian approximation)

$$\begin{aligned}
2S[g] &= \text{Tr} \ln \left\{ \partial_\tau + \mu + \frac{\hat{p}^2}{2m} + \frac{i}{2\tau} g \Lambda g^{-1} - J \sigma^S \sigma_3^T \mathbf{S} \right\} \\
&= \text{Tr} \ln \left\{ \partial_\tau + \mu + \frac{\mathbf{p}^2 + 2\mathbf{p}\hat{q}}{2m} - J \sigma^S \sigma_3^T \mathbf{S} + \frac{i}{2\tau} \Lambda + \frac{i}{2\tau} \Lambda W + \frac{i}{4\tau} \Lambda W^2 \right\} \\
&= \text{Tr} \ln \left\{ [\mathcal{G}_0^S]^{-1} + \frac{\mathbf{p}\hat{q}}{m} + \partial_\tau + \frac{i}{2\tau} \Lambda W + \frac{i}{4\tau} \Lambda W^2 \right\} \\
&= \text{Tr} \ln \left\{ 1 + \mathcal{G}_0^S \left(\frac{\mathbf{p}\hat{q}}{m} + \partial_\tau + \frac{i}{2\tau} \Lambda W + \frac{i}{4\tau} \Lambda W^2 \right) \right\} \\
&= \text{Tr} \left\{ \mathcal{G}_0^S \left(\frac{\mathbf{p}\hat{q}}{m} + \partial_\tau + \frac{i}{2\tau} \Lambda W + \frac{i}{4\tau} \Lambda W^2 \right) \right\} - \frac{1}{2} \left\{ \mathcal{G}_0^S \left(\frac{\mathbf{p}\hat{q}}{m} + \partial_\tau + \frac{i}{2\tau} \Lambda W + \frac{i}{4\tau} \Lambda W^2 \right) \right\}^2 \\
&\quad + \frac{1}{6} \text{Tr} \left\{ \mathcal{G}_0^S \left(\frac{\mathbf{p}\hat{q}}{m} + \partial_\tau + \frac{i}{2\tau} \Lambda W + \frac{i}{4\tau} \Lambda W^2 \right) \right\}^3 - \dots
\end{aligned}$$

In the second line we neglected a term proportional to \hat{q}^2 , and in the fourth and the last line we neglected constant contributions. Also we employed the fact that in order to find corrections to the conductivity up to order $O(1/(\epsilon_F \tau)^2)$ we can rely on the Gaussian approximation, that is we only need to expand to second order in the generators W . We now want to find for each order in J the most relevant contributions. Using that every Greens function after integration over fast momenta contributes by a factor τ (see Eq. (A.1)) (i.e. terms with higher derivatives are corrections of the order $(\omega_m \tau)^k \ll 1$ and $(D\mathbf{q}^2)^k \tau \ll 1, k > 0$) we find for the J^0 -order

$$\begin{aligned}
S_{J=0}[W] &= \frac{i}{8\tau} \text{Tr} \{ \mathcal{G}_0 \Lambda W^2 \} + \frac{1}{16\tau^2} \text{Tr} \{ \mathcal{G}_0 \Lambda W \mathcal{G}_0 \Lambda W \} - \frac{i}{8\tau} \text{Tr} \{ \mathcal{G}_0 \partial_\tau \mathcal{G}_0 \Lambda W^2 \} \\
&\quad - \frac{1}{16\tau^2} \text{Tr} \{ \mathcal{G}_0 \partial_\tau \mathcal{G}_0 \Lambda W \mathcal{G}_0 \Lambda W \} + \frac{i}{16\tau} \text{Tr} \left\{ \mathcal{G}_0 \frac{\mathbf{p}\hat{q}}{m} \mathcal{G}_0 \frac{\mathbf{p}\hat{q}}{m} \mathcal{G}_0 \Lambda W^2 \right\} + \dots + O(W^3).
\end{aligned}$$

We proceed by writing $\mathcal{G}_0(\mathbf{p}) = \frac{1}{2}(1 + \Lambda) \mathcal{G}_0^r(\mathbf{p}) + \frac{1}{2}(1 - \Lambda) \mathcal{G}_0^a(\mathbf{p})$, where $\mathcal{G}_0^{r/a}(p) = (-\frac{p^2}{2m} + \mu \pm i/2\tau)^{-1}$ and employ the identity

$$\int d^d \mathbf{p} [G_0^r(\mathbf{p})]^{k+1} [G_0^a(\mathbf{p})]^{m+1} = (-1)^k 2\pi i \nu^{k+m} \binom{k+m}{m} \tau^{k+m+1}, \quad (\text{A.1})$$

in order to find for the $J = 0$ contribution,

$$S_{J=0}[W] = S_\sigma^2[W] = -\frac{\pi\nu}{8} \sum_{n_1 n_2} \int d^d \mathbf{q} \text{Tr} \{ (D\mathbf{q}^2 + 2\hat{\epsilon}\Lambda) W_{n_1 n_2}(\mathbf{q}) W_{n_2 n_1}(-\mathbf{q}) \}.$$

Turning to contributions with non-vanishing J we again neglect those terms containing derivatives ∂_τ and \hat{q} (they constitute corrections of the order $\omega_m \tau \ll 1$ and $D\mathbf{q}^2 \tau \ll 1$). This leaves us with the following three terms

$$\begin{aligned}
S[J \neq 0, W] &= \frac{iJ}{8\tau} \text{Tr} \{ \mathcal{G}_0 \sigma^S \sigma_3^T \mathbf{S} \mathcal{G}_0^S \Lambda W^2 \} + \frac{J}{8\tau^2} \text{Tr} \{ \mathcal{G}_0 \sigma^S \sigma_3^T \mathbf{S} \mathcal{G}_0^S \Lambda W \mathcal{G}_0 \Lambda W \} \\
&\quad + \frac{J^2}{16\tau^2} \text{Tr} \{ \mathcal{G}_0 \sigma^S \sigma_3^T \mathbf{S} \mathcal{G}_0^S \Lambda W \mathcal{G}_0 \sigma^S \sigma_3^T \mathbf{S} \mathcal{G}_0^S \Lambda W \},
\end{aligned}$$

where we employed that $\mathcal{G}_0^S = \mathcal{G}_0 + J \mathcal{G}_0 \sigma^S \sigma_3^T \mathbf{S} \mathcal{G}_0^S$. Using the decomposition of \mathcal{G}_0 in retarded and advanced components we can see that the first term vanishes, since

$$\begin{aligned}
\text{Tr} \{ \mathcal{G}_0 \sigma^S \sigma_3^T \mathbf{S} \mathcal{G}_0^S \Lambda W^2 \} &= \text{const.} \int d^d \mathbf{p} \mathcal{G}_0^R \mathcal{G}_0^A \text{Tr} \{ (1 \mp \Lambda) \sigma^S \sigma_3^T \mathbf{S} (1 + J \mathcal{G}_0^S \sigma^S \sigma_3^T \mathbf{S}) (1 \pm \Lambda) \Lambda W^2 \} \\
&= \text{const.} \int d^d \mathbf{p} \mathcal{G}_0^R \mathcal{G}_0^A \text{Tr} \{ \sigma^S \sigma_3^T \mathbf{S} (1 + J \mathcal{G}_0^S \sigma^S \sigma_3^T \mathbf{S}) (1 \pm \Lambda) (1 \mp \Lambda) \Lambda W^2 \},
\end{aligned}$$

and $(1 \mp \Lambda)(1 \pm \Lambda) = 0$. The second term, on the other hand, acquires the form

$$\begin{aligned}
& -\frac{J}{8\tau^2} \text{Tr} \left\{ \mathcal{G}_0 \sigma \mathbf{S} \mathcal{G}_0^S \Lambda W \mathcal{G}_0^S \Lambda W \right\} \\
& = -\frac{J}{16\tau^2} \sum_p \mathcal{G}_0^R(\mathbf{p}) \mathcal{G}_0^R(\mathbf{p}) \mathcal{G}_0^A(\mathbf{p}) \text{Tr} \left\{ (\sigma^S \sigma_3^T \mathbf{S} + J \sigma^S \sigma_3^T \mathbf{S} \mathcal{G}_0^S \sigma^S \sigma_3^T \mathbf{S}) \Lambda W^2 (1 + \Lambda) \right\} \\
& \quad - \frac{J}{16\tau^2} \sum_p \mathcal{G}_0^R(\mathbf{p}) \mathcal{G}_0^A(\mathbf{p}) \mathcal{G}_0^A(\mathbf{p}) \text{Tr} \left\{ (\sigma^S \sigma_3^T \mathbf{S} + J \sigma^S \sigma_3^T \mathbf{S} \mathcal{G}_0^S \sigma^S \sigma_3^T \mathbf{S}) \Lambda W^2 (1 - \Lambda) \right\} \\
& = -\frac{\pi \nu i J}{4} \text{Tr} \left\{ (\sigma^S \sigma_3^T \mathbf{S} + J \sigma^S \sigma_3^T \mathbf{S} \mathcal{G}_0^S \sigma^S \sigma_3^T \mathbf{S}) \Lambda W^2 \right\},
\end{aligned}$$

and the last may be written as

$$\begin{aligned}
& \frac{1}{16\tau^2} \text{Tr} \left\{ \mathcal{G}_0 \sigma \mathbf{S} \mathcal{G}_0^S \Lambda W \mathcal{G}_0 \sigma^S \sigma_3^T \mathbf{S} \mathcal{G}_0^S \Lambda W \right\} \\
& = \frac{1}{16\tau^2} \sum_{p'} \sum_p \mathcal{G}_0^R(\mathbf{p}) \mathcal{G}_0^A(\mathbf{p}) \mathcal{G}_0^R(\mathbf{p}') \mathcal{G}_0^A(\mathbf{p}') \\
& \quad \text{Tr} \left\{ (\sigma^S \sigma_3^T \mathbf{S} + J \sigma^S \sigma_3^T \mathbf{S} \mathcal{G}_0^S \sigma^S \sigma_3^T \mathbf{S}) \Lambda W (\sigma^S \sigma_3^T \mathbf{S} + J \sigma^S \sigma_3^T \mathbf{S} \mathcal{G}_0^S \sigma^S \sigma_3^T \mathbf{S}) \Lambda W \right\}.
\end{aligned}$$

Integration over the fast momenta we find Eqs. (2.26), (2.27) and (2.28). We notice that since the magnetic impurity is a hard scatterer, i.e. incoming momenta are scattered over the whole Fermi-sphere, every Greens function between two local spins gives a term $\int d^d \mathbf{p} \mathcal{G}_0(\mathbf{p})$. That is every order in J comes with a free integration over the Fermi-sphere and thus the k -th order in J gives a correction $\sim (J\nu L^d)^k$. In the case of soft scatterers different contributions are dominant; see the evaluation of the corrections to $1/\tau_\varphi$ from mixed diagrams and higher orders in n_S in the text and in Appendix A.7 and A.8 for a discussion of this point.

A.2 Spin-singlet and spin-triplet channels

In this appendix we separate the effective degrees of freedom (Diffuson and Cooperon), which describe the joined propagation of two spin-1/2 particles, into its spin-singlet and spin-triplet contributions. To this end we remind that the spin-singlet state is by definition the one-dimensional space on which the action of the spin SU(2) is trivial. Introduction of a Zeeman-term allows for a further identification of the spin-triplet states with z -component $m = -1, 0, 1$.

A.2.1 Spin-singlet channels

By definition the spin SU(2) acts trivial on the spin-singlet state. For a representation of the action of SU(2) on the Diffuson and Cooperon, respectively, we go back to the definitions,

$$\Psi = \frac{1}{\sqrt{2}} \begin{pmatrix} \psi \\ -i\sigma_2^S \bar{\psi}^t \end{pmatrix}_T, \quad \bar{\Psi} = \frac{1}{\sqrt{2}} (\bar{\psi} \quad -i\psi^t \sigma_2^S)_T, \quad Q \propto \Psi \otimes \bar{\Psi}, \quad (\text{A.2})$$

and remind that the Diffuson corresponds to the T-space diagonal terms, $\mathcal{D} \propto \chi \otimes \bar{\chi}$. That is, the action of the SU(2) is given by the *complex* adjunct representation,

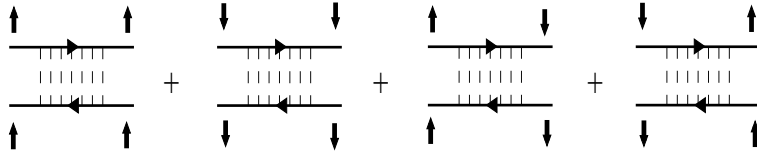
$$\chi \otimes \bar{\chi} \rightarrow g\chi \otimes \bar{\chi}g^\dagger, \quad (\text{A.3})$$

from which we read off the invariant singlet sub-space spanned by $\mathcal{D}_{S=0} = s_D \otimes \sigma_0^S$. The Cooperon on the other hand is given by the T-space off-diagonal terms, $\mathcal{C} \propto \chi \otimes \chi^t \sigma_2^S$. Therefore the SU(2) acts by the *real* conjugate representation,

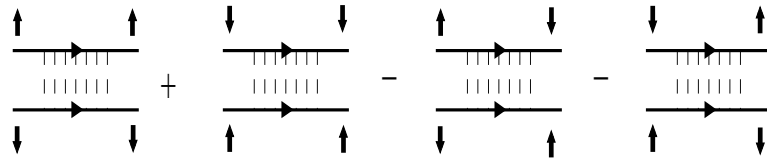
$$\chi \otimes \chi^t \sigma_2^S \rightarrow g\chi \otimes \chi^t g^t \sigma_2^S, \quad (\text{A.4})$$

which also has the one-dimensional invariant subspace $\mathcal{C}_{S=0} = s_C \otimes \sigma_0^S$. For completeness we give the diagrammatic representation of the Diffuson and Cooperon singlet-states in terms of advanced and retarded Greens functions.

Spin-singlet Diffuson



Spin-singlet Cooperon



A.2.2 Spin-triplet channels

The triplet components of Diffuson and Cooperon are spanned by the generators, W , proportional to $\sigma_1^S, \sigma_2^S, \sigma_3^S$. In order to find the $S_z = -1, 0, 1$ components we introduce a Zeeman term into the Hamiltonian,

$$H_{\text{Zee}} = \int d^d \mathbf{x} \bar{\chi}(\mathbf{x}) \mathbf{B}_z \sigma_3^S \chi(\mathbf{x}), \quad (\text{A.5})$$

where \mathbf{B}_z is a (homogeneous) external magnetic field defining the z -axis of the coordinate system. Introduction of a time-reversed component and following the steps for the derivation of the σ -model one ends up with the following additional contribution to the σ -model action

$$S_{\text{Zee}}[W] = \sum_{n_1 n_2} \int d^d \mathbf{x} \text{tr} \{ \mathbf{B}_z \sigma_3^S \sigma_3^T \Lambda_{n_1} W_{n_1 n_2} W_{n_2 n_1} \}. \quad (\text{A.6})$$

Separation into Diffuson and Cooperon contributions one obtains

$$S_{\text{Zee}}[\mathcal{D}^{++}] = \sum_{n_1 n_2} \int d^d \mathbf{x} \text{tr} \{ \mathbf{B}_z \Lambda_{n_1} [\sigma_3^S, \mathcal{D}_{n_1 n_2}^{++}] \mathcal{D}_{n_2 n_1}^{++} \} \quad (\text{A.7})$$

$$S_{\text{Zee}}[\mathcal{C}^{+-} \mathcal{C}^{-+}] = \sum_{n_1 n_2} \int d^d \mathbf{x} \text{tr} \{ \mathbf{B}_z \Lambda_{n_1} [\sigma_3^S, \mathcal{C}_{n_1 n_2}^{+-}]_+ \mathcal{C}_{n_2 n_1}^{-+} \}. \quad (\text{A.8})$$

Notice that the Cooperon-singlet is not diagonal in the Zeeman term (i.e. an invariant subspace of). This results from the fact that the magnetic field in the time-reversed space comes with a minus sign. In order to distinguish the Cooperon-triplet components one may work for the Cooperon with the model Hamiltonian

$$S_{\text{Zee}}[W^C] = \sum_{n_1 n_2} \int d^d \mathbf{x} \text{tr} \{ \mathbf{B}_z \sigma_3^S \Lambda_{n_1} W_{n_1 n_2}^C W_{n_2 n_1}^C \}, \quad (\text{A.9})$$

	singlet	triplet $m = 0$	triplet $m = 1$	triplet $m = -1$
Diffuson	$\mathcal{D}_{S=0} = s^D \otimes \sigma_0^S$	$\mathcal{D}_{S=1,0} = t_0^D \otimes \sigma_3^S$	$\mathcal{D}_{S=1,1} = \tau_1^D \otimes (\sigma_1^S + i\sigma_2^S)$	$\mathcal{D}_{S=1,-1} = \tau_{-1}^D \otimes (\sigma_1^S - i\sigma_2^S)$
Cooperon	$\mathcal{C}_{S=0} = s^C \otimes \sigma_0^S$	$\mathcal{C}_{S=1,0} = t_0^C \otimes \sigma_3^S$	$\mathcal{C}_{S=1,1} = \tau_1^C \otimes (\sigma_1^S + i\sigma_2^S)$	$\mathcal{C}_{S=1,-1} = \tau_{-1}^C \otimes (\sigma_1^S - i\sigma_2^S)$

Table A.1: Separation of Diffuson and Cooperon into its spin-singlet and spin-triplet contributions

which takes the form

$$S_{Zee}[\mathcal{C}^{+-}\mathcal{C}^{-+}] = \sum_{n_1 n_2} \int d^d \mathbf{x} \text{tr} \{ \mathbf{B}_z \Lambda_{n_1} [\sigma_3^S, \mathcal{C}_{n_1 n_2}^{+-}] \mathcal{C}_{n_2 n_1}^{-+} \}. \quad (\text{A.10})$$

However, we only use Eq. (A.10) in order to identify the $m = -1, 0, 1$ triplet states. A physical B -field makes the modes $W^C \propto \sigma_3^S \pm \sigma_0^S$ massive, while $W^C \propto \sigma_1^S, \sigma_2^S$ are not affected. With Eqs. (A.7), (A.10) it follows that the $S_z = 0$ triplet-Diffuson and -Cooperon are given by $W_{S=1} \propto t_0 \otimes \sigma_3^S$ whereas the $m = \pm 1$ states are linear combinations of $W_{S=1} \propto t_1 \otimes \sigma_1^S$ and $W_{S=1} \propto t_2 \otimes \sigma_2^S$. To be more precise, the latter diagonalize the Hamiltonian, i.e.

$$\begin{aligned} (\bar{t}_1 \quad \bar{t}_2)_{nn'} & \begin{pmatrix} \Pi_{nn'} & -i\mathbf{B}_z \\ i\mathbf{B}_z & \Pi_{nn'} \end{pmatrix} \begin{pmatrix} t_1 \\ t_2 \end{pmatrix}_{n'n} \\ &= \frac{1}{2} (\bar{t}_1 + i\bar{t}_2 \quad \bar{t}_1 - i\bar{t}_2)_{nn'} \begin{pmatrix} \Pi_{nn'} + \mathbf{B}_z & \\ & \Pi_{nn'} - \mathbf{B}_z \end{pmatrix} \begin{pmatrix} t_1 - it_2 \\ t_1 + it_2 \end{pmatrix}_{n'n} \\ &\equiv (\bar{\tau}_1 \quad \bar{\tau}_2)_{nn'} \begin{pmatrix} \Pi_{nn'} + \mathbf{B}_z & \\ & \Pi_{nn'} - \mathbf{B}_z \end{pmatrix} \begin{pmatrix} \tau_1 \\ \tau_2 \end{pmatrix}_{n'n}, \end{aligned} \quad (\text{A.11})$$

where $\bar{t}_{nn'}$ and $t_{nn'}$ again denote contributions with $n < 0, n' > 0$ and $n > 0, n' < 0$ (correspondingly for s and τ) and $\Pi_{nn'}^{-1} = D\mathbf{q}^2 + i\epsilon_{n-n'}$ is the propagator of the standard nonlinear σ -model action. In summary, contributions from the spin-triplet channels to the action are

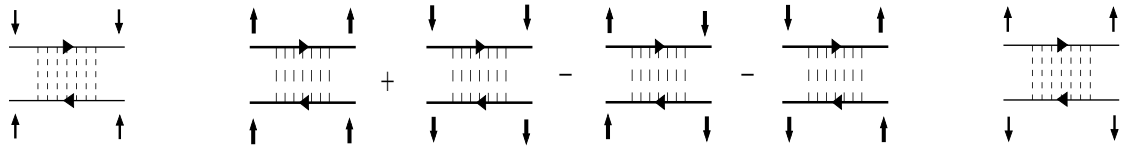
$$S_\sigma[\bar{t}_0 t_0] = \int d^d \mathbf{q} \text{tr}_R \{ \Pi^{-1} \bar{t}_0 t_0 \} \quad (\text{A.12})$$

$$S_\sigma[\bar{\tau}_1 \tau_1] = \int d^d \mathbf{q} \text{tr}_R \{ [\Pi^{-1} + \mathbf{B}_z] \bar{\tau}_1 \tau_1 \} \quad (\text{A.13})$$

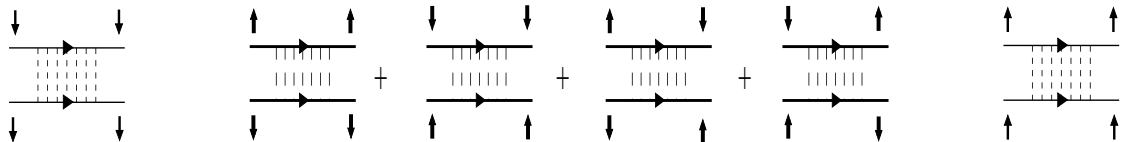
$$S_\sigma[\bar{\tau}_{-1} \tau_{-1}] = \int d^d \mathbf{q} \text{tr}_R \{ [\Pi^{-1} - \mathbf{B}_z] \bar{\tau}_{-1} \tau_{-1} \}. \quad (\text{A.14})$$

The results of this section are summarized in Table A.1 and a diagrammatic representation of the triplet states in terms of Greens functions is depicted below.

Spin-triplet Diffusons: $m = -1, 0$ and 1



Spin-triplet Cooperons: $m = -1, 0$ and 1



A.3 Response kernels in Gaussian approximation

In this appendix we derive the response kernels for the calculation of weak localization corrections to the conductivity (WL) and the Aharonov-Bohm oscillations (AB), Eqs. (2.55)-(2.56) and Eqs. (2.94)-(2.96).

We start out from the definition of the (homogeneous) dc-conductivity in a d -dimensional system in the linear-response approximation, $\sigma = -\frac{K(\omega)}{i\omega}$, where

$$K(\omega_m) \equiv \frac{1}{d} \sum_{i=1}^d \frac{\delta^2 F[\mathbf{a}]}{\delta \mathbf{a}_0^i(\omega_m) \delta \mathbf{a}_0^i(-\omega_m)} \quad (\text{A.15})$$

is the linear response kernel, \mathbf{a}_0 denotes the homogeneous component $\mathbf{a}(\mathbf{q} = 0)$ of the vector potential and the analytical continuation $i\omega_m \rightarrow \omega + i0$ has to be done. Next we perform an expansion in the generators W to second order (Notice that we introduced \mathbf{a} into the action Eq. (2.26) by minimally coupling, $i\partial \mapsto i\partial + e[\mathbf{a}\sigma_3^\top, \cdot]$). In 0^{th} order fluctuation matrices, W , the source term of action Eq. (2.26) takes the form,

$$S_{\text{dia}}^0[\mathbf{a}] = \frac{e^2 \pi \nu D}{4} \text{tr} \{ \mathbf{a} \sigma_3^\top \Lambda \mathbf{a} \sigma_3^\top \Lambda - 2 \mathbf{a} \mathbf{a} \},$$

leading to (here and in the following summation over repeated indices is implicit)

$$K_{\text{mf}}(i\omega_m) = \frac{e^2 \pi \nu D}{\beta} \text{tr} \{ 2n_1 - \Lambda_{n_1} (\Lambda_{n_1+m} + \Lambda_{n_1-m}) \},$$

which gives the Drude conductivity, σ^D . The second order contribution to the source action contains a "diamagnetic" ($\propto \mathbf{a}^2$) and a "paramagnetic" ($\propto \mathbf{a}$) term,

$$\begin{aligned} S_{\text{dia}}^2[W, \mathbf{a}] &= \frac{e^2 \pi \nu D}{4} \text{tr} \{ \mathbf{a} \sigma_3^\top \Lambda W(\mathbf{q}) \mathbf{a} \sigma_3^\top \Lambda W(-\mathbf{q}) + \mathbf{a} \sigma_3^\top \Lambda \mathbf{a} \sigma_3^\top \Lambda W(\mathbf{q}) W(-\mathbf{q}) \} \\ S_{\text{para}}^2[W, \mathbf{a}] &= \frac{e \pi \nu D}{2} \text{tr} \{ \mathbf{a} \mathbf{q} \sigma_3^\top W(\mathbf{q}) W(-\mathbf{q}) \}. \end{aligned}$$

Since \mathbf{a} is diagonal in T-space, the contributions from matrices diagonal (Diffuson) and off-diagonal (Cooperon) in T-space decouple, i.e. the source term in Gaussian approximation can be separated into its Cooperon and Diffuson contributions. Depending on the experiment that we want to describe we keep only one of these terms: The WL experiment involves only the Cooperon, while the AB experiment in general involves Cooperon and Diffuson degrees of freedom. Yet at already moderate magnetic fields the Cooperon-contribution may be neglected.

A.3.1 Response kernel for weak localization experiment

Referring to the parametrization of Eq. (2.29), the Cooperon-contribution to the diamagnetic source term is

$$S_{\text{dia}}^2[\mathcal{C}^{+-} \mathcal{C}^{-+}] = \frac{e^2 \pi \nu D}{2\beta} \mathbf{a}_{m_1} \mathbf{a}_{m_2} \text{tr}_{\mathbf{R} \otimes \mathbf{S}} \{ [\mathcal{C}_{n_1-m_2, n_2}^{+-}(\mathbf{q}) + \mathcal{C}_{n_1, n_2-m_2}^{+-}(\mathbf{q})] \mathcal{C}_{n_2, n_1+m_1}^{-+}(\mathbf{q}) \} \text{sign} [n_1(n_1 + m)].$$

In the absence of any interactions there is only one possible contraction, resulting from

$$K_{\text{dia}}^0(i\omega_m) = \frac{e^2 \pi \nu D}{\beta} \text{tr} \{ \mathcal{C}_{n_1, n_2+m}^{+-}(\mathbf{q}) \mathcal{C}_{n_2, n_1+m}^{-+}(-\mathbf{q}) \} \text{sign} [n_1(n_1 + m)]$$

and leading to Eq. (2.55). In the presence of (perturbatively treated) interactions there are several possible ways to perform contractions between $S_{\text{dia}}^2[\mathcal{C}]$ and $S_{\text{int}}^2[\mathcal{C}]$, i.e. we have to keep all terms in S_{dia}^2 . This leads to

$$K_{\text{dia}}(i\omega_m) = \frac{e^2\pi\nu D}{\beta} \text{tr} \left\{ [\mathcal{C}_{n_1+m,n_2}^{+-}(\mathbf{q}) + \mathcal{C}_{n_1,n_2+m}^{+-}(\mathbf{q})] \mathcal{C}_{n_2,n_1+m}^{-+}(-\mathbf{q}) \right\} \text{sign} [n_1(n_1 + m_1)].$$

The paramagnetic contribution to the source-term action,

$$S_{\text{para}}^2[\mathcal{C}^{+-}\mathcal{C}^{-+}] = \frac{e\pi\nu D}{2\beta^{1/2}} \mathbf{q} \mathbf{a}_{m_1} \text{tr}_{\mathbf{R} \otimes \mathbf{T}} \left\{ \mathcal{C}_{n_1,n_2}^{+-}(\mathbf{q}) \mathcal{C}_{n_2,n_1+m_1}^{-+}(-\mathbf{q}) \right\} \Theta(n_1(n_1 + m_1)),$$

may be expanded to second order, i.e. $e^{S_{\text{para}}} = 1 + S_{\text{para}} + \frac{1}{2}S_{\text{para}}^2$. Performing one contractions one finds (for a d -dimensional system)

$$\begin{aligned} \langle S_{\text{para}}^2[\mathcal{C}^{+-}\mathcal{C}^{-+}] S_{\text{para}}^2[\mathcal{C}^{+-}\mathcal{C}^{-+}] \rangle \\ = \frac{(e\pi\nu D)^2}{\beta} \frac{\mathbf{q}^2}{d} \mathbf{a}_{m_1} \mathbf{a}_{m_2} \Pi_{n_1 n_2}^{\mathbf{C}} \text{tr}_{\mathbf{R} \otimes \mathbf{T}} \left\{ [\mathcal{C}_{n_1-m_2,n_2}^{+-}(\mathbf{q}) + \mathcal{C}_{n_1,n_2-m_2}^{+-}(\mathbf{q})] \mathcal{C}_{n_2,n_1+m_1}^{-+}(-\mathbf{q}) \right\} \Theta(n_1(n_1 + m_1)), \end{aligned}$$

i.e.

$$K_{\text{para}}(i\omega_m) = \frac{2(e\pi\nu D)^2}{\beta} \frac{\mathbf{q}^2}{d} \Pi_{n_1 n_2}^{\mathbf{C}}(\mathbf{q}) \text{tr}_{\mathbf{R} \otimes \mathbf{T}} \left\{ [\mathcal{C}_{n_1+m,n_2}^{+-}(\mathbf{q}) + \mathcal{C}_{n_1,n_2+m}^{+-}(\mathbf{q})] \mathcal{C}_{n_2,n_1+m}^{-+}(-\mathbf{q}) \right\} \Theta(n_1(n_1 + m)).$$

Notice that in the absence of interactions there are no possible contractions from S_{para} . The sum of diamagnetic and paramagnetic contributions may be organized as follows

$$\begin{aligned} K_{\text{dia}}(i\omega_m) + K_{\text{para}}(i\omega_m) = \frac{e^2\pi\nu D}{\beta} \left\{ \left[1 + 2\pi\nu D \frac{\mathbf{q}^2}{d} \Pi_{n_1 n_2}^{\mathbf{C}}(\mathbf{q}) \right] \Theta(n_1(n_1 + m)) - \Theta(-n_1(n_1 + m)) \right\} \\ \text{tr}_{\mathbf{R} \otimes \mathbf{T}} \left\{ [\mathcal{C}_{n_1+m,n_2}^{+-}(\mathbf{q}) + \mathcal{C}_{n_1,n_2+m}^{+-}(\mathbf{q})] \mathcal{C}_{n_2,n_1+m}^{-+}(-\mathbf{q}) \right\}. \end{aligned}$$

Employing that (after the contractions) the final term contains two further Cooperon-propagators, $\Pi^{\mathbf{C}}$, one may write the propagator in the first line as a derivative, i.e.

$$\begin{aligned} K_{\text{dia}}(i\omega_m) + K_{\text{para}}(i\omega_m) = \frac{e^2\pi\nu D}{\beta} \left\{ \left[1 + \mathbf{q}_1 \frac{d}{d\mathbf{q}_1} \right] \Theta(n_1(n_1 + m)) - \Theta(-n_1(n_1 + m)) \right\} \\ \text{tr}_{\mathbf{R} \otimes \mathbf{S}} \left\{ [\mathcal{B}_{n_1+m,n_2}^{+-}(\mathbf{q}) + \mathcal{B}_{n_1,n_2+m}^{+-}(\mathbf{q})] \mathcal{B}_{n_2,n_1+m}^{-+}(-\mathbf{q}) \right\}. \end{aligned}$$

Partial integration in \mathbf{q}_1 reveals that the first contribution is exactly zero, leaving us with

$$\begin{aligned} K_{\text{dia}}(i\omega_m) + K_{\text{para}}(i\omega_m) \\ = -\frac{e^2\pi\nu D}{\beta} \text{tr}_{\mathbf{R} \otimes \mathbf{S}} \left\{ [\mathcal{B}_{n_1+m,n_2}^{+-}(\mathbf{q}) + \mathcal{B}_{n_1,n_2+m}^{+-}(\mathbf{q})] \mathcal{B}_{n_2,n_1+m}^{-+}(-\mathbf{q}) \right\} \Theta(-n_1(n_1 + m)), \end{aligned}$$

which gives Eqs. (2.55) and (2.56). Notice that in the end only those terms where the current-vertex changes causality contribute.

A.3.2 Response kernel for Aharonov-Bohm oscillations

We now turn to the AB-response kernel and restrict to the Diffuson-contribution and a (quasi)1-d geometry. The AB are found from the typical sample-to-sample fluctuations, $\text{var } g = \langle g^2 \rangle - (\langle g \rangle)^2$. Ensemble fluctuations are most conveniently computed by enlarging the internal field-space by a fluctuation sector F. The vector-potential becomes a matrix in F-space, $\mathbf{a} = \begin{pmatrix} \mathbf{a}^1 & \\ & \mathbf{a}^2 \end{pmatrix}_{\mathbf{F}}$, and fluctuations are obtained from

$$\text{var } g = \frac{1}{L^2} \frac{1}{\omega_{m_1} \omega_{m_2}} \frac{\delta^4 F[\mathbf{a}]}{\delta \mathbf{a}_{m_1}^1 \delta \mathbf{a}_{-m_1}^1 \delta \mathbf{a}_{m_2}^2 \delta \mathbf{a}_{-m_2}^2} \Big|_{i\omega_{m_1}, i\omega_{m_2} \rightarrow i0},$$

where, \mathbf{a}^i is a (homogeneous) vector potential pointing along the wire. Connected diagrams contain only generators with off-diagonal components in F-space. Separation into dia- and paramagnetic contributions gives, $S_{\mathbf{a}}^2 = S_{\text{dia}}^2 + S_{\text{para}}^2$, where

$$S_{\text{dia}}^2[\mathcal{D}] = \frac{e^2 \pi \nu D}{2\beta} \text{tr}_{\text{R} \otimes \text{S}} \{ [\mathbf{a}_{m_1} \mathbf{a}_{m_2} \mathcal{D}_{n_1-m_2, n_2}^{++}(\mathbf{q}) + \mathbf{a}_{m_1} \mathcal{D}_{n_1, n_2+m_2}^{++}(\mathbf{q}) \mathbf{a}_{m_2}] \mathcal{D}_{n_2, n_1+m_1}^{++}(\mathbf{q}) \} \text{sign}[n_1(n_1 + m_1)]$$

$$S_{\text{para}}^2[\mathcal{D}] = \frac{e \pi \nu D}{2\beta^{1/2}} \mathbf{q} \text{tr}_{\text{R} \otimes \text{T}} \{ \mathbf{a}_{m_1} \mathcal{D}_{n_1, n_2}^{++}(\mathbf{q}) \mathcal{D}_{n_2, n_1+m_1}^{++}(-\mathbf{q}) \} \Theta(n_1(n_1 + m_1)).$$

Expansion to fourth order, i.e. $e^{S^2[\mathbf{a}]} = 1 + S^2[\mathbf{a}] + \dots$, obtains

$$K_{\text{AB}} = \frac{1}{2!} \langle S_{\text{dia}}^2 S_{\text{dia}}^2 \rangle + \frac{3}{3!} \langle S_{\text{dia}}^2 S_{\text{para}}^2 S_{\text{para}}^2 \rangle + \frac{1}{4!} \langle S_{\text{para}}^2 S_{\text{para}}^2 S_{\text{para}}^2 S_{\text{para}}^2 \rangle.$$

We now perform contractions in fluctuation matrices of the paramagnetic term, in order to end up with a contribution quartic in \mathcal{D} . To this end we use that (in $d=1$)

$$\langle S_{\text{para}}^2[\mathcal{D}^{++}] S_{\text{para}}^2[\mathcal{D}^{++}] \rangle$$

$$= \frac{2(e\pi\nu D)^2}{\beta} \frac{\mathbf{q}^2}{d} \Pi_{n_1 n_2}^{\text{D}} \text{tr}_{\text{R} \otimes \text{T}} \{ [\mathbf{a}_{m_1} \mathbf{a}_{m_2} \mathcal{D}_{n_1-m_2, n_2}^{++}(\mathbf{q}) - \mathbf{a}_{m_1} \mathcal{D}_{n_1, n_2+m_2}^{++}(\mathbf{q}) \mathbf{a}_{m_2}] \mathcal{D}_{n_2, n_1+m_1}^{++}(-\mathbf{q}) \} \Theta(n_1(n_1 + m_1)),$$

in order to organize K_{AB} as follows

$$K_{\text{AB}} = \frac{(e^2 \pi \nu D)^2}{8\beta^2} \text{tr}_{\text{R} \otimes \text{T}} \{ \mathcal{O}[\mathbf{a}, n_1 n_2, m_1] \} \text{tr}_{\text{R} \otimes \text{T}} \{ \mathcal{O}[\mathbf{a}, n'_1 n'_2, m'_1] \} \left[\text{sign}(n_1(n_1 + m_1)) \text{sign}(n'_1(n'_1 + m'_1)) \right.$$

$$\left. + \pi \nu D \mathbf{q}^2 \Pi_{n_1 n_2}^{\text{D}} \Theta(n_1(n_1 + m_1)) \text{sign}(n'_1(n'_1 + m'_1)) + \pi \nu D)^2 \mathbf{q}^4 [\Pi_{n_1 n_2}^{\text{D}}]^2 \Theta(n_1(n_1 + m_1)) \Theta(n'_1(n'_1 + m'_1)) \right].$$

Here we used the short notation

$$\text{tr}_{\text{R} \otimes \text{T}} \{ \mathcal{O}[\mathbf{a}, n_1 n_2, m_1] \} = \text{tr}_{\text{R} \otimes \text{T}} \{ [\mathbf{a}_{m_1} \mathbf{a}_{m_2} \mathcal{D}_{n_1-m_2, n_2}^{++}(\mathbf{q}) - \mathbf{a}_{m_1} \mathcal{D}_{n_1, n_2+m_2}^{++}(\mathbf{q}) \mathbf{a}_{m_2}] \mathcal{D}_{n_2, n_1+m_1}^{++}(-\mathbf{q}) \}.$$

Writing $\text{sign}(n_1(n_1 + m_1)) = \Theta(n_1(n_1 + m_1)) - \Theta(-n_1(n_1 + m_1))$ one can verify that the term proportional to $\Theta(n_1(n_1 + m_1))\Theta(-n'_1(n'_1 + m'_1))$ does not give any contributions when doing the contractions in \mathcal{D} and therefore

$$K_{\text{AB}} = \frac{(e^2 \pi \nu D)^2}{8\beta^2} \text{tr}_{\text{R} \otimes \text{T}} \{ \mathcal{O}[\mathbf{a}, n_1 n_2, m_1] \} \text{tr}_{\text{R} \otimes \text{T}} \{ \mathcal{O}[\mathbf{a}, n'_1 n'_2, m'_1] \}$$

$$\left[\Theta(-n_1(n_1 + m_1))\Theta(-n'_1(n'_1 + m'_1)) + \left(1 + (\pi \nu D)^2 \mathbf{q}^4 [\Pi_{n_1 n_2}^{\text{D}}]^2 \Theta(n_1(n_1 + m_1))\Theta(n'_1(n'_1 + m'_1)) \right) \right].$$

Again, we employ that the final expression contains two more Diffuson-propagators in order to write Π^{D} as a derivative. Doing partial integrations it may then be seen that, again, only those terms survive, where causality is changed at the current vertex, i.e.

$$K_{\text{AB}} = \frac{(e^2 \pi \nu D)^2}{\beta^2} \text{tr}_{\text{R} \otimes \text{T}} \{ \mathcal{O}[\mathbf{a}, n_1 n_2, m_1] \} \text{tr}_{\text{R} \otimes \text{T}} \{ \mathcal{O}[\mathbf{a}, n'_1 n'_2, m'_1] \} \Theta(-n_1(n_1 + m_1))\Theta(-n'_1(n'_1 + m'_1)).$$

Performing the derivative with respect to \mathbf{a}^i we find $\text{var } g = K_\nu + K_D$, where (1,2 denotes F-space components)

$$K_\nu = \frac{(e^2 \pi \nu D)^2}{\beta^2 L^2 \omega_{m_1} \omega_{m_2}} \sum_{-m_1 < n_1 < 0} \sum_{-m_2 < n_2 < 0} \text{tr}_{\mathbf{R} \otimes \mathbf{S}} \{ \bar{C}_{n_1+m_2, n_2}^{12}(\mathbf{q}) C_{n_2, n_1+m_1}^{21}(-\mathbf{q}) \} \text{tr}_{\mathbf{R} \otimes \mathbf{S}} \{ \bar{C}_{n'_1+m'_2, n'_2}^{12}(\mathbf{q}) C_{n'_2, n'_1+m'_1}^{21}(-\mathbf{q}) \}$$

$$K_D = \frac{(e^2 \pi \nu D)^2}{\beta^2 L^2 \omega_{m_1} \omega_{m_2}} \sum_{-m_1 < n_1 < 0} \sum_{-m_2 < n_2 < 0} \text{tr}_{\mathbf{R} \otimes \mathbf{S}} \{ \bar{C}_{n_1, n_2+m_2}^{12}(\mathbf{q}) \bar{C}_{n_2, n_1+m_1}^{21}(-\mathbf{q}) \} \text{tr}_{\mathbf{R} \otimes \mathbf{S}} \{ C_{n'_1, n'_2+m'_2}^{12}(\mathbf{q}) C_{n'_2, n'_1+m'_1}^{21}(-\mathbf{q}) \}.$$

The first and second term describe ensemble fluctuations of the density of states, ν , and the diffusion constant, D , respectively [22]. (For notational convenience we did not write out the T-space indices $+/ -$.)

A.4 Some details

In this appendix we show that $I_d(\Omega, \tau_\varphi) \sim [\Omega^2 + 1/\tau_\varphi^2]^{\frac{d-4}{4}}$. Using that

$$I_d(\Omega, \tau_\varphi) = \int d^d q \frac{1}{(Dq^2 + 1/\tau_\varphi)^2 + \Omega^2} = \frac{1}{D^{d/2} \Omega} \text{Im} \int d^d q \frac{1}{q^2 + 1/\tau_\varphi - i\Omega} \quad (\text{A.16})$$

one finds up to orders $O\left(\frac{\Omega^2}{1/\tau_\varphi^2 + \Omega^2}\right)$

- in $d = 1$

$$I_1(\Omega, \tau_\varphi) = \frac{2\pi}{D^{1/2} \Omega} \text{Im} \frac{1}{\sqrt{1/\tau_\varphi - i\Omega}} \sim \frac{\pi}{D^{1/2}} \frac{1}{(1/\tau_\varphi^2 + \Omega^2)^{3/4}} \quad (\text{A.17})$$

- in $d = 2$

$$I_2(\Omega, \tau_\varphi) = \frac{-\pi}{D\Omega} \text{Im} \ln[1/\tau_\varphi - i\Omega] \sim \frac{\pi}{D} \frac{1}{(1/\tau_\varphi^2 + \Omega^2)^{1/2}} \quad (\text{A.18})$$

- in $d = 3$

$$I_3(\Omega, \tau_\varphi) = \frac{-8\pi^2}{D^{3/2} \Omega} \text{Im} \sqrt{1/\tau_\varphi - i\Omega} \sim \frac{4\pi^2}{D^{3/2}} \frac{1}{(1/\tau_\varphi^2 + \Omega^2)^{1/4}} \quad (\text{A.19})$$

Here we used in $d = 1$ (and similar in $d = 3$) that

$$\text{Im} \frac{1}{\sqrt{1/\tau_\varphi - i\Omega}} = \frac{1}{(1/\tau_\varphi^2 + \Omega^2)^{1/4}} \text{Im} e^{i/2 \arcsin \frac{\Omega}{\sqrt{1/\tau_\varphi^2 + \Omega^2}}}.$$

Furthermore we employed that $\sin x = \frac{\sin 2x}{2 \cos x}$ and $|\Omega/\sqrt{1/\tau_\varphi^2 + \Omega^2}| < 1$ in order to approximate

$$\text{Im} \frac{1}{\sqrt{1/\tau_\varphi - i\Omega}} = \frac{\Omega}{(1/\tau_\varphi^2 + \Omega^2)^{3/4}} \frac{1}{2 \cos \frac{1}{2} \arcsin \frac{\Omega}{\sqrt{1/\tau_\varphi^2 + \Omega^2}}} = \frac{\Omega}{2(1/\tau_\varphi^2 + \Omega^2)^{3/4}} \left(1 + O\left(\frac{\Omega^2}{1/\tau_\varphi^2 + \Omega^2}\right)\right).$$

In $d = 2$ we approximated

$$\arcsin \frac{\Omega}{\sqrt{1/\tau_\varphi^2 + \Omega^2}} = \frac{\Omega}{\sqrt{1/\tau_\varphi^2 + \Omega^2}} \left(1 + O\left(\frac{\Omega^2}{1/\tau_\varphi^2 + \Omega^2}\right)\right).$$

Taking into account the higher orders gives only corrections of numerical factors but no parametrical different results in the estimate of the inelastic vertex contributions (notice e.g. that $\frac{1}{\cos \frac{1}{2} \arcsin \frac{\Omega}{\sqrt{1/\tau_\varphi^2 + \Omega^2}}} < \sqrt{2}$).

A.5 Some more details

In this appendix we want to show that assuming that the inelastic vertex, $\Gamma_{\text{in}}(\Omega)$ is a peaked function of width ΔE the correction to the WL due to inelastic processes is given by

$$\frac{\Delta\sigma_2}{\Delta\sigma_{\text{WL}}} \sim \max \left\{ \left(\frac{1}{\Delta E \tau_\varphi} \right)^{(4-d)/2}, \frac{1}{\Delta E \tau_\varphi} \right\} \quad (\text{A.20})$$

This may be seen as follows: We showed that the first order corrections from the vertex take the form

$$\Delta\sigma_2 = \int d\epsilon \int d\Omega \tilde{f}(\epsilon, \Omega) \Gamma(\epsilon, \Omega) I_d(\Omega). \quad (\text{A.21})$$

We write the vertex as a sum of its elastic and inelastic part, $\Gamma = \Gamma_{\text{el}} + \Gamma_{\text{in}}$ and approximate the elastic part by $\Gamma_{\text{el}}(\Omega) = \frac{\Omega}{\tau_\varphi} \delta(\Omega)$, such that

$$\Delta\sigma_{\text{el}} = \int d\epsilon \int d\Omega \tilde{f}(\epsilon, \Omega) \Gamma_{\text{el}}(\epsilon, \Omega) I_d(\Omega) = \int d\Omega \frac{1}{\tau_\varphi} I_d(\Omega) \delta(\Omega) \sim \tau_\varphi^{(2-d)/2} \sim \Delta\sigma_{\text{WL}} \quad (\text{A.22})$$

Assuming that Γ_{in} is a peaked function in Ω of width ΔE , we may approximate it by $\Gamma_{\text{in}}(\Omega) = \frac{\Omega}{\tau_\varphi} \frac{\Delta E}{\Omega^2 + \Delta E^2}$. Then we can use that for any integer $m > 0$

$$\int \frac{d\Omega}{2\pi} \frac{1}{(\Omega^2 + 1/\tau_\varphi^2)^m} \frac{\Delta E}{\Omega^2 + \Delta E^2} \sim \frac{1}{\Delta E} \left(\frac{1}{1/\tau_\varphi^2 + \Delta E^2} \right)^m + \frac{\tau_\varphi^{2m-1}}{\tau_\varphi^2 + \Delta E^2}, \quad (\text{A.23})$$

where we further assumed that $\Delta E \tau_\varphi \gg 1$ and kept only the leading order terms. As this holds for any integer $m > 0$, one finds (by analytical continuation)

$$\begin{aligned} \Delta\sigma_2 &= \frac{\Delta E}{\tau_\varphi} \int d\Omega \frac{1}{(1/\tau_\varphi^2 + \Omega^2)^{(4-d)/4}} \frac{1}{\Omega^2 + \Delta E^2} \\ &\sim \tau_\varphi^{(2-d)/2} \left(\frac{1}{(1 + (\Delta E \tau_\varphi)^2)^{(4-d)/4}} + \frac{\Delta E \tau_\varphi}{1 + (\Delta E \tau_\varphi)^2} \right) \\ &= \Delta\sigma_{\text{WL}} \max \left\{ \left(\frac{1}{\Delta E \tau_\varphi} \right)^{(4-d)/2}, \frac{1}{\Delta E \tau_\varphi} \right\}. \end{aligned} \quad (\text{A.24})$$

A.6 Renormalized perturbation theory for the Anderson model

At temperatures well below the Kondo temperature, i.e. $T \ll T_K$ analytic calculations can be performed within the framework of a Fermi liquid approach based on perturbation theory for the Anderson model [19]. In the single impurity Anderson model one describes the conduction band electrons coupled to the local magnetic moment centered at the origin by

$$H = H_{\text{ce}}(c^\dagger, c) + H_{\text{d}}(d^\dagger, d) + H_{\text{hyb.}}(c^\dagger, c, d^\dagger, d),$$

where H_{ce} describes the dynamics of the conduction band electrons (see Eq. (2.1)),

$$H_{\text{d}} = \sum_{\sigma} (\epsilon_{\text{d}} - \mu) d_{\sigma}^{\dagger} d_{\sigma} + U n_{\text{d}\uparrow} n_{\text{d}\downarrow}$$

is the Hubbard Hamiltonian for the local impurity and

$$H_{\text{hyb.}} = V \sum_{\mathbf{k}\sigma} (d_{\sigma}^{\dagger} c_{\sigma} + \text{h.c.})$$

is the hybridization of the local level with the conduction band. One recovers the physics of Kondo model in the limit of strong on-site repulsion U . The strongly interacting model can be treated within a renormalized perturbation theory [19], where the free d-electrons Greens function is given by

$$\mathcal{G}_d(\epsilon_n) = \langle d_n^{\dagger} d_n \rangle = \frac{1}{i\epsilon_n + iT_K \text{sgn}(n)},$$



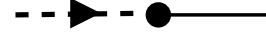
the interaction between d-electrons takes the form

$$V = T_K d_{n+m}^{\dagger} d_n d_{n'}^{\dagger} d_{n'+m}$$



and the hybridization is

$$H_{\text{hyb.}} = \left(\frac{T_K}{\nu} \right)^{\frac{1}{2}} \sum_{\mathbf{k}\sigma} (d_n^{\dagger} c_n + \text{h.c.}).$$

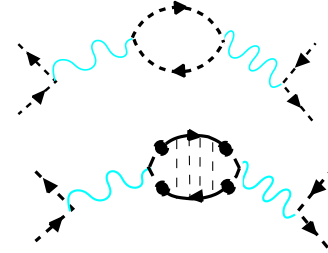


Notice that, as we are interested only in orders of magnitude we just give the relevant energy scales, neglecting factors of π or $2, \dots$. The diagrammatic representation for the d-electron Green's function, the hybridization and the d-electron interaction is given on the right hand side.

Effective Interactions:

$$V^R(\Omega) = \frac{n_S T_K^2}{T_K - i\Omega}$$

$$V_{\text{screen.}}^R(\Omega) = \frac{n_S^2}{\nu} \frac{D\mathbf{q}^2}{D\mathbf{q}^2 - i\Omega}$$



A.7 Fluctuations of the Kondo-temperature

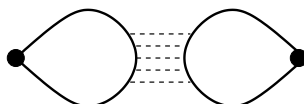
We use the following defining equation for the Kondo temperature,

$$\int_{T_K}^{E_F} d\omega \frac{\nu(\omega)}{\omega} = \frac{1}{J}, \quad (\text{A.25})$$

and find for its fluctuations

$$\left(\frac{\delta T_K}{T_K} \right)^2 = \frac{1}{\nu^2} \int_{T_K}^{E_F} d\omega \int_{T_K}^{E_F} d\omega' \frac{\langle \delta \nu(\omega) \delta \nu(\omega') \rangle}{\omega \omega'}. \quad (\text{A.26})$$

Here ν denotes the local DOS. In order to find the effect of disorder on the Kondo temperature, we therefore have to calculate the mesoscopic fluctuations of the local DOS. Their leading contribution is given by the following diagram,



$$\propto \int (dp) \mathcal{G}_p^R \mathcal{G}_p^A \int (dp') \mathcal{G}_{p'}^R \mathcal{G}_{p'}^A \int (dq) \Pi_q^{C/D}(\omega)$$

which gives

$$\langle \delta\nu(\epsilon + \omega) \delta\nu(\epsilon) \rangle = \nu \operatorname{Re} \int (dq) \frac{1}{D\mathbf{q}^2 - i\omega}. \quad (\text{A.27})$$

Evaluation of the integral in quasi-1d and $d = 2, 3$ gives

$$\operatorname{Re} \int (dq) \frac{1}{D\mathbf{q}^2 - i\omega} = \begin{cases} \frac{1}{L_{\perp}^2} \frac{\omega^{-1/2}}{D^{1/2}}, & \text{quasi-1d} \\ \frac{1}{D} \ln[\omega\tau] & d = 2 \\ \frac{1}{\sqrt{\tau}} \frac{1}{D^{3/2}} & d = 3. \end{cases} \quad (\text{A.28})$$

Finally, we obtain for the fluctuations of the Kondo temperature in quasi-1d and $d = 3$

$$\left(\frac{\delta T_K}{T_K} \right)^2 \sim \begin{cases} \frac{1}{k_F l} \frac{1}{(k_F^2 L_{\perp})^2} \sqrt{\frac{E_F}{T_K}} & \text{quasi-1d} \\ \frac{1}{(k_F l)^2} \frac{1}{(J\nu)^2} & d = 3. \end{cases} \quad (\text{A.29})$$

The case of $d = 2$ has to be treated with some more care and gives

$$\left(\frac{\delta T_K}{T_K} \right)^2 \sim \frac{1}{k_F l} \frac{1}{(J\nu)^3} \quad d = 2. \quad (\text{A.30})$$

These results were stated in Eq. (2.76).

A.8 Limits of applicability: Cross-over temperatures for the dephasing-rate

Restricting to low temperatures, $T \ll T_K$, we calculate contributions to the dephasing rate, resulting from different types of diagrams that were neglected in formula Eq. (2.52). These diagrams include mixed scattering processes from static and dynamic disorder and are depicted in Figs 1(a) and (b) below. In order to obtain analytically expressions we employ renormalized perturbation theory, valid for temperatures $T \ll T_K$, and summarized in Appendix A.6. As we are only interested in parametric dependencies of $1/\tau_{\varphi}$ we may calculate it from self-energy diagrams with $1/\tau_{\varphi}$ included self-consistently as the IR cut-off,

$$\frac{1}{\tau_{\varphi}} = \int_{\tau_{\varphi}^{-1}} d\Omega \frac{\Omega}{T \sinh^2 \left[\frac{\Omega}{2T} \right]} V(\Omega), \quad (\text{A.31})$$

i.e. we do not explicitly take into account the vertex contributions. Here V represents an effective interaction different for each diagram.

Dephasing-rate in Fermi liquid regime: In a first step we evaluate the dephasing-rate Eq. (2.81) obtained from neglecting mixed scattering from static and dynamic disorder in the low temperature regime $T \ll T_K$. The relevant diagram for the very low temperature regime is depicted in Fig. 1(a). Below we show that

$$V^{(a)}(\Omega) = \frac{n_S \Omega}{\nu T_K^2}, \quad (\text{A.32})$$

and therefore

$$\frac{1}{\tau_{\varphi}^a} = \frac{n_S}{\nu} \left(\frac{T}{T_K} \right)^2 \quad \text{in } d = 1, 2, 3. \quad (\text{A.33})$$

In a next step we compare result Eq. (A.33) with corrections arising from the interplay between interactions and scattering from static impurities. The role of correlations disorder/interactions may be explored in terms of the diagrams shown in Fig. 1(b) and (c). On face of it, these diagrams are smaller by factors of $1/(k_F l)$ than the leading contributions, Eq. (A.33). This suppression results from the fact that quantum interference maintained across the impurity limits the momentum exchange to values $< l^{-1}$ much smaller than k_F . However, in the very low T regime, that we are considering, the enhanced infrared singularity caused by the presence of additional Diffuson/Cooperon modes may over-compensate this phase space suppression factor.

Interplay between scattering from static and dynamical impurities – linear order in n_S : First we look at diagrams linear order in n_S as depicted in Fig. 1(b). Below we show that

$$V^{(b)}(\Omega) = \frac{n_S}{\nu^2 T_K^2} \frac{\Omega}{D^{d/2}} \begin{cases} \frac{\Omega^{-1/2}}{(k_F L_\perp)^2}, & \text{quasi-1d} \\ 1, & d = 2 \\ \tau^{-1/2}, & d = 3 \end{cases} \quad (\text{A.34})$$

and therefore

$$\frac{1}{\tau_\varphi^b} = \frac{n_S}{\nu^2 T_K^2} \frac{1}{D^{d/2}} \begin{cases} \frac{T^{3/2}}{(k_F L_\perp)^2} & \text{quasi-1d} \\ T^2, & d = 2 \\ T^2 \tau^{-1/2}, & d = 3. \end{cases} \quad (\text{A.35})$$

Interplay between scattering from static and dynamical impurities – Higher order in n_S : Finally we account for scattering processes from different magnetic impurities. At very low T the Kondo impurities become indistinguishable from a conventional disordered Fermi liquid with short-range momentum-conserving interactions. Therefore the dephasing-rate should be dominated by Altshuler-Aronov-Khmelnitsky [1] type processes, shown in Fig. 1(c). Although these type of processes give corrections which contribute only at order n_S^2 they become important at low temperatures, since they scale as $T^{2/3}$, T and $T^{3/2}$ in $d = 1, 2, 3$, respectively. More precisely, we find from the diagrams, that

$$V^{(c)}(\Omega) = \frac{n_S^2}{\nu^3 T_K^2} \frac{\Omega^{d/2-1}}{D^{d/2}} \begin{cases} \frac{1}{(k_F L_\perp)^2}, & \text{quasi-1d} \\ 1 & d=2,3, \end{cases} \quad (\text{A.36})$$

which results in

$$\frac{1}{\tau_\varphi^c} = \frac{n_S^2}{\nu^3 T_K^2} \frac{1}{D^{d/2}} \begin{cases} \frac{T \tau_\varphi^{1/2}}{(k_F L_\perp)^2} & \text{quasi-1d} \\ T^{d/2}, & d = 2, 3. \end{cases} \quad (\text{A.37})$$

Employing that $D = \frac{E_F \tau}{m}$ and $\nu_d = m^{d/2} E_F^{d/2-1}$ we find the cross-over temperatures given in Eq. (2.79).

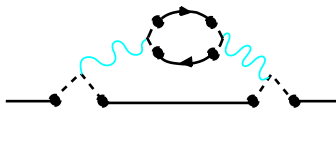


Fig. 1a

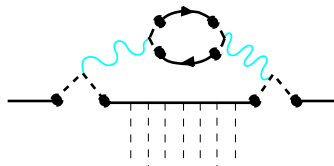


Fig. 1b

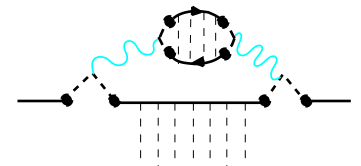
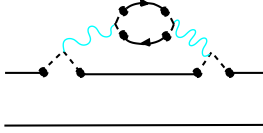
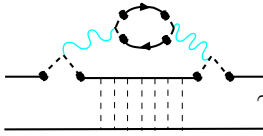
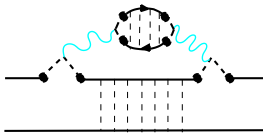


Fig. 1c

A.8.1 Evaluation of the diagrams

The explicit analytical expression for the diagrams depicted in Fig. 1(a), (b) and (c) are

-  $\sim \nu \tau^2 \frac{n_S}{T_K^2} \frac{T_K}{T_K \nu} \int d\Omega \left(\coth \left[\frac{\Omega}{2T} \right] - \tanh \left[\frac{\epsilon + \Omega}{2T} \right] \right) \left\{ \text{Im} \frac{T_K^2}{T_K - i\Omega} \right\}$
-  $\sim \nu \tau^2 \frac{n_S}{\nu^2 T_K^2} \int d\Omega \left(\coth \left[\frac{\Omega}{2T} \right] - \tanh \left[\frac{\epsilon + \Omega}{2T} \right] \right) \left\{ \text{Im} \frac{T_K^2}{T_K - i\Omega} \right\} \int (dq) \frac{1}{D\mathbf{q}^2 - i\Omega}$
-  $\sim \nu \tau^2 \frac{n_S^2}{\nu^2 T_K^2} \int d\Omega \left(\coth \left[\frac{\Omega}{2T} \right] - \tanh \left[\frac{\epsilon + \Omega}{2T} \right] \right) \int (dq) \left\{ \text{Im} \frac{1}{\nu} \frac{D\mathbf{q}^2}{D\mathbf{q}^2 - i\Omega} \right\} \frac{1}{D\mathbf{q}^2 - i\Omega}.$

Here we employed the propagators for the Fermi liquid regime derived in Appendix A.6. Employing the averaged over electron-energies according to $\langle \dots \rangle = \int d\epsilon [-f'_F](\dots)$, with f_F the Fermi-distribution function and using the identity,

$$\int d\epsilon \left(\frac{d}{d\epsilon} \tanh \left[\frac{\epsilon}{2T} \right] \right) \left(\coth \left[\frac{\Omega}{2T} \right] - \tanh \left[\frac{\epsilon + \Omega}{2T} \right] \right) = \frac{\Omega}{T \sinh^2 \left[\frac{\Omega}{2T} \right]},$$

we find Eq. (A.31) with Eqs. (A.32), (A.34) and (A.36).

A.9 Analytical continuation

We supply the analytical continuation of the inelastic vertex corrections to the conductivity, $\Delta\sigma_1$ and $\Delta\sigma_2$.

A.9.1 Self-energy corrections $\Delta\sigma_1$

We begin with the self-energy corrections, $\Delta\sigma_1$, depicted in Fig. 2.7. These are given by the sums

$$\Delta\sigma_1 = \frac{\text{const.}}{\omega} \left(\sum_{-m < n_1 < 0, n_2 > 0} + \sum_{n_1 < 0, 0 < n_2 < m} \right) \Pi_{n_1 n_2}^C \Pi_{n_1 n_2}^C \Gamma_{\text{inel}}(n_1, n_2, m = 0).$$

The Lehmann-representation (see Appendix A.10) reveals that Γ_{inel} has cuts along the following branches

- $\text{Im } \epsilon_1 = \epsilon_{n_1} = 0$
- $\text{Im } \epsilon_2 = \epsilon_{n_2} = 0$

- $\text{Im}(\epsilon_1 + \epsilon_2) = \epsilon_{n_1+n_2} = 0$
- $\text{Im}(\epsilon_1 - \epsilon_2) = \epsilon_{n_1-n_2} = 0$.

Since the frequencies $\epsilon_{n_1}, \epsilon_{n_2}$ are restricted to the ranges $n_1 < 0$ and $n_2 > 0$ one may identify two different analytic continuations of the vertex Γ_{inel} :

(A)	Γ_A	$\text{Im } \epsilon_1 < -\text{Im } \epsilon_2$	$\text{Im } \epsilon_1 < 0, \text{Im } \epsilon_2 > 0$
(B)	Γ_B	$\text{Im } \epsilon_1 > -\text{Im } \epsilon_2$	$\text{Im } \epsilon_1 < 0, \text{Im } \epsilon_2 > 0$

Table A.2: Analytical Continuations of Γ_{inel} leading to Γ_A and Γ_B .

We first perform the summation over frequencies ϵ_{n_1} by means of contour-integral, see e.g. [40]. We notice that the analytical continuation of the vertex as a function of ϵ_1 is independent of the other variable, ϵ_2 and therefore we may assume that $n_1 < -m$ ($n_2 > m$) [40]. The resulting function in ϵ_2 has branch cuts along the lines $\text{Im } \epsilon_2 = 0$ ($\text{Im } \epsilon_2 = -\omega_m$). Exchanging the summation over Matsubara-frequencies ϵ_{n_2} for an integral along a contour (as e.g. given in [40]) one gets

$$\begin{aligned} & \sum_{-m < n_1 < 0} \sum_{n_2 > 0} \Pi_{n_1 n_2}^C \Pi_{n_1 n_2}^C \Gamma_{\text{inel}}(n_1, n_2) \\ &= -\frac{1}{(4T\pi)^2} \int d\epsilon_1 d\epsilon_2 \Pi_{\epsilon_1 \epsilon_2}^C \Pi_{\epsilon_1 \epsilon_2}^C \left(\tanh \left[\frac{\epsilon_1 + \omega}{2T} \right] - \tanh \left[\frac{\epsilon_1}{2T} \right] \right) \tanh \left[\frac{\epsilon_2}{2T} \right] \Gamma_B(\epsilon_1, \epsilon_2) \end{aligned}$$

and

$$\begin{aligned} & \sum_{n_1 < 0} \sum_{0 < n_2 < m} \Pi_{n_1 n_2}^C \Pi_{n_1 n_2}^C \Gamma_{\text{inel}}(n_1, n_2) \\ &= \frac{1}{(4T\pi)^2} \int d\epsilon_1 d\epsilon_2 \Pi_{\epsilon_1 \epsilon_2}^C \Pi_{\epsilon_1 \epsilon_2}^C \left(\tanh \left[\frac{\epsilon_2}{2T} \right] - \tanh \left[\frac{\epsilon_2 - \omega}{2T} \right] \right) \tanh \left[\frac{\epsilon_1}{2T} \right] \Gamma_A(\epsilon_1, \epsilon_2) \end{aligned}$$

and therefore

$$\begin{aligned} & \lim_{\omega \rightarrow 0} \frac{1}{\omega} \left(\sum_{-m < n_1 < 0} \sum_{n_2 > 0} + \sum_{n_1 < 0} \sum_{0 < n_2 < m} \right) \Pi_{n_1 n_2}^C \Pi_{n_1 n_2}^C \Gamma_{\text{inel}}(n_1, n_2) \\ &= -\frac{1}{(4T\pi)^2} \int d\epsilon_1 d\epsilon_2 \left(\frac{d}{d\epsilon_1} \tanh \left[\frac{\epsilon_1}{2T} \right] \right) \tanh \left[\frac{\epsilon_2}{2T} \right] (\Pi_{\epsilon_1 \epsilon_2}^C \Pi_{\epsilon_1 \epsilon_2}^C \Gamma_B(\epsilon_1, \epsilon_2) - \Pi_{\epsilon_2 \epsilon_1}^C \Pi_{\epsilon_2 \epsilon_1}^C \Gamma_A(\epsilon_2, \epsilon_1)). \end{aligned}$$

Defining $\epsilon_2 \equiv \epsilon + \Omega$ and $\epsilon_1 \equiv \epsilon$ we notice that the function

$$f^+(\epsilon, \Omega) \equiv \Pi_{\epsilon_1 \epsilon_2}^C \Pi_{\epsilon_1 \epsilon_2}^C \Gamma_B(\epsilon_1, \epsilon_2)$$

is analytic in the upper half-plane $\text{Im } \Omega > 0$ and

$$f^-(\epsilon, \Omega) \equiv \Pi_{\epsilon_2 \epsilon_1}^C \Pi_{\epsilon_2 \epsilon_1}^C \Gamma_A(\epsilon_2, \epsilon_1)$$

is analytic in the lower half-plane $\text{Im } \Omega < 0$. Furthermore one can see from the Lehmann representation that $\Gamma_A(\epsilon_1, \epsilon_2) = [\Gamma_B(\epsilon_2, \epsilon_1)]^*$ and therefore

$$\begin{aligned} & \lim_{\omega \rightarrow 0} \frac{1}{\omega} \left(\sum_{-m < n_1 < 0} \sum_{n_2 > 0} + \sum_{n_1 < 0} \sum_{0 < n_2 < m} \right) \Pi_{n_1 n_2}^C \Pi_{n_1 n_2}^C \Gamma_{\text{inel}}(n_1, n_2) \\ &= \frac{i}{8T^2\pi^2} \text{Im} \int d\epsilon_1 d\epsilon_2 \Pi_{\epsilon_1 \epsilon_2}^C \Pi_{\epsilon_1 \epsilon_2}^C \left(\frac{d}{d\epsilon_1} \tanh \left[\frac{\epsilon_1}{2T} \right] \right) \tanh \left[\frac{\epsilon_2}{2T} \right] \Gamma_B(\epsilon_1, \epsilon_2), \end{aligned}$$

leading to Eq. (2.67).

A.9.2 Vertex corrections $\Delta\sigma_2$

Next we turn to the vertex contributions, $\Delta\sigma_2$, as depicted in Fig. ???. These are given by the sums

$$\Delta\sigma_2 = \frac{\text{const.}}{\omega} \sum_{-m < n_1} \sum_{n_2 < 0} \Pi_{n_1 n_2 + m}^C \Pi_{n_2 n_1 + m}^C \Gamma_{\text{inel}}(n_1, n_2, m).$$

Again we refer to the Lehmann-representation in Appendix A.10, in order to see that Γ has cuts along the branches

- $\text{Im } \epsilon_1 = \epsilon_{n_1} = 0$
- $\text{Im } \epsilon_2 = \epsilon_{n_2} = 0$
- $\text{Im}(\epsilon_1 + \omega) = \epsilon_{n_1 + m} = 0$
- $\text{Im}(\epsilon_2 + \omega) = \epsilon_{n_2 + m} = 0$
- $\text{Im}(\epsilon_1 + \epsilon_2 + \omega_m) = \epsilon_{n_1 + n_2 + m} = 0$
- $\text{Im}(\epsilon_1 - \epsilon_2) = \epsilon_{n_1 - n_2} = 0$.

Since the frequencies $\epsilon_{n_1}, \epsilon_{n_2}$ are restricted to the range $-\omega_m < \epsilon_{n_1}, \epsilon_{n_2} < 0$ one may identify four different analytic continuations of the vertex, see Table A.9.2.

(I)	Γ_I	$\text{Im } \epsilon_1 < -\text{Im}(\epsilon_2 + \omega)$	$\text{Im } \epsilon_2 > \text{Im } \epsilon_1$
(II)	Γ_{II}	$\text{Im } \epsilon_1 > -\text{Im}(\epsilon_2 + \omega)$	$\text{Im } \epsilon_2 > \text{Im } \epsilon_1$
(III)	Γ_{III}	$\text{Im } \epsilon_1 > -\text{Im}(\epsilon_2 + \omega)$	$\text{Im } \epsilon_2 < \text{Im } \epsilon_1$
(IV)	Γ_{IV}	$\text{Im } \epsilon_1 < -\text{Im}(\epsilon_2 + \omega)$	$\text{Im } \epsilon_2 < \text{Im } \epsilon_1$

Table A.3: Analytical Continuations of Γ_{inel} leading to $\Gamma_I, \Gamma_{II}, \Gamma_{III}$ and Γ_{IV} .

Proceeding as before (we may assume that $\epsilon_{n_1} > -\epsilon_{n_1 + m}$) and following [40] we first perform the summation over frequencies ϵ_{n_1} . We notice that the analytical continuation of the vertex as a function of ϵ_1 is independent of the other variable, ϵ_2 and therefore may assume that $\epsilon_{n_1} > -\epsilon_{n_1 + m}$ [40]. The resulting function in ϵ_2 has branch cuts along the lines $\text{Im } \epsilon_2 = 0$ and $\text{Im } \epsilon_2 = -\omega_m$. Exchanging the summation over Matsubara-frequencies ϵ_{n_2} for an contour-integral we finally get

$$\begin{aligned} & \lim_{\omega \rightarrow 0} \frac{1}{\omega} \sum_{-m < n_1, n_2 < 0} \Pi_{n_1 n_2 + m}^C \Pi_{n_2 n_1 + m}^C \Gamma_{\text{inel}}(\epsilon_{n_1}, \epsilon_{n_2}, \omega_m) |_{i\omega_m \rightarrow \omega + i0} \\ &= \frac{1}{(4T\pi)^2} \int d\epsilon_1 d\epsilon_2 \Pi_{\epsilon_1 - \epsilon_2}^C \Pi_{\epsilon_2 - \epsilon_1}^C \left(\frac{d}{d\epsilon_2} \tanh \left[\frac{\epsilon_2}{2T} \right] \right) \left[\right. \\ & \quad \left(\coth \left[\frac{\epsilon_1 + \epsilon_2}{2T} \right] - \tanh \left[\frac{\epsilon_1}{2T} \right] \right) (\Gamma_{III} - \Gamma_{IV})(\epsilon_1, \epsilon_2) \\ & \quad \left. + \left(\coth \left[\frac{\epsilon_1 - \epsilon_2}{2T} \right] - \tanh \left[\frac{\epsilon_1}{2T} \right] \right) (\Gamma_{II} - \Gamma_{III})(\epsilon_1, \epsilon_2) \right] \end{aligned}$$

Using the notation of Appendix A.10 we separate Γ into a 2-, 3- and 4-component,

$$\begin{aligned} & \lim_{\omega \rightarrow 0} \frac{1}{\omega} \sum_{-m < n_1, n_2 < 0} \Pi_{n_1 n_2 + m}^C \Pi_{n_2 n_1 + m}^C \Gamma_{\text{inel}}(\epsilon_{n_1}, \epsilon_{n_2}, \omega_m) |_{i\omega_m \rightarrow \omega + i0} \\ &= \pm \frac{1}{(4T\pi)^2} \int d\epsilon_1 d\epsilon_2 \Pi_{\epsilon_1 - \epsilon_2}^C \Pi_{\epsilon_2 - \epsilon_1}^C \left(\frac{d}{d\epsilon_2} \tanh \left[\frac{\epsilon_2}{2T} \right] \right) \left[\right. \\ & \quad \left(\coth \left[\frac{\epsilon_1 - \epsilon_2}{2T} \right] - \tanh \left[\frac{\epsilon_1}{2T} \right] \right) (\Gamma^2 + J\Gamma^3 + J^2\Gamma_1^4)(\epsilon_1, \epsilon_2) \\ & \quad \left. + \left(\coth \left[\frac{\epsilon_1 + \epsilon_2}{2T} \right] - \tanh \left[\frac{\epsilon_1}{2T} \right] \right) J^2\Gamma_2^4(\epsilon_1, -\epsilon_2) \right], \end{aligned}$$

leading to Eq. (2.68).

A.10 Lehmann representation

We give the Lehmann representation for the self-energy and the different two-, three- and four-vertices introduced in Tables VII and VIII of Appendix A.9. Although it turned out that we do not need their explicit expressions for the evaluation of $1/\tau_\varphi$, I give these for reasons of documentation. The reader is invited to skip this section.

In the following we use the short notation $\Theta_{12} \equiv \Theta(\tau_1 - \tau_2)$, $\Theta_{123} \equiv \Theta(\tau_1 - \tau_2)\Theta(\tau_2 - \tau_3)$, etc. $E_a \equiv E_a - \mu N_a$, $\Xi_{ab} \equiv E_a - E_b$, $(S)_{ab} \equiv \langle \Psi_a | S | \Psi_b \rangle$.

A.10.1 Self-energy

We start with the self energy-contribution,

$$\Sigma(n_1) \equiv \langle (Sc)_{n_1}^\alpha (c^\dagger S)_{n_1}^\alpha \rangle = \frac{1}{\beta} \int d\tau_1 d\tau_2 e^{i\epsilon_{n_1}(\tau_1 - \tau_2)} \langle T_\tau (Sc)^\alpha(\tau_1) (c^\dagger S)^\alpha(\tau_2) \rangle,$$

and insert an exact eigenbasis to find

$$\langle (Sc)^\alpha(\tau_1) (c^\dagger S)^\alpha(\tau_2) \rangle = \mathcal{Z}^{-1} \sum_{ab} (cS)_{ab}^\alpha (c^\dagger S)_{ba}^\alpha e^{\Xi_{ab}(\tau_1 - \tau_2)} \left(e^{-\beta E_a} \Theta_{12} - e^{-\beta E_b} \Theta_{21} \right).$$

Fourier transformation then leads to

$$\langle (Sc)_{n_1}^\alpha (c^\dagger S)_{n_1}^\alpha \rangle = \mathcal{Z}^{-1} \sum_{ab} (cS)_{ab}^\alpha (c^\dagger S)_{ba}^\alpha \frac{e^{-\beta E_a} + e^{-\beta E_b}}{\Xi_{ab} + i\epsilon_{n_1}}.$$

Performing the analytical continuations,

$$\begin{aligned} \Sigma^R(n) &= \mathcal{Z}^{-1} \sum_{ab} (cS)_{ab}^\alpha (c^\dagger S)_{ba}^\alpha \frac{e^{-\beta E_a} + e^{-\beta E_b}}{\Xi_{ab} + \epsilon + i0}, \quad \text{for } n > 0 \\ \Sigma^A(n) &= \mathcal{Z}^{-1} \sum_{ab} (cS)_{ab}^\alpha (c^\dagger S)_{ba}^\alpha \frac{e^{-\beta E_a} + e^{-\beta E_b}}{\Xi_{ab} + \epsilon - i0}, \quad \text{for } n < 0, \end{aligned}$$

one has

$$\text{Im } \Sigma^R(\epsilon) \equiv -\pi \mathcal{Z}^{-1} \sum_{ab} (cS)_{ab}^\alpha (c^\dagger S)_{ba}^\alpha \left(e^{-\beta E_a} + e^{-\beta E_b} \right) \delta(\Xi_{ab} + \epsilon)$$

A.10.2 Two-vertex

Turning to the two-vertex

$$\Gamma^2(n_1, n_2) \equiv \langle S_{n_2 - n_1}^\alpha S_{n_1 - n_2}^\alpha \rangle = \frac{1}{\beta} \int d\tau_1 d\tau_2 e^{i\epsilon_{n_2 - n_1}(\tau_1 - \tau_2)} \langle T_\tau S^\alpha(\tau_1) S^\alpha(\tau_2) \rangle,$$

we insert the exact eigenbasis and find

$$\Gamma^2(\tau_1, \tau_2) = \mathcal{Z}^{-1} \sum_{ab} S_{ab}^\alpha S_{ba}^\alpha e^{\Xi_{ab}(\tau_1 - \tau_2)} \left(e^{-\beta E_a} \Theta_{12} + e^{-\beta E_b} \Theta_{21} \right),$$

which after Fourier transformation leads to

$$\Gamma^2(n_1, n_2) = \mathcal{Z}^{-1} \sum_{ab} S_{ab} S_{ba} \frac{e^{-\beta E_a} - e^{-\beta E_b}}{\Xi_{ab} + i\epsilon_{n_2 - n_1}}$$

and the analytical continuations are given by

$$\begin{aligned} \Gamma_{II}^2 - \Gamma_{III}^2(\epsilon_1, \epsilon_2) &= iA(\epsilon_2 - \epsilon_1) \equiv \Gamma^2(\epsilon_1, \epsilon_2) \\ \Gamma_{III}^2 - \Gamma_{IV}^2(\epsilon_1, \epsilon_2) &= 0, \end{aligned}$$

where

$$A(\omega) \equiv \frac{\pi}{2} \mathcal{Z}^{-1} \sum_{ab} S_{ab}^\alpha S_{ba}^\alpha (e^{-\beta E_a} - e^{-\beta E_b}) \delta(\Xi_{ab} + \omega).$$

Furthermore we want to mention that looking at Table VI of Appendix A.9 one finds $\Gamma_B^2(\epsilon_2, \epsilon_1) = [\Gamma_A^2(\epsilon_1, \epsilon_2)]^*$.

A.10.3 Three-vertex

Since we are interested in the analytical continuations of Γ appearing in the vertex corrections to the conductivity, we may use the symmetrized form of the three-vertex

$$\Gamma^{(3)}(n_1, n_2, m) \equiv \langle S_{n_2 - n_1}^{\alpha\beta} [(Sc)_{n_1 + m}^\beta (c^\dagger S)_{n_2 + m}^\alpha + (Sc)_{n_1}^\beta (c^\dagger S)_{n_2}^\alpha] \rangle.$$

The expectation value is that of the (imaginary) time-ordered product,

$$\Gamma^3(n_1, n_2, m) \equiv \frac{1}{\beta^{3/2}} \int d\tau_1 d\tau_2 d\tau_3 e^{i\epsilon_{n_2 - n_1} \tau_1} \left[e^{i\epsilon_{n_1 + m} \tau_2 - i\epsilon_{n_2 + m} \tau_3} + e^{i\epsilon_{n_1} \tau_2 - i\epsilon_{n_2} \tau_3} \right] \langle T_\tau S(\tau_1) Sc(\tau_2) c^\dagger S(\tau_3) \rangle.$$

We start from

$$\Gamma^3(\tau_1, \tau_2, \tau_3) \equiv \langle T_\tau S^{\alpha\beta}(\tau_1) (Sc)^\beta(\tau_2) (c^\dagger S)^\alpha(\tau_3) \rangle$$

and group the six terms appearing in the time-ordered product in two families emerging from cyclic permutations

$$\Gamma^3(\tau_1, \tau_2, \tau_3) = \Gamma_{123}^3(\tau_1, \tau_2, \tau_3) - \Gamma_{132}^3(\tau_1, \tau_2, \tau_3).$$

Each family Γ_{ijk}^3 consists of three terms. Those coming from the ordering $1 > 2 > 3$ are given by

$$\begin{aligned} \Gamma_{123}^3(\tau_1, \tau_2, \tau_3) &= \mathcal{Z}^{-1} \sum_{abc} (S)_{ab}^{\alpha\beta} (Sc)_{bc}^\beta (c^\dagger S)_{ca}^\alpha \\ &\times \left[e^{-\beta E_a} e^{\Xi_{ab}(\tau_1 - \tau_2)} e^{\Xi_{ac}(\tau_2 - \tau_3)} \Theta_{123} + e^{-\beta E_b} e^{\Xi_{bc}(\tau_2 - \tau_3)} e^{\Xi_{ba}(\tau_3 - \tau_1)} \Theta_{231} - e^{-\beta E_c} e^{\Xi_{ca}(\tau_3 - \tau_1)} e^{\Xi_{cb}(\tau_1 - \tau_2)} \Theta_{312} \right]. \end{aligned}$$

The second family arises from the ordering $1 > 3 > 2$ and cyclic permutations. We get it from the above expression by simple substitution $\tau_2 \leftrightarrow \tau_3$. Changing also $a \leftrightarrow b$ we get

$$\begin{aligned} \Gamma_{132}^3(\tau_1, \tau_2, \tau_3) &= \mathcal{Z}^{-1} \sum_{abc} (S)_{ba}^{\alpha\beta} (Sc)_{cb}^\beta (Sc^\dagger)_{ac}^\alpha \\ &\times \left[e^{-\beta E_a} e^{\Xi_{ab}(\tau_2 - \tau_1)} e^{\Xi_{ac}(\tau_3 - \tau_2)} \Theta_{321} + e^{-\beta E_b} e^{\Xi_{bc}(\tau_3 - \tau_2)} e^{\Xi_{ba}(\tau_1 - \tau_3)} \Theta_{132} - e^{-\beta E_c} e^{\Xi_{ca}(\tau_1 - \tau_3)} e^{\Xi_{cb}(\tau_2 - \tau_1)} \Theta_{213} \right]. \end{aligned}$$

Next we Fourier-transform the above expressions and insert the frequencies according to Eq. (A.38) which leads us to (e.g. [40],[41])

$$\begin{aligned} \beta^{1/2}\Gamma^3(n_1, n_2, m) = & \mathcal{Z}^{-1} \sum_{abc} (S)_{ab}^{\alpha\beta} (Sc)_{bc}^{\beta} (c^\dagger S)_{ca}^{\alpha} \left[\frac{e^{-\beta E_a}}{\Xi_{ab} + i\epsilon_{n_2-n_1}} \left(\frac{1}{\Xi_{ac} + i\epsilon_{n_2}} + \frac{1}{\Xi_{ac} + i\epsilon_{n_2+m}} \right) \right. \\ & + \frac{e^{-\beta E_b}}{\Xi_{ba} + i\epsilon_{n_1-n_2}} \left(\frac{1}{\Xi_{bc} + i\epsilon_{n_1}} + \frac{1}{\Xi_{bc} + i\epsilon_{n_1+m}} \right) \\ & \left. - \frac{e^{-\beta E_c}}{(\Xi_{ca} - i\epsilon_{n_2})(\Xi_{cb} - i\epsilon_{n_1})} - \frac{e^{-\beta E_c}}{(\Xi_{ca} - i\epsilon_{n_2+m})(\Xi_{cb} - i\epsilon_{n_1+m})} \right] \\ & - \mathcal{Z}^{-1} \sum_{abc} (S)_{ba}^{\alpha\beta} (Sc)_{cb}^{\beta} (c^\dagger S)_{ac}^{\alpha} \left[\frac{e^{-\beta E_a}}{\Xi_{ab} - i\epsilon_{n_2-n_1}} \left(\frac{1}{\Xi_{ac} - i\epsilon_{n_2}} + \frac{1}{\Xi_{ac} - i\epsilon_{n_2+m}} \right) \right. \\ & + \frac{e^{-\beta E_b}}{\Xi_{ba} - i\epsilon_{n_1-n_2}} \left(\frac{1}{\Xi_{bc} - i\epsilon_{n_1}} + \frac{1}{\Xi_{bc} - i\epsilon_{n_1+m}} \right) \\ & \left. - \frac{e^{-\beta E_c}}{(\Xi_{ca} + i\epsilon_{n_2})(\Xi_{cb} + i\epsilon_{n_1})} - \frac{e^{-\beta E_c}}{(\Xi_{ca} + i\epsilon_{n_2+m})(\Xi_{cb} + i\epsilon_{n_1+m})} \right]. \end{aligned}$$

Finally, we read off the analytical continuations of the three-vertex

$$\begin{aligned} \Gamma_{\text{II}}^3 - \Gamma_{\text{III}}^3(\epsilon_1, \epsilon_2) &= -\frac{i4\pi}{\beta^{1/2}} \int d\omega \mathcal{P}\left(\frac{1}{\omega}\right) \left[B_1(\omega - \epsilon_2, \omega - \epsilon_1) - B_2(\omega + \epsilon_2, \omega + \epsilon_1) \right] \equiv \Gamma^3(\epsilon_1, \epsilon_2) \\ \Gamma_{\text{IV}}^3 - \Gamma_{\text{III}}^3(\epsilon_1, \epsilon_2) &= 0, \end{aligned}$$

where \mathcal{P} denotes the principal part and we used the spectral functions

$$\begin{aligned} B_1(\omega_1, \omega_2) &\equiv 2\pi \mathcal{Z}^{-1} \sum_{abc} (S)_{ab}^{\alpha\beta} (Sc)_{bc}^{\beta} (c^\dagger S)_{ca}^{\alpha} \left(e^{-\beta E_a} - e^{-\beta E_b} \right) \delta(\Xi_{ca} + \omega_1) \delta(\Xi_{cb} + \omega_2), \\ B_2(\omega_1, \omega_2) &\equiv 2\pi \mathcal{Z}^{-1} \sum_{abc} (S)_{ba}^{\alpha\beta} (Sc)_{cb}^{\beta} (c^\dagger S)_{ac}^{\alpha} \left(e^{-\beta E_a} - e^{-\beta E_b} \right) \delta(\Xi_{ca} + \omega_1) \delta(\Xi_{cb} + \omega_2). \end{aligned}$$

In order to find the analytical continuations of the three-vertex entering Eqs. (2.67), (2.68), we use the Lehmann representation ($m = 0$)

$$\begin{aligned} & \beta^{1/2}\Gamma^3(n_1, n_2) \\ &= \mathcal{Z}^{-1} \sum_{abc} (S)_{ab}^{\alpha\beta} (Sc)_{bc}^{\beta} (c^\dagger S)_{ca}^{\alpha} \left[\frac{e^{-\beta E_a}}{\Xi_{ab} + i\epsilon_{n_2-n_1}} \frac{1}{\Xi_{ac} + i\epsilon_{n_2}} + \frac{e^{-\beta E_b}}{\Xi_{ba} + i\epsilon_{n_1-n_2}} \frac{1}{\Xi_{bc} + i\epsilon_{n_1}} - \frac{e^{-\beta E_c}}{(\Xi_{ca} - i\epsilon_{n_2})(\Xi_{cb} - i\epsilon_{n_1})} \right] \\ & \quad - \mathcal{Z}^{-1} \sum_{abc} (S)_{ba}^{\alpha\beta} (Sc)_{cb}^{\beta} (c^\dagger S)_{ac}^{\alpha} \left[\frac{e^{-\beta E_a}}{\Xi_{ab} - i\epsilon_{n_2-n_1}} \frac{1}{\Xi_{ac} - i\epsilon_{n_2}} + \frac{e^{-\beta E_b}}{\Xi_{ba} - i\epsilon_{n_1-n_2}} \frac{1}{\Xi_{bc} - i\epsilon_{n_1}} - \frac{e^{-\beta E_c}}{(\Xi_{ca} + i\epsilon_{n_2})(\Xi_{cb} + i\epsilon_{n_1})} \right] + n_1 \leftrightarrow n_2. \end{aligned}$$

Using the definitions of Table VII in Appendix A.9, one again finds that $\Gamma_{\text{B}}^3(\epsilon_2, \epsilon_1) = [\Gamma_{\text{A}}^3(\epsilon_1, \epsilon_2)]^*$.

A.10.4 Four-vertex

The four-vertex corrections are given by the four-point function

$$\Gamma^4(n_1, n_2, m) \equiv \langle (Sc)_{n_1+m}^\alpha (c^\dagger S)_{n_2+m}^\beta (Sc)_{n_2}^\beta (c^\dagger S)_{n_1}^\alpha \rangle,$$

or in (imaginary-) time representation

$$\Gamma^4(n_1, n_2, m) \equiv \frac{1}{\beta^2} \int d\tau_1 d\tau_2 d\tau_3 d\tau_4 e^{i\epsilon_{n_1+m}\tau_1 + i\epsilon_{n_2}\tau_2 - i\epsilon_{n_2+m}\tau_3 - i\epsilon_{n_1}\tau_4} \langle T_\tau (Sc)^\alpha(\tau_1) (Sc)^\beta(\tau_2) (Sc^\dagger)^\beta(\tau_3) (Sc^\dagger)^\alpha(\tau_4) \rangle.$$

Again, we start from the time-ordered product

$$\Gamma^4(\tau_1 \tau_2 \tau_3 \tau_4) \equiv \langle T_\tau (Sc)^\alpha(\tau_1) (Sc)^\beta(\tau_2) (Sc^\dagger)^\beta(\tau_3) (Sc^\dagger)^\alpha(\tau_4) \rangle$$

Following the same strategy as before we group the 24 terms of the time-ordered product in six families arising from cyclic permutations, i.e.

$$\Gamma^4 = \Gamma_{1234}^4 - \Gamma_{1243}^4 - \Gamma_{1324}^4 + \Gamma_{1342}^4 + \Gamma_{1423}^4 - \Gamma_{1432}^4.$$

The family emerging from the order $1 > 2 > 3 > 4$ has the Lehmann representation

$$\begin{aligned} \Gamma_{1234}^4(\tau_1 \tau_2 \tau_3 \tau_4) &= \mathcal{Z}^{-1} \sum_{abcd} (Sc)_{ab}^\alpha (Sc)_{bc}^\beta (Sc^\dagger)_{cd}^\beta (Sc^\dagger)_{da}^\alpha \left[\right. \\ &e^{-\beta E_a} e^{\Xi_{ab}(\tau_1 - \tau_2) + \Xi_{ac}(\tau_2 - \tau_3) + \Xi_{ad}(\tau_3 - \tau_4)} \Theta_{1234} - e^{-\beta E_b} e^{\Xi_{bc}(\tau_2 - \tau_3) + \Xi_{bd}(\tau_3 - \tau_4) + \Xi_{ba}(\tau_4 - \tau_1)} \Theta_{2341} \\ &\left. + e^{-\beta E_c} e^{\Xi_{cd}(\tau_3 - \tau_4) + \Xi_{ca}(\tau_4 - \tau_1) + \Xi_{cb}(\tau_1 - \tau_2)} \Theta_{3412} - e^{-\beta E_d} e^{\Xi_{da}(\tau_4 - \tau_1) + \Xi_{db}(\tau_1 - \tau_2) + \Xi_{dc}(\tau_2 - \tau_3)} \Theta_{4123} \right] \end{aligned}$$

The contributions corresponding to cycles from the remaining orders are

$$\begin{aligned} \Gamma_{1243}^4(\tau_1 \tau_2 \tau_3 \tau_4) &= \mathcal{Z}^{-1} \sum_{abcd} (Sc)_{ab}^\alpha (Sc)_{bc}^\beta (Sc^\dagger)_{cd}^\alpha (Sc^\dagger)_{da}^\beta \left[\right. \\ &e^{-\beta E_a} e^{\Xi_{ab}(\tau_1 - \tau_2) + \Xi_{ac}(\tau_2 - \tau_4) + \Xi_{ad}(\tau_4 - \tau_3)} \Theta_{1243} - e^{-\beta E_b} e^{\Xi_{bc}(\tau_2 - \tau_4) + \Xi_{bd}(\tau_4 - \tau_3) + \Xi_{ba}(\tau_3 - \tau_1)} \Theta_{2431} \\ &\left. + e^{-\beta E_c} e^{\Xi_{cd}(\tau_4 - \tau_3) + \Xi_{ca}(\tau_3 - \tau_1) + \Xi_{cb}(\tau_1 - \tau_2)} \Theta_{4312} - e^{-\beta E_d} e^{\Xi_{da}(\tau_3 - \tau_1) + \Xi_{db}(\tau_1 - \tau_2) + \Xi_{dc}(\tau_2 - \tau_4)} \Theta_{3124} \right] \end{aligned}$$

$$\begin{aligned} \Gamma_{1324}^4(\tau_1 \tau_2 \tau_3 \tau_4) &= \mathcal{Z}^{-1} \sum_{abcd} (Sc)_{ab}^\alpha (Sc^\dagger)_{bc}^\beta (Sc)_{cd}^\beta (Sc^\dagger)_{da}^\alpha \left[\right. \\ &e^{-\beta E_a} e^{\Xi_{ab}(\tau_1 - \tau_3) + \Xi_{ac}(\tau_3 - \tau_2) + \Xi_{ad}(\tau_2 - \tau_4)} \Theta_{1324} - e^{-\beta E_b} e^{\Xi_{bc}(\tau_3 - \tau_2) + \Xi_{bd}(\tau_2 - \tau_4) + \Xi_{ba}(\tau_4 - \tau_1)} \Theta_{3241} \\ &\left. + e^{-\beta E_c} e^{\Xi_{cd}(\tau_2 - \tau_4) + \Xi_{ca}(\tau_4 - \tau_1) + \Xi_{cb}(\tau_1 - \tau_3)} \Theta_{2413} - e^{-\beta E_d} e^{\Xi_{da}(\tau_4 - \tau_1) + \Xi_{db}(\tau_1 - \tau_3) + \Xi_{dc}(\tau_3 - \tau_2)} \Theta_{4132} \right] \end{aligned}$$

$$\begin{aligned} \Gamma_{1342}^4(\tau_1 \tau_2 \tau_3 \tau_4) &= \mathcal{Z}^{-1} \sum_{abcd} (Sc)_{ab}^\alpha (Sc^\dagger)_{bc}^\beta (Sc^\dagger)_{cd}^\alpha (Sc)_{da}^\beta \left[\right. \\ &e^{-\beta E_a} e^{\Xi_{ab}(\tau_1 - \tau_3) + \Xi_{ac}(\tau_3 - \tau_4) + \Xi_{ad}(\tau_4 - \tau_2)} \Theta_{1342} - e^{-\beta E_b} e^{\Xi_{bc}(\tau_3 - \tau_4) + \Xi_{bd}(\tau_4 - \tau_2) + \Xi_{ba}(\tau_2 - \tau_1)} \Theta_{3421} \\ &\left. + e^{-\beta E_c} e^{\Xi_{cd}(\tau_4 - \tau_2) + \Xi_{ca}(\tau_2 - \tau_1) + \Xi_{cb}(\tau_1 - \tau_3)} \Theta_{4213} - e^{-\beta E_d} e^{\Xi_{da}(\tau_2 - \tau_1) + \Xi_{db}(\tau_1 - \tau_3) + \Xi_{dc}(\tau_3 - \tau_4)} \Theta_{2134} \right] \end{aligned}$$

$$\begin{aligned}
\Gamma_{1423}^4(\tau_1\tau_2\tau_3\tau_4) &= \mathcal{Z}^{-1} \sum_{abcd} (Sc)_{ab}^\alpha (Sc^\dagger)_{bc}^\alpha (Sc)_{cd}^\beta (Sc^\dagger)_{da}^\beta \left[\right. \\
&e^{-\beta E_a} e^{\Xi_{ab}(\tau_1-\tau_4)+\Xi_{ac}(\tau_4-\tau_2)+\Xi_{ad}(\tau_2-\tau_3)} \Theta_{1423} - e^{-\beta E_b} e^{\Xi_{bc}(\tau_4-\tau_2)+\Xi_{bd}(\tau_2-\tau_3)+\Xi_{ba}(\tau_3-\tau_1)} \Theta_{4231} \\
&\left. + e^{-\beta E_c} e^{\Xi_{cd}(\tau_2-\tau_3)+\Xi_{ca}(\tau_3-\tau_1)+\Xi_{cb}(\tau_1-\tau_4)} \Theta_{2314} - e^{-\beta E_d} e^{\Xi_{da}(\tau_3-\tau_1)+\Xi_{db}(\tau_1-\tau_4)+\Xi_{dc}(\tau_4-\tau_2)} \Theta_{3142} \right]
\end{aligned}$$

$$\begin{aligned}
\Gamma_{1432}^4(\tau_1\tau_2\tau_3\tau_4) &= \mathcal{Z}^{-1} \sum_{abcd} (Sc)_{ab}^\alpha (Sc^\dagger)_{bc}^\alpha (Sc^\dagger)_{cd}^\beta (Sc)_{da}^\beta \left[\right. \\
&e^{-\beta E_a} e^{\Xi_{ab}(\tau_1-\tau_4)+\Xi_{ac}(\tau_4-\tau_3)+\Xi_{ad}(\tau_3-\tau_2)} \Theta_{1432} - e^{-\beta E_b} e^{\Xi_{bc}(\tau_4-\tau_3)+\Xi_{bd}(\tau_3-\tau_2)+\Xi_{ba}(\tau_2-\tau_1)} \Theta_{4321} \\
&\left. + e^{-\beta E_c} e^{\Xi_{cd}(\tau_3-\tau_2)+\Xi_{ca}(\tau_2-\tau_1)+\Xi_{cb}(\tau_1-\tau_4)} \Theta_{3214} - e^{-\beta E_d} e^{\Xi_{da}(\tau_2-\tau_1)+\Xi_{db}(\tau_1-\tau_4)+\Xi_{dc}(\tau_4-\tau_3)} \Theta_{2143} \right].
\end{aligned}$$

Analogue to the three-vertex we bring it into a “nicer” form by exchanging $a \leftrightarrow b$ and $c \leftrightarrow d$ in the fourth, fifth and sixth term and grouping the first with the sixth, the second with the fourth and the third with the fifth term

$$\begin{aligned}
\Gamma_{1234}^4 - \Gamma_{1432}^4 &= \mathcal{Z}^{-1} \sum_{abcd} \left\{ (Sc)_{ab}^\alpha (Sc)_{bc}^\beta (Sc^\dagger)_{cd}^\beta (Sc^\dagger)_{da}^\alpha \left[\right. \right. \\
&e^{-\beta E_a} e^{\Xi_{ab}(\tau_1-\tau_2)+\Xi_{ac}(\tau_2-\tau_3)+\Xi_{ad}(\tau_3-\tau_4)} \Theta_{1234} - e^{-\beta E_b} e^{\Xi_{bc}(\tau_2-\tau_3)+\Xi_{bd}(\tau_3-\tau_4)+\Xi_{ba}(\tau_4-\tau_1)} \Theta_{2341} \\
&+ e^{-\beta E_c} e^{\Xi_{cd}(\tau_3-\tau_4)+\Xi_{ca}(\tau_4-\tau_1)+\Xi_{cb}(\tau_1-\tau_2)} \Theta_{3412} - e^{-\beta E_d} e^{\Xi_{da}(\tau_4-\tau_1)+\Xi_{db}(\tau_1-\tau_2)+\Xi_{dc}(\tau_2-\tau_3)} \Theta_{4123} \left. \right] \\
&- (Sc)_{ba}^\alpha (Sc^\dagger)_{ad}^\alpha (Sc^\dagger)_{dc}^\beta (Sc)_{cb}^\beta \left[\right. \\
&e^{-\beta E_a} e^{\Xi_{ba}(\tau_1-\tau_2)+\Xi_{ca}(\tau_2-\tau_3)+\Xi_{da}(\tau_3-\tau_4)} \Theta_{4321} - e^{-\beta E_b} e^{\Xi_{cb}(\tau_2-\tau_3)+\Xi_{db}(\tau_3-\tau_4)+\Xi_{ab}(\tau_4-\tau_1)} \Theta_{1432} \\
&\left. + e^{-\beta E_c} e^{\Xi_{dc}(\tau_3-\tau_4)+\Xi_{ac}(\tau_4-\tau_1)+\Xi_{bc}(\tau_1-\tau_2)} \Theta_{2143} - e^{-\beta E_d} e^{\Xi_{ad}(\tau_4-\tau_1)+\Xi_{bd}(\tau_1-\tau_2)+\Xi_{cd}(\tau_2-\tau_3)} \Theta_{3214} \right] \left. \right\}
\end{aligned}$$

$$\begin{aligned}
\Gamma_{1243}^4 - \Gamma_{1342}^4 &= \mathcal{Z}^{-1} \sum_{abcd} \left\{ (Sc)_{ab}^\alpha (Sc)_{bc}^\beta (Sc^\dagger)_{cd}^\alpha (Sc^\dagger)_{da}^\beta \left[\right. \right. \\
&e^{-\beta E_a} e^{\Xi_{ab}(\tau_1-\tau_2)+\Xi_{ac}(\tau_2-\tau_4)+\Xi_{ad}(\tau_4-\tau_3)} \Theta_{1243} - e^{-\beta E_b} e^{\Xi_{bc}(\tau_2-\tau_4)+\Xi_{bd}(\tau_4-\tau_3)+\Xi_{ba}(\tau_3-\tau_1)} \Theta_{2431} \\
&+ e^{-\beta E_c} e^{\Xi_{cd}(\tau_4-\tau_3)+\Xi_{ca}(\tau_3-\tau_1)+\Xi_{cb}(\tau_1-\tau_2)} \Theta_{4312} - e^{-\beta E_d} e^{\Xi_{da}(\tau_3-\tau_1)+\Xi_{db}(\tau_1-\tau_2)+\Xi_{dc}(\tau_2-\tau_4)} \Theta_{3124} \left. \right] \\
&- (Sc)_{ba}^\alpha (Sc^\dagger)_{ad}^\beta (Sc^\dagger)_{dc}^\alpha (Sc)_{cb}^\beta \left[\right. \\
&e^{-\beta E_a} e^{\Xi_{ba}(\tau_1-\tau_2)+\Xi_{ca}(\tau_2-\tau_4)+\Xi_{da}(\tau_4-\tau_3)} \Theta_{3421} - e^{-\beta E_b} e^{\Xi_{cb}(\tau_2-\tau_4)+\Xi_{db}(\tau_4-\tau_3)+\Xi_{ab}(\tau_3-\tau_1)} \Theta_{1342} \\
&\left. + e^{-\beta E_c} e^{\Xi_{dc}(\tau_4-\tau_3)+\Xi_{ac}(\tau_3-\tau_1)+\Xi_{bc}(\tau_1-\tau_2)} \Theta_{2134} - e^{-\beta E_d} e^{\Xi_{ad}(\tau_3-\tau_1)+\Xi_{bd}(\tau_1-\tau_2)+\Xi_{cd}(\tau_2-\tau_4)} \Theta_{4213} \right] \left. \right\}
\end{aligned}$$

$$\begin{aligned}
& \Gamma_{1324}^4 - \Gamma_{1423}^4 \\
&= \mathcal{Z}^{-1} \sum_{abcd} \left\{ (Sc)_{ab}^\alpha (Sc^\dagger)_{bc}^\beta (Sc)_{cd}^\beta (Sc^\dagger)_{da}^\alpha \left[\right. \right. \\
& \quad e^{-\beta E_a} e^{\Xi_{ab}(\tau_1 - \tau_3) + \Xi_{ac}(\tau_3 - \tau_2) + \Xi_{ad}(\tau_2 - \tau_4)} \Theta_{1324} - e^{-\beta E_b} e^{\Xi_{bc}(\tau_3 - \tau_2) + \Xi_{bd}(\tau_2 - \tau_4) + \Xi_{ba}(\tau_4 - \tau_1)} \Theta_{3241} \\
& \quad + e^{-\beta E_c} e^{\Xi_{cd}(\tau_2 - \tau_4) + \Xi_{ca}(\tau_4 - \tau_1) + \Xi_{cb}(\tau_1 - \tau_3)} \Theta_{2413} - e^{-\beta E_d} e^{\Xi_{da}(\tau_4 - \tau_1) + \Xi_{db}(\tau_1 - \tau_3) + \Xi_{dc}(\tau_3 - \tau_2)} \Theta_{4132} \left. \right] \\
& \quad - (Sc)_{ba}^\alpha (Sc^\dagger)_{ad}^\alpha (Sc)_{dc}^\beta (Sc^\dagger)_{cb}^\beta \left[\right. \\
& \quad e^{-\beta E_a} e^{\Xi_{ba}(\tau_1 - \tau_3) + \Xi_{ca}(\tau_3 - \tau_2) + \Xi_{da}(\tau_2 - \tau_4)} \Theta_{4231} - e^{-\beta E_b} e^{\Xi_{cb}(\tau_3 - \tau_2) + \Xi_{db}(\tau_2 - \tau_4) + \Xi_{ab}(\tau_4 - \tau_1)} \Theta_{1423} \\
& \quad + e^{-\beta E_c} e^{\Xi_{dc}(\tau_2 - \tau_4) + \Xi_{ac}(\tau_4 - \tau_1) + \Xi_{bc}(\tau_1 - \tau_3)} \Theta_{3142} - e^{-\beta E_d} e^{\Xi_{ad}(\tau_4 - \tau_1) + \Xi_{bd}(\tau_1 - \tau_3) + \Xi_{cd}(\tau_3 - \tau_2)} \Theta_{2314} \left. \right] \left. \right\}.
\end{aligned}$$

Fourier-transformation then leads to (see also [40])

$$\begin{aligned}
& \Gamma_{1234}^4 - \Gamma_{1432}^4 \\
&= \beta^{-1} \mathcal{Z}^{-1} \sum_{abcd} \left\{ (Sc)_{ab}^\alpha (Sc)_{bc}^\beta (Sc^\dagger)_{cd}^\beta (Sc^\dagger)_{da}^\alpha \left[\right. \right. \\
& \quad \frac{e^{-\beta E_a}}{(\Xi_{ab} + i\epsilon_{n_1+m})(\Xi_{ac} + i\epsilon_{n_1+n_2+m})(\Xi_{ad} + i\epsilon_{n_1})} - \frac{e^{-\beta E_b}}{(\Xi_{bc} + i\epsilon_{n_2})(\Xi_{bd} - i\omega_m)(\Xi_{ba} - i\epsilon_{n_1+m})} \\
& \quad + \frac{e^{-\beta E_c}}{(\Xi_{cd} - i\epsilon_{n_2+m})(\Xi_{ca} - i\epsilon_{n_1+n_2+m})(\Xi_{cb} - i\epsilon_{n_2})} - \frac{e^{-\beta E_d}}{(\Xi_{da} - i\epsilon_{n_1})(\Xi_{db} + i\omega_m)(\Xi_{dc} + i\epsilon_{n_2+m})} \left. \right] \\
& \quad + (Sc)_{ba}^\alpha (Sc^\dagger)_{ad}^\alpha (Sc^\dagger)_{dc}^\beta (Sc)_{cb}^\beta \left[\right. \\
& \quad \frac{e^{-\beta E_a}}{(\Xi_{ab} - i\epsilon_{n_1+m})(\Xi_{ac} - i\epsilon_{n_1+n_2+m})(\Xi_{ad} - i\epsilon_{n_1})} - \frac{e^{-\beta E_b}}{(\Xi_{bc} - i\epsilon_{n_2})(\Xi_{bd} + i\omega_m)(\Xi_{ba} + i\epsilon_{n_1+m})} \\
& \quad + \frac{e^{-\beta E_c}}{(\Xi_{cd} + i\epsilon_{n_2+m})(\Xi_{ca} + i\epsilon_{n_1+n_2+m})(\Xi_{cb} + i\epsilon_{n_2})} - \frac{e^{-\beta E_d}}{(\Xi_{da} + i\epsilon_{n_1})(\Xi_{db} - i\omega_m)(\Xi_{dc} - i\epsilon_{n_2+m})} \left. \right] \left. \right\}
\end{aligned}$$

$$\begin{aligned}
& \Gamma_{1243}^4 - \Gamma_{1342}^4 \\
&= \beta^{-1} \mathcal{Z}^{-1} \sum_{abcd} \left\{ (Sc)_{ab}^\alpha (Sc)_{bc}^\beta (Sc^\dagger)_{cd}^\alpha (Sc^\dagger)_{da}^\beta \left[\right. \right. \\
& \quad \frac{e^{-\beta E_a}}{(\Xi_{ab} + i\epsilon_{n_1+m})(\Xi_{ac} + i\epsilon_{n_1+n_2+m})(\Xi_{ad} + i\epsilon_{n_2+m})} - \frac{e^{-\beta E_b}}{(\Xi_{bc} + i\epsilon_{n_2})(\Xi_{bd} - i\epsilon_{n_1-n_2})(\Xi_{ba} - i\epsilon_{n_1+m})} \\
& \quad + \frac{e^{-\beta E_c}}{(\Xi_{cd} - i\epsilon_{n_1})(\Xi_{ca} - i\epsilon_{n_1+n_2+m})(\Xi_{cb} - i\epsilon_{n_2})} - \frac{e^{-\beta E_d}}{(\Xi_{da} - i\epsilon_{n_2+m})(\Xi_{db} + i\epsilon_{n_1-n_2})(\Xi_{dc} + i\epsilon_{n_1})} \left. \right] \\
& \quad + (Sc)_{ba}^\alpha (Sc^\dagger)_{ad}^\beta (Sc^\dagger)_{dc}^\alpha (Sc)_{cb}^\beta \left[\right. \\
& \quad \frac{e^{-\beta E_a}}{(\Xi_{ab} - i\epsilon_{n_1+m})(\Xi_{ac} - i\epsilon_{n_1+n_2+m})(\Xi_{ad} - i\epsilon_{n_2+m})} - \frac{e^{-\beta E_b}}{(\Xi_{bc} - i\epsilon_{n_2})(\Xi_{bd} + i\epsilon_{n_1-n_2})(\Xi_{ba} + i\epsilon_{n_1+m})} \\
& \quad + \frac{e^{-\beta E_c}}{(\Xi_{cd} + i\epsilon_{n_1})(\Xi_{ca} + i\epsilon_{n_1+n_2+m})(\Xi_{cb} + i\epsilon_{n_2})} - \frac{e^{-\beta E_d}}{(\Xi_{da} + i\epsilon_{n_2+m})(\Xi_{db} - i\epsilon_{n_1-n_2})(\Xi_{dc} - i\epsilon_{n_1})} \left. \right] \left. \right\}
\end{aligned}$$

$$\begin{aligned}
& \Gamma_{1324}^4 - \Gamma_{1423}^4 \\
&= \beta^{-1} \mathcal{Z}^{-1} \sum_{abcd} \left\{ (Sc)_{ab}^\alpha (Sc^\dagger)_{bc}^\beta (Sc)_{cd}^\beta (Sc^\dagger)_{da}^\alpha \left[\frac{e^{-\beta E_a}}{(\Xi_{ab} + i\epsilon_{n_1+m})(\Xi_{ac} + i\epsilon_{n_1-n_2})(\Xi_{ad} + i\epsilon_{n_1})} - \frac{e^{-\beta E_b}}{(\Xi_{bc} - i\epsilon_{n_2+m})(\Xi_{bd} - i\omega_m)(\Xi_{ba} - i\epsilon_{n_1+m})} \right. \right. \\
&+ \left. \frac{e^{-\beta E_c}}{(\Xi_{cd} + i\epsilon_{n_2})(\Xi_{ca} - i\epsilon_{n_1-n_2})(\Xi_{cb} + i\epsilon_{n_2+m})} - \frac{e^{-\beta E_d}}{(\Xi_{da} - i\epsilon_{n_1})(\Xi_{db} + i\omega_m)(\Xi_{dc} - i\epsilon_{n_2})} \right] \\
&+ (Sc)_{ba}^\alpha (Sc^\dagger)_{ad}^\alpha (Sc)_{dc}^\beta (Sc^\dagger)_{cb}^\beta \left[\frac{e^{-\beta E_a}}{(\Xi_{ab} - i\epsilon_{n_1+m})(\Xi_{ac} - i\epsilon_{n_1-n_2})(\Xi_{ad} - i\epsilon_{n_1})} - \frac{e^{-\beta E_b}}{(\Xi_{bc} + i\epsilon_{n_2+m})(\Xi_{bd} + i\omega_m)(\Xi_{ba} + i\epsilon_{n_1+m})} \right. \\
&+ \left. \left. \frac{e^{-\beta E_c}}{(\Xi_{cd} - i\epsilon_{n_2})(\Xi_{ca} + i\epsilon_{n_1-n_2})(\Xi_{cb} - i\epsilon_{n_2+m})} - \frac{e^{-\beta E_d}}{(\Xi_{da} + i\epsilon_{n_1})(\Xi_{db} - i\omega_m)(\Xi_{dc} + i\epsilon_{n_2})} \right] \right\}.
\end{aligned}$$

The analytical continuation leads to the following functions

$$\begin{aligned}
\Gamma_1^4(\epsilon_1, \epsilon_2) \equiv \Gamma_{II}^4 - \Gamma_{III}^4(\epsilon_1, \epsilon_2) = & i\beta^{-1} \int d\omega_1 d\omega_2 \frac{1}{\omega_1 + \epsilon_1 + i0} \left(\frac{C_1(\omega_1, \epsilon_2 - \epsilon_1, \omega_2)}{\omega_2 + \epsilon_1 - i0} - \frac{D_1(\omega_1, \epsilon_2 - \epsilon_1, \omega_2)}{\omega_2 - \epsilon_2 + i0} \right) \\
& - i\beta^{-1} \int d\omega_1 d\omega_2 \frac{1}{\omega_1 - \epsilon_1 - i0} \left(\frac{C_2(\omega_1, -\epsilon_2 + \epsilon_1, \omega_2)}{\omega_2 - \epsilon_1 + i0} - \frac{D_2(\omega_1, -\epsilon_2 + \epsilon_1, \omega_2)}{\omega_2 + \epsilon_2 - i0} \right),
\end{aligned}$$

where we introduced the following spectral densities

$$\begin{aligned}
C_1(\omega_1, \omega_2, \omega_3) &\equiv 2\pi \mathcal{Z}^{-1} \sum_{abcd} (Sc)_{ab}^\alpha (Sc)_{cd}^\beta (Sc^\dagger)_{bc}^\beta (Sc^\dagger)_{da}^\alpha (e^{-\beta E_a} - e^{-\beta E_c}) \delta(\Xi_{ba} + \omega_1) \delta(\Xi_{ca} + \omega_2) \delta(\Xi_{da} + \omega_3) \\
C_2(\omega_1, \omega_2, \omega_3) &\equiv 2\pi \mathcal{Z}^{-1} \sum_{abcd} (Sc)_{ba}^\alpha (Sc)_{dc}^\beta (Sc^\dagger)_{cb}^\beta (Sc^\dagger)_{ad}^\alpha (e^{-\beta E_a} - e^{-\beta E_c}) \delta(\Xi_{ba} + \omega_1) \delta(\Xi_{ca} + \omega_2) \delta(\Xi_{da} + \omega_3) \\
D_1(\omega_1, \omega_2, \omega_3) &\equiv 2\pi \mathcal{Z}^{-1} \sum_{abcd} (Sc)_{ab}^\alpha (Sc)_{da}^\beta (Sc^\dagger)_{bc}^\beta (Sc^\dagger)_{cd}^\alpha (e^{-\beta E_a} - e^{-\beta E_c}) \delta(\Xi_{ba} + \omega_1) \delta(\Xi_{ca} + \omega_2) \delta(\Xi_{da} + \omega_3) \\
D_2(\omega_1, \omega_2, \omega_3) &\equiv 2\pi \mathcal{Z}^{-1} \sum_{abcd} (Sc)_{ba}^\alpha (Sc)_{ad}^\beta (Sc^\dagger)_{cb}^\beta (Sc^\dagger)_{dc}^\alpha (e^{-\beta E_a} - e^{-\beta E_c}) \delta(\Xi_{ba} + \omega_1) \delta(\Xi_{ca} + \omega_2) \delta(\Xi_{da} + \omega_3)
\end{aligned}$$

and

$$\begin{aligned}
\Gamma_2^4(\epsilon_1, \epsilon_2) \equiv \Gamma_{III}^4 - \Gamma_{IV}^4(\epsilon_1, \epsilon_2) = & -i\beta^{-1} \int d\omega_1 d\omega_2 \frac{1}{\omega_1 + \epsilon_1 + i0} \left(\frac{C_3(\omega_1, -\epsilon_2 - \epsilon_1, \omega_2)}{\omega_2 + \epsilon_1 - i0} - \frac{D_3(\omega_1, -\epsilon_2 - \epsilon_1, \omega_2)}{\omega_2 + \epsilon_2 + i0} \right) \\
& + i\beta^{-1} \int d\omega_1 d\omega_2 \frac{1}{\omega_1 - \epsilon_1 - i0} \left(\frac{C_4(\omega_1, \epsilon_2 + \epsilon_1, \omega_2)}{\omega_2 - \epsilon_1 + i0} - \frac{D_4(\omega_1, \epsilon_2 + \epsilon_1, \omega_2)}{\omega_2 - \epsilon_2 - i0} \right),
\end{aligned}$$

where

$$\begin{aligned}
C_3(\omega_1, \omega_2, \omega_3) &\equiv 2\pi \mathcal{Z}^{-1} \sum_{abcd} (Sc)_{ab}^\alpha (Sc)_{bc}^\beta (Sc^\dagger)_{cd}^\beta (Sc^\dagger)_{da}^\alpha (e^{-\beta E_a} - e^{-\beta E_c}) \delta(\Xi_{ba} + \omega_1) \delta(\Xi_{ca} + \omega_2) \delta(\Xi_{da} + \omega_3) \\
C_4(\omega_1, \omega_2, \omega_3) &\equiv 2\pi \mathcal{Z}^{-1} \sum_{abcd} (Sc)_{ba}^\alpha (Sc)_{cb}^\beta (Sc^\dagger)_{dc}^\beta (Sc^\dagger)_{ad}^\alpha (e^{-\beta E_a} - e^{-\beta E_c}) \delta(\Xi_{ba} + \omega_1) \delta(\Xi_{ca} + \omega_2) \delta(\Xi_{da} + \omega_3) \\
D_3(\omega_1, \omega_2, \omega_3) &\equiv 2\pi \mathcal{Z}^{-1} \sum_{abcd} (Sc)_{ab}^\alpha (Sc)_{bc}^\beta (Sc^\dagger)_{da}^\beta (Sc^\dagger)_{cd}^\alpha (e^{-\beta E_a} - e^{-\beta E_c}) \delta(\Xi_{ba} + \omega_1) \delta(\Xi_{ca} + \omega_2) \delta(\Xi_{da} + \omega_3) \\
D_4(\omega_1, \omega_2, \omega_3) &\equiv 2\pi \mathcal{Z}^{-1} \sum_{abcd} (Sc)_{ba}^\alpha (Sc)_{cb}^\beta (Sc^\dagger)_{ad}^\beta (Sc^\dagger)_{dc}^\alpha (e^{-\beta E_a} - e^{-\beta E_c}) \delta(\Xi_{ba} + \omega_1) \delta(\Xi_{ca} + \omega_2) \delta(\Xi_{da} + \omega_3)
\end{aligned}$$

Again, it can be seen that $\Gamma_B^4(\epsilon_2, \epsilon_1) = [\Gamma_B^4(\epsilon_1, \epsilon_1)]^*$.

Summarizing, we find the following analytical continuations of Γ_{in}

$$\begin{aligned}
\Gamma^2(\epsilon_1, \epsilon_2) &= iA(\epsilon_2 - \epsilon_1) \\
\Gamma^3(\epsilon_1, \epsilon_2) &= -\frac{i2}{\beta^{1/2}} \int d\omega \mathcal{P}\left(\frac{1}{\omega}\right) \left[B_1(\omega - \epsilon_2, \omega - \epsilon_1) - B_2(\omega + \epsilon_2, \omega + \epsilon_1) \right] \\
\Gamma_1^4(\epsilon_1, \epsilon_2) &= i\beta^{-1} \int d\omega_1 d\omega_2 \frac{1}{\omega_1 + \epsilon_1 + i0} \left(\frac{C_1(\omega_1, \epsilon_2 - \epsilon_1, \omega_2)}{\omega_2 + \epsilon_1 - i0} - \frac{D_1(\omega_1, \epsilon_2 - \epsilon_1, \omega_2)}{\omega_2 - \epsilon_2 + i0} \right) \\
&\quad - i\beta^{-1} \int d\omega_1 d\omega_2 \frac{1}{\omega_1 - \epsilon_1 - i0} \left(\frac{C_2(\omega_1, -\epsilon_2 + \epsilon_1, \omega_2)}{\omega_2 - \epsilon_1 + i0} - \frac{D_2(\omega_1, -\epsilon_2 + \epsilon_1, \omega_2)}{\omega_2 + \epsilon_2 - i0} \right) \\
\Gamma_2^4(\epsilon_1, \epsilon_2) &= -i\beta^{-1} \int d\omega_1 d\omega_2 \frac{1}{\omega_1 + \epsilon_1 + i0} \left(\frac{C_3(\omega_1, -\epsilon_2 - \epsilon_1, \omega_2)}{\omega_2 + \epsilon_1 - i0} - \frac{D_3(\omega_1, -\epsilon_2 - \epsilon_1, \omega_2)}{\omega_2 + \epsilon_2 + i0} \right) \\
&\quad + i\beta^{-1} \int d\omega_1 d\omega_2 \frac{1}{\omega_1 - \epsilon_1 - i0} \left(\frac{C_4(\omega_1, \epsilon_2 + \epsilon_1, \omega_2)}{\omega_2 - \epsilon_1 + i0} - \frac{D_4(\omega_1, \epsilon_2 + \epsilon_1, \omega_2)}{\omega_2 - \epsilon_2 - i0} \right)
\end{aligned}$$

Looking at the integrals over ϵ_1, ϵ_2 (see Eqs. (2.67), (2.68)) we notice that we can exchange $\epsilon_i \rightarrow -\epsilon_i$ in the second terms of Γ^3 and Γ^4 , i.e.

$$\begin{aligned}
\Gamma^2(\epsilon_1, \epsilon_2) &= iA(\epsilon_2 - \epsilon_1) \\
\Gamma^3(\epsilon_1, \epsilon_2) &= \frac{i2}{\beta^{1/2}} \int d\omega \mathcal{P}\left(\frac{1}{\omega}\right) \left[B_1(\omega + \epsilon_2, \omega + \epsilon_1) + B_2(\omega + \epsilon_2, \omega + \epsilon_1) \right] \\
\Gamma_1^4(\epsilon_1, \epsilon_2) &= i\beta^{-1} \int d\omega_1 d\omega_2 \left[\frac{C_1(\omega_1, \epsilon_2 - \epsilon_1, \omega_2)}{(\omega_1 + \epsilon_1 + i0)(\omega_2 + \epsilon_1 - i0)} + \frac{C_2(\omega_1, \epsilon_2 - \epsilon_1, \omega_2)}{(\omega_1 + \epsilon_1 - i0)(\omega_2 + \epsilon_1 + i0)} \right. \\
&\quad \left. - \frac{D_1(\omega_1, \epsilon_2 - \epsilon_1, \omega_2)}{(\omega_1 + \epsilon_1 + i0)(\omega_2 - \epsilon_2 + i0)} - \frac{D_2(\omega_1, \epsilon_2 - \epsilon_1, \omega_2)}{(\omega_1 + \epsilon_1 - i0)(\omega_2 - \epsilon_2 - i0)} \right] \\
\Gamma_2^4(\epsilon_1, \epsilon_2) &= -i\beta^{-1} \int d\omega_1 d\omega_2 \left[\frac{C_3(\omega_1, -\epsilon_1 - \epsilon_2, \omega_2)}{(\omega_1 + \epsilon_1 + i0)(\omega_2 + \epsilon_1 - i0)} + \frac{C_4(\omega_1, -\epsilon_1 - \epsilon_2, \omega_2)}{(\omega_1 + \epsilon_1 - i0)(\omega_2 + \epsilon_1 + i0)} \right. \\
&\quad \left. - \frac{D_3(\omega_1, -\epsilon_1 - \epsilon_2, \omega_2)}{(\omega_1 + \epsilon_1 + i0)(\omega_2 + \epsilon_2 + i0)} - \frac{D_4(\omega_1, -\epsilon_1 - \epsilon_2, \omega_2)}{(\omega_1 + \epsilon_1 - i0)(\omega_2 + \epsilon_2 - i0)} \right].
\end{aligned}$$

The spectral functions are given by

$$\text{Im } \Sigma^{\text{R}}(\omega) \equiv -\pi \mathcal{Z}^{-1} \sum_{ab} (Sc)_{ab}^{\alpha} (c^{\dagger} S)_{ba}^{\alpha} \left(e^{-\beta E_a} + e^{-\beta E_b} \right) \delta(\Xi_{ab} + \omega)$$

$$A(\omega) \equiv 2\pi \mathcal{Z}^{-1} \sum_{ab} S_{ab}^{\alpha} S_{ba}^{\alpha} \left(e^{-\beta E_a} - e^{-\beta E_b} \right) \delta(\Xi_{ab} + \omega)$$

$$B_1(\omega_1, \omega_2) \equiv 2\pi \mathcal{Z}^{-1} \sum_{abc} (S)_{ab}^{\alpha\beta} (Sc)_{bc}^{\beta} (c^{\dagger} S)_{ca}^{\alpha} \left(e^{-\beta E_a} - e^{-\beta E_b} \right) \delta(\Xi_{ac} + \omega_1) \delta(\Xi_{bc} + \omega_2)$$

$$B_2(\omega_1, \omega_2) \equiv 2\pi \mathcal{Z}^{-1} \sum_{abc} (S)_{ba}^{\alpha\beta} (Sc)_{cb}^{\beta} (c^{\dagger} S)_{ac}^{\alpha} \left(e^{-\beta E_a} - e^{-\beta E_b} \right) \delta(\Xi_{ac} + \omega_1) \delta(\Xi_{bc} + \omega_2)$$

$$C_1(\omega_1, \omega_2, \omega_3) \equiv 2\pi \mathcal{Z}^{-1} \sum_{abcd} (Sc)_{ab}^{\alpha} (Sc)_{cd}^{\beta} (Sc^{\dagger})_{bc}^{\beta} (Sc^{\dagger})_{da}^{\alpha} \left(e^{-\beta E_a} - e^{-\beta E_c} \right) \delta(\Xi_{ba} + \omega_1) \delta(\Xi_{ca} + \omega_2) \delta(\Xi_{da} + \omega_3)$$

$$C_2(\omega_1, \omega_2, \omega_3) \equiv 2\pi \mathcal{Z}^{-1} \sum_{abcd} (Sc)_{ba}^{\alpha} (Sc)_{dc}^{\beta} (Sc^{\dagger})_{cb}^{\beta} (Sc^{\dagger})_{ad}^{\alpha} \left(e^{-\beta E_a} - e^{-\beta E_c} \right) \delta(\Xi_{ba} + \omega_1) \delta(\Xi_{ca} + \omega_2) \delta(\Xi_{da} + \omega_3)$$

$$D_1(\omega_1, \omega_2, \omega_3) \equiv 2\pi \mathcal{Z}^{-1} \sum_{abcd} (Sc)_{ab}^{\alpha} (Sc)_{da}^{\beta} (Sc^{\dagger})_{bc}^{\beta} (Sc^{\dagger})_{cd}^{\alpha} \left(e^{-\beta E_a} - e^{-\beta E_c} \right) \delta(\Xi_{ba} + \omega_1) \delta(\Xi_{ca} + \omega_2) \delta(\Xi_{da} + \omega_3)$$

$$D_2(\omega_1, \omega_2, \omega_3) \equiv 2\pi \mathcal{Z}^{-1} \sum_{abcd} (Sc)_{ba}^{\alpha} (Sc)_{ad}^{\beta} (Sc^{\dagger})_{cb}^{\beta} (Sc^{\dagger})_{dc}^{\alpha} \left(e^{-\beta E_a} - e^{-\beta E_c} \right) \delta(\Xi_{ba} + \omega_1) \delta(\Xi_{ca} + \omega_2) \delta(\Xi_{da} + \omega_3)$$

$$C_3(\omega_1, \omega_2, \omega_3) \equiv 2\pi \mathcal{Z}^{-1} \sum_{abcd} (Sc)_{ab}^{\alpha} (Sc)_{bc}^{\beta} (Sc^{\dagger})_{cd}^{\beta} (Sc^{\dagger})_{da}^{\alpha} \left(e^{-\beta E_a} - e^{-\beta E_c} \right) \delta(\Xi_{ba} + \omega_1) \delta(\Xi_{ca} + \omega_2) \delta(\Xi_{da} + \omega_3)$$

$$C_4(\omega_1, \omega_2, \omega_3) \equiv 2\pi \mathcal{Z}^{-1} \sum_{abcd} (Sc)_{ba}^{\alpha} (Sc)_{cb}^{\beta} (Sc^{\dagger})_{dc}^{\beta} (Sc^{\dagger})_{ad}^{\alpha} \left(e^{-\beta E_a} - e^{-\beta E_c} \right) \delta(\Xi_{ba} + \omega_1) \delta(\Xi_{ca} + \omega_2) \delta(\Xi_{da} + \omega_3)$$

$$D_3(\omega_1, \omega_2, \omega_3) \equiv 2\pi \mathcal{Z}^{-1} \sum_{abcd} (Sc)_{ab}^{\alpha} (Sc)_{bc}^{\beta} (Sc^{\dagger})_{da}^{\beta} (Sc^{\dagger})_{cd}^{\alpha} \left(e^{-\beta E_a} - e^{-\beta E_c} \right) \delta(\Xi_{ba} + \omega_1) \delta(\Xi_{ca} + \omega_2) \delta(\Xi_{da} + \omega_3)$$

$$D_4(\omega_1, \omega_2, \omega_3) \equiv 2\pi \mathcal{Z}^{-1} \sum_{abcd} (Sc)_{ba}^{\alpha} (Sc)_{cb}^{\beta} (Sc^{\dagger})_{ad}^{\beta} (Sc^{\dagger})_{dc}^{\alpha} \left(e^{-\beta E_a} - e^{-\beta E_c} \right) \delta(\Xi_{ba} + \omega_1) \delta(\Xi_{ca} + \omega_2) \delta(\Xi_{da} + \omega_3).$$

Appendix B

Appendix (Disordered Luttinger Liquid)

B.1 l_0 -independent contributions from the “ $\text{tr} \ln$ ”-expansion

In this appendix we want to show that there are no further l_0 -independent contributions from the “ $\text{tr} \ln$ ”-expansion than those considered in the text, i.e. the term depending on T from the linear order expansion, $S^{(1)}[T]$, and the term where T equals to the unit matrix from the second order expansion, $S^{(2)}[T]$. To this end we go back to the series-expansion of the “ $\text{tr} \ln$ ”,

$$S[T, X_1, X_2] = \frac{1}{2} \sum_{k=1} \frac{(-1)^k}{k} \text{tr} \{ \mathcal{G}_\Lambda [X_1 + X_2] \}^k,$$

where

$$X_{\tau\tau'}^1(x) = [T^{-1}(\partial T)]_{\tau\tau'}(x) \quad (\text{B.1})$$

$$X_{\tau\tau'}^2(x) = [T^{-1} [\mu + ia\sigma_3\sigma_3^T] T]_{\tau\tau'}(x). \quad (\text{B.2})$$

For a systematic analysis of the various contributions we introduce the matrix $O_{\tau\tau'}(x)$ which is local in space and non-local in time and the field $\phi(x, \tau)$ both local in space and time. ϕ represents the source-fields (or a fluctuating “interaction”-field) and results from X^2 with T and T^{-1} being the unit matrices, while O resembles the remaining contributions. To be precise, O takes into account X^1 and those contributions from X^2 in which at least one of the matrices T or T^{-1} differs from 1. Notice that in energy-representation $O_{nn'}$ is only non-vanishing inside an energy range $|n|, |n'| < n_0$ where ϵ_{n_0} is some high-energy-scale limiting the applicability of our low-energy model. So let us take a look at the terms from the expansion depending only on ϕ ,

$$S[\phi] = \frac{1}{2} \sum_{k=1} \frac{(-1)^k}{k} \text{tr} \{ \mathcal{G}_\Lambda \phi \}^k.$$

In energy/momentum representation the k -th order takes the form (for convenience we here restrict to the $+$ -sector)

$$\begin{aligned}
& \text{tr}\{g_{\Lambda}^+ \phi\}^k \\
&= \sum_n \sum_{m_1} \dots \sum_{m_{k-1}} \int dp \int dq_1 \dots \int dq_{k-1} \\
& \quad \frac{1}{z \pm \frac{i}{2l_0}} \frac{1}{z + z_1 \pm \frac{i}{2l_0}} \frac{1}{z + z_1 + z_2 \pm \frac{i}{2l_0}} \dots \frac{1}{z + z_1 + z_2 + \dots + z_{k-1} \pm \frac{i}{2l_0}} \\
& \quad \phi(z_1) \phi(z_2) \phi(z_3) \dots \phi(z_k) \phi(-z_1 - z_2 - \dots - z_k) \\
&= \sum_n \sum_{m_1} \dots \sum_{m_{k-1}} \int dp \int dq_1 \dots \int dq_{k-1} \Gamma^k(z, z_1, \dots, z_{k-1}) \phi(z_1) \phi \dots \phi(z_k) \phi(-z_1 - z_2 - \dots - z_k),
\end{aligned}$$

where we introduced the short notation $z = p + i\epsilon_n$ and $z_i = q_i + i\omega_{m_i}$ and the sign $\pm \frac{i}{2l_0}$ is that of ϵ_n . We may now divide the energy-sums into a part, where all energies have the same sign (i.e. all Greens functions g^+ are either *all* retarded or *all* advanced) and a part where the product of the k Greens functions contains g^+ with *different* causal structure. Starting with the later we use that $\frac{1}{z \pm \frac{i}{2l_0}} = \frac{1}{z \pm \frac{i}{2l_0}} \sum_{l=0}^{\infty} \frac{z_1^l}{[z \pm \frac{i}{2l_0}]^l}$ in order to write

$$\begin{aligned}
& \Gamma^k(z, z_1, \dots, z_{k-1}) \\
&= \sum_{l_1=0}^{\infty} \dots \sum_{l_{k-1}=0}^{\infty} \frac{1}{[z \pm \frac{i}{2l_0}]^k} \frac{1}{[z \pm \frac{i}{2l_0}]^{l_1}} \frac{1}{[z \pm \frac{i}{2l_0}]^{l_2}} \dots \frac{1}{[z \pm \frac{i}{2l_0}]^{l_{k-1}}} z_1^{l_1} (z_1 + z_2)^{l_2} \dots (z_1 + \dots + z_{k-1})^{l_{k-1}}.
\end{aligned}$$

Performing the ϵ -integral we find

$$\int d\epsilon \Gamma^k(z, z_1, \dots, z_{k-1}) \propto \sum_{l_1=0}^{\infty} \dots \sum_{l_{k-1}=0}^{\infty} l_0^{k-1} (l_0 z_1)^{l_1} (l_0 [z_1 + z_2])^{l_2} \dots (l_0 [z_1 + \dots + z_{k-1}])^{l_{k-1}},$$

which vanishes for $l_0 = 0$ (as discussed in the text keeping only the l_0 -independent contributions we may equally set l_0 in the calculations). Notice that taking $l_0 = 0$ is well-defined as all remaining integrals are convergent: $\int dp$ due to momentum cut-off Λ and those over ω_{m_i} and q_i due to $\phi(\omega_i, q_i)$. This procedure works for $k > 1$. For $k = 1$ the source-field has vanishing arguments, $\phi(z_1 = 0)$, and therefore is zero.

Next we turn to the case where all g^+ are either retarded or advanced, e.g.

$$\begin{aligned}
& \Gamma^k(z, z_1, \dots, z_{k-1}) \\
&= \sum_{l_1=0}^{\infty} \dots \sum_{l_{k-1}=0}^{\infty} \frac{1}{[z - \frac{i}{2l_0}]^k} \frac{1}{[z - \frac{i}{2l_0}]^{l_1}} \frac{1}{[z - \frac{i}{2l_0}]^{l_2}} \dots \frac{1}{[z - \frac{i}{2l_0}]^{l_{k-1}}} z_1^{l_1} (z_1 + z_2)^{l_2} \dots (z_1 + \dots + z_{k-1})^{l_{k-1}} \\
&= \sum_{l_1=0}^{\infty} \dots \sum_{l_{k-1}=0}^{\infty} \frac{1}{[z - \frac{i}{2l_0}]^{k+l_1+\dots+l_{k-1}}} z_1^{l_1} (z_1 + z_2)^{l_2} \dots (z_1 + \dots + z_{k-1})^{l_{k-1}}.
\end{aligned}$$

In this case we first integrate over ϵ (which for advance g^+ has to be positive) and then over p , i.e.

$$\begin{aligned}
& \int_0^\infty d\epsilon \int_{-\Lambda}^\Lambda dp \Gamma^k(z, z_1, \dots, z_{k-1}) \\
& \propto \int_{-\Lambda}^\Lambda dp \sum_{l_1=0}^\infty \dots \sum_{l_{k-1}=0}^\infty \frac{1}{[p - \frac{i}{2l_0}]^{k-1+l_1+\dots+l_{k-1}}} z_1^{l_1} (z_1 + z_2)^{l_2} \dots (z_1 + \dots z_{k-1})^{l_{k-1}} \\
& \propto \sum_{l_1=0}^\infty \dots \sum_{l_{k-1}=0}^\infty \left(\frac{1}{[\Lambda - \frac{i}{2l_0}]^{k-2+l_1+\dots+l_{k-1}}} - \frac{1}{[-\Lambda - \frac{i}{2l_0}]^{k-2+l_1+\dots+l_{k-1}}} \right) \\
& \quad z_1^{l_1} (z_1 + z_2)^{l_2} \dots (z_1 + \dots z_{k-1})^{l_{k-1}} \\
& \propto \sum_{l_1=0}^\infty \dots \sum_{l_{k-1}=0}^\infty \frac{l_0^{k-1+l_1+\dots+l_{k-1}}}{[1 + 4\Lambda^2 l_0^2]^{l_1+\dots+l_{k-1}-1}} z_1^{l_1} (z_1 + z_2)^{l_2} \dots (z_1 + \dots z_{k-1})^{l_{k-1}} + O(l_0^{k+l_1+\dots+l_{k-1}}) \\
& \propto \sum_{l_1=0}^\infty \dots \sum_{l_{k-1}=0}^\infty \frac{l_0^{k-1}}{[1 + 4\Lambda^2 l_0^2]^{l_1+\dots+l_{k-1}-1}} (l_0 z_1)^{l_1} (l_0 [z_1 + z_2])^{l_2} \dots (l_0 [z_1 + \dots z_{k-1}])^{l_{k-1}} \\
& \quad + O(l_0^{k+l_1+\dots+l_{k-1}}),
\end{aligned}$$

which again vanishes for $l_0 = 0$. Again setting $l_0 = 0$ is a well defined procedure since the remaining integrals are well-behaved. This argument only holds whenever $k > 2$. The $k = 2$ contribution was calculated in the text and the $k = 1$ case we already considered above. We conclude that of all contributions containing “only” sources only the $k = 2$ contribution with g^\pm both retarded or both advanced is l_0 -independent, i.e. does not vanish for $l_0 = 0$.

So let us turn to those contributions from the “ $\text{tr} \ln$ ”-expansion that only involve O 's, i.e.

$$S[O] = \frac{1}{2} \sum_{k=1} \frac{(-1)^k}{k} \text{tr} \{g_\Lambda^+ O\}^k.$$

The explicit form of the k^{th} order contribution is

$$\begin{aligned}
\text{tr} \{g_\Lambda^+ O\}^k &= \sum_n \sum_{n_1} \dots \sum_{n_{k-1}} \int dp \int dq_1 \dots \int dq_{k-1} \\
& \quad \frac{1}{z \pm \frac{i}{2l_0}} \frac{1}{z + z_1 \pm \frac{i}{2l_0}} \frac{1}{z + z_1 + z_2 \pm \frac{i}{2l_0}} \dots \frac{1}{z + z_1 + z_2 + \dots + z_{k-1} \pm \frac{i}{2l_0}} \\
& \quad \text{tr} \{O_{nn_1}(q_1) O_{n_1 n_2}(q_2) O_{n_2 n_3}(q_3) \dots O_{n_{k-1} n}(q_{k-1})\} \\
&= \sum_n \sum_{m_1} \dots \sum_{m_{k-1}} \int dp \int dq_1 \dots \int dq_{k-1} \\
& \quad \Gamma^k(z, z_1, \dots, z_{k-1}) \text{tr} \{O_{nn_1}(q_1) O_{n_1 n_2}(q_2) O_{n_2 n_3}(q_3) \dots O_{n_{k-1} n}(q_{k-1})\}.
\end{aligned}$$

Again, we may distinguish the situation where all g^\pm have the *same* analytical structure from the one where g^\pm 's appear in their retarded *and* advanced version. Starting with the former we perform the p -integral and find

$$\begin{aligned}
& \int dp \Gamma^k(z, z_1, \dots, z_{k-1}) \\
&= \int dp \sum_{l_1=0}^\infty \dots \sum_{l_{k-1}=0}^\infty \frac{1}{[z \pm \frac{i}{2l_0}]^k} \frac{1}{[z \pm \frac{i}{2l_0}]^{l_1}} \frac{1}{[z \pm \frac{i}{2l_0}]^{l_2}} \dots \frac{1}{[z \pm \frac{i}{2l_0}]^{l_{k-1}}} z_1^{l_1} (z_1 + z_2)^{l_2} \dots (z_1 + \dots z_{k-1})^{l_{k-1}} \\
&\propto \sum_{l_1=0}^\infty \dots \sum_{l_{k-1}=0}^\infty l_0^{k-1} (l_0 z_1)^{l_1} (l_0 [z_1 + z_2])^{l_2} \dots (l_0 [z_1 + \dots z_{k-1}])^{l_{k-1}}
\end{aligned}$$

which again vanishes for $l_0 = 0$ (the remaining integrals are well-behaved). Notice that this time it is the fact that $O_{nn'}$ is only non-vanishing inside some energy range $|n|, |n'| < n_0$ that makes the ϵ -integrals convergent. In the case of plain sources we had to perform the ϵ -integral (i.e. the n -summation) as this was not restricted. (In the above situation we cannot perform the ϵ -integral as O still depends on ϵ). Again, this argument holds for $k > 1$ and the case $k = 1$ was considered in the text.

Turning to the situation of $k > 1$ where all g^\pm 's have the same analytical structure we may perform the p -integral, by closing the contour in the half plane of the complex plane, where $\Gamma(p)$ has no poles, e.g.

$$\begin{aligned} & \int dp \Gamma^k(z, z_1, \dots, z_{k-1}) \\ &= \int dp \frac{1}{z - \frac{i}{2l_0}} \frac{1}{z + z_1 - \frac{i}{2l_0}} \frac{1}{z + z_1 + z_2 - \frac{i}{2l_0}} \dots \frac{1}{z + z_1 + z_2 + \dots + z_{k-1} - \frac{i}{2l_0}} = 0. \end{aligned}$$

Again, the remaining integrals are well behaved. We conclude, that the only non-vanishing contributions from the expansion of “tr ln” containing only O 's stems from the linear order expansion (i.e. $k = 1$). This term has been considered in the text.

Turning to terms from the “tr ln”-expansion containing contributions from ϕ and O (case 3) we observe that for $k > 2$ we may apply the same argument as in the case where all contributions contained only ϕ 's (case 1). The reason therefore is that in case 3 there is always a free ϵ -integral, in the sense that ϵ just enters in the g^\pm . We may therefore perform the free ϵ -integral and the argument used in case 1 applies. In the case of the $k = 2$ contribution, linear in ϕ and linear O we may apply the argument used in the case of only O 's (case 2) as the energy-integrals are restricted due to the presence of O . Therefore all “mixed” contributions containing ϕ as well as O vanish.

To summarize: In this appendix we showed that the “tr ln”-expansion has just two l_0 -independent (i.e. non-vanishing for $l_0 = 0$) contributions. These are

- $\text{tr} \{ \mathcal{G}_\Lambda [\hat{\mu} + i\hat{a}\sigma_3\sigma_3^\top] \mathcal{G}_\Lambda [\hat{\mu} + i\hat{a}\sigma_3\sigma_3^\top] \}$
- $\text{tr} \{ \mathcal{G}_\Lambda T^{-1} [\partial + \hat{\mu} + i\hat{a}\sigma_3\sigma_3^\top] T \},$

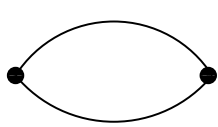
where in the second expression at least one of the matrices T or T^{-1} has to differ from unity. These terms were considered in the text: The first term is the diamagnetic contribution second order in the sources, and the second term accounts for its paramagnetic contribution. The fact that going beyond the second order in sources gives no further contributions results from the “higher-loop cancelation”, as stated in the text. In this sense our approach is closely related to the functional bosonization method with the difference lying in the fact, that in our approach the paramagnetic contributions are taken into account by coupling to a bosonic matrix-field, introduced in order to decouple the disorder average induced interaction between the electrons.

B.2 Diagrammatic evaluation of the density/density correlation function

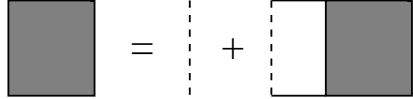
In this appendix we supply the explicit calculation of the density/density correlation function for the Green's functions dressed by forward scattering disorder length, i.e.

$$g_n^\pm(p) = \frac{1}{-i\epsilon_n \pm p - \frac{i}{2l_0} \text{sgn}(n)}. \quad (\text{B.3})$$

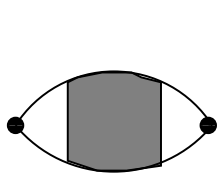
The paramagnetic contribution to the density/density correlation function is given by the sum of two diagrams depicted in Fig.3.2, where the single particle lines consist of a retarded and an advanced contribution. The individual contributions calculate as



$$\begin{aligned} & \text{Re} \left\{ T \sum_{-m < n < 0} \int \frac{dp}{2\pi} \frac{1}{p + q + i\epsilon_{n+m} + \frac{i}{2l_0}} \frac{1}{p + i\epsilon_n - \frac{i}{2l_0}} \right\} \\ &= \frac{1}{2\pi} \text{Im} \left\{ \frac{\omega_m}{q + i\omega_m + i/l_0} \right\} \end{aligned} \quad (\text{B.4})$$



$$\mathcal{D}(\omega_m, q) = \frac{1}{l_0 - \frac{i}{q + i\omega_m + i/l_0}} = \frac{1}{l_0} \frac{1 - iql_0 + \omega_m l_0}{\omega_m l_0 - iql_0} \quad (\text{B.5})$$



$$\begin{aligned} & \text{Re} \left\{ \frac{1}{T} \sum_{-m < n < 0} \int \left\{ \frac{dp}{2\pi} \frac{1}{p + q + i\epsilon_{n+m} + \frac{i}{2l_0}} \frac{1}{p + i\epsilon_n - \frac{i}{2l_0}} \right\}^2 \times \mathcal{D}(\omega_m, q) \right\} \\ &= \frac{-\omega_m}{2\pi l_0} \text{Re} \left\{ \left(\frac{1}{q + i\omega_m + i/l_0} \right)^2 \frac{1 - iql_0 + \omega_m l_0}{\omega_m l_0 - iql_0} \right\} \\ &= \frac{1}{2\pi} \text{Im} \left\{ \frac{\omega_m}{(\omega_m l_0 - iql_0)(q + i\omega_m + i/l_0)} \right\}. \end{aligned} \quad (\text{B.6})$$

B.3 Regularization of the propagator

We stated in the text, that before considering higher loop corrections to the Gaussian propagator one has to modify the model in order to account for the limit of resolution set by the momentum cut-off Λ . This is done in this appendix. To be precise, we “soften” the δ -correlated disorder by taking the correlation function

$$\langle u(x)u(x') \rangle_u = 2l_0^{-1} \delta(x - x' + a),$$

where a is e.g. Gaussian distributed, $p(a) = e^{-a^2/\lambda^2}$. This choice corresponds to Gaussian distributed disorder,

$$\langle u(x)u(x') \rangle = 2l_0^{-1} e^{-(x-x')^2/\lambda^2}.$$

In the following we take the correlation length $\lambda \ll l_0$ to be the smallest length-scale in the system (e.g. may think of λ as the lattice spacing, i.e. $\lambda = \Lambda^{-1}$). Going through the same steps as before the Hubbard-Stratonovich field is now $Q = Q(x, x + a)$. As a is negligible small the saddle-point analysis is unchanged and the Goldstone-modes are $Q(x, x + a) = T(x + a)\Lambda T^{-1}(x)$. Since we can think of $a \rightarrow 0$ the only modification results in “regularizing” the pole-integral of the first order term in the expansion of “ $\text{tr} \ln$ ”

$$\begin{aligned} & \sum_n \int dx \text{tr} \{ \mathcal{G}_n^\Lambda(x, x + a) X_{nn}^1(x + a, x) \} \\ &= \frac{1}{L} \sum_{np} \sum_{mq} \text{tr} \left\{ \mathcal{G}_{n,p}^\Lambda T_{\pm, nn+m}^{-1}(q) [\omega_m \pm iq] T_{\pm, n+mn}(-q) e^{-ia(p-q)} \right\}. \end{aligned}$$

Using that

$$\sum_p g_{n,p}^\pm e^{-iap} = \int \frac{dp}{2\pi} \frac{e^{-iap}}{\pm p - i\epsilon_n} = \pm \theta(\mp na) e^{-\epsilon_n a}$$

we find (notice the factor $1/2$ compared to $a = 0$, since in the latter case: $\theta(sna)e^{-\epsilon_n a} = \frac{1}{2}$) and we neglect $e^{-\epsilon a}$ as it is irrelevant

$$S_{\text{reg}}^0[T_{\pm}] = -\frac{1}{2} \sum_{nm,q} \text{tr} \left\{ \Lambda_n T_{\pm,nn+m}^{-1}(q) [\omega_m \pm iq] e^{\pm i a q} \theta(\pm n a) T_{\pm,n+mn}(-q) \right\}.$$

In Gaussian approximation this leads to the Diffuson-action (notice that the factor two is compensated by combining $\theta(sa) + \theta(-sa)$ in order to get $e^{i s q |a|}$)

$$S_{\text{reg}}^0[\mathcal{D}_s] = - \sum_{m>0} \sum_{-m < n < 0} \sum_q \text{tr} \left\{ \bar{D}_{s,nn+m}^{\text{ff}}(q) [\omega_m + s i q] e^{i s q |a|} D_{s,n+mn}^{\text{ff}}(-q) \right\}$$

Averaging according to $\langle \dots \rangle = \int da(\dots) p(a)$ the regularized propagator now takes the form

$$\langle \bar{D}_{s,nn+m}^{\text{ff}}(x) D_{s,n+mn}^{\text{ff}}(x') \rangle_{S_{\text{reg}}^0} = \begin{cases} \langle \bar{D}_{s,nn+m}^{\text{ff}}(x) D_{s,n+mn}^{\text{ff}}(x') \rangle_{S^0}, & s(x-x') > \lambda \\ 0, & s(x-x') < \lambda. \end{cases}$$

That is, introducing Gaussian correlated disorder, with a finite, yet very small correlation length, λ , the effective particle-hole propagator gives only non-vanishing contributions if the particle (hole) travel at least over the distance λ . This is compatible with the fact that we consider left- and right moving particles and use the UV cut-off Λ in all momentum integrals and therefore, e.g. the density-density correlation function, $\langle \rho^{\pm}(x) \rho^{\pm}(x') \rangle$, should only be evaluated for values $|x-x'| > \Lambda^{-1}$ (we may set $\lambda = \Lambda^{-1}$). In summary, softening the (unphysical) δ -correlated disorder sets the local (in the sense that $|x-x'| < \Lambda^{-1}$) particle-hole propagator to zero, but leaves it unchanged on regular scales $\gtrsim \Lambda^{-1}$. Notice also that the regularization only works this way because electrons and holes can only travel in one direction. All considerations made here also apply for the Cooperon. The source part of the action, S_{Sou} remains unchanged.

B.4 Equivalence of Eq.(3.68) and Eq.(3.72)

In this appendix we want to show how to obtain Eq.(3.68) from Eq.(3.72). Starting out from

$$S[\varphi] + S_{\text{Sou}}[\mu, a] = \frac{1}{2} \int d^2 x \varphi^t G^{-1} \varphi + \text{tr} \ln \{ \partial \} + \frac{1}{2\pi} \int d^2 x (J + \varphi)^t \Pi (J + \varphi), \quad (\text{B.7})$$

where

$$J = \begin{pmatrix} \mu + i a \\ \mu - i a \end{pmatrix} \quad \text{and} \quad \Pi_m(q) = \begin{pmatrix} \Pi_m^+(q) & \\ & \Pi_m^-(q) \end{pmatrix} \quad \text{where} \quad \Pi_m^{\pm}(q) = \frac{q}{q \pm i \omega_m}. \quad (\text{B.8})$$

We introduce some more matrices,

$$D_m(q) = \begin{pmatrix} q + i \omega_m & q + i \omega_m \\ -q + i \omega_m & q - i \omega_m \end{pmatrix} \quad (\text{B.9})$$

$$L_m(q) = D_{-m}^t(-q) \Pi_m(q) D_m(q) = \begin{pmatrix} q^2 & i \omega_m q \\ i \omega_m q & q^2 \end{pmatrix} \quad (\text{B.10})$$

$$g_m(q) = D_{-m}^t(-q) G^{-1} D_m(q) = \frac{1}{g_1 g_2} \begin{pmatrix} g_2 \omega_m^2 + g_1 q^2 & i \omega_m q (g_1 - g_2) \\ i \omega_m q (g_1 - g_2) & -g_1 \omega_m^2 - g_2 q^2 \end{pmatrix}, \quad (\text{B.11})$$

and replace the “ $\text{tr} \ln \{ \partial \}$ ” by a bosonic field integral,

$$- \int d^2 x \chi \partial \chi \rightarrow \frac{1}{2} \int d^2 x \Theta^t L \Theta, \quad (\text{B.12})$$

where $\Theta = \begin{pmatrix} \theta_1 \\ \theta_2 \end{pmatrix}$. Now we introduce $\varphi = DK$ and shift $\Theta \rightarrow \Theta - \pi^{-1/2} [D^{-1}J + K]$ leading to

$$\begin{aligned} S[K] + S[\Theta] + S_{\text{Sou.}}[\mu, a] \\ = \frac{1}{2} \int d^2x K^t g K + \frac{1}{2} \int d^2x \Theta^t L \Theta + \frac{1}{2\pi} \int d^2x (D^{-1}J + K)^t L (D^{-1}J + K) \\ \rightarrow \frac{1}{2} \int d^2x K^t g K + \frac{1}{2} \int d^2x \Theta^t L \Theta + \frac{1}{2\sqrt{\pi}} \int d^2x \left[(D^{-1}J + K)^t L \Theta + \Theta L (D^{-1}J + K) \right]. \end{aligned}$$

Integration over K and then over Θ gives

$$\begin{aligned} \frac{1}{2} \int d^2x K^t g K + \frac{1}{2} \int d^2x \Theta^t L \Theta + \frac{1}{2\sqrt{\pi}} \int d^2x \left[(D^{-1}J + K)^t L \Theta + \Theta L (D^{-1}J + K) \right] \\ \rightarrow \frac{1}{2} \int d^2x \Theta^t [L + L^t g^{-1} L] \Theta + \frac{1}{2\sqrt{\pi}} \int d^2x [J^t \Pi D \Theta + \Theta^t D^t \Pi J] \\ \rightarrow \frac{1}{2\pi} \int d^2x J^t \Pi D [L + L^t g^{-1} L]^{-1} D^t \Pi J \end{aligned}$$

Finally, applying that

$$\Pi D = iq \begin{pmatrix} 1 & -1 \\ 1 & 1 \end{pmatrix} \quad L + L^t g^{-1} L = \begin{pmatrix} (1 - \frac{g_2}{2\pi}) q^2 & i\omega_m q \\ i\omega_m q & (1 + \frac{g_2}{2\pi}) q^2 \end{pmatrix} \quad (\text{B.13})$$

one returns to action Eq. (3.68), i.e.

$$\begin{aligned} S[a, \mu] \\ = \frac{1}{2\pi} \sum_{m,q} \left\{ \frac{vq^2}{v^2 q^2 + \omega_m^2} [g \mu_{mq} \mu_{-m,-q} - g^{-1} a_{mq} a_{-m,-q}] + \frac{\omega_m q}{v^2 q^2 + \omega_m^2} [\mu_{mq} a_{-m,-q} + a_{mq} \mu_{-m,-q}] \right\}. \end{aligned} \quad (\text{B.14})$$

B.5 Equivalence of Eq.(3.72) and Eq.(3.74)

In this appendix we want to show the equivalence of Eq.(3.72) and Eq.(3.74). To this end we merely have to make sure that

$$\text{tr} \ln \{\mathcal{G}_\Lambda^{-1}\} = \text{tr} \ln \{\mathcal{G}_0^{-1}\},$$

where $\mathcal{G}_0 = \partial^{-1}$ and $\mathcal{G}_\Lambda = [\partial - \frac{i}{2l_0} \Lambda]^{-1}$. Since

$$\text{tr} \ln \{\mathcal{G}_\Lambda^{-1}\} = \text{tr} \ln \{\partial\} + \text{tr} \ln \left\{ 1 + \frac{i}{2l_0} \mathcal{G}_0 \Lambda \right\},$$

this amounts to showing that

$$\text{tr} \ln \left\{ 1 + \frac{i}{2l_0} \mathcal{G}_0 \Lambda \right\} = 0,$$

and may be done as follows:

$$\begin{aligned}
\text{tr} \ln \left\{ 1 + \frac{i}{2l_0} \mathcal{G}_0 \Lambda \right\} &= - \sum_{k=1}^{\infty} \frac{1}{k} \text{tr} \left\{ \frac{i}{2l_0} \mathcal{G}_0 \Lambda \right\}^k \\
&= - \sum_{k=1}^{\infty} \frac{1}{k} \sum_{n,p} \text{tr} \left\{ \frac{i}{2l_0} \mathcal{G}_0(n,p) \Lambda_n \right\}^k \\
&= - \sum_{k=1}^{\infty} \frac{1}{k} \sum_{|p| < \Lambda} \left(\sum_{n>0} \left\{ \left[\frac{i}{2l_0} g_0^+(n,p) \right]^k + \left[\frac{i}{2l_0} g_0^-(n,p) \right]^k \right\} \right. \\
&\quad \left. + \sum_{n<0} \left\{ \left[\frac{-i}{2l_0} g_0^+(n,p) \right]^k + \left[\frac{-i}{2l_0} g_0^-(n,p) \right]^k \right\} \right)
\end{aligned}$$

Substituting $g_n^{\pm}(p) = \frac{-1}{i\epsilon_n \mp p}$ we get

$$\begin{aligned}
\frac{1}{k} \sum_{n>0} \left[\frac{i}{2l_0} g_n^{\pm}(p) \right]^k &= \frac{1}{k} \sum_{n>0} \left(\frac{-i}{2l_0[i\epsilon_n \mp p]} \right)^k = \frac{T}{k} \int_0^{\infty} \frac{d\epsilon}{2\pi} \left(\frac{-1}{2l_0[\epsilon \pm ip]} \right)^k = -\frac{T}{2\pi} \left(\frac{\pm i}{2l_0 p} \right)^{k-1} \\
\frac{1}{k} \sum_{n<0} \left[\frac{-i}{2l_0} g_n^{\pm}(p) \right]^k &= \frac{1}{k} \sum_{n<0} \left(\frac{i}{2l_0[i\epsilon_n \mp p]} \right)^k = \frac{T}{k} \int_{-\infty}^0 \frac{d\epsilon}{2\pi} \left(\frac{1}{2l_0[\epsilon \pm ip]} \right)^k = \frac{T}{2\pi} \left(\frac{\mp i}{2l_0 p} \right)^{k-1}
\end{aligned}$$

and therefore

$$\begin{aligned}
- \sum_{|p| < \Lambda} \sum_{k=1}^{\infty} \frac{1}{k} \sum_{n>0} \left\{ \left[\frac{i}{2l_0} g_0^+(n,p) \right]^k + \left[\frac{i}{2l_0} g_0^-(n,p) \right]^k \right\} &= \frac{T}{2\pi} \int_{-\Lambda}^{\Lambda} \frac{dp}{2\pi} \sum_{k=0}^{\infty} \left[\left(\frac{i}{2l_0 p} \right)^k + \left(\frac{-i}{2l_0 p} \right)^k \right] \\
&= \frac{T}{2\pi} \int_{-\Lambda}^{\Lambda} \frac{dp}{2\pi} \left[\frac{1}{1 - i/2l_0 p} + \frac{1}{1 + i/2l_0 p} \right] \\
&= \frac{T}{2\pi} \int_{-\Lambda}^{\Lambda} \frac{dp}{2\pi} \frac{4l_0 p^2}{1 + 4l_0^2 p^2},
\end{aligned}$$

which vanishes for $l_0 \rightarrow 0$ (notice that the remaining integral is finite, due to the cut-off Λ). In the second line used that $l_0 p < \Lambda^{-1} p < 1$). For $n < 0$ one can proceed in the same way.

B.6 Dephasing rates

This appendix is included for reasons of documentation and may be skipped by the reader. In order to show the different role of the vertex contributions played in context of the Diffuson and Cooperon, respectively. To this end we perform the m -summation leading to

$$\sum_m \sum_q V_m^s(q) \Pi_m^s(q) [\theta(n_1(n_1 + m)) \theta(n_2(n_2 + m))] = -\frac{2}{L\pi} \sum_q \int d\Omega \frac{1}{\sinh \left[\frac{\Omega}{2T} \right]} \text{Im} V_{\Omega}^{\text{R},s}(q) \text{Re} \Pi_{\Omega}^{\text{R},s}(q) \quad (\text{B.15})$$

It is convenient to change to a time picture, such that for the Diffuson (elastic contributions from self-energy and vertex $\delta_{m,0}$ cancel)

$$\begin{aligned}
&\frac{1}{2} \langle S_{\text{coup}}[\mathcal{D}, \phi] S_{\text{coup}}[\mathcal{D}, \phi] \rangle \\
&= \frac{4T}{L} \sum_{s=\pm} \sum_{q'} \int dt_1 dt_2 \int dq \int d\Omega \frac{\text{Im} V_{\Omega}^{\text{R},s}(q)}{\sinh \left[\frac{\Omega}{2T} \right]} \text{Re} \Pi_{\Omega}^{\text{R},s}(q) \left\{ 1 - \cos[\Omega(t_1 - t_2)] \right\} \text{tr} \left\{ \mathcal{D}_{t_1 t_2}^{\text{s},\text{ff}}(q') \mathcal{D}_{t_2 t_1}^{\text{s},\text{ff}}(-q') \right\},
\end{aligned}$$

where again the first contributions are the self-energy and the second the vertex contributions. The time difference $t_1 - t_2$ is the time difference the electron and hole arrive at some space point x and $\ll \Omega^{-1}$. That is one may set $\cos[\Omega(t_1 - t_2)] = 1$ for all energies $\Omega \lesssim T$ and find that self-energy and vertex contributions cancel in the one-loop approximation.

For the Cooperon on the other hand analytical continuation and changing to a time representation gives

$$\begin{aligned} & \frac{1}{2} \langle S_{\text{coup}}[\mathcal{C}, \phi] S_{\text{coup}}[\mathcal{C}, \phi] \rangle \\ &= \frac{4T}{L} \sum_{s=\pm} \sum_{q'} \int dt_1 dt_2 \int dq \int d\Omega \frac{\text{Im } V_{\Omega}^{\text{R},s}(q)}{\sinh\left[\frac{\Omega}{T}\right]} \text{Re } \Pi_{\Omega}^{\text{R},s}(q) \left\{ 1 - \cos[\Omega(t_1 + t_2)] \right\} \text{tr} \left\{ \mathcal{C}_{t_1 t_2}^{\text{s,ff}}(q') \mathcal{C}_{t_2 t_1}^{\text{s,ff}}(-q') \right\}. \end{aligned}$$

As the typical traveling time of the particle-hole excitation is given by the dephasing time τ_{ϕ} one has $t_1 + t_2 \sim \tau_{\phi}$. Therefore we may approximate $1 - \cos[\Omega(t_1 + t_2)] = \Theta(|\Omega| - \tau_{\phi}^{-1})$ and find that the vertex contribution cuts off energies $\Omega \lesssim \tau_{\phi}^{-1}$.

B.7 Inclusion of back-scattering disorder

In this appendix we want to show, that the only contributions from

$$S[T] = -\frac{1}{2} \text{tr} \ln \{1 + \mathcal{G}_{\Lambda}[X_1 + X_2 + X_3]\}, \quad (\text{B.16})$$

involving X_3 is given by

$$S_{\text{bs}}[T] = -\frac{1}{16l_1} \sum_{nn'} \text{tr} \{ [T \Lambda T^{-1}]_{nn'}(q) \sigma_1 [T \Lambda T^{-1}]_{n'n}(-q) \sigma_1 \}. \quad (\text{B.17})$$

Here $X_{nn'}^3(x) = [T^{-1} v \sigma_1 T]_{nn'}(x)$.

The argument goes as follows: X^3 is off-diagonal in \pm -space. Therefore all contributions from v are even powers in v . Expansion of the exponential function gives various terms containing v . Let us consider first terms containing products of traces, as e.g.

$$\text{tr} \{ \mathcal{G} X^i \mathcal{G} T^{-1} v \sigma_1 T \mathcal{G} T^{-1} v \sigma_1 T \} \text{tr} \{ \mathcal{G} X^i \mathcal{G} T^{-1} v \sigma_1 T \mathcal{G} T^{-1} v \sigma_1 T \}.$$

If one performs the disorder average pairing (Wick contracting) v 's from different traces one ends up with terms as

$$\text{tr} \{ X^i(x) \mathcal{G}(x, x') [T^{-1} \sigma_1 T](x') \mathcal{G}(x', x) [T^{-1} \sigma_1 T](x) \} \text{tr} \{ X^i(x') \mathcal{G}(x', x) [T^{-1} \sigma_1 T](x) \mathcal{G}(x, x') [T^{-1} \sigma_1 T](x') \}.$$

Such terms vanish, as we showed in Appendix B.1. Therefore in order to obtain non-vanishing contributions all pairings of v 's (Wick contractions) have to be done within the same trace. The lowest order contribution in v and \mathcal{G} is

$$\begin{aligned} \text{tr} \{ \mathcal{G} T^{-1} v \sigma_1 T \mathcal{G} T^{-1} v \sigma_1 T \} &= \int dx \text{tr} \{ \mathcal{G}(x, x) [T^{-1} \sigma_1 T](x) \mathcal{G}(x, x) [T^{-1} \sigma_1 T](x) \} \\ &= \frac{1}{4l_1} \int dx \frac{1}{L^2} \sum_{pp'} \text{tr} \{ \mathcal{G}(p) [T^{-1} \sigma_1 T](x) \mathcal{G}(p') [T^{-1} \sigma_1 T](x) \} \\ &= -\frac{1}{16l_1} \int dx \text{tr} \{ \Lambda [T^{-1} \sigma_1 T](x) \Lambda [T^{-1} \sigma_1 T](x) \}, \end{aligned}$$

where in the last line we used that $\frac{1}{L} \sum_p \mathcal{G}_n(p) = \frac{i}{2} \Lambda_n$. A contribution which is of the same order in v but next order in \mathcal{G} is

$$\text{tr} \{ \mathcal{G} X^i \mathcal{G} T^{-1} v \sigma_1 T \mathcal{G} T^{-1} v \sigma_1 T \} = \text{tr} \{ \mathcal{G}(x, x') X^i(x') \mathcal{G}(x', x'') [T \sigma_1 T](x'') \mathcal{G}(x'', x) [T^{-1} \sigma_1 T](x) \}.$$

This term vanishes by the same arguments as employed in Appendix B.1. All higher powers in v or \mathcal{G} correspond (after disorder average) to those cases considered in Appendix B.1, i.e. they all vanish. Therefore expansion of “tr ln” followed by an expansion of exponential function containing v gives

$$\begin{aligned} e^{\text{tr} \ln \{1 + \mathcal{G}_\Lambda [X_1 + X_2 + X_3]\}} &= e^{\text{tr} \ln \{1 + \mathcal{G}_\Lambda [X_1 + X_2]\}} \sum_k \frac{1}{k!} \left(\text{tr} \{ \mathcal{G} T^{-1} v \sigma_1 T \mathcal{G} T^{-1} v \sigma_1 T \} \right)^k \\ &= e^{\text{tr} \ln \{1 + \mathcal{G}_\Lambda [X_1 + X_2]\}} \left(\frac{-1}{16l_1} \text{tr} \{ T \Lambda T^{-1} \sigma_1 T \Lambda T^{-1} \sigma_1 \} \right)^k \\ &= \exp \left\{ \text{tr} \ln \{1 + \mathcal{G}_\Lambda [X_1 + X_2]\} - \frac{1}{16l_1} \text{tr} \{ T \Lambda T^{-1} \sigma_1 T \Lambda T^{-1} \sigma_1 \} \right\}. \end{aligned}$$

B.8 Some details

In this appendix we supply some details of the calculations done in section 3.8.

B.8.1 Analytical continuation of $S_\chi[\mathcal{C}^{\text{fb}} \mathcal{C}^{\text{bf}}]$

In this appendix we explicitly show that the interaction processes contained in

$$S_\chi[\mathcal{C}_s^{\text{fb}} \mathcal{C}_s^{\text{bf}}] = \frac{1}{2l_1} \int d^2x \text{tr} \left\{ \mathcal{C}_s^{\text{fb}} \mathcal{C}_s^{\text{bf}} \Lambda e^{i\chi^f} \Lambda e^{-i\chi^f} \right\} \quad (\text{B.18})$$

are solely given by high energy processes, i.e. $S_\chi[\mathcal{C}_s^{\text{fb}} \mathcal{C}_s^{\text{bf}}]$ is irrelevant for the discussion of dephasing. The explicit form of Eq.(B.18) is given by

$$\begin{aligned} S_\chi[\mathcal{C}_s^{\text{fb}} \mathcal{C}_s^{\text{bf}}] &= \frac{1}{4l_1} \int dx \sum_{n, m > 0} \text{tr} \{ (\mathcal{C}_s^{\text{fb}} \mathcal{C}_s^{\text{bf}})_{nn} \} \left(e^{i\chi^f} \right)_m \left(e^{-i\chi^f} \right)_{-m} \text{sgn}(n) [\text{sgn}(n+m) + \text{sgn}(n-m)] \\ &= \frac{1}{2l_1} \int dx \sum_{n, m > 0} \text{tr} \{ (\mathcal{C}_s^{\text{fb}} \mathcal{C}_s^{\text{bf}})_{nn} \} \left(e^{i\chi^f} \right)_m \left(e^{-i\chi^f} \right)_{-m} \text{sgn}(n) \theta(|n| - m) \end{aligned} \quad (\text{B.19})$$

Using the off-diagonal matrices, \bar{C} and C , introduced in section 3.2.3 gives

$$\begin{aligned} S_\chi[\mathcal{C}_s^{\text{fb}} \mathcal{C}_s^{\text{bf}}] &= -\frac{1}{4l_1} \int dx \sum_{n < 0, n' > 0} \sum_{-n > m > 0} \text{tr} \{ \bar{C}_{nn'} C_{n'n} \} \left(e^{i\chi^f} \right)_m \left(e^{-i\chi^f} \right)_{-m} \\ &\quad + \frac{1}{4l_1} \int dx \sum_{n < 0, n' > 0} \sum_{n' > m > 0} \text{tr} \{ \bar{C}_{nn'} C_{n'n} \} \left(e^{i\chi^f} \right)_m \left(e^{-i\chi^f} \right)_{-m}. \end{aligned} \quad (\text{B.20})$$

The analytical continuation of the bosonic frequency ω_m is done along the “low-energy” cut through $\omega_m = 0$ and the high energy contour through $\omega_m = \epsilon_n$. After analytical continuation the first line in Eq.(B.20) takes the form

$$(1) \propto - \int d\epsilon \int d\epsilon' \int d\Omega \tanh \left[\frac{\epsilon}{2T} \right] \tanh \left[\frac{\epsilon'}{2T} \right] \text{tr} \{ \bar{C}_{\epsilon\epsilon'} C_{\epsilon'\epsilon} \} \left(\coth \left[\frac{\Omega}{2T} \right] - \tanh \left[\frac{\epsilon - \Omega}{2T} \right] \right) V^R(\Omega), \quad (\text{B.21})$$

where $V^R(\Omega)$ is the analytically continued retarded component of $\langle (e^{i\chi^f})_m (e^{-i\chi^f})_{-m} \rangle$. The term proportional to \coth comes from the “low energy” cut, and, in the Keldysh formalism results from the correlation function containing only classical Coulomb fields.

The second term, on the other hand gives

$$(2) \propto \int d\epsilon \int d\epsilon' \int d\Omega \tanh\left[\frac{\epsilon}{2T}\right] \tanh\left[\frac{\epsilon'}{2T}\right] \text{tr}\{\bar{C}_{\epsilon\epsilon'} C_{\epsilon'\epsilon}\} \left(\coth\left[\frac{\Omega}{2T}\right] - \tanh\left[\frac{\epsilon' + \Omega}{2T}\right] \right) V^R(\Omega). \quad (\text{B.22})$$

Summing these two contributions therefore one obtains

$$S_\chi[\mathcal{C}_s^{\text{fb}} \mathcal{C}_s^{\text{bf}}] = \propto \int d\epsilon \int d\epsilon' \int d\Omega \tanh\left[\frac{\epsilon}{2T}\right] \tanh\left[\frac{\epsilon'}{2T}\right] \text{tr}\{\bar{C}_{\epsilon\epsilon'} C_{\epsilon'\epsilon}\} \tanh\left[\frac{\epsilon - \Omega}{2T}\right] [V^R(\Omega) - V^R(-\Omega)]. \quad (\text{B.23})$$

That is, the low energy contribution cancels and only the contribution containing interaction processes with high energy exchange survives. In Keldysh formalism these interaction processes are described by interaction fields with a quantum component.

B.8.2 Poisson summation

The Poisson-summation is done as follows:

$$\begin{aligned} & \sum_q \frac{1}{(v_F q + \Omega + i\tau_\varphi^{-1})(v_F q - \Omega - i\tau_\varphi^{-1})} \\ &= \sum_{m=-\infty}^{\infty} \frac{1}{\left[\frac{2\pi v_F}{L}(m + \frac{2\phi}{\phi_0}) + \Omega + i\tau_\varphi^{-1}\right] \left[\frac{2\pi v_F}{L}(m + \frac{2\phi}{\phi_0}) - \Omega - i\tau_\varphi^{-1}\right]} \\ &= \left(\frac{L}{2\pi v_F}\right)^2 \sum_{m=-\infty}^{\infty} \frac{1}{[m + x + y + i\gamma][m + x - y - i\gamma]} \\ &= \left(\frac{L}{2\pi v_F}\right)^2 \sum_{m=-\infty}^{\infty} \int d\phi \frac{1}{[\phi + y + i\gamma][\phi - y - i\gamma]} e^{i2\pi\phi m} e^{-i2\pi x m} \\ &= \left(\frac{L}{2\pi v_F}\right)^2 \sum_{m>0} \left\{ \int d\phi \frac{1}{[\phi + y + i\gamma][\phi - y - i\gamma]} e^{i2\pi\phi m} e^{-i2\pi x m} \right. \\ &\quad \left. + \int d\phi \frac{1}{[\phi + y + i\gamma][\phi - y - i\gamma]} e^{-i2\pi\phi m} e^{i2\pi x m} \right\} + \phi\text{-independent} \\ &= i2\pi \left(\frac{L}{2\pi v_F}\right)^2 \sum_{m>0} \frac{e^{i2\pi y m} e^{-2\pi\gamma m} \cos[2\pi m x]}{y + i\gamma} + \phi\text{-independent}, \end{aligned}$$

where $y = \frac{L}{2\pi v_F} \Omega$, $x = \frac{2\phi}{\phi_0}$, $\gamma = \frac{L}{2\pi v_F l_1}$ and $\theta = \frac{TL}{2\pi v_F}$.

B.8.3 Performing the y -integral

The y -integral in Eq.(3.189) is done by a contour integral, closing the contour in the upper half plane, i.e.

$$\begin{aligned} \int dy \frac{y \coth\left[\frac{y}{2\theta}\right] e^{i2\pi m y}}{y + i\gamma} &= (i2\pi)(2\theta) \sum_{m'>0} \frac{e^{-8\pi^2 m m' \theta}}{1 + \gamma/4\pi\theta m'} = i4\pi\theta \sum_{m'>0} e^{-8\pi^2 m m' \theta} + O(1/T\tau_\varphi) \\ &= i2\pi\theta \frac{e^{-4\pi^2 m \theta}}{\sinh[4\pi^2 m \theta]} + O(1/T\tau_\varphi) = \frac{iTL}{v_F} \frac{e^{-\frac{2\pi m TL}{v_F}}}{\sinh\left[\frac{2\pi m TL}{v_F}\right]} + O(1/T\tau_\varphi). \end{aligned}$$

B.8.4 Coulomb field propagator

The Coulomb field propagator is given by

$$\begin{aligned}
S(\tau) &= \frac{T}{2L} \sum_{mq} \langle \chi_{-m}(q) \chi_m(-q) \rangle (1 - \cos[\omega_m \tau]) \\
&= \frac{T}{L} \sum_{mq} \frac{g_2}{(v_F q)^2 + \omega_m^2 + \kappa |\omega_m|} (1 - \cos[\omega_m \tau]) \\
&= \frac{g_2 T}{v_F} \sum_{m>0} \frac{1}{\sqrt{\omega_m^2 + \kappa \omega_m}} (1 - \cos[\omega_m \tau]) \\
&\approx \frac{g_2 T}{v_F} \sum_{m>0} \left(\frac{1}{\omega_m} - \frac{\kappa}{2\omega_m^2} \right) (1 - \cos[\omega_m \tau]) \\
&= S^a(\tau) + S^b(\tau).
\end{aligned}$$

Using the high energy cut-off $e^{-\omega_m/\Lambda}$ (the precise form of the cut of is of no relevance) the first sum can be evaluated with help of the identity [6] (for $N \gg 1$ and $\text{Re}(z) \gg 1/N$)

$$\sum_{m=1}^N \frac{1 - e^{-mz}}{m} \approx \ln[1 - e^{-z}] + \ln N, \quad (\text{B.24})$$

as follows:

$$\begin{aligned}
S^a(\tau) &\approx \frac{g_2 T}{4\pi T v_F} \sum_{m>0} \frac{1 - e^{m(i2\pi T\tau - 0)}}{m} + \tau \leftrightarrow -\tau \\
&= \frac{g_2}{4\pi v_F} \left(2 \ln \left[\frac{\Lambda}{T} \right] + \ln[1 - e^{-i2\pi T\tau - 0}] + \ln[1 - e^{i2\pi T\tau - 0}] \right) \\
&= \frac{g_2}{4\pi v_F} \left(2 \ln \left[\frac{\Lambda}{T} \right] + \ln[\sin^2[2\pi T\tau + i0]] \right) .. \quad (\text{B.25})
\end{aligned}$$

The second term may be evaluated with help of the identity [12]

$$2T \sum_{m \neq 0} \frac{1 - e^{i\omega_m \tau}}{\omega_m^2} = |\tau| - T\tau^2$$

and gives

$$S^b(\tau) = -\frac{g_2 \kappa T}{2v_F} \sum_{m>0} \frac{1 - \cos[\omega_m \tau]}{\omega_m^2} = \frac{g_2 \kappa}{8v_F} (T\tau^2 - |\tau|), \quad (\text{B.26})$$

with $\kappa = \frac{g_2 v_F}{2\pi l_1}$.

Danksagung

An dieser Stelle möchte ich allen Personen danken, die zum Gelingen dieser Arbeit beigetragen haben. Mein besonderer Dank gilt Alexander Altland für die interessante Themenstellung sowie dafür, mein Interesse an der mesoskopischen Physik geweckt zu haben. Ihm und Achim Rosch danke ich für ihre unkomplizierte, wertvolle Betreuung. Weiterhin danke ich Julia Meyer für eine wunderbare Zeit in Columbus. Nicht unerwähnt bleiben sollen natürlich die vielen anregende Diskussionen mit Fabrizio Anfuso, Inga Fischer, Dominic Grün, Rolf Helmes, Peter Jung, Julia Meyer, Jan Müller und Chushun Tian.

Erklärung

Ich versichere, daß ich die von mir vorgelegte Dissertation selbständig angefertigt, die benutzten Quellen und Hilfsmittel vollständig angegeben und die Stellen der Arbeit — einschließlich Tabellen, Karten und Abbildungen, die anderen Werken im Wortlaut oder dem Sinn nach entnommen sind — in jedem Einzelfall als Entlehnung kenntlich gemacht habe; daß diese Dissertation noch keiner anderen Fakultät oder Universität zur Prüfung vorgelegen hat, daß sie — abgesehen von unten angegebenen Teilpublikationen — noch nicht veröffentlicht worden ist sowie, daß ich eine solche Veröffentlichung vor Abschluß des Promotionsverfahrens nicht vornehmen werde. Die Bestimmungen der Promotionsordnung sind mir bekannt. Die von mir vorgelegte Dissertation ist von Herrn Prof. Dr. Alexander Altland betreut worden.

Köln, den 18. Dezember 2006

Teilpublikationen

- T. Micklitz, T. A. Costi, A. Altland and A. Rosch, Phys. Rev. Lett. **96**, 226601 (2006).
- F. Mallet, J. Ericsson, D. Mailly, S. Ünlübayir, D. Reuter, A. Melnikov, A. D. Wieck, T. Micklitz, A. Rosch, T.A. Costi, L. Saminadayar, and C. Bäuerle, Phys. Rev. Lett. **97**, 226804 (2006).
- T. Micklitz, T. A. Costi, A. Altland and A. Rosch, cond-mat/0610304 (submitted to PRB).

Lebenslauf

Persönliche Daten

Name	Tobias Micklitz
Geburtsdatum	12.08.1973
Geburtsort	München
Familienstand	ledig
Staatsangehörigkeit	deutsch

Schulbildung

1980–1984	Bucholzer-Grundschule (Witten, NRW)
1984–1991	Schiller-Gymnasium (Witten, NRW)
1991–1993	Friedrich-Wilhelm Gymnasium (Köln)
Juni 1993	Abitur

Juni 1993–Juni 1994	Kibbutzaufenthalt (Urim, Israel)
Juni 1994–September 1995	Zivildienst

Hochschulstudium

Oktober 1995	Immatrikulation an der Universität zu Köln
Juli 1997–April 1998	Studiengang: Regionalwissenschaften Lateinamerika (Diplom) Unterbrechung des Studiums für einen Auslandsaufenthalt an der Universität Fortaleza (Ceará, Brasilien)
Juli 1998	Vordiplom
Oktober 1998	Fachwechsel: Physik (Diplom)
Juli 2000	Vordiplom
Februar 2003	Diplom
seit März 2003	Anfertigung der vorliegenden Dissertation

Arbeitsverhältnisse

Oktober 2000–Juli 2001	Studentische Hilfskraft am Mathematischen Institut
August 2001–Februar 2003	Studentische Hilfskraft am Institut für Theoretische Physik
seit März 2003	Wissenschaftlicher Mitarbeiter (ibidem)